Dedicated to

my parents

Al and Rhoda Cox

A STUDY OF HORIZONTAL AND DOWN HILL TWO-PHASE OIL-WATER FLOW

BY

ALDEN LEROY COX JR, B.S. P.En.

THESIS

Presented to the Faculty of the Graduate School of

The University of Texas at Austin

in Partial Fulfillment

of the Requirements

for the Degree of

MASTER OF SCIENCE IN ENGINEERING

THE UNIVERSITY OF TEXAS AT AUSTIN

August 1985

ACKNOWLEDGEMENTS

My deepest appreciation and gratitude go to my supervisors, Dr. A. D. Hill and Dr. A. L. Podio, whose supervision, advice and encouragement made this thesis a valuable learning experience.

I would like to thank Ray Flores, Bob Hamilton and Jim Wortham for their help and expertise with the setup and operation of the experimental flow system. K. G. Morrison also helped by securing certain necessary parts for the flow system.

Fellow graduate students Grant Scott, Scott Schmidt, Jay Akers, Tom Lowe and Joel Rood assisted me in various ways in the completion of this project. Grant Scott helped me use the University computer system. Scott Schmidt showed me how to use the Zeta plotter. Jay Akers helped me use the IBM script system through which my appendices were printed. Finally, Tom Lowe and Joel Rood let me use their Apple Macintosh computers to draw certain figures found in this thesis, which proved very time saving.

I would like to acknowledge the companies that comprise the Stimulation, Logging and Formation Damage Research Program for their financial assistance during my work on this project.

Final thanks go to my family whose positive attitude and caring kept me going during the rough times.

Alden Leroy Cox Jr.

The University of Texas at Austin

August 1985

ABSTRACT

Concurrent oil and water flow in inclined pipes is a common occurrence in deviated wells and production gathering systems. To predict properties associated with non-emulsified oil and water flow such as pressure gradient, two-phase flow correlations developed for gas-liquid flow or average flow properties of the oil and water must be used.

The objective of this work was to study water holdup (water holdup defined as the in-situ fraction of the pipe occupied by water), and see what, if any, parameters have an effect on its magnitude. Flow pattern formation was also studied to determine its effect on holdup.

The oil-water flow experiments were conducted with a flow loop constructed of 2 inch ID clean plastic pipe using a wide range of oil and water flow rates and involving inclination angles of 0, -15 and -30 degrees from horizontal. For each set of flowing conditions, the system was allowed to reach steady-state, then the flow regime was observed and the water holdup was measured. From the experiments, the flow regimes associated with oil-water flow differed greatly from flow regimes encountered with gas-liquid flow. It seems apparent that when comparing experimental flow regime data with modified and established gas-liquid dimensionless parameters there exists no meaningful correlation. Holdup data obtained indicates that it does vary according to certain parameters which include pipe inclination, flow patterns, and input fraction of water.

TABLE OF CONTENTS

PAGE

LIST OF TABLES

LIST OF FIGURES

FIGURE PAGE

FIGURE PAGE

FIGURE PAGE

CHAPTER I

INTRODUCTION

GENERAL ASPECTS OF THE PROBLEM

The simultaneous flow of oil and water in pipes is a common occurrence in oil production systems, occurring from the well perforations to the final stage of separation. Many times the oil and water will flow as separate phases rather than as an emulsion. At times when this happens, the measurement of certain flow properties, such as holdup of the more dense phase (holdup as used in this paper will be referred to as the volume fraction of pipe occupied by the more dense phase), or the prediction of pressure drop, becomes complicated by some of the same factors that make gas-liquid flow properties difficult to measure. Pipe inclination can further complicate the flow condition, which will affect both flow patterns and related holdups. The most common area where inclined oil-water flow occurs is in oil production. An example is shown in Figure 1. Offshore oil fields tend to have the most inclined flow because well deviation can range from vertical to 80 degrees from vertical.

With the increase in offshore drilling and production, there is an increase in the transportation of well fluids through pipelines over long distances. Most well fluids are composed of oil and gas and frequently contain water. Water fractions will tend to increase over the productive life of the well. Therefore, water must be considered

when predicting flow behavior that will be used in the designing of wells, production facilities and pipelines.

An extensive amount of research has been published in previous years concerning multi-phase flow in pipes. The fluids used have varied from a gas and a liquid to two liquids that are immiscible. A majority of the work has involved gas-liquid flow through vertical or horizontal pipe. Inclined flow was treated throughout these studies as a variation of these two situations. Present studies indicate that in horizontal gas-liquid flow, pressure gradients are higher with the presence of water. These pressure increases tend to be caused by an increase in the apparent viscosity of the liquid near the interface of the two phases. The failure to plan for this pressure increase can lead to decreased productivity in wells and decreased capacities in pipelines. Likewise, the failure to account for slippage between oil and water phases can make separation designs ineffective.

These facts just discussed necessitate the need to further study oil-water inclined flow. The significant parameters to be studied are pipe inclination and water input flow rates and their effect on water holdup and flow patterns in two-phase oil-water flow.

PREVIOUS INVESTIGATIONS INVOLVING TWO-PHASE FLOW

A voluminous amount of research has been conducted in the area of multi-phase flow in pipes since it is common in the nuclear, chemical and petroleum industries. A majority of the work involves gas-liquid two-phase flow in horizontal and vertical pipes. The main objective of

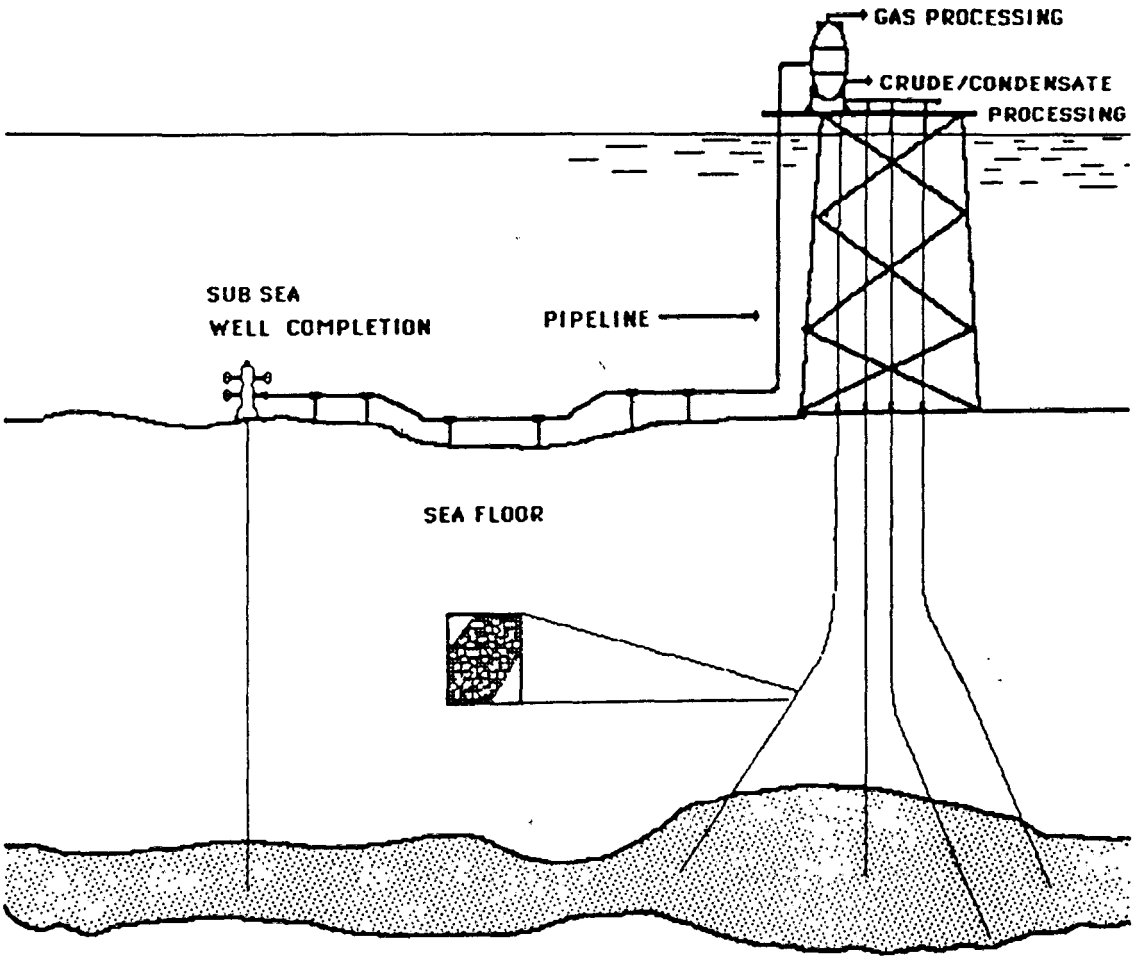

Figure 1

An Example of Offshore Inclined Oil-Water Flow

these studies was to relate pressure drop as a function of various two-phase flow conditions. A few studies have included pipe inclination as a parameter but most were only concerned with a few degrees from horizontal because of its applicability to pipelines in hilly regions.

Dukler et al.[1] listed five approaches to the correlation of gas-liquid flow. These are:

1. Empirical correlations alone
2. Empirical correlations with dimensional analysis
3. Empirical correlations utilizing similarity analysis and model theory.
4. Mathematical analysis and theoretical development of equations using simplified physical models.
5. Semi-empirical correlations developed from the conservation of energy and momentum equations using experimental data to evaluate the transport terms.

To improve pressure drop correlations in gas-liquid flow, complex conditions were added by researchers. Pressure drop correlations were improved by the development of liquid holdup correlations. Then, to help improve the holdup correlations, flow regime correlations were developed. One of the first flow regime maps that, at different input fractions, describes the different flow patterns was developed by Duns and Ros[2] and published in 1963. This work involved correlations for vertical gas-liquid flow. Also, they described five distinct flow patterns - bubble flow, plug flow, slug flow, froth flow and mist flow. "Heading" was a term given to slug flow because a region was observed in the flow regime where the liquid seemed to be falling back along the

wall of the pipe. Previously, in 1961, Ros[3] had published results of a study that was conducted on gas-liquid flow in vertical pipe. These results involved a dimensional analysis that used liquid density, interfacial tension and gravity as repeated variables. Hagedorn[4] in 1963 used this work to correlate vertical two-phase flow in his Ph.D. dissertation.

There have been few studies on the effect of pipe inclination on gas-liquid two-phase flow. Most of this work involved angles within approximately 15 degrees of horizontal. DeGance and Atherton[5] reviewed several pressure drop correlations for gas-liquid flow for inclined and vertical pipe. They concluded that over the entire range of possible angles, there is no one valid, general correlation for all pipe sizes.

Gregory[6] published a study in 1975 in which several correlations were compared using data that was available for angles from 0 degrees to 10 degrees of horizontal. He determined that the correlations of Lockhart and Martinelli[7] and of Guzhov[8] were the best available. However, it is fascinating that neither correlation contained any allowance for pipe inclination.

Beggs and Brill[9] experimented with gas-liquid flow with different angles, ranging from vertical upflow to vertical downflow. They concluded that maximum liquid holdup occurred at approximately 55 degrees from horizontal in upwards flow. From this a correlation for gas-liquid flow was developed which included the important parameter of pipe inclination.

Over the years, it has been noted that liquid-liquid flow has not received the attention that gas-liquid flow has received, but more

research is being done to remedy the situation. Some of the work involved the addition of water to reduce pressure loss in horizontal pipe flow of viscous oil. A study of the flow regimes possible in horizontal liquid-liquid flow was experimentally conducted by Russell, et al.[10] The flow patterns observed in this flow were stratified, bubble and mixed flow. Pressure drop readings and holdup data were taken while observing the flow regimes.

Stratified flow consisted of the more dense fluid flowing along the bottom of the pipe and the less dense fluid travelling above. Bubble flow was interpreted as globules of one phase flowing within the other phase. Finally, mixed flow was defined as a combination of the two other flow regimes. Charles et al.[11] studied two equal density liquids in two-phase flow. They determined that with a constant oil flow rate, an increase in the water flow rate will produce the following flow regimes: water drops in oil; concentric oil in water; oil slugs in water; oil bubbles in water and finally oil drops in water.

Guzhov et al.[12] conducted a complex study on the structural forms of liquid-liquid flow. This flow regime study involved flowing oil-water horizontally through 1½ inch diameter pipe, observing and photographing the structural form of the flow. The structural forms of the flow of oil-water were as follows:

1. stratified flow
2. stratified flow with a dense layer of oil in water emulsion at the boundary.
3. dense emulsion with very dense packing of oil globules in water.

4. complete emulsion flow
   (a) oil in water
   (b) stratified oil in water and water in oil emulsions
   (c) water in oil emulsion

From the data gathered, a flow regime map was developed which showed eight structural forms of oil-water flow which were dependent upon input oil fraction and mixture velocity.

Soot and Knudsen[13] experimented with downward oil-water flow. Throughout the course of their work they used a dispersed oil phase that was carried in a continuous water phase. The end result is that the flow regime resembled a gas-liquid bubble flow pattern. Pressure drop and holdup correlations were developed for this particular flow pattern and then the correlations were compared with other data to see if there is any change. A standard deviation of 20 to 30% was noted.

A study completed by Mukherjee et al.[14] experimented with diesel oil and water at various angles of inclination from ±30 degrees to ±90 degrees. Upward vertical flow is indicated by an angle of +90 degrees while downward vertical flow is indicated by -90 degrees and horizontal flow is designated by an angle of 0 degrees. They gathered holdup and frictional pressure drop data and correlated these to the input fraction, pipe inclination, Froude Number and Reynolds number of the particular flow condition. One of their recommendations was that "future studies should not exclude the important inclination angles between 30 degrees and -30 degrees".

It was concluded, after reviewing the previous literature concerning gas-liquid and liquid-liquid two-phase flow, that there is a

conspicuous absence of work involving liquid-liquid downhill flow. Therefore, there needs to be more study conducted with two-phase liquid-liquid flow at negative inclinations.

SCOPE OF EXPERIMENTAL WORK

The experimental data was collected from a test flow loop located in the Petroleum Engineering Building on the campus of the University of Texas at Austin.

The test loop shown in a schematic diagram in Figure 2 was constructed of clear plexiglass pipe and was used to study certain predetermined parameters. The parameters varied were: (1) the oil flow rate (50-700 B/D), (2) the water flow rate (50-700 B/D), (3) the pipe inclination (0 degrees, -15 degrees, and -30 degrees) with -15 degrees and -30 degrees designated as downhill flow. The parameters studied were water holdup and flow regimes.

Oil and water were pumped through the system simultaneously, at a certain inclination angle with the oil rate held constant and the water rate incremented from 50 - 700 B/D, while observing the corresponding flow regimes at each set of flow rates. This process was repeated with a different oil rate held constant and the water rate incremented until all the selected oil rates at a certain angle were tested. Then the angle was changed and this process repeated. This allows for the effect of oil and water rate changes and inclination angle on flow regimes.

Within this experimental work, holdup will be studied to see what, if any, parameters have an effect on its magnitude.

Flow patterns will be defined and evaluated to understand their effect on holdup.

Holdup was measured by using two "quick closing" pneumatic ball valves. This allows for the effect of varied oil and water flow rates and pipe inclination on holdup to be studied.

The data collected was from 363 test runs with each run repeated twice to get an "average" for the particular run.

The next chapter describes the apparatus needed for the experimental test flow loop and also discusses testing procedures.

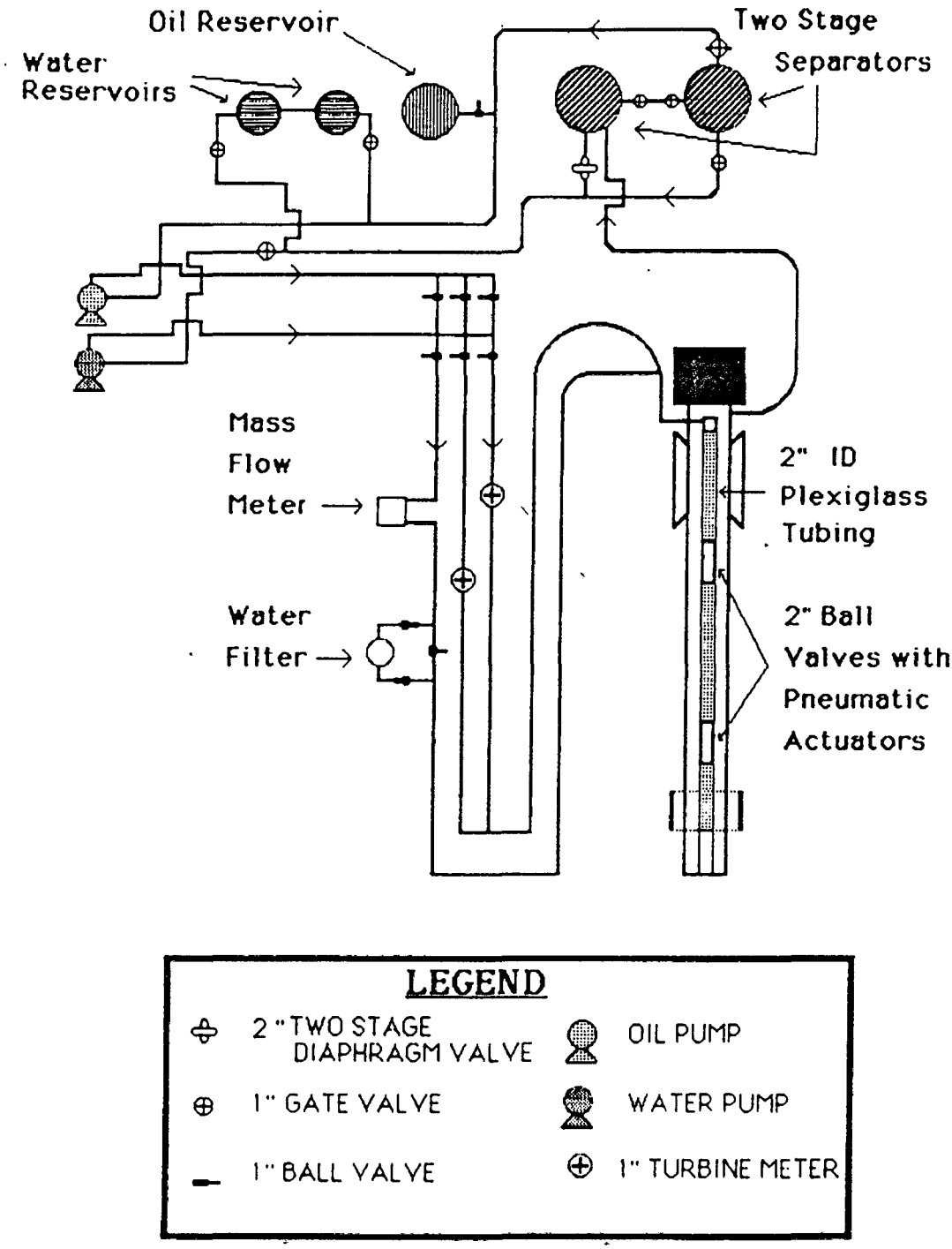

Figure 2

Schematic Diagram of Test Flow Loop

CHAPTER II

EXPERIMENTAL APPARATUS AND TESTING PROCEDURE

EXPERIMENTAL APPARATUS

A test flow system was designed and constructed to obtain experimental data. The flow system consists of a flow loop, two two-stage vertical separators, an oil reservoir, two water reservoirs, two centrifugal pumps, measuring equipment and a filtering system.

Flow Loop

The flow loop consisted of 2-inch diameter, clear, plexiglass pipe mounted along a steel beam. The pipe is mounted on the top and bottom of the steel beam with a 180 degrees elbow mounted at the end of the loop, to allow the test liquid to flow around and through the bottom pipe. The pipe has four 2-inch "quick-closing" pneumatic ball valves which make it possible to measure quantitatively the holdup of the more dense phase. After the flow is stabilized, the valves will be closed, capturing the oil-water stream which when allowed to separate, will give an indication of the holdup under flowing conditions. The beam is mounted on a fulcrum which allows inclinations up to 30 degrees from horizontal to be used. Since the pipe is mounted on either side of the beam, upward and downward flow, and related holdups can be studied simultaneously. Two metal bars with drilled holes are at the "U" shaped end of the pipe which can be used to lock the beam at a desired angle.

At the opposite end of the beam, weights are mounted to allow for easy upward and downward movement of the flow loop. Side views of the flow loop are shown in Figure 3 and 4.

Two-Stage Vertical Separators

Each separator is 6½ feet in height and is 2 feet in diameter with a capacity of 150 gallons or 3.6 barrels and stand side-by-side. Water is removed from each separator through a drain at the bottom. Water from the right separator flows through a two-inch gate valve along 2-inch pipe toward the water pump. The water from the left separator flows through a 2-inch two diaphragm valve into the 2-inch pipe mixing with the water from the other separator. The water then flows to the water pump. Oil is removed only from the right separator through a 2-inch gate valve about 2/3 of the way up the separator well within the oil column. Once past the valve the 2-inch pipe is nippled down into 1-inch pipe which continues all the way to the oil pump. The mixed stream of oil and water is discharged from the clear, plexiglass flow loop through 2-inch pipe into the upper 1/3 of the left separator. The separators are connected through valves by two flexible hoses, the top hose allows oil flow between the separators and the bottom hose allows water to flow from one separator to the other. The levels of oil and water were kept at a certain height to assure that only oil was being drawn into the oil pump and water was flowing to the water pump. Four sight glasses were installed to monitor the liquid levels.

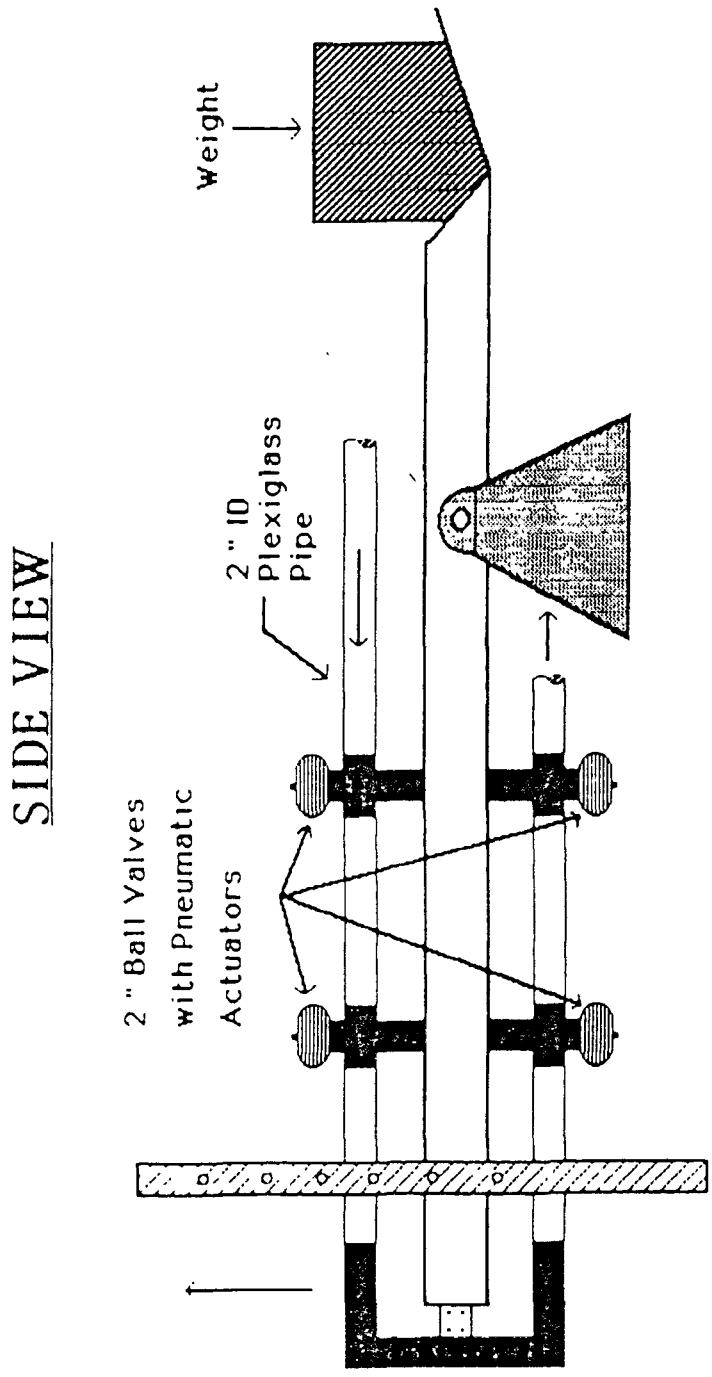

Figure 3

Side View of Flow Loop

Figure 4

Side View of Flow Loop

Oil Reservoir

Oil storage consisted of a 55 gallon drum placed to the left of the two separators. It is connected to the oil discharge pipe by a 1-inch pipe with a "tee" which was nippled down from a 2-inch pipe which is mounted through a hole in the top of the reservoir. A 1" ball valve is used to seal off the reservoir from the oil line. The drum has a 1-inch pipe which has a valve that allows pressurized nitrogen to be pumped in, which forces the oil to be pushed out of the reservoir and into the oil line when needed.

Water Reservoirs

Water storage consisted of two 5 foot high cylinders with 1½ foot diameters each having a capacity of approximately 66 gallons or 1.6 barrels. Each reservoir has a 2-inch pipe with a gate valve that is connected at the 4 foot level. Water from the system can be discharged into each reservoir through this two-inch pipe. Water can be discharged from the two reservoirs by 1-inch pipe that is connected near the bottom of each reservoir. 1-inch gate valves are used to seal off the reservoirs from the water discharge pipe. There is a 1-inch pipe that connects both reservoirs at the 4-3/4 foot level to prevent overflow.

Pumping System

Oil and water from the separators were pumped by two 1½x1x6 Worthington centrifugal pumps, model D1011 with 3 horsepower motors. Each pump has a discharge rating of 100 gallons per minute. Each pump discharges its respective liquid into a manifold which, in turn, routes

the water stream to a mass flow meter and the oil stream to a turbine meter located down stream.

Measuring Equipment

The metering of the oil and water was accomplished by a calibrated turbine meter and mass flow meter, respectively. The turbine meter is a Daniel 1401-1P which has a flow capacity of 60 GPM with a 181A transducer mounted on top. The mass flow meter is a model C50 made by Micro Motion, Inc. It has a flow capacity of 440 lbs/min (2400 GPM).

MEASUREMENT OF PARAMETERS

Both a turbine meter and mass flow meter were used to measure the flow rates of oil and water in the flow system. Since the mass flow meter was calibrated at the factory an additional calibration was not performed. The mass flow meter was, however, used to calibrate the turbine meter. The Daniel turbine meter's readout is in percent flow (%), therefore, to convert the readout to barrels per day (B/D), the mass flow meter was used in series with the turbine meter to make the conversion. First, the readout of the mass flow meter was in lbm/min, so for convenience, it was necessary to calculate a conversion factor that could be used to change lbm/min to B/D. So for oil:

$$\frac{\text{lbm}}{\text{min}} \times \frac{\text{ft}^3}{62.4\ \text{lbm}\ (0.754)} \times \frac{\text{Barrel}}{5.615\ \text{ft}^3} \times \frac{1440\ \text{min}}{\text{Day}} =$$

5.45 (Reading from mass flow meter) = B/D

Similarly for water, the conversion factor = 4.11

Secondly, 24 runs with 100% oil were made while recording the readouts of the mass flow meter and turbine meter, respectively. The results are listed in Table I. Next, to check the linearity of the turbine meter, a plot of turbine meter (% flow) vs. mass flow meter (B/D) was made, with a best fit line drawn through the points. Figure 5 shows the finished plot and best fit line. Finally, to convert the % flow readings to B/D, start at a flow rate on the X axis, then proceed vertically until the best fit line is reached. Then move horizontally to the Y axis. This number is the corresponding % flow reading for the chosen oil flow rate in B/D.

This method was used throughout the experiment to determine the oil flow rate through the turbine meter. This procedure was duplicated using water instead of oil so that the turbine meter could be used to measure either oil or water flow rates. Table II and Figure 6 show the results and final plot for water, respectively.

TABLE I

LINEARITY CHECK OF TURBINE METERS

(100% oil)

Mass Flow meter B/D	Daniel Meter % Flow
327	20.0
300.0	18.0
245.0	16.0
128.0	8.0
341.0	13.0
41.0	2.0
170.0	10.0
60.0	4.0
273.0	17.0
169.0	11.0
98.0	6.0
202.0	12.0
420.0	27.0
19.0	0.2
455.0	29.0
142.0	8.0
510.0	34.0
185.0	12.0
561.0	37.0
76.0	4.0
600.0	40.0
387.0	24.0
643.0	40.0
218.0	14.0

LINEARITY AND CALIBRATION CHECK OF
FLOWMETER FOR OIL FLOWRATES

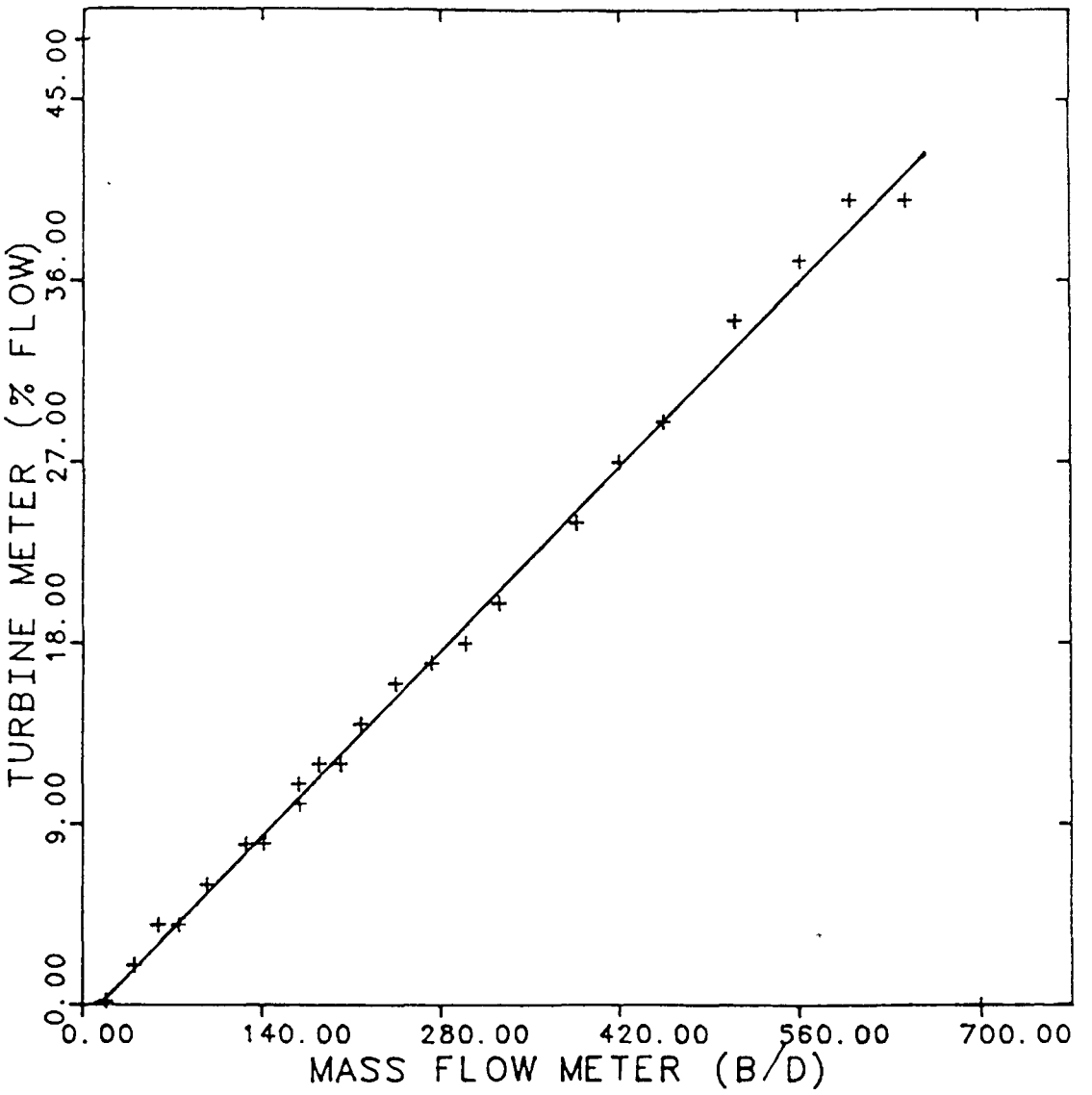

Figure 5

Plot of Turbine Meter Readout vs. Mass Flow Meter Readout

TABLE II

LINEARITY CHECK OF TURBINE METERS

(100% water)

Mass Flow meter B/D	Daniel Meter % Flow
127.0	7.0
789.0	42.0
575.0	31.0
300.0	18.0
103.0	6.0
86.0	6.0
66.0	4.0
49.0	3.0
33.0	2.0
177.0	10.0
100.0	9.0
127.0	8.0
201.0	12.0
246.0	14.0
308.0	17.0
349.0	19.0
395.0	22.0
452.0	24.0
493.0	27.0
555.0	30.0
604.2	33.0
653.5	36.0
703.0	38.0
748.0	41.0

LINEARITY AND CALIBRATION CHECK OF
FLOW METER FOR WATER FLOW RATES

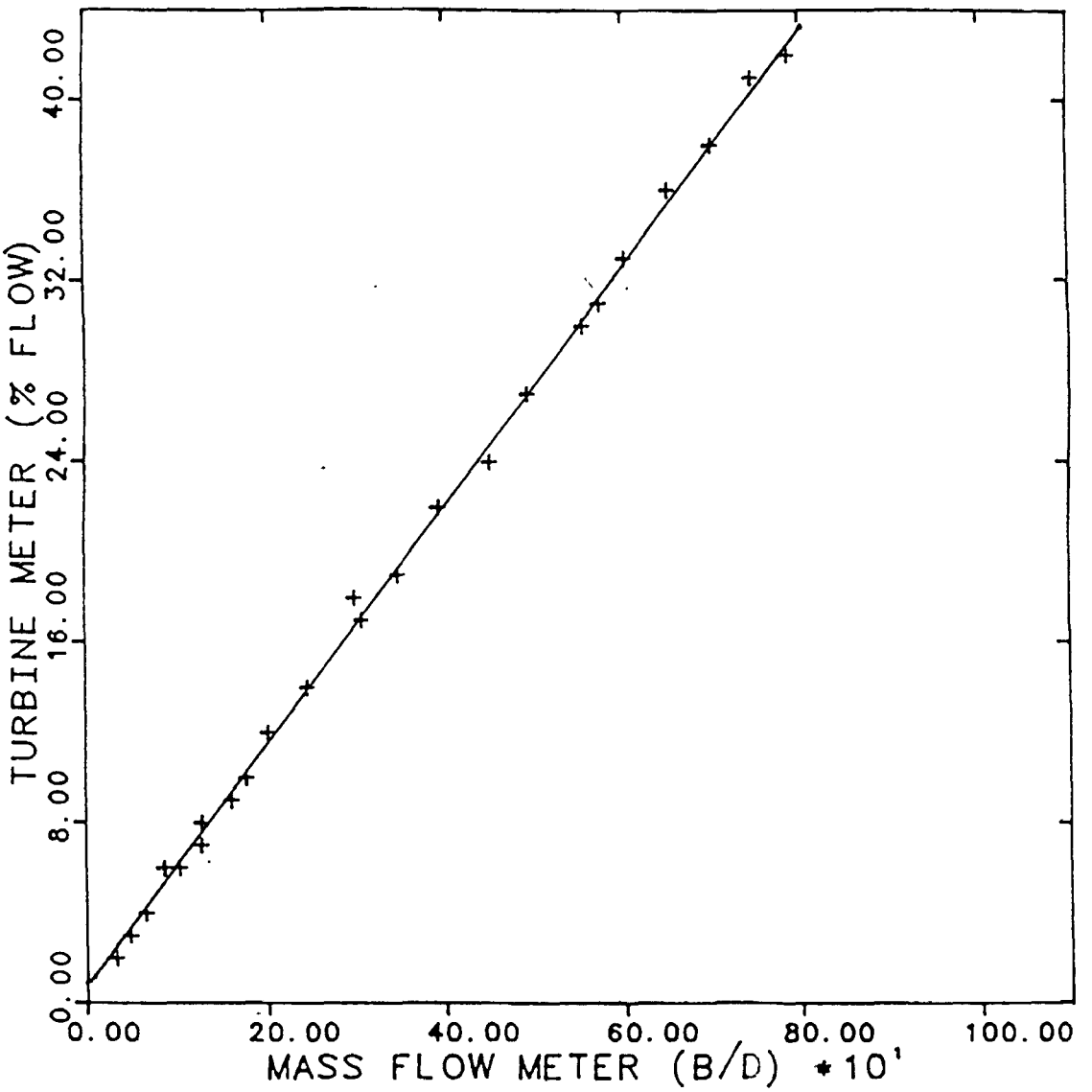

Figure 6

Plot of Turbine Meter Readout vs. Mass Flow Meter Readout

According to Eaton et al.[15] the measurement of holdup can be accomplished several ways, and these methods usually fall into two categories.

1) Indirect holdup measurement
   a) Acoustic velocity in a two-phase mixture
   b) Electric resistivity of a two-phase mixture
   c) Thermal conductivity of a two phase mixture
   d) Capacitance of a two-phase mixture

2) Direct holdup measurement
   a) Sampling probes
   b) Photography
   c) Direct measurement by use of quick-closing valves

From a review of the literature concerning holdup, direct measurement by quick closing ball valves was the best method possible under the present circumstances.

The valves were placed approximately 4 feet apart on both the top and bottom sections of the plexiglass tubing in the flow loop. Figure 7 shows a drawing of the pipe and closed ball valves. There is a section between the end of the pipe to the ball in the ball valve where the volume must be determined. This volume is shown in Figure 8. This "blind" section volume can be determined by subtracting the volume of water that is left in the pipe and outside the valve from the initial input volume of water. Figure 9 shows an example at 30 degrees. It follows that:

at 30°

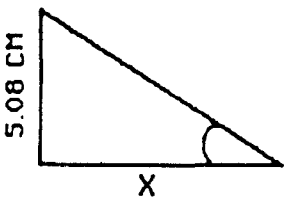

$\frac{y}{x}$ = tan 30° x = 8.7988 cm.

Volume (valve) = Volume (input) - Volume (water outside the valve)

To calculate the volume of the fluid outside the blind section

Volume (pipe) = $\pi r^2 L$

where L = x/2 = $\frac{8.80}{2}$ = 4.40 cm.

Volume (pipe) = π (2.54 cm)^2 (4.40 cm) = 89.17 cm^3 or 89.17 cc

If 250 cc of fluid was present in the pipe, then,

V (ball valve) = (250 - 89.17) cc = 160.93 cc

Tests were conducted at different inclinations to see varying valve volumes that could be expected.

Angle (degrees)	Input volume (cc)	X-Distance* (cm)	Area (cm^2)	x/2 (cm)	Volume§ Outside valve(cc)	V ball valve(cc)
10	455	28.8	20.27	14.40	291.96	163.0
20	304	13.96	20.27	6.98	141.44	162.6
25	281	10.89	20.27	5.45	110.40	170.6
30	250	8.80	20.27	4.40	89.17	160.8

* x = y/tan θ
§ V = $\pi r^2 (x/2)$

so,

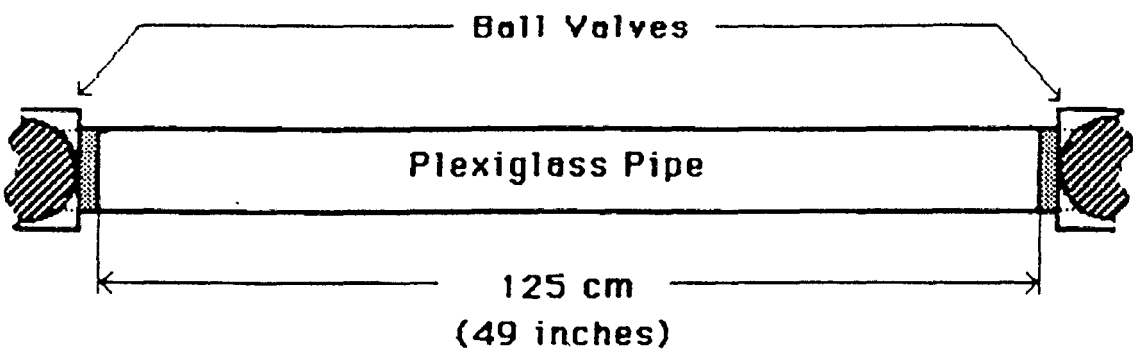

Figure 7

Pipe and Closed Ball Valves

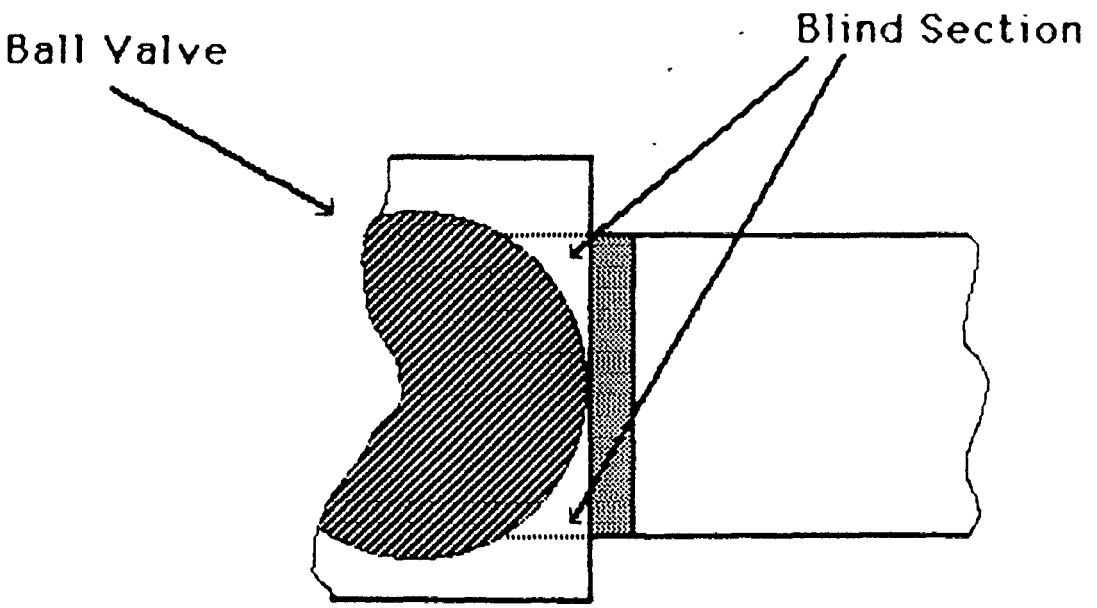

Figure 8

Ball Valve and Blind Section

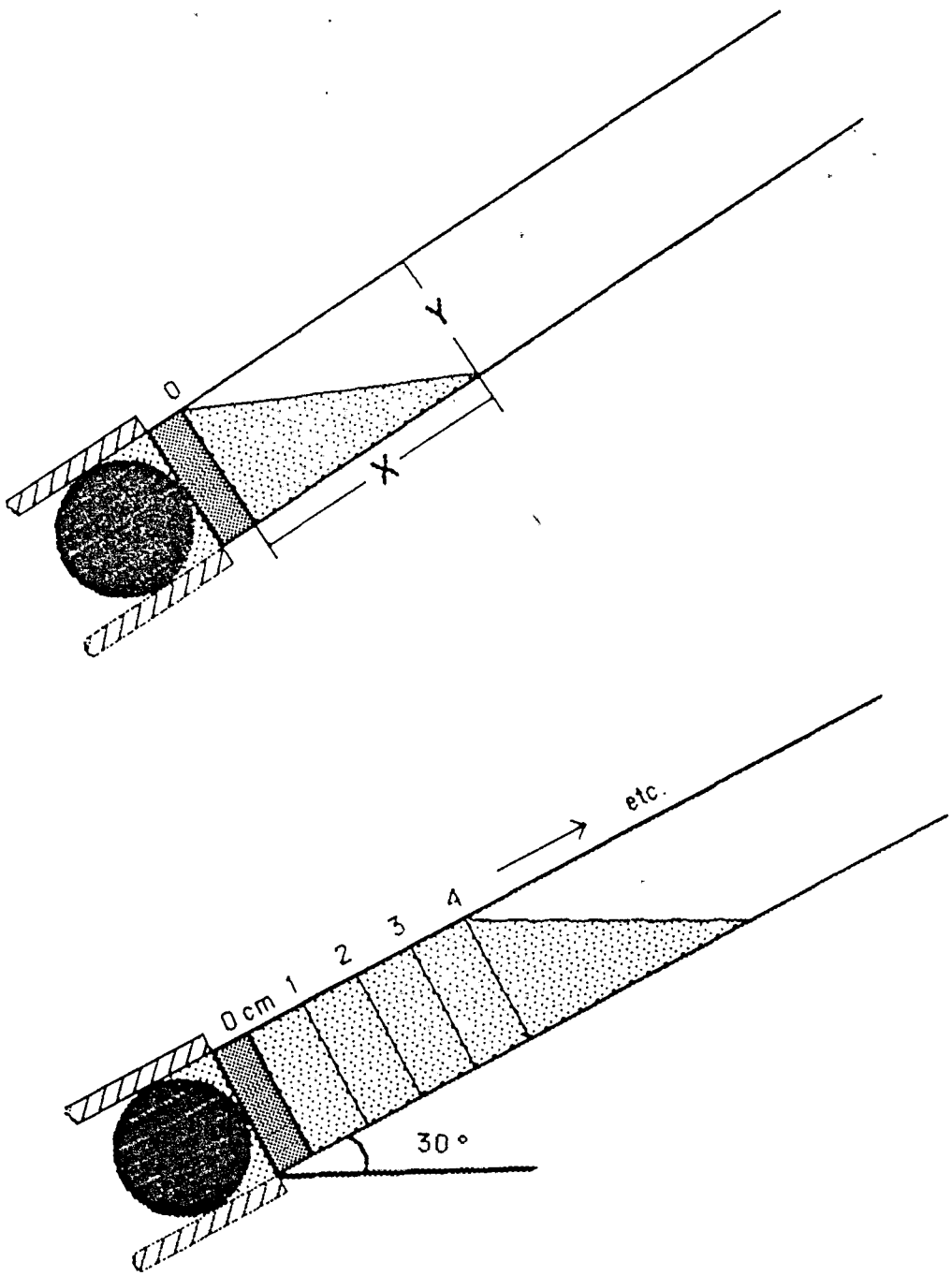

Figure 9

Ball Valve and Liquid Level Markings

the ball valve volume, V_{bv}, will be calculated as follows:

$$V_{bv} = (163+162.6+170.6+160.83)/4 = 164 \text{ cc}$$

now, the volume of pipe is

$$V_p = \pi r^2 L = \pi(2.54\text{cm})^2(125 \text{ cm}) = 2533.5 \text{ cm}^3$$

therefore the total volume of the pipe including both "blind" valve section volumes is

$$V_{PT} = \text{pipe volume} + \text{valve volumes} = 2533.5 + 164 + 164$$
$$= 2861.5 \text{ cc}$$

To be able to read what the captured holdup volume is, increment lines must be marked on the plexiglass pipe between the valves. Marks at 1 cm intervals will be used.

So for 0 cm mark:

Volume (0) = 89.17 + 164 = 253.2 cc;

for 1 cm mark:

Volume (1) = 253.2 cc + $\pi r^2 L$

= 253.2 cc + $\pi(2.54 \text{ cm})^2$ (1 cm)

= 273.5 cc

Therefore, at 30 degrees, each 1 cm adds 20.3 cc. The other angles use a similar calculation:

Angle (Degrees)	V (cc)	Volume added for each cm (cc)
5	752.4	20.3
10	457.0	20.3
15	356.1	20.3
20	305.4	20.3
25	274.4	20.3
30	253.2	20.3

Apparatus Problems

In the course of using the flow system, certain problems developed that needed to be solved. The first, and most troublesome problem, was bacteria growth in the oil. Since Soltrol 130 is a distilled mineral oil, it lacks key components, that diesel oil, for example, may contain to keep bacteria growth in check. When the experiment first started, bacteria growth was minimal. However, as the experiments proceeded, a large quantity of bacteria was encountered. At first, the growth was assumed to be algae, however, repeated attempts to kill the growth using chlorine and bleach proved unsuccessful. Next a sample was taken for analysis and at that time it was determined that instead of just algae, the growth was a strain of algae bacteria. From that point, an algicide was considered for use in the management of the bacteria. Several chemical companies were contacted and Hydrochem was chosen. The biocide selected for use was A 706 Algicide. The quantity needed is one pint for every 300 gallons.

After repeated application, the bacteria was finally under control but the biocide tended to make the water somewhat opaque. This tradeoff was considered satisfactory for the remaining experimentation.

Since some of the experimentation depended on distinct phases of oil and water an emulsion was not wanted. Considering that the flow rates of oil and water were each approaching 700 B/D, the possibility of creating an emulsion was increased. So, the method decided upon for the elimination of the emulsion was the use of a demulsifier. Magna Corporation, a Baker International Company, provided a demulsifier known as DI-Chem 354 for use in the oil and water mixture. The proper

concentration needed is 1 cc of demulsifier for every 100 gallons of fluid to be treated. Therefore, approximately 3 cc of DI-Chem 354 was used. Each time the water was changed, new demulsifier was added.

EXPERIMENTAL PROCEDURE

Experimental data that was obtained from each test consisted of visual observation of the flow pattern, angle of inclination, fluid flow rates and water holdup. There was no problem making visual observations with the clear plexiglass pipe in the flow loop. Each test consisted of taking three separate readings of holdup. It took 5 minutes for the system to reach steady-state each time.

The complete procedure for each test took an average of 15 minutes and consisted of the following steps:

(1) The desired flow rate of oil was set by adjusting a ball valve in the oil line in the manifold and noting the turbine meter readout. The water flow rate was set in a similar manner except that the flow rate was metered through a mass flow meter.

(2) After the flow rates were set, the flow loop inclination angle was set for that test run.

(3) When the flow stream reached steady-state, approximately 5 minutes later, a visual observation of the flow pattern was made and its appearance recorded. Still photographs of each different flow regime were taken at this time.

(4) Finally, the switch that controls the pneumatic valves was thrown, the valves closed and 30 seconds later, after the two phases separated, water holdup was measured.

(5) The valves were then opened and the procedure was repeated twice more at that angle of inclination.

These steps were followed for each test run. The water flow rates varied from 50 to 700 B/D. The oil rate also varied from 50 to 700 B/D. The total liquid flow rate ranged from a low of 100 B/D to a high of 1400 B/D. The physical properties of the two test liquids are listed in Table III.

TABLE III

Physical Properties of Test Liquids

SOLTROL 130*

PROPERTIES	TYPICAL	SPECIFICATIONS
Distillation range, initial boiling point, F	349	335 min-360 max
10% Condensed, F	355	345 min-365 max
50% Condensed, F	364	355 min-370 max
90% Condensed, F	382	370 min-390 max
End point, F	406	380 min-410 max
Specific gravity of liquid at 60 60 F	0.754	0.750 min-0.760 max
API gravity at 60 F	56.2	
Density of liquid at 60 F, lb/ft^3	46.98	
Bromine number	0.6	
Flash point by TCT, F at 760 mm	133	125 min
Color, Saybolt	+30	25 min
Sulfur content, weight percent	0.0004	
Unsulfonated residue, volume percent	99.0	
Acidity, distillation residue	Neutral	Neutral
Aniline point, F	185	182 min-188 max
Copper corrosion, 3 hrs at 212 F	1	1 max
Kauri-Butanol value	25.3	23 min-27 max
Evaporation rate, minutes	10	
Kinematic viscosity, cs at 32 F	2.775	
cs at 100 F	1.382	

*Available through Phillips Petroleum Company

Water

PROPERTIES	TYPICAL
Boiling Point, F	212
Specific gravity of liquid at 60°F	1.0
Density of liquid at 60°F, lb/ft^3	62.34
Kinematic viscosity, cs at 77°F	0.9935

CHAPTER III

EXPERIMENTAL RESULTS

FLOW REGIMES

OBJECTIVES OF THE FLOW REGIME STUDY

The ability to predict the flow regime in a liquid-liquid system at a specific set of parameters such as flow rate, fluid properties and pipe geometry would be of great importance when designing pipelines and facilities in which liquid-liquid flow will occur.

One possible method used in predicting these flow patterns are presented by means of flow regime maps. These maps basically consist of plotting two independent flow parameters, such as the flow rates or velocities of each phase, with each pattern or regime occupying a certain portion of the plot.

A large majority of the flow regime maps, like the maps presented in this section, are limited to the parameters and conditions under which they occurred. Therefore, the realistic usage of these flow pattern maps have limitations.

If a flow regime map was produced that used generalized parameters instead of specific parameters, this would be the ultimate solution to this problem.

For gas-liquid flow there exists a number of flow pattern maps that use generalized flow parameters. In 1954, Baker[16] proposed one

of the earliest flow regime maps. In the ensuing years, other flow regime maps were introduced using both dimensionless and dimensional coordinates. Taitel and Dukler (1976), proposed a generalized, dimensionless, gas-liquid flow regime map based on a mechanistic model for transition boundaries between the regimes. The study placed an emphasis on the mechanisms of these transitions. This method then took into account other parameters such as pipe inclination for flow regime prediction.

In liquid-liquid flow, most flow regime maps have used superficial phase velocities as the flow parameters. One important study on flow regimes conducted with horizontal liquid-liquid flow was completed by Russell et al.[10] The conclusion reached was that the horizontal flow of two immiscible liquids produced three possible flow patterns: bubble, stratified and mixed. Another liquid-liquid flow study, this time involving equal density liquids, was conducted by Charles et al.[11] They concluded that with the oil rate constant, and increasing the water rate, the flow regimes created ranged from water drops in oil to oil drops in water with a combination of each occurring in between.

From the work that has been previously presented, there is a large amount of research involving horizontal gas-liquid flow regime maps with a smaller amount of inclined gas-liquid flow maps. In liquid-liquid flow, most work has involved horizontal flow regime maps. There are very few studies involving inclined liquid-liquid flow regime prediction and mapping.

Since the work by Taitel et al.[17] involves a generalized gas-liquid flow regime correlation, it could be possible to modify this correlation to include all the criteria for liquid-liquid flow. This author's objective, therefore, is to generate flow regime maps for liquid-liquid flow for horizontal and downhill flow (negative angles) using data gathered experimentally. Also, the flow regime data can be compared with results obtained with Taitel et al.'s modified gas-liquid flow regime map to see if there is any agreement at all with the experimental data.

Some of the names and descriptions of the flow regimes encountered are based on established industry definitions. However, certain flow patterns are different from any other definition found. The flow regimes that are labeled by an asterisk (*) are not an industry standard but were developed to describe flow patterns observed in this study.

DEFINITIONS OF LIQUID-LIQUID FLOW REGIMES

The following descriptions of the flow regimes encountered during the experimentation will indicate the angle of inclination at which it occurred, describe the flow pattern and present a photograph of the actual flow regime. The flow patterns are listed in the order in which they were observed at a preset angle of inclination and as the flow rates of oil and water were increased. The flow patterns that occurred are:

A. Horizontal Flow (0 degrees)

(1) Stratified Smooth (SS)

The two liquids flow as distinct phases with the lighter phase on top and the denser phase flowing along the bottom of the pipe and there exists a waveless interface between the phases. An example of this regime is shown in a photograph in Figure 10.

(2) Stratified Wavy (SW)

The flow regime is essentially the same as stratified smooth, except that at the interface ripples and waves are present. Figure 11 shows a photograph of the flow regime.

(3) Stratified Bubble (SB)*

This flow regime is identified by a phase separation with water bubbles flowing in the upper phase of oil while oil bubbles tend to flow in the denser water phase with a distinct oil-water interface. This regime is displayed in a photograph in Figure 12.

(4) Massive Bubble (MB)*

This regime is characterized by no phase separation. Oil bubbles are flowing in a continuous phase of water. The oil bubbles tend to be dispersed evenly through the water phase. A photograph of this regime is Figure 13.

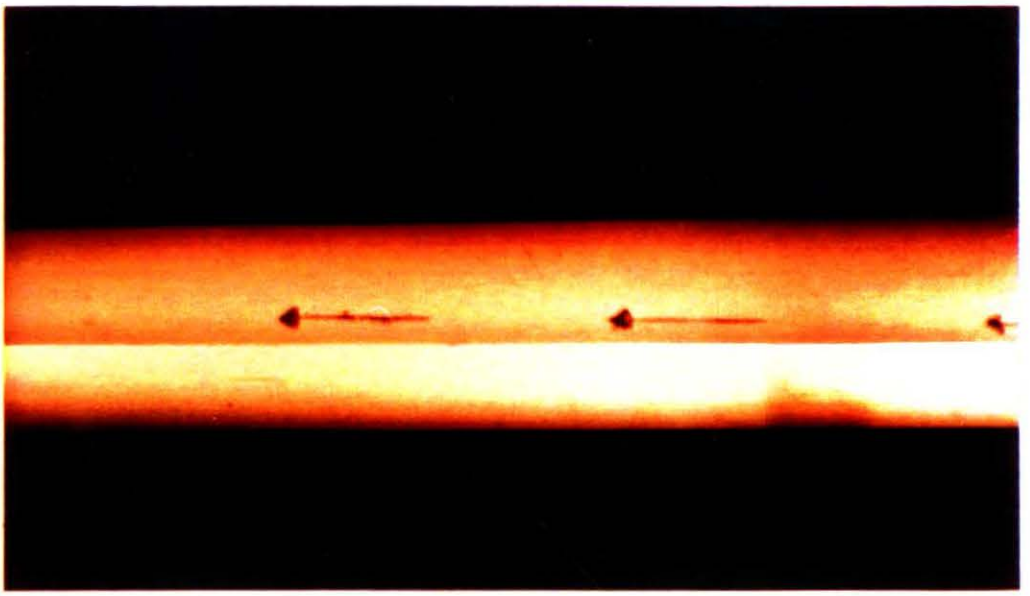

Figure 10

Stratified Smooth Flow Regime

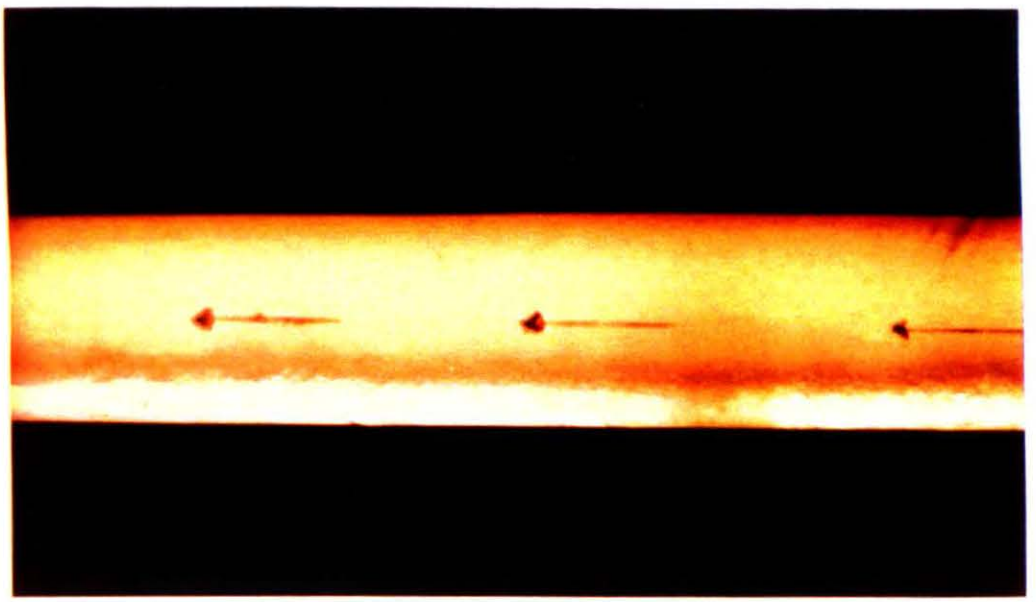

Figure 11

Stratified Wavy Flow Regime

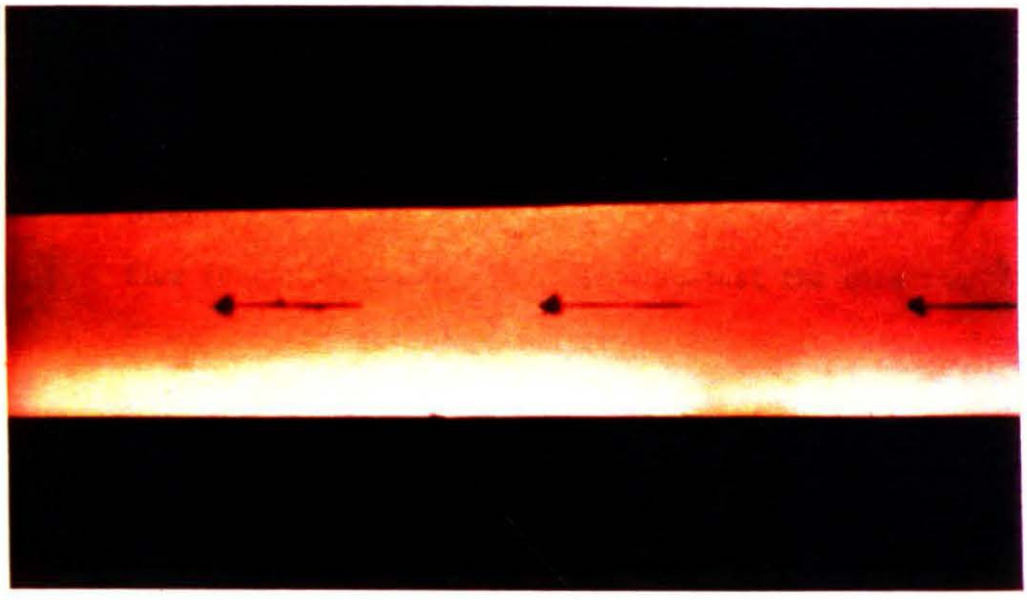

Figure 12

Stratified Bubble Flow Regime

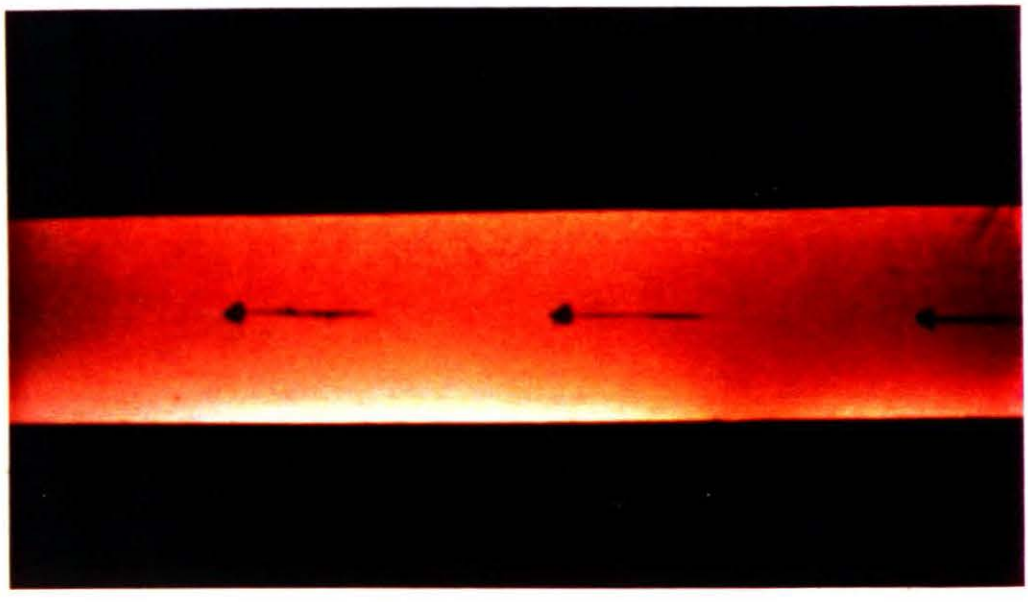

Figure 13

Massive Bubble Flow Regime

B. Down Hill Flow (-15 degrees)

(1) Stratified Wavy with Churning (SWC)*

This flow pattern is similar to the stratified wavy flow pattern because of a distinct phase separation and wavy interface, however, the oil stream and bubbles tend to flow in a churning motion upwards against the direction of flow, from the interface toward the top of the pipe. Some of these bubbles seem to drift upwards along the top of the pipe as the rest of the oil phase flows downward. The more dense phase of water seems to travel faster or "slip by" the oil phase. This regime is described by a photograph in Figure 14.

(2) Stratified Wavy (SW)

This regime is essentially the same as the pattern observed in horizontal flow. The waves on the interface are somewhat flatter than the waves in horizontal flow. Figure 15 is a photograph of this regime.

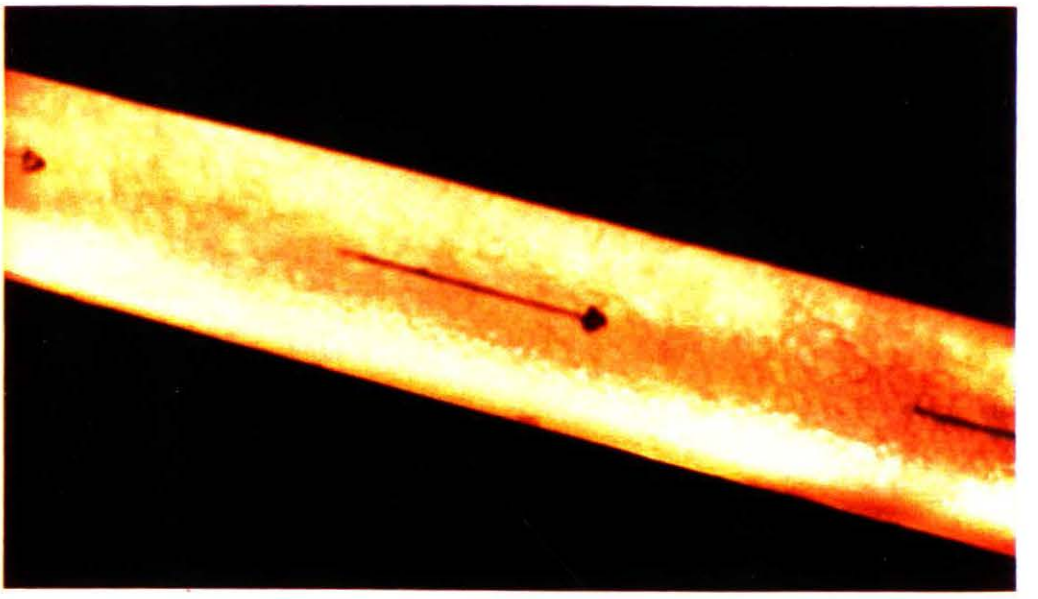

Figure 14

Stratified Wavy with Churning Flow Regime

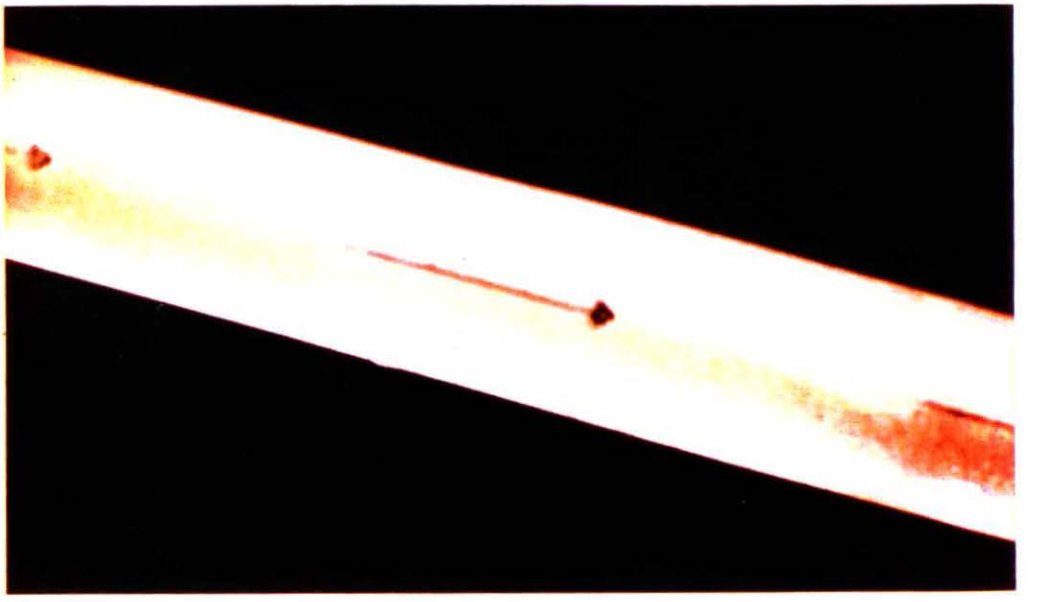

Figure 15

Stratified Wavy Flow Regime

(3) Stratified Bubble (SB)*

The description of this regime reflects the same characteristics as the flow pattern encountered in horizontal flow. A photograph of this regime appears in Figure 16.

(4) Massive Bubble (MB)*

This flow pattern is unchanged from horizontal to inclined flow. Figure 17 shows a photograph of the pattern at this particular angle.

C. Down Hill Flow (-30 degrees)

(1) Stratified Wavy with Churning (SWC)*

Similar to the flow pattern observed at -15 degrees, this regime is depicted in a photograph in Figure 18.

(2) Stratified Wavy (SW)

The regime is identical to the stratified wavy regimes observed at horizontal and at an angle of -15 degrees. A photograph detailing this pattern is shown in Figure 19.

(3) Stratified Bubble (SB)*

This regime resembles stratified bubble flow at horizontal and at -15 degrees. Figure 20 displays a photograph.

(4) Massive Bubble (MB)*

The description of this regime is identical to the regimes observed at horizontal and at -15 degrees. A photograph of this pattern is in Figure 21.

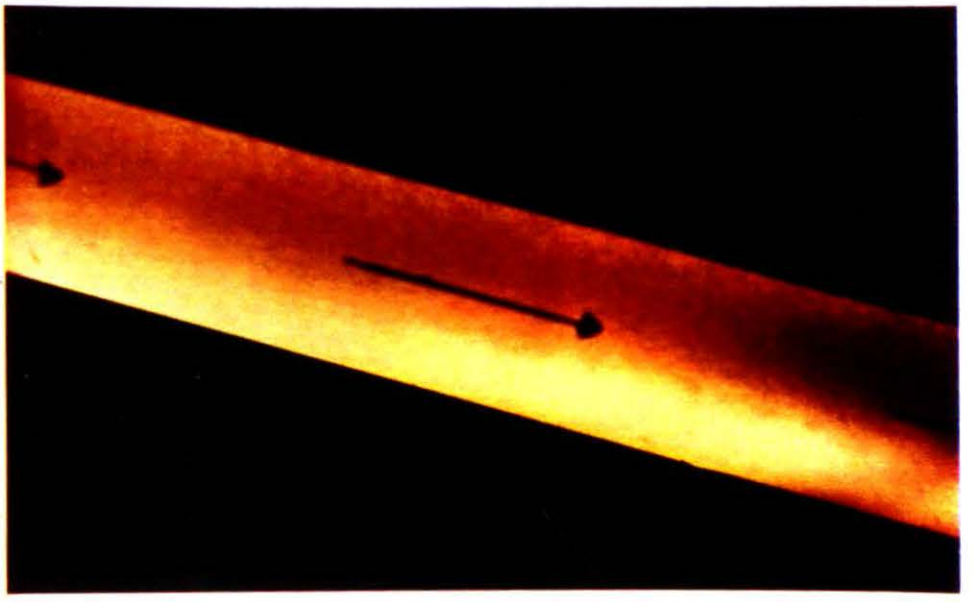

Figure 16

Stratified Bubble Flow Regime

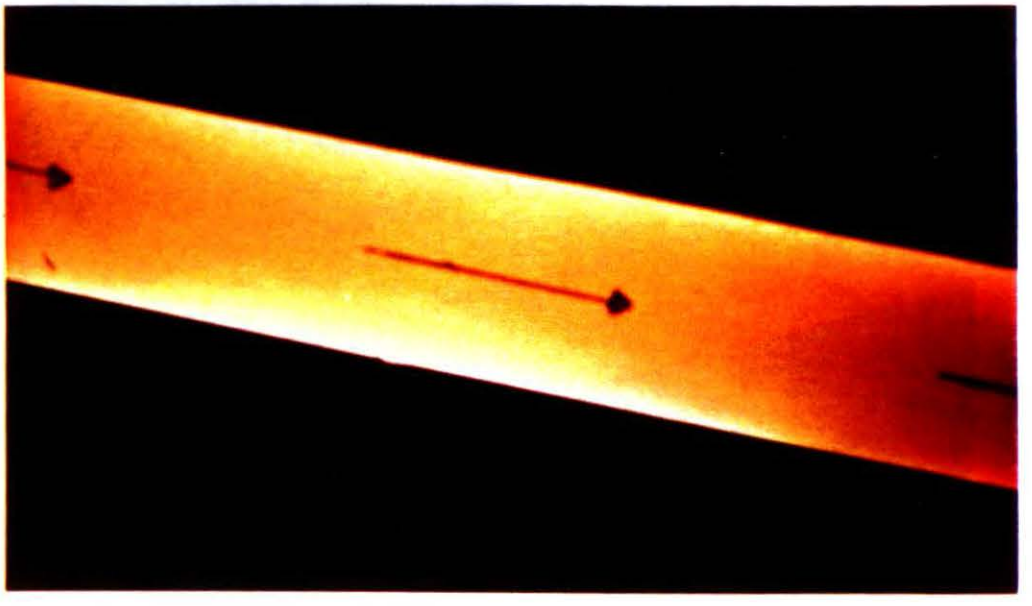

Figure 17

Massive Bubble Flow Regime

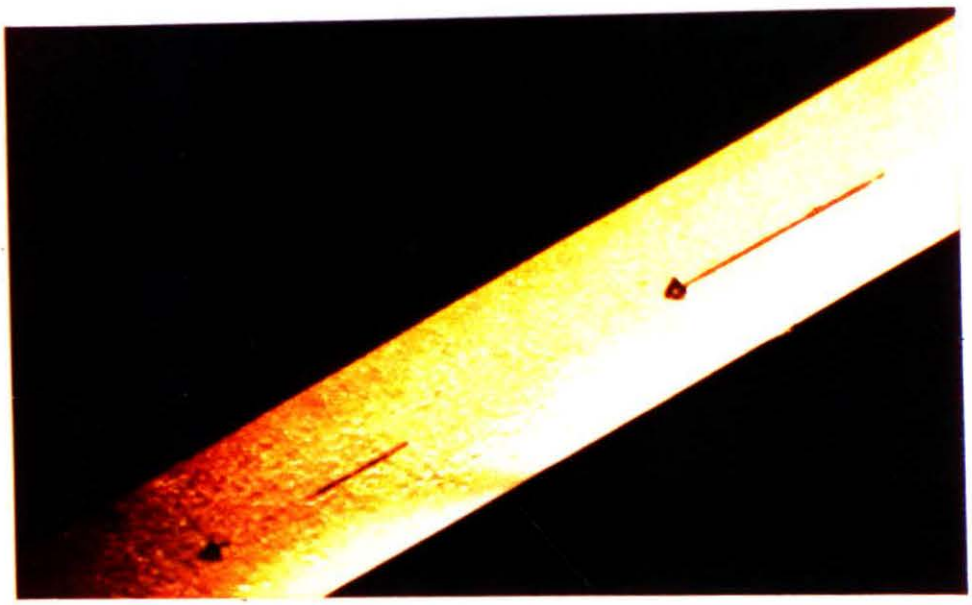

Figure 18

Stratified Wavy with Churning Flow Regime

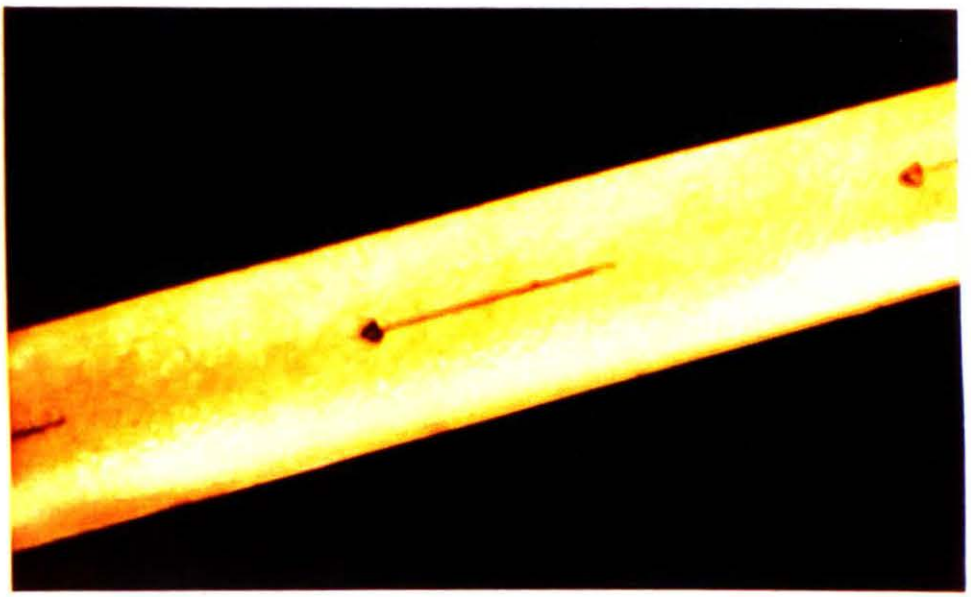

Figure 19

Stratified Wavy Flow Regime

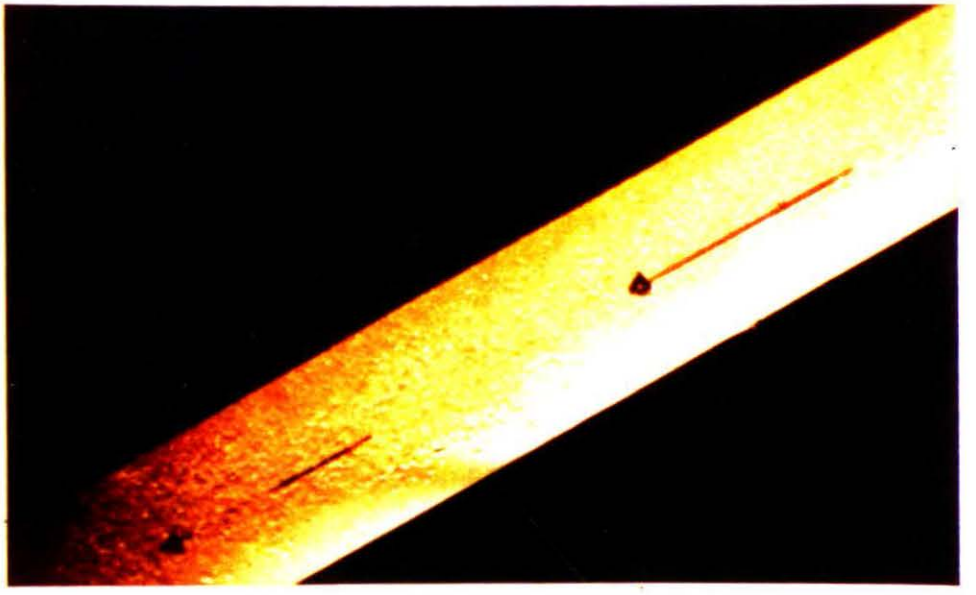

Figure 20

Stratified Bubble Flow Regime

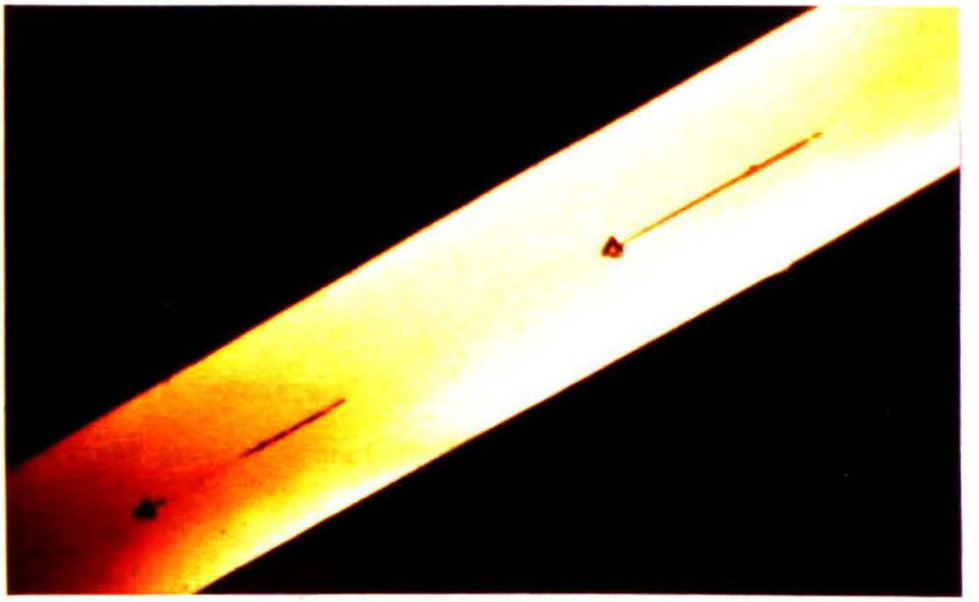

Figure 21

Massive Bubble Flow Regime

LIQUID-LIQUID FLOW REGIME MAPS GENERATED FROM EXPERIMENTAL DATA

Data for the generation of the three flow regime maps to be presented was gathered using the experimental flow loop discussed previously. The oil flow rate will be held constant while the water flow rate is varied from 50-700 B/D (0.15 - 2.1 ft/sec). The velocities just presented represent superficial velocities. Superficial velocity of a phase is the average velocity of the phase if it filled the entire pipe, or, as if it were a single phase. The velocities encountered in the future will be considered superficial unless otherwise noted. The range of the oil flow rates is the same as the flow rates for water. A majority of the possible flow rate combinations was observed, with each corresponding flow regime noted. After all the data for horizontal flow was collected the angle of inclination of the pipe was changed and the process was repeated for -15 degrees and -30 degrees, respectively. The data points were plotted on standard coordinates with oil velocity on the X-axis and water velocity on the Y-axis.

The following explanations of the three generated flow regime maps will indicate at which approximate velocities of oil and water that transition boundaries occur and show that at these boundaries the transition from one pattern to another was not well defined and the lines represent gradual transitions.

A. Liquid-Liquid Flow Regime Map for 0 degrees

For this angle of inclination, there exists three flow regime boundaries separating four flow patterns for the range of oil and water

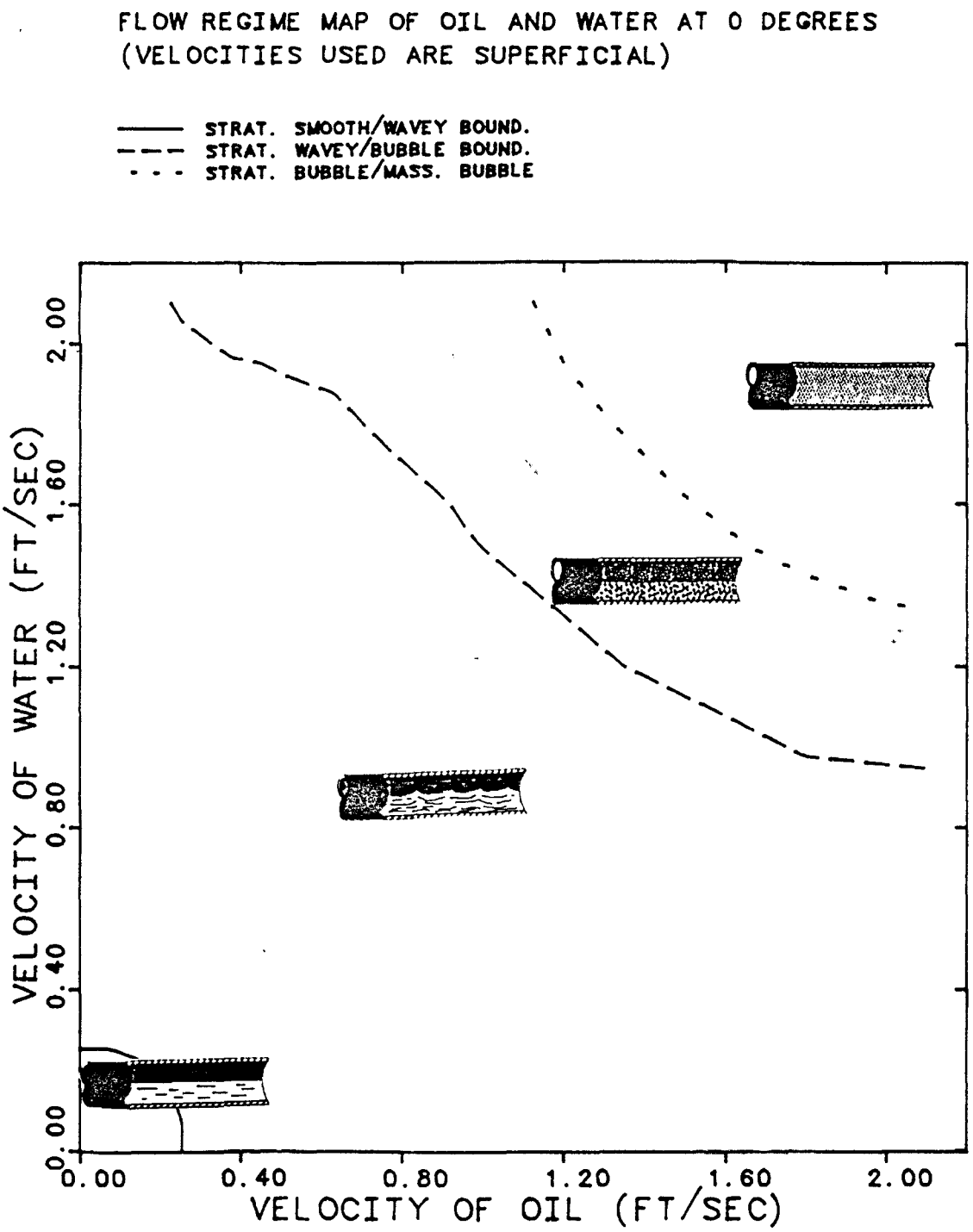

Figure 22

Flow Regime Map for Oil and Water

parameters investigated. The parameters used in these flow regime maps are the superficial velocities of each liquid phase. Superficial velocity of a phase is defined as the flow rate of that phase divided by the cross-sectional area of the pipe in which it is flowing. The regime boundaries are listed in the order in which they appeared during the experimentation. The flow regime boundaries are shown on a map in Figure 22. The boundaries are:

(1) Stratified Smooth/Stratified Wavy

The stratified smooth flow pattern was observed in the lower end of the oil and water velocities studied. This regime occurred at a minimum total superficial velocity of 0.18 ft/sec to a maximum of 0.45 ft/sec. This maximum total velocity designates the approximate region where the transition from stratified smooth to stratified wavy flow took place. This transition could be cause by turbulence from the higher flow velocities.

(2) Stratified Wavy/Stratified Bubble

As the total superficial velocity of the oil and water was increased from 0.45 ft/sec, the waves on the interface the two phases became smaller and bubbles from each phase started to gather in the other phase near the interface. At a minimum total velocity of 2.33 ft/sec, (V_{so} = 0.23 ft/sec and V_{sw} = 2.1 ft/sec), the transition between stratified wavy and stratified bubble flow was beginning

to occur. This transition was observed at various total velocities, from the minimum velocity just mentioned up to a maximum total velocity of 3.03 ft/s (V_{so} = 2.1 ft/sec and V_{sw} = 0.93 ft/sec). This transition boundary tends to occur when the turbulence of the two liquids cause bubbles from each liquid to flow in the continuous phase of the other liquid with the interface showing a slightly less wavy interface than in stratified wavy flow.

(3) Stratified Bubble/Massive Bubble

This flow boundary was observed to occur at a total superficial velocity of approximately 3.0 ft/sec. It ranges from V_{so} = 1.7 ft/sec and V_{sw} = 1.3 ft/sec to V_{so} = 1.3 ft/sec and V_{sw} = 1.7 ft/sec. The transition from stratified bubble to massive bubble seems to be caused by greater turbulence in both phases from the increase in the flow velocity of each liquid. Massive bubble flow was observed at the highest velocities achieved in the experimentation.

Figure 23 shows drawings prepared from photographs of the oil and water mixture used in the experimentation showing the variation in the flow pattern with the oil velocity remaining fixed at 1.5 ft/sec and the water velocity being varied, from 0.3 ft/sec to 1.8 ft/sec.

FLOW PATTERNS 0 DEGREES	SUPERFICIAL OIL VELOCITY, Vsw (FT/SEC)
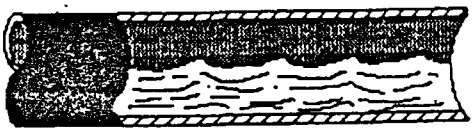 OIL AND WATER STRATIFIED WAVY →	0.75
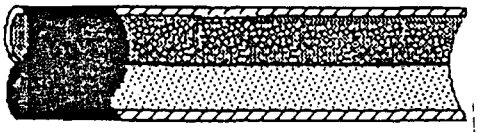 OIL BUBBLES IN WATER WATER BUBBLES IN OIL →	1.40
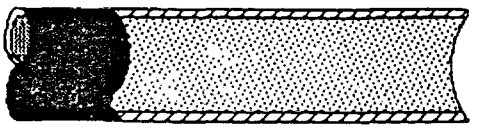 OIL BUBBLES IN WATER →	1.80

Figure 23

Flow Regime Variation with Water Velocity

for a Low Fixed Oil Velocity of 1.5 ft/sec

B. Liquid-Liquid Flow Regime Map for -15 Degrees

For this angle of inclination below horizontal, four flow regimes exist separated by three transition boundaries for the range of oil and water parameters studied. The following list of transition boundaries are in the order in which they were observed during the experiments. These flow regime boundaries are shown on a map in Figure 24. The boundaries are:

(1) Stratified Wavy with Churning/Stratified Wavy

The stratified wavy with churning flow pattern was observed over the entire range of water velocities with an oil velocity from 0.15 to 0.38 ft/sec. The maximum oil velocity of 0.38 ft/sec indicates the area where the churning motion in the oil phase is broken up by turbulence and the entire oil phase starts to flow in the general downward direction of flow.

(2) Stratified Wavy/Stratified Bubble

As the total superficial velocity of the oil and water approached 2.4 ft/sec (V_{so} = 0.3 ft/sec and V_{sw} = 2.1 ft/sec) the interface between the oil and water developed smaller waves, and bubbles from the oil phase tended to flow in the water phase and the same phenomena occurred in the oil phase with water bubbles. The maximum total velocity in which the transition from wavy to stratified bubble flow occurred was at 2.85 ft/sec (V_{so} = 2.1 ft/sec and V_{sw} = 0.75 ft/sec).

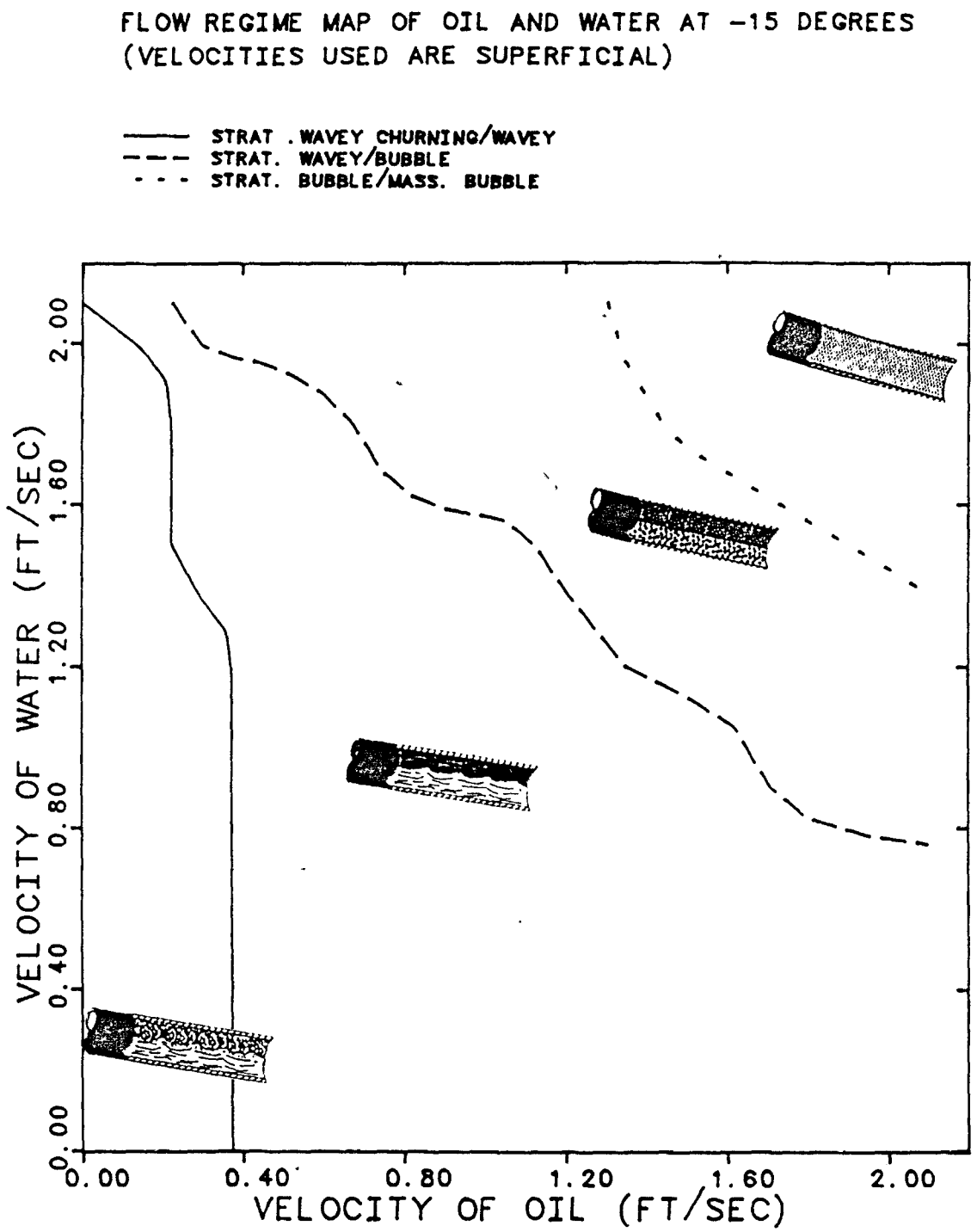

Figure 24

Flow Regime Map for Oil and Water

(3) Stratified Bubble/Massive Bubble

This last transition boundary occurs at the upper end of the range of flow velocities studied during the experimentation. Starting at a minimum total superficial velocity of 3.24 ft/sec (V_{so} = 1.5 ft/sec and V_{sw} = 1.74 ft/sec) to a maximum velocity of 3.45 ft/sec (V_{so} = 1.35 ft/sec and V_{sw} = 2.1 ft/sec or V_{so} = 2.1 ft/sec and V_{sw} = 1.35 ft/sec). The presence of increased turbulence in both phases at the increased flow velocities causes oil bubbles to form and flow in a continuous phase of water.

Figure 25 depicts drawings prepared from photographs of the oil and water mixture used in the experimentation showing the variation in the flow regimes with the water superficial velocity held constant at 1.5 ft/sec, and the oil superficial velocity being varied from 0.23 ft/sec to 2.1 ft/sec.

FLOW PATTERNS

-15 DEGREES

SUPERFICIAL OIL VELOCITY, Vsw (FT/SEC)

0.23

OIL AND WATER STRATIFIED WAVY WITH OIL CHURNING

0.38

OIL AND WATER STRATIFIED WAVY

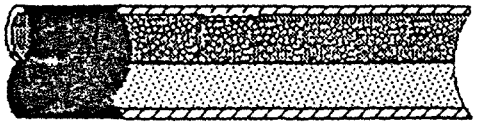

1.40

OIL BUBBLES IN WATER
WATER BUBBLES IN OIL

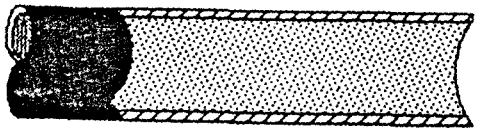

2.10

OIL BUBBLES IN WATER

Figure 25

Flow Regime Variation with Oil Velocity for a Low Fixed Water Velocity of 1.5 ft/sec

C. Liquid-Liquid Flow Regime Map for -30 Degrees

This angle of inclination is the largest inclination studied in the present experiments. Three boundaries of transition separate four flow regimes formed by the ranges of flow velocities investigated. The flow pattern boundaries are listed in the order in which they appeared during the experiments. The flow regime map which details these boundaries is shown in Figure 26. The transition boundaries are:

(1) Stratified Wavy with Churning/Stratified Wavy

This transition boundary is the same as the similar boundary for -15 degrees. The only difference between these boundaries is the minimum and maximum superficial velocities at which each occurs. This transition boundary begins to occur when the velocity of oil approaches 0.38 ft/sec with the water velocity ranging from 0.15 ft/sec to 1.2 ft/sec. Beyond this maximum velocity, the boundary is formed at oil velocities less than 0.38 ft/sec.

(2) Stratified Wavy/Stratified Bubble

This boundary of transition occurred in the same manner as the similar transition boundary at -15 degrees. However, the total superficial velocities needed to achieve this transition are slightly smaller than the velocities needed at -15 degrees. The minimum total velocity needed is approximately 2.33 ft/sec (V_{so} = 1.13 ft/sec and V_{sw} = 1.2 ft/sec). The maximum velocities range from 2.48

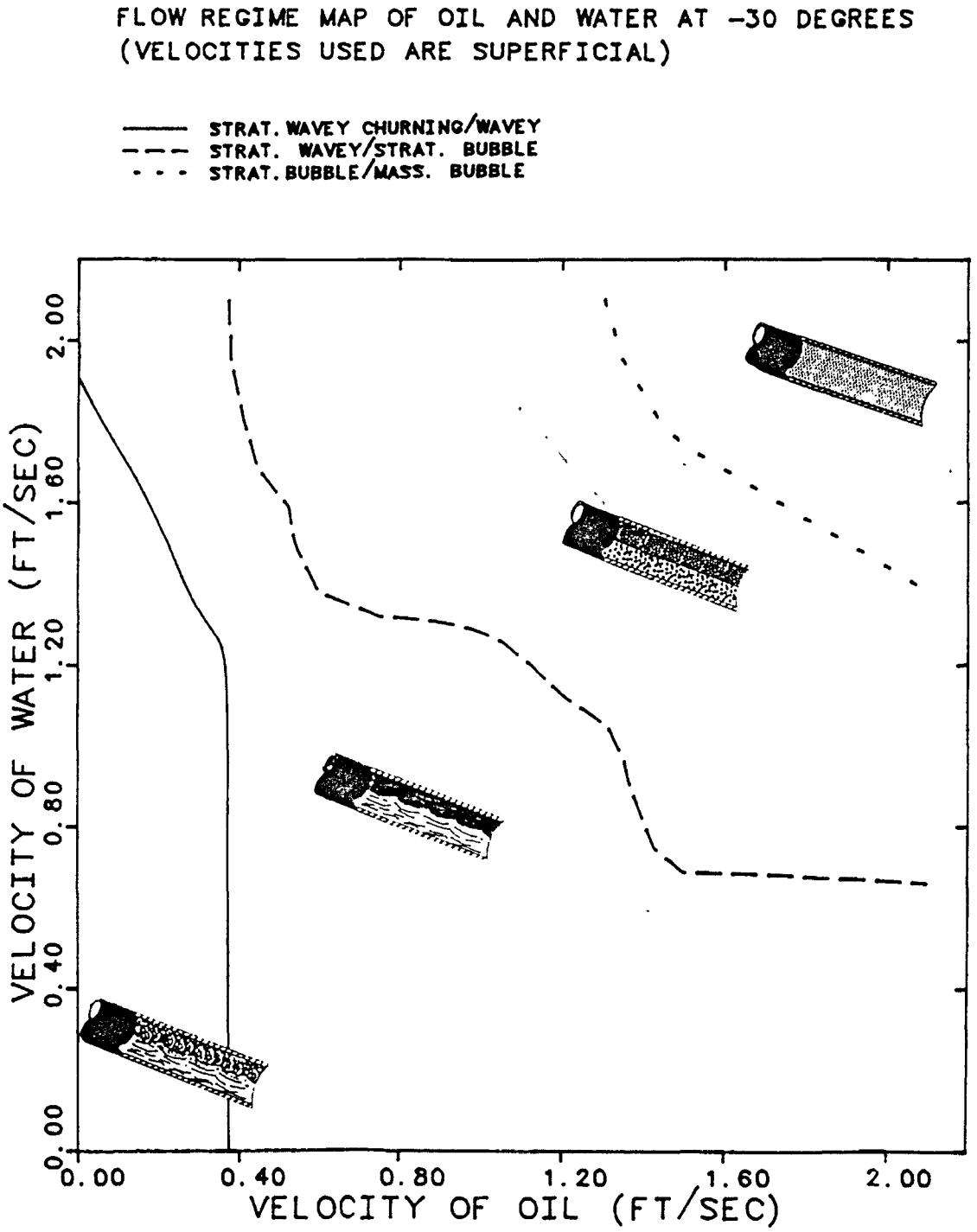

Figure 26

Flow Regime Map for Oil and Water

ft/sec (V_{so} = 0.38 ft/sec and V_{sw} = 2.1 ft/sec) to 2.78 ft/sec (V_{so} = 2.1 ft/sec and V_{sw} = 0.68 ft/sec).

(3) Stratified Bubble/Massive Bubble

This transition was observed occurring during the part of the experiments where the largest flow velocities were used. This transition boundary occurs in the same manner as the similar boundary at -15 degrees. The total superficial velocities where this transition occurred is also approximately the same. The minimum total velocity needed for transition to begin is 3.24 ft/sec with a maximum total velocity approaching 3.45 ft/sec.

Figure 27 shows drawings made from photographs of the oil and water mixture used in the experiments, which shows the variation in the flow regimes with the water superficial velocity remaining constant at 1.8 ft/sec and the oil superficial velocity being varied from 0.8 ft/sec to 1.8 ft/sec.

FLOW PATTERNS -30 DEGREES	SUPERFICIAL OIL VELOCITY, Vsw (FT/SEC)
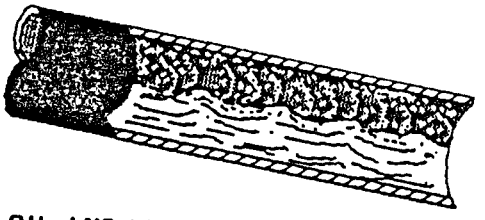 OIL AND WATER STRATIFIED WAVY WITH OIL CHURNING ⟶	0.80
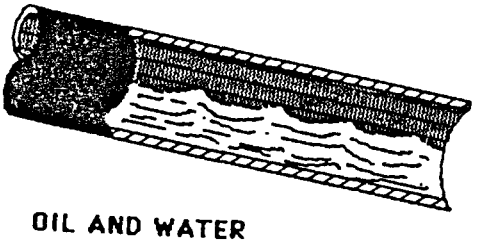 OIL AND WATER STRATIFIED WAVY ⟶	0.38
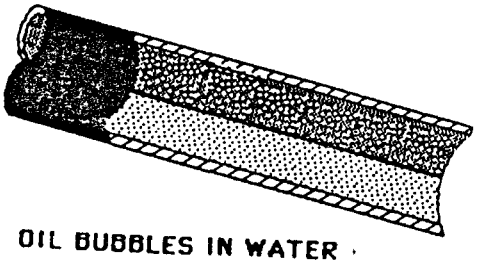 OIL BUBBLES IN WATER WATER BUBBLES IN OIL ⟶	1.15
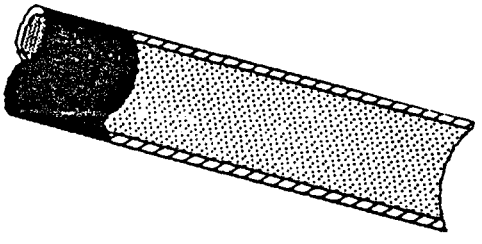 OIL BUBBLES IN WATER ⟶	1.80

Figure 27

Flow Regime Variation with Oil Velocity

For a Fixed Water Velocity of 1.8 ft/sec

From an analysis of the flow regime maps just presented, there is a noticeable difference between certain flow patterns in horizontal flow and flow patterns observed in inclined flow. For example, stratified smooth flow exists at certain superficial velocities of oil and water in horizontal flow, however, with inclined flow, stratified smooth flow did not occur over the entire range of oil and water superficial velocities. This same observation can be made concerning the stratified wavy with churning flow pattern and inclined flow. Over a range of oil and water parameters in inclined flow, stratified wavy with churning did occur, yet, this pattern did not exist under any flow conditions in horizontal flow. The rest of the flow patterns, stratified wavy, stratified bubble and massive bubble, however, do exist at all three inclinations at different superficial velocities of oil and water. This, then, suggests that inclination angle will affect the formation of certain flow regimes. It was noted that there was no appreciable difference in flow regime patterns from -15 to -30 degrees, and the transition boundaries at both angles differed only slightly in the superficial velocities of oil and water. The big difference in flow regime formation is the change of the angle of inclination from horizontal (0 degrees) to an inclination below horizontal (-15 and -30 degrees).

GENERALIZED GAS-LIQUID FLOW REGIME MAP

Taitel and Dukler[17] developed a theoretical model for gas-liquid flow which predicts the relationship between certain parameters at which flow regime transitions take place. These parameters are: gas and liquid mass flow rates, properties of the fluids, pipe diameter, and angle of inclination from horizontal. The mechanisms for these transitions are based upon physical concepts which are completely predictive and, as such, no actual flow regime data was used in their development.

The five flow regimes considered are stratified smooth, stratified wavy, intermittent (slug and plug), dispersed bubble and annular-annular dispersed liquid. When the theory is manipulated into dimensionless form the following five groups are created:

$$X = \left(\frac{|(dP/dx)_L^S|}{|(dP/dx)_G^S|} \right)^{\frac{1}{2}}$$

$$T = \left(\frac{|(dP/dx)_L^S|}{(\rho_L - \rho_G) g \cos \alpha} \right)^{\frac{1}{2}}$$

$$Y = \frac{(\rho_L - \rho_G) g \sin \alpha}{|(dP/dx)_G^S|}$$

$$F = \frac{\rho_G}{\sqrt{\rho_L - \rho_G}} \quad \frac{U_G^S}{\sqrt{D g \cos \alpha}}$$

$$K = F \left(\frac{D\, U_L^S}{\nu_L} \right)^{\frac{1}{2}} = F \left[(R_e)_L^S \right]^{\frac{1}{2}}$$

Since all velocities and pressure gradients used are calculated from superficial conditions, these five dimensionless groups can be determined with data gathered from the flow system during operation. The transitions of interest are controlled by the following dimensionless groups:

Stratified to annular	X, F, Y
Stratified to intermittent	X, F, Y
Intermittent to dispersed bubble	X, T, Y
Stratified smooth to stratified wavy	X, K, Y
Annular dispersed liquid to intermittent and to dispersed bubble	X, Y

The theoretical transition boundaries for Y = 0 (horizontal flow) are displayed on a generalized two-dimensional flow regime map in Figure 28. Maps that are similar except that they are for angles of inclinations other than horizontal can be constructed by using another value for Y calculated from certain equations that will be discussed later. Since this work is a parametric study of the effect of operating variables on regime boundaries with the coordinates being superficial velocities of gas and liquid, there is a relatively low sensitivity to pipe diameter in an air-water system at low pressure and small line sizes. However, some boundaries can shift due to larger line sizes,

gases at higher pressure and slight inclinations of the pipe. The generalized map in Figure 28 does, however, take all of these operational factors into account and can offer confidence in the prediction of flow regimes.

According to Taitel and Dukler, Baker[16] proposed the most durable of all two-phase gas-liquid flow maps, and there have been others (White and Huntington;[18] Govier and Omer;[19] Kosterin[20]). In 1970, Al-Sheikh et al.[21] defined a variety of dimensionless groups and using the Dukler two-phase flow data bank evaluated the suitability of various pairs for the mapping of flow regimes. They reached the conclusion that no two groups characterized all of the transitions and all the data. Later, Mandhane et al.[22] created a flow regime map based on coordinates of superficial gas and liquid velocity using a larger data base.

A lack of precision in describing visual observations causes part of the overall problem with two-phase flow regime maps. There are numerous possible classifications suggested, for example, smooth stratified, wavy, semiannular, bubble, annular, froth, dispersed bubble, dispersed liquid, plug and slug flow, to name a few. Hubbard and Dukler[23] who based their work on studies of the spectral distribution of wall pressure fluctuations, suggested that each observation represents the superposition of three basic patterns: segregated, intermittent and dispersed flow. This concept, however, does not distinguish between stratified and annular flow, or dispersed liquid or dispersed gas flow regimes and these differences can cause concern.

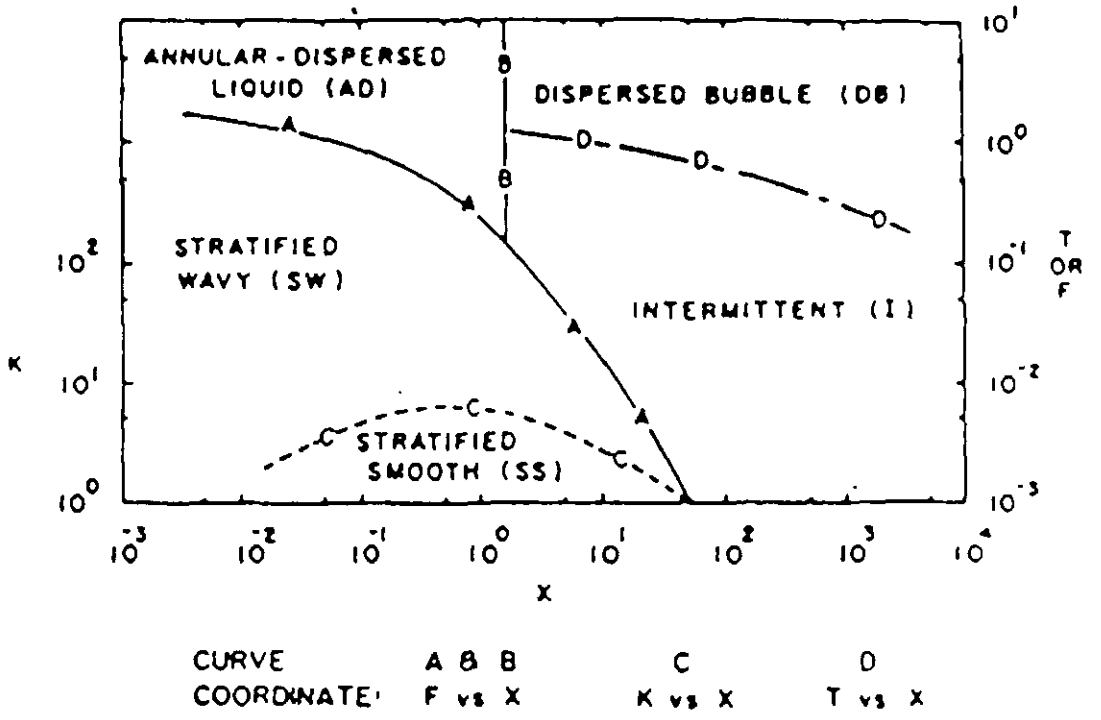

Figure 28

Generalized Flow Regime Map for Horizontal Two-Phase Flow

Taitel and Dukler (1976)

In the following, developed by Taitel and Dukler, a mechanistic model was developed for unambiguous analytical prediction of the transition between the flow regimes.

The following analysis considers the conditions for transition between five basic flow regimes: smooth stratified (SS), wavy stratified (SW), intermittent (I), (slug and plug), annular with dispersed liquid (AD) and dispersed bubble (DB). Slug, according to Hubbard and Dukler[23] and elongated bubble flow are all considered different conditions of intermittent flow. Annular dispersed liquid flow is the condition in which there can be a small or large amount of liquid dispersed annularly or semiannularly, throughout the pipe.

In their paper, Taitel and Dukler state that stratified flow starts the analysis of the transitions between flow regimes. Their approach is to envision a stratified liquid and then discover the mechanism that can cause the flow pattern to change and also what flow pattern it will change to.

Since the existence of stratified flow is important to this particular study, the first step is the development of a generalized relationship for stratified flow.

Equilibrium Stratified Flow

Taitel and Dukler first considered smooth, equilibrium stratified flow as detailed in Figure 29.

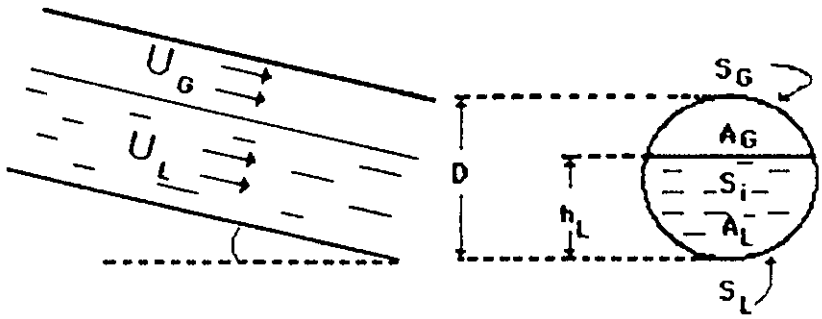

Figure 29

Equilibrium Stratified Flow

Taitel and Dukler (1976)

A momentum balance on each phase yields Equation (1) and Equation (2).

$$- A_L \left(\frac{dP}{dx} \right) - \tau_{WL} S_L + \tau_i S_i + \rho_L A_L g \sin \alpha = 0 \qquad (1)$$

$$- A_G \left(\frac{dP}{dx} \right) - \tau_{WG} S_G + \tau_i S_i + \rho_G A_L g \sin \alpha = 0 \qquad (2)$$

Making the pressure drop in the two phases equal and setting Equation (1) equal to Equation (2), the following will result

$$\tau_{WG} \frac{S_G}{A_G} - \tau_{WL} \frac{S_L}{A_L} + \tau_i S_i \left(\frac{1}{A_L} + \frac{1}{A_G} \right) + (\rho_L - \rho_G) g \sin \alpha = 0 \quad (3)$$

The shear stresses are evaluated as

$$\tau_{WL} = f_L \frac{\rho_L U_L^2}{2} \qquad \tau_{WG} = f_G \frac{\rho_G U_G^2}{2} \qquad \tau_i = f_i \frac{\rho_G (U_G - U_i)^2}{2} \quad (4)$$

the friction factors of liquid and gas are evaluated from

$$f_L = C_L \left(\frac{D_L U_L}{\nu_L} \right)^{-n} \qquad f_G = C_G \left(\frac{D_G U_G}{\nu_G} \right)^{-m} \quad (5)$$

where D_L and D_G are the hydraulic diameter evaluated with a method suggested by Agrawal et al. 1973[24]:

$$D_L = \frac{4A_L}{S_L} \qquad D_G = \frac{4A_G}{S_G + S_i} \quad (6)$$

This then implies that the liquid resistance to the wall is similar to that of open channel flow and that of gas to conduit flow. Gazley,[25] established that $f_i \cong f_G$ for smooth stratified flow. A very small error will result when assuming smooth stratified flow because most transitions occur in stratified flow with a wavy interface. At the flow rates where the transition occurs, $U_G >> U_i$. Therefore, the gas side interfacial shear stress is evaluated with the same equation that is used with the gas shear at the wall. In their work, Taitel and Dukler used the following coefficients: $C_L = C_G = 16$, $n = m = 1.0$ for laminar flow and $C_L = C_G = 0.046$, $n = m = 0.2$ is associated with turbulent flow.

It is helpful in this situation to transform the previous equations into a dimensionless form. The variables are D for length, D^2 for area, U_L^S and U_G^S are superficial velocities for liquid and gas, respectively. By using a tilde (~) to indicate dimensionless quantities, Equations (3), with (4) and (5) becomes:

$$X^2 \left((\tilde{U}_L \tilde{D}_L)^{-n} \tilde{U}_L^2 \frac{\tilde{S}_L}{\tilde{A}_L} \right) - \left((\tilde{U}_G \tilde{D}_G)^{-m} \tilde{U}_G^2 \left(\frac{\tilde{S}_G}{\tilde{A}_G} + \frac{\tilde{S}_i}{\tilde{A}_L} + \frac{\tilde{S}_i}{\tilde{A}_G} \right) \right) - 4Y = 0 \qquad (7)$$

where

$$X^2 = \frac{\frac{4C_L}{D} \left(\frac{U_L^S D}{\nu_L} \right)^{-n} \frac{\rho_L (U_L^S)^2}{2}}{\frac{4C_G}{D} \left(\frac{U_G^S D}{\nu_G} \right)^{-m} \frac{\rho_G (U_G^S)^2}{2}} = \frac{|(dP/dx)_L^S|}{|(dP/dx)_G^S|} \qquad (8)$$

$$Y = \frac{(\rho_L - \rho_G) g \sin \alpha}{\frac{4C_G}{D} \left(\frac{U_G^S D}{\nu_G} \right)^{-m} \frac{\rho_G (U_G^S)^2}{2}} = \frac{(\rho_L - \rho_G) g \sin \alpha}{|(dP/dx)_G^S|} \qquad (9)$$

The quantity $|(dP/dx)^S|$ indicates the pressure drop if just one phase is flowing in the pipe. Therefore, X is the parameter that was developed by Lockhart and Martinelli[26] and can be calculated directly with the flow rates, property of the fluids and pipe diameter known. Y indicates

the relative forces acting upon the liquid in the direction of flow due to the effect of gravity and pressure drop and is zero when the pipe is at horizontal. Y also can be calculated with the knowledge of certain parameters. All dimensionless variables with the ~ will depend on only $\tilde{h}_L$ which is equal to h_L/D. This can be seen from the following

$$\tilde{A}_L = 0.25\left[\pi - \cos^{-1}(2\tilde{h}_L-1) + (2\tilde{h}_L-1)\sqrt{1-(2\tilde{h}_L-1)^2}\right] \tag{10}$$

$$\tilde{A}_G = 0.25\left[\cos^{-1}(2\tilde{h}_L-1) - (2\tilde{h}_L-1)\sqrt{1-(2\tilde{h}_L-1)^2}\right] \tag{11}$$

$$\tilde{S}_L = \pi - \cos^{-1}(2\tilde{h}_L-1) \tag{12}$$

$$\tilde{S}_G = \cos^{-1}(2\tilde{h}_L-1) \tag{13}$$

$$\tilde{S}_i = \sqrt{1-(2\tilde{h}_L-1)^2} \tag{14}$$

$$\tilde{U}_L = \tilde{A}/\tilde{A}_L \tag{15}$$

$$\tilde{U}_G = \tilde{A}/\tilde{A}_G \tag{16}$$

Therefore, each X-Y pair will correspond to a certain h_L/D value for all parameters of pipe size, fluid properties, flow rate and pipe inclination where stratified flow occurs. Turbulent flow of both the gas and liquid is considered ($n = m = 0.2$, $C_G = C_L = 0.046$) when solving Equation (7) because it is of greatest practical application. These results are displayed in Figure 12 with solid lines. Turbulent-laminar flow of liquid and gas results with $n = 0.2$, $m = 1.0$, $C_L = 0.046$, $C_G = 16$ are also shown in Figure 30 with dashed lines. Both results are

similar to each other. The decision on whether turbulent or laminar flow will exist in each phase should be based upon the calculated Reynolds number which depends on actual velocity and hydraulic diameter of each phase, not on the superficial velocity and diameter.

Transition Between Stratified (S) and Intermittent (I) or Annular-Dispersed Liquid (AD) Regimes - Line A

Hubbard and Dukler[23] through extensive research involving gas-liquid flow, both experimental and analytical, have shown that, at first, stratified flow will occur at the inlet part of the pipe when the conditions for intermittent flow exist. Increasing the liquid rate will start a rise in the liquid level which causes the formation of a rapidly rising wave that will most likely block the flow. When the gas rate is lowered, this blockage forms a complete bridge, then slug or plug flow will result. However, at higher gas rates, there is not enough liquid flowing to form or even maintain a bridge, therefore, the liquid wave is swept up and around the pipe to form an annulus and could be trapped if there is a high enough gas rate. This process just described is the transition from stratified flow to either intermittent or annular flow. This transition will occur when conditions allow for rapid wave growth.

Under stratified flow conditions, with gas flowing on top, when the gas rate is accelerated, the pressure in the upper phase of gas will decrease due to the Bernoulli effect, which then allows the liquid wave to grow. However, gravity acting on the wave will tend to make it collapse. The Kelvin-Helmholtz theory (Milne-Thomson)[27] provides a

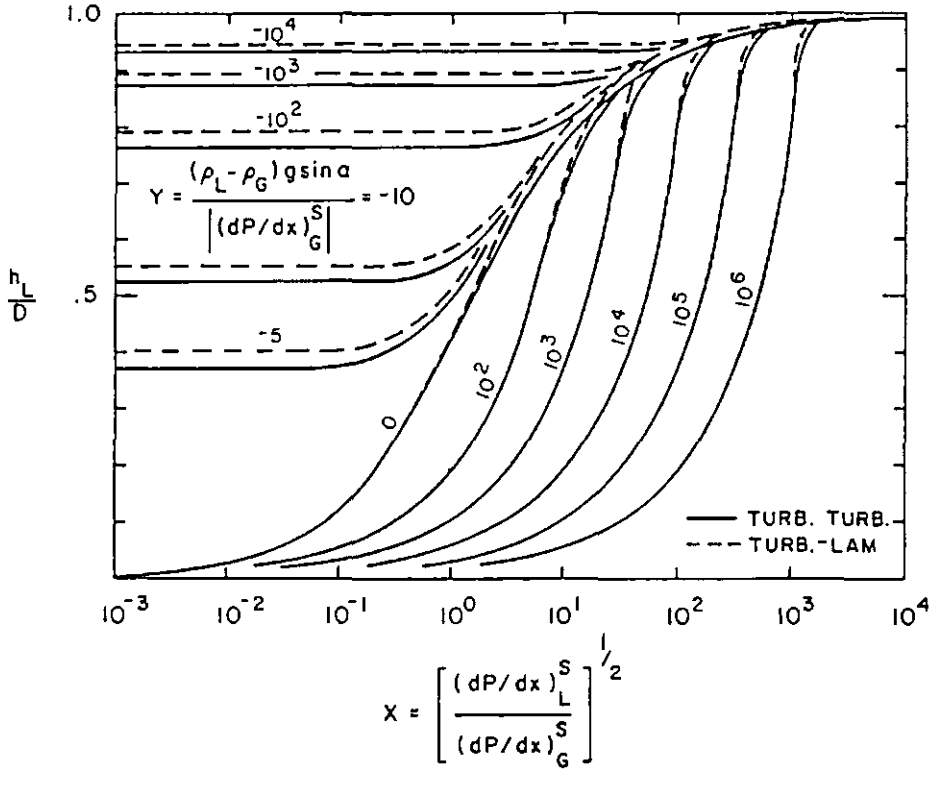

Figure 30

Equilibrium Liquid Level For Stratified Flow

(Turbulent Liquid, Turbulent or Laminar Gas).

Taitel and Dukler (1976)

criterion for wave stability of infinitesimal amplitude on a sheet of liquid flowing between two horizontal plates. The equation for propagation of these waves is described as:

$$m\rho(U-c)^2 \coth mh + m\ell' (U'-c)^2 \coth mh' = g(\rho-\rho') + Tm^2 \quad (17)$$

which for the gas-liquid case results in,

$$m\rho_L (U_L - c)^2 \coth mh_L + m\rho_G (U_G - c)^2 \coth mh_G = g(\rho_L - \rho_G) + Tm^2 \quad (18)$$

where $m = 2\pi/\lambda$ is the wave number, c the velocity of the wave, T the surface tension, ρ_L and ρ_G the density of the liquid and gas phases, h_L and h_G is the height of each gas and liquid phase, respectively.

Taitel and Dukler considered waves of a sufficient length that $mh_L << 1$, $mh_G << 1$, surface tension is negligible, $\rho_L >> \rho_G$, $U_G >> U_L$. Therefore, combining these assumptions into an analysis at the interface of the two phases in a stationary wave (with $c = 0$) the following equation used in their paper results.

$$U_G > \left(\frac{g (\rho_L - \rho_G) h_G}{\rho_G} \right)^{0.5} \quad (19)$$

Therefore, according to the theory, if this equation is satisfied, waves will grow. This analysis is used with finite waves between two parallel plates on a flat sheet of liquid. Next finite waves on stratified liquid in an inclined pipe were analyzed using a finite solitary wave on a flat horizontal surface, as depicted in Figure 31.

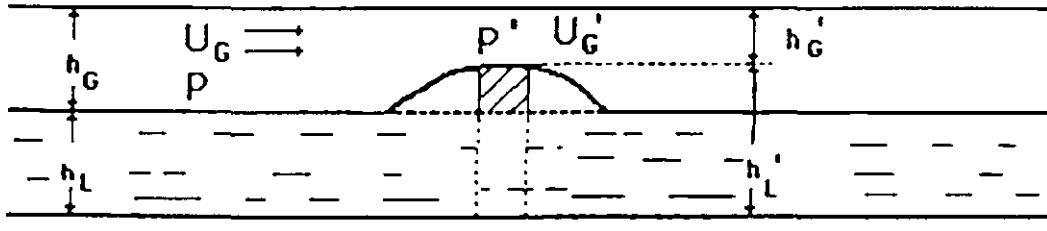

Figure 31

Instability for a Solitary Wave

Taitel and Dukler (1976)

Taitel et al. examined the specific case of a motionless finite wave, where the condition for wave growth is:

$$P - P' > (h_G - h_G')(\rho_L - \rho_G)g \qquad (20)$$

where $$P - P' = \tfrac{1}{2}\rho_G(U_G'^2 - U_G^2) \qquad (21)$$

which is a variation of Bernoulli's equation for pressure change in a gas with negligible hydrostatic effects.

If $U_G^1 = U_G h_G / h'_G$

then the equation becomes

$$\tfrac{1}{2}\rho_G\left[\left(\frac{U_G h_G}{h'_G}\right)^2 - U_G^2\right] > (h_G - h_G^1)(\rho_L - \rho_G)g$$

$$U_G^2 > \frac{2}{\rho_G}\left[\frac{(h_G - h_G^1)}{\left(\frac{h_G^2}{h'^2_G} - 1\right)}\right](\rho_L - \rho_G)g$$

Simplifying the equation

$$U_G^2 > \frac{2}{\rho_G}\left[\frac{1}{\frac{h_G}{h_{G'}}\left(\frac{h_G}{h_G^1} + 1\right)}\right](\rho_L - \rho_G)g$$

$$U_G > C_1\left[\frac{g(\rho_L - \rho_G)h_G}{\rho_G}\right]^{0.5} \tag{22}$$

where

$$C_1 = \left[\frac{2}{\frac{h_G}{h_{G'}}\left(\frac{h_G}{h_G^1} + 1\right)}\right]^{0.5} \tag{23}$$

If Equation (22) is satisfied, the flow pattern is not stratified.

Taitel et al. states that for an infinitesimal disturbance, $h_G/h_G' \rightarrow 1.0$ and $C_1 \rightarrow 1.0$ which will reduce Equation (22) to Equation (19). This analysis can be extended to pipe geometry and will use the stability equation with a variation in the dimensionless term to yield

$$\tfrac{1}{2} \rho_G (U_G'^2 - U_G^2) > (h_G - h_G')(\rho_L - \rho_G) g$$

when the pipe is inclined from horizontal

$$\tfrac{1}{2} \rho_G (U_G'^2 - U_G^2) > (h_L' - h_L)(\rho_L - \rho_G)_g \cos \alpha$$

If $U_G' = A/A_G'$, then

$$\tfrac{1}{2} \rho_G \left(\frac{A^2}{A_G'^2} - U_G^2 \right) > (h_L' - h_L)(\rho_L - \rho_G) g \cos \alpha$$

Simplification shows

$$U_G > \left(\frac{2(\rho_L - \rho_G) g \cos \alpha (h_L' - h_L)}{\rho_G} \frac{A_G'^2}{A_G^2 - A_G'^2} \right)^{0.5} \tag{24}$$

A_G' can be expanded in a Taylor series around A_G when involving small, finite disturbances.

The previous equation will then simplify to:

$$U_G > C_2 \left(\frac{(\rho_L - \rho_G) g \cos \alpha A_G}{\rho_G \, dA_L/dh_L} \right)^{0.5} \tag{25}$$

where $C_2 \cong A_G' / A_G$

With an infinitesimal disturbance where $A_{G'} \rightarrow A_G$ then $C_2 \cong 1.0$. When the equilibrium liquid level approaches the pipe top, and A_G is small, waves which then appear will make $C_2 \cong 0$. However, if there is a low liquid level, the appearance of a small, finite wave will have little or no effect on the size of the air gap and thus $C_2 \cong 1.0$. Taitel and Dukler, using these facts, concluded that C_2 can be defined as:

$$C_2 = 1 - \frac{h_L}{D} \tag{26}$$

In summary, Taitel et al. used Equation (25) and Equation (26) to define the conditions for flow regime transition from stratified (S) to intermittent (I) and to annular dispersed liquid (AD) flow in pipes.

The final version of the dimensionless form was arrived at by:

$$U_G > C_2 \left[\frac{(\rho_L - \rho_G)\, g \cos \alpha\, A_G}{\rho_G \quad dA_L/dh_L} \right]^{0.5}$$

with

$$\tilde{U}_G = \frac{U_G}{U_{GS}} \quad , \quad \tilde{A}_G = \frac{A_G}{D^2} \quad , \quad \tilde{A}_L = \frac{A_L}{D^2} \quad , \quad \tilde{h}_L = \frac{h_L}{D}$$

therefore,

$$\frac{V_G^2}{C_2^2}\left[\left(\frac{\rho_G}{\rho_L - \rho_G}\right)\frac{dA_L/dh_L}{g\cos\alpha\, A_G}\right] > 1$$

$$\frac{V_G^2 \quad V_G^{s^2}}{C_2^2}\left[\left(\frac{\rho_G}{\rho_L - \rho_G}\right)\left[\frac{d\,(\tilde{A_L} \times D^2)}{d\,(\tilde{h}_L \times D)}\right]\right] \geq 1$$

Rearranging,

$$F^2\left[\frac{1}{C_2^2}\quad\frac{\tilde{U}_G^2 \quad d\tilde{A}_L/\,\tilde{dh}_L}{\tilde{A}_G}\right] \geq 1 \tag{27}$$

where F is a Froude number modified by the density ratio:

$$F = \frac{\rho_G}{\sqrt{\rho_L - \rho_G}} \quad \frac{U_G^s}{\sqrt{D\, g \cos\alpha}} \tag{28}$$

Transition Between Intermittent (I) and Annular Dispersed Liquid (AD) Regimes - Line B

As shown previously, Equation (27) presents the specific criteria upon which finite waves that are generated on stratified liquid can be expected to grow. Two different events could take place when such criteria are satisfied and wave growth occurs. When the supply of liquid is large enough, a stable slug can be formed. However, if the liquid level is inadequate, the wave on the liquid will, instead, be swept up around the interior of the pipe, and annular or annular mist flow occurs. From this, Taitel and Dukler suggested that the liquid level in the stratified equilibrium flow will dictate whether intermittent or annular flow will eventually develop within the pipe. They also conclude that if the equilibrium level is above the center line of the pipe, intermittent flow will develop, and if $h_L/D < 0.5$, annular or annular dispersed liquid flow will occur. The authors defend their choice of $h_L/D = 0.5$ as follows: when a wave of finite height or amplitude begins to grow because of suction occurring over the crest of the wave, liquid must then be supplied to the wave from the liquid film next to it, and therefore, a trough or depression forms there. If the wave is perceived as a sinusoid, then when the level is above the center line of the pipe, the peak will reach the top of the pipe before its trough reaches the bottom, and from there, gas passage blockage occurs and slugging is the end result. However, when the liquid level is below

the center line, the reverse is true and slugging would then be impossible.

Since this flow regime transition takes place at a constant value of $h_L/D = 0.5$, Figure 30, shows that a single Martinelli value, X, characterizes the change in the flow regime for any value of the inclination parameter Y. When the flow occurs in a horizontal tube, according to Taitel et al., X = 1.6, and is plotted in Figure 10 as line B. The location of the boundary now will define two distinct flow regimes as movement across line A occurs; from stratified to intermittent (S/I) flow for X values greater than 1.6 and stratified to annular dispersed liquid (S/AD) flow for X values less than 1.6.

Finally, for the transition between stratified and intermittent flow, the previous analysis suggests a sharp, distinct change, unlike the transition between intermittent and annular dispersed liquid (I/AD) which is gradual since it is impossible to distinguish between slug flow, and annular flow with large, rolling waves.

Transition between Stratified Smooth (SS) and Stratified Wavy (SW) Regimes - Line C

Taitel and Dukler, in their paper state that the region known as stratified is composed of two subregions: stratified smooth (SS) and stratified wavy (SW). The waves are generated by gas flow where the velocity of the gas is sufficiently high to form waves but not high enough to cause rapid wave growth which will lead to a transition to intermittent or annular flow regimes.

Wave generation is considered an extremely complicated phenomena and is best understood as the result of viscous dissipation in the wave being overcome by pressure and shear work on the wave.

Jeffreys[28] stated the following criteria for the generation of waves:

$$(U_G - c)^2 c > \frac{4V_L\, g(\rho_L - \rho_G)}{s\rho_G} \tag{29}$$

where s is the sheltering coefficient which, according to Jeffreys should approximate 0.03. However, Benjamin[29] stated that s should have a value ranging from 0.01 to 0.03 based on extensive experimentation and theory. Taitel et al. assumed that $S \cong 0.01$.

The variable c indicates the velocity of the wave propagation. $U_G >> c$ in conditions where a transition will probably take place. Theories addressing wave propagation have advanced the concept that the

ratio of the wave velocity to the mean of the film velocity (C/U_L) will decrease as the Reynolds number of the liquid associated with the particular flow conditions increases. Taitel et al. cited data from Fulford,[30] Brock[31] and Chu[32] to confirm this concept. At turbulent flow conditions, where a high Reynolds number is certain, the ratio just discussed approaches 1.0 to 1.5. Because knowing the precise transition boundary is not that important, for simplicity, the relation $U_L = c$ is now introduced.

When these approximations are used in conjunction with Equation (29), the criterion for the transition from stratified smooth to stratified wavy becomes:

$$U_G \geq \left(\frac{4V_L(\rho_L - \rho_G)\ g \cos \alpha}{s\ \rho_G\ U_L} \right)^{0.5} \tag{30}$$

This equation converted into the dimensionless form by Taitel et al. is:

$$K \geq \frac{2}{\sqrt{\tilde{U}_L}\ \tilde{U}_G\ \sqrt{S}} \tag{31}$$

where K approximates the product of the Froude number (modified) and the square root of the Reynolds number determined by superficial parameters:

$$K^2 = F^2\ Re_L^s = \left(\frac{\rho_G\ (U_G^s)^2}{(\rho_L - \rho_G)\ D\ g \cos \alpha} \right) \left(\frac{D\ U_L^s}{\nu_L} \right) \tag{32}$$

Transition Between Intermittent (I) and Dispersed Bubble (DB) Regimes - Line D

Taitel et al. states that values of X (Martinelli parameter) which lie in the intermittent flow regime area, will most likely "bridge" the pipe thus forming a slug and an associated gas bubble. If the liquid flow rate is high and the gas rate is somewhat lower, the equilibrium level is above the pipe center line and approaches the pipe top. Since the liquid phase has a high flow rate the slower gas phase tends to mix somewhat with the liquid. This indicates that the transition from intermittent flow to dispersed bubble flow can occur when the fluctuations in turbulent flow are large enough to overcome the force of gas buoyancy which tries to keep the gas above the liquid at the top of the pipe.

The buoyancy force per unit length of the gas region is defined as:

$$F_B = g \cos \alpha \, (\rho_L - \rho_G) \, A_G \tag{33}$$

In using a method discussed by Levich[33] the force associated with turbulence is designated by:

$$F_T = \tfrac{1}{2} \rho_L \overline{v'^2} S_i \tag{34}$$

where v' equals the radial velocity fluctuation whose root-mean-square approximates the friction velocity. Therefore:

$$\bar{v}'^{2\,\frac{1}{2}} = U_* = U_L \left(\frac{f_L}{2} \right)^{\frac{1}{2}} \tag{35}$$

Dispersion of gas, according to Taitel et al. will take place when $F_T \geq F_B$ or if:

$$U_L \geq \left(\frac{4A_G}{S_i} \quad \frac{g \cos \alpha}{f_L} \quad (1 - \frac{\rho_G}{\rho_L}) \right)^{0.5} \tag{36}$$

Conversion to dimensionless form, Equation (36) becomes

$$T^2 \geq \left(\frac{8 \tilde{A}_G}{\tilde{S}_i \tilde{U}_L^2 (\tilde{U}_L \tilde{D}_L)^{-n}} \right) \tag{37}$$

where

$$T = \left(\frac{\frac{4 C_L}{D} \left(\frac{U_L^S D}{\nu_L} \right)^{-n} \frac{\rho_L U_L^{S^2}}{2}}{(\rho_L - \rho_G) \; g \cos \alpha} \right)^{0.5}$$

$$= \left(\frac{|(dP/dx)_L^S|}{(\rho_L - \rho_G) \; g \cos \alpha} \right)^{0.5} \tag{38}$$

T can approximate the ratio of turbulent to gravity forces which act directly in the gas.

SUMMARY OF RESULTS

The Generalized Flow Regime Map

Taitel and Dukler summarize the results from their work in the following manner:

Line A represents the boundary where a transition from stratified (S) to intermittent (I) or annular-dispersed liquid (AD) occurs, with the parameters for the boundary being F vs X. The generalized map in Figure 10, shows an area where F - X values satisfy Equation (27). This result depends upon the premise that waves of a finite size will grow and either block or sweep around the pipe when the force due to the Bernoulli effect above the wave overcomes the force of gravity acting on the wave. Therefore, all X values to the left of Line A indicate conditions where stratified flow will occur.

Line B indicates the transition between annular-dispersed liquid (AD) and intermittent (I) or dispersed bubble (DB) flow. This boundary occurs at a constant value of X. This occurs if the liquid supply in a growing wave is large enough to form a slug which happens only when $h_L/D \geq 0.5$. Any time $h_L/D < 0.5$, the liquid will be swept around the pipe into an annular flow pattern.

Representing the transition between stratified smooth (SS) and stratified wavy (SW) flow, line C is a function of the K - X parameters and indicates which K - X values that satisfy Equation (31). This boundary is based upon Jeffreys' model and its assumption that the condition for the transfer of energy to the liquid in order to generate waves with the wave velocity is approximated by the mean velocity of the

liquid film and the sheltering coefficient estimated by Benjamin. If the K value is lower than line C in the K - X plane, there is insufficient gas flow to create wave formation.

Line D locates the Intermittent to dispersed bubble flow transition boundary. This boundary indicates the conditions where turbulent forces within the liquid approximate the buoyant forces which cause the gas to rise to the pipe top. This line indicates which T - X pairs satisfy Equation (14). Any T value below the line will represent conditions where the turbulence is not strong enough to cause gas mixing, and elongated gas bubbles which indicate intermittent flow will form.

COMPARISON OF EXPERIMENTAL DATA TO MODIFIED GAS-LIQUID FLOW REGIME MAP

Since Taitel and Dukler have generated a gas-liquid flow regime map based on generalized dimensionless variables, a modification of the variables to fit given liquid-liquid flow parameters is feasible. The flow pattern definitions will remain the same from gas-liquid flow when referring to the regime definitions in liquid-liquid flow. Stratified smooth and stratified wavy flow will be segregated oil and water with either a smooth or wavy interface. Intermittent flow will be slug or plug flow with oil being the slug in water and dispersed bubble flow will consist of oil bubbles in water. Finally, annular-dispersed liquid will indicate oil flowing through water which is dispersed as an annulus around the inside of the pipe.

In Appendix I, an outlined procedure for the modification of the generalized dimensionless variables used by Taitel et al. is presented. Also, a computer program, FMAP, which generates the appropriate variables for the present flow system and an example output is presented.

Within Appendix II, two computer programs are listed that calculate the Martinelli parameter X for horizontal and inclined flow, respectively. Included with the two programs are example output listings. The Martinelli parameter along with data from the program FMAP will be used with another computer program, DUKMAP, which is presented in Appendix III to generate the dimensionless variables that will be used to create a flow regime map for specific liquid-liquid flow parameters. From this output generated, plots are developed which show how the experimental data compares with the theoretical flow regime transition boundaries.

Plots were generated for oil-water flow at horizontal (0 degrees) and downhill flow (-15 degrees and -30 degrees). The angle of inclination and the oil flow rate will affect the Martinelli parameter, therefore, the oil flow rates used in the plots will include 100, 300, 500 and 700 B/D, respectively.

For horizontal flow, the generalized flow regime map was plotted to include all the transition boundaries, Figure 32, did resemble the map generated by Taitel et al., Figure 28. Therefore, it seems possible the some similarity between the gas-liquid flow regime map and the liquid-liquid flow regime map just generated does exist.

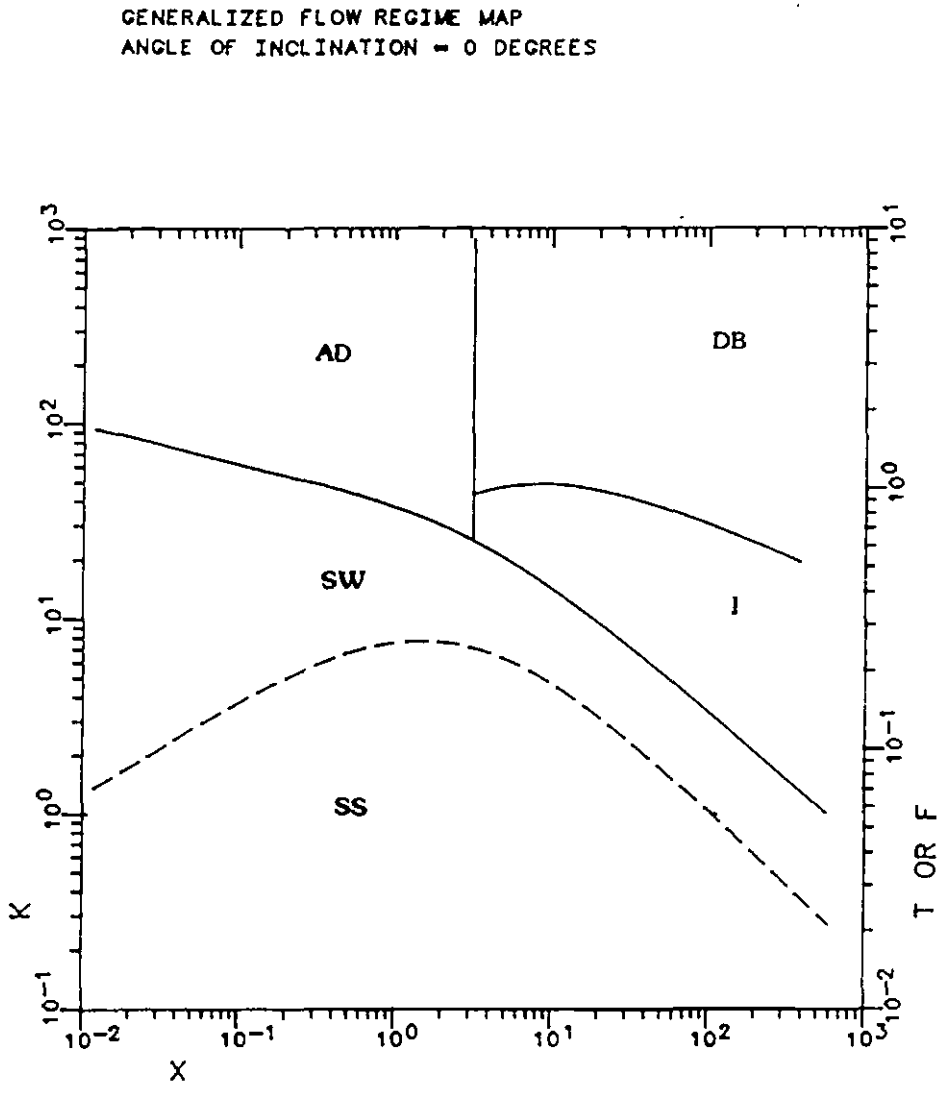

Figure 32

Generalized Flow Regime Map

However, when comparing the flow data generated by the program FMAP with the flow regime map developed by program DUKMAP for line A, Figure 33, there seems to be no agreement since stratified wavy flow and massive bubble flow fall into the same area of the flow regime map, annular-dispersed liquid. When Line B was plotted and compared with the appropriate data, Figure 34, again, no logical correlation was noticed. Yet, when the Line C was generated and the experimental data was plotted there was agreement. Figure 35 shows how the stratified smooth point that was observed in the experimentation did fall into the area of the plot designated for stratified smooth flow. The next closest point which fell right on Line C could possibly be considered stratified smooth since the ripples in that flow regime were extremely small and very hard to detect. All other points tended to fall into the stratified wavy area of the map, which seems logical since there were only two regimes possible in the plot, stratified smooth and stratified wavy. Figure 36 again showed no possible agreement with the Line D plot. All the points fell within the intermittent flow area which would indicate some type of slug or plug flow which is not indicated by any of the flow regime observations in the data points. The only transition boundary that came even close to being sensible was the Line C correlation. Even that correlation was not sufficient to prove that the flow map generated by modification of the gas-liquid dimensionless variables is completely feasible since all other possible comparisons were not reasonable.

COMPARISON OF FLOW DATA TO GENERALIZED FLOW
REGIME MAP (DUKLER & TAITEL)
TRANSITION BETWEEN STRATIFIED (S) AND INTERMITTENT
(I) OR ANNULAR-DISPERSED LIQUID (AD) REGIMES
ANGLE OF INCLINATION = 0 DEGREES

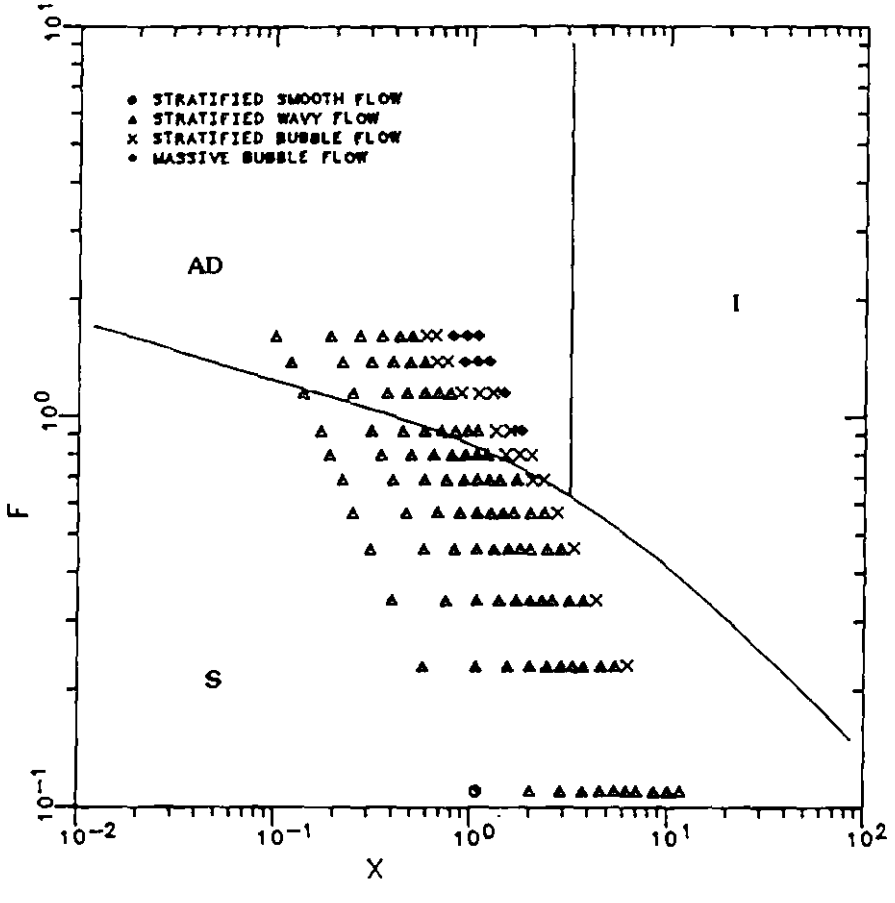

Figure 33

Comparison of Flow Data to Generalized Flow Regime Map (Taitel & Dukler)

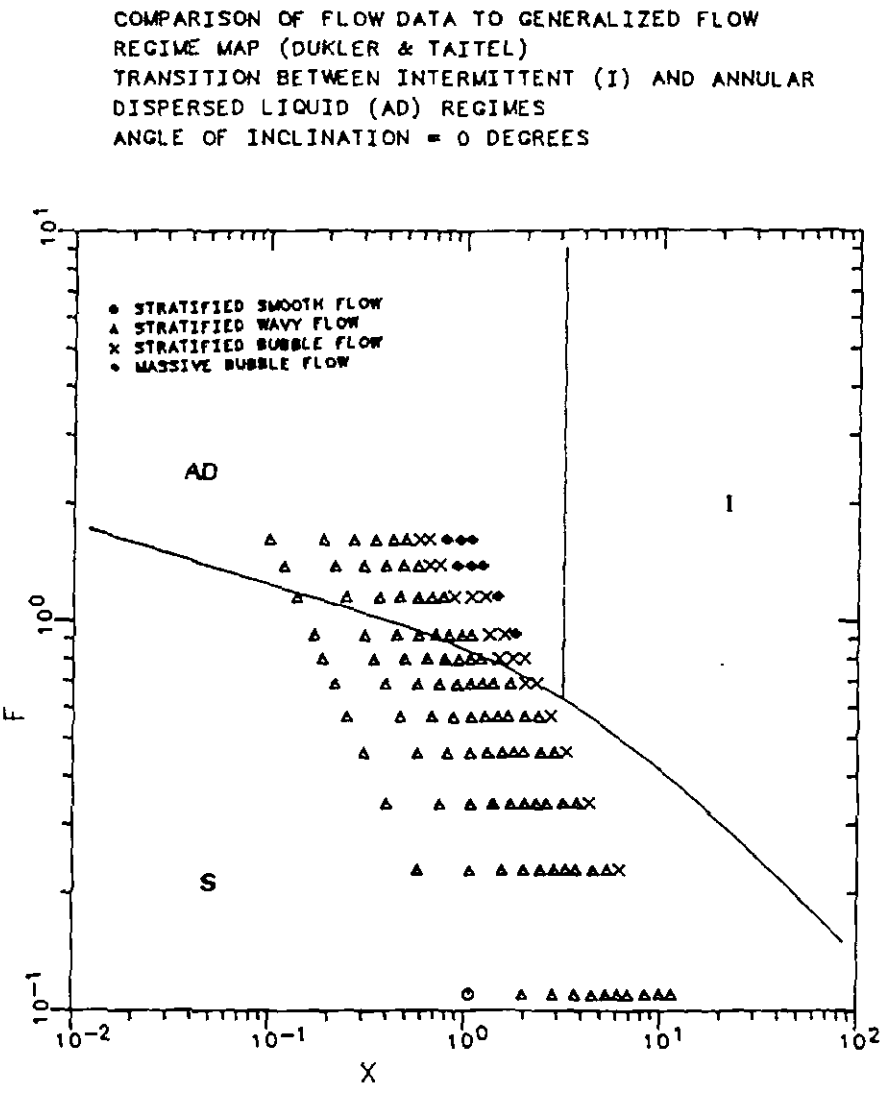

Figure 34

Comparison of Flow Data to Generalized Flow Regime Map (Taitel & Dukler)

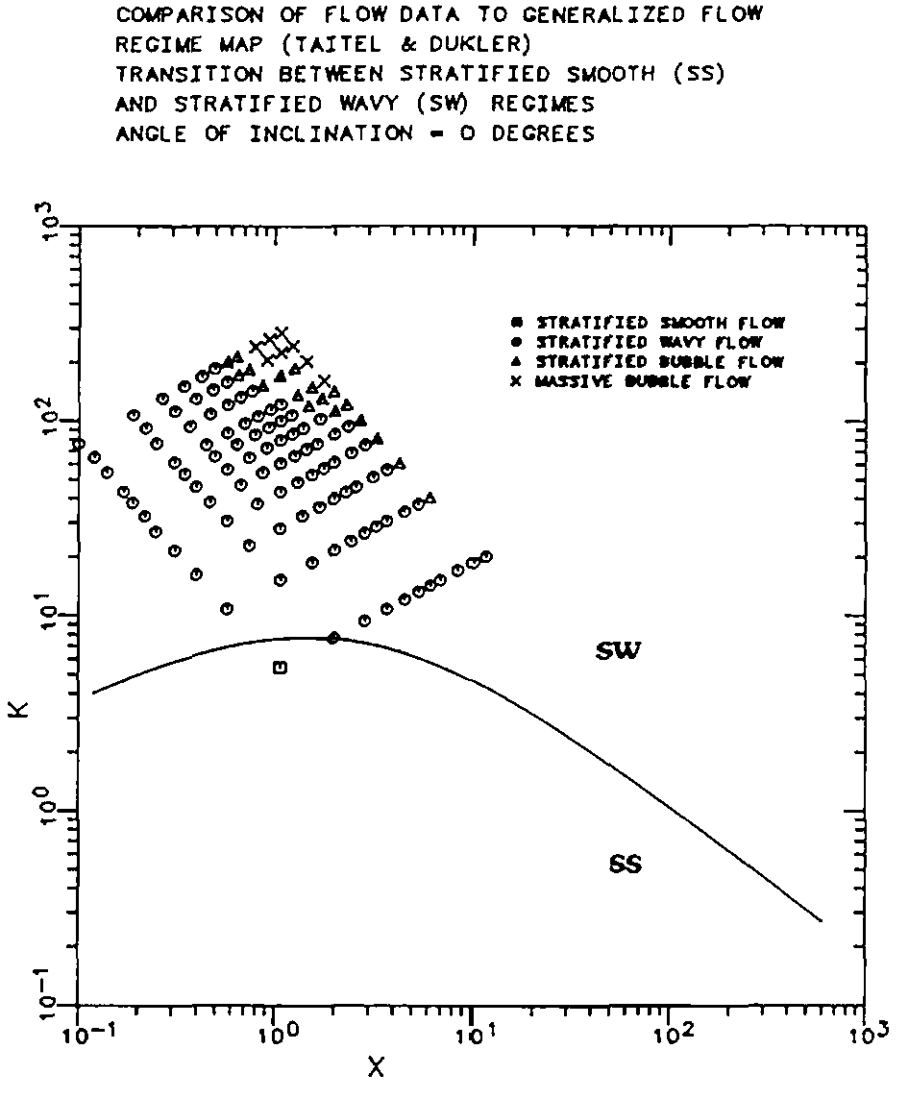

Figure 35

Comparison of Flow Data to Generalized Flow Regime Map (Taitel & Dukler)

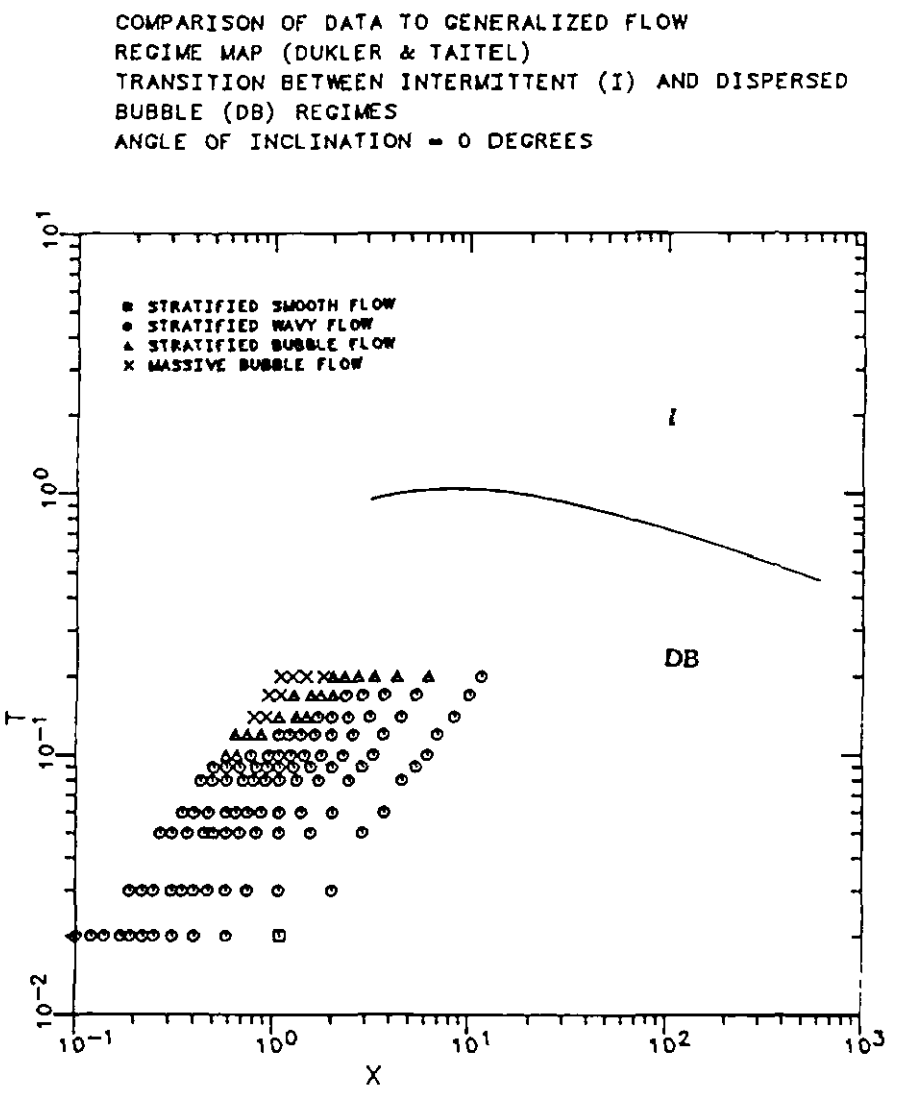

Figure 36

Comparison of Flow Data to Generalized Flow Regime Map (Taitel & Dukler)

Next, downhill flow was taken in account when generating the next set of plots dealing with the comparison of calculated transition boundaries and experimental data.

The generalized map in Figure 37 for an oil flow rate of 100 B/D and an angle of inclination of -15 degrees, shows distorted boundary lines when compared to the generalized map at horizontal flow. The Martinelli parameter X is dependent on the oil flow rate and angle of inclination of flow from horizontal so this would account for the fact that there will be some changes in the shape of the flow regime transition boundaries. Since any change in the oil rate and pipe angle will affect the boundaries, a separate map for every different oil flow rate that is used at a certain angle will need be generated. The flow regime map generated for Line A, Figure 38, has all of the related data points in the stratified region. However, when this plot is compared to the plot at Line B, Figure 39, the data tends to be confusing. The same data points are used for Line B but the results are not reasonable. The data falls in neither the intermittent nor the annular-dispersed liquid region but is within the stratified section of the plot. Also the data in the B line plot falls neither in the intermittent nor the annular-dispersed flow regime. For the plot of Line C, Figure 40, all of the data points plot in the stratified wavy region. However, there are no stratified smooth flow regime data points available to check and see if this flow boundary is correct. Finally the Line D plot, Figure 41, details the transitional boundary line between intermittent and dispersed bubble flow. In this plot, all the data is positioned below Line D, within the region of intermittent flow. Since none of the flow

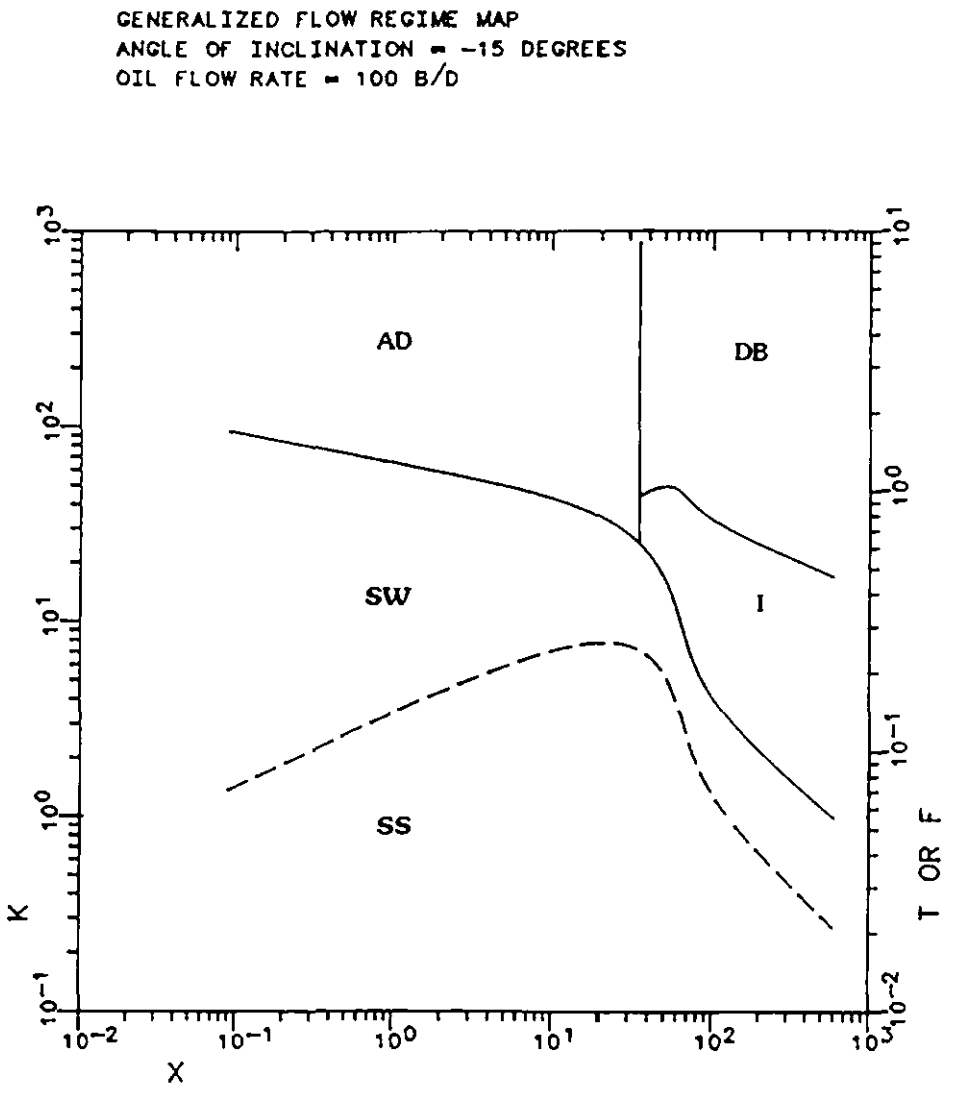

Figure 37

Generalized Flow Regime Map

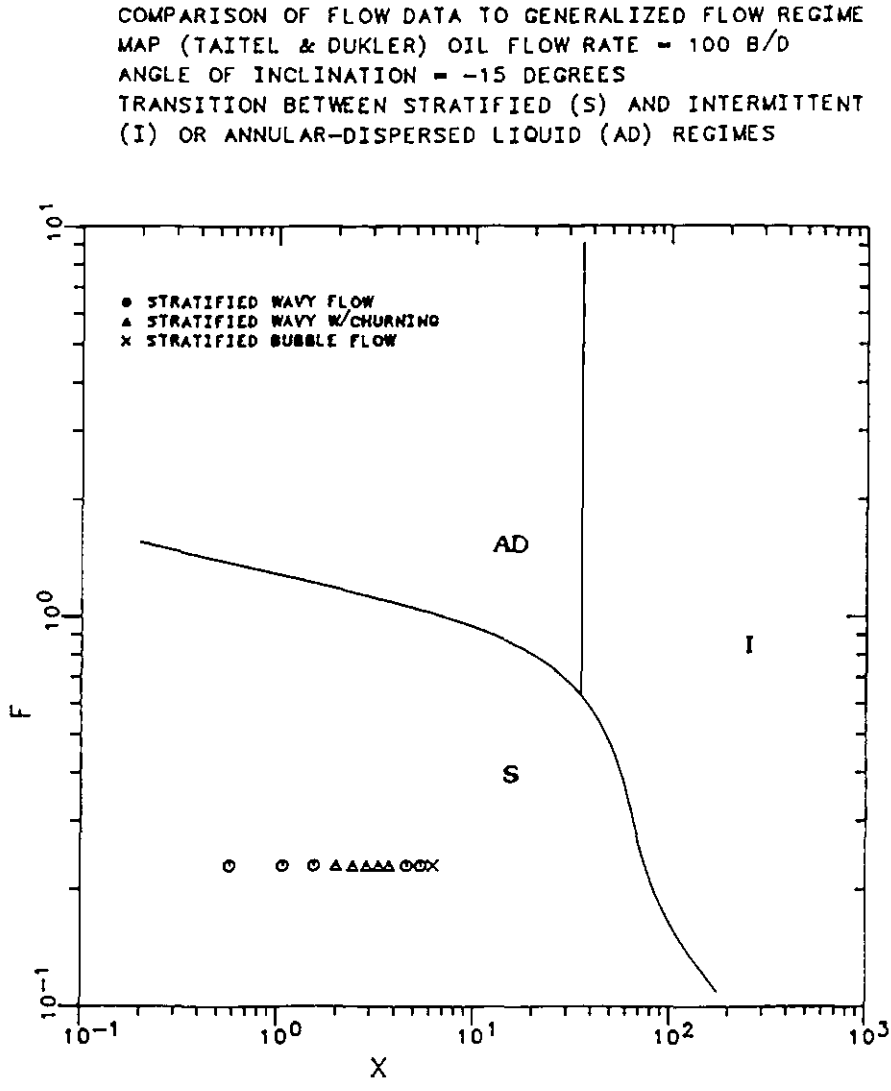

Figure 38

Comparison of Flow Data to Generalized Flow Regime Map (Taitel & Dukler)

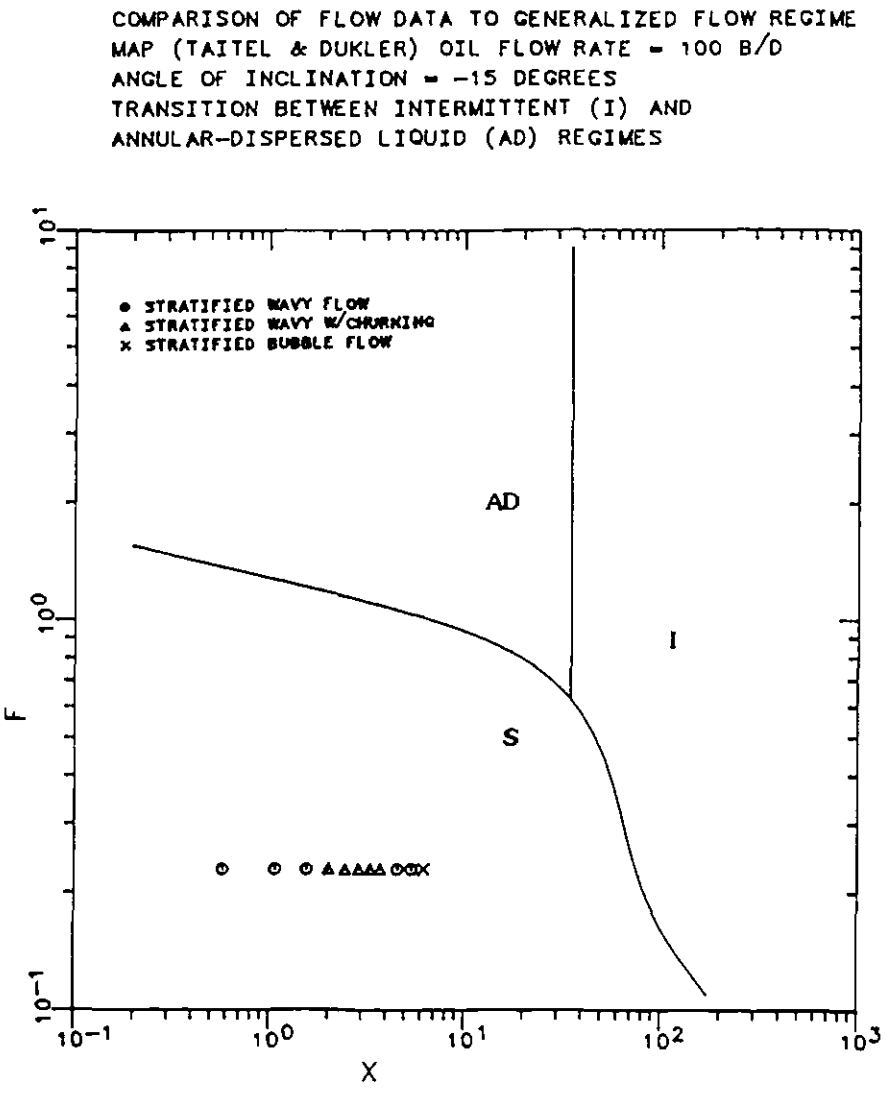

Figure 39

Comparison of Flow Data to Generalized Flow Regime Map (Taitel & Dukler)

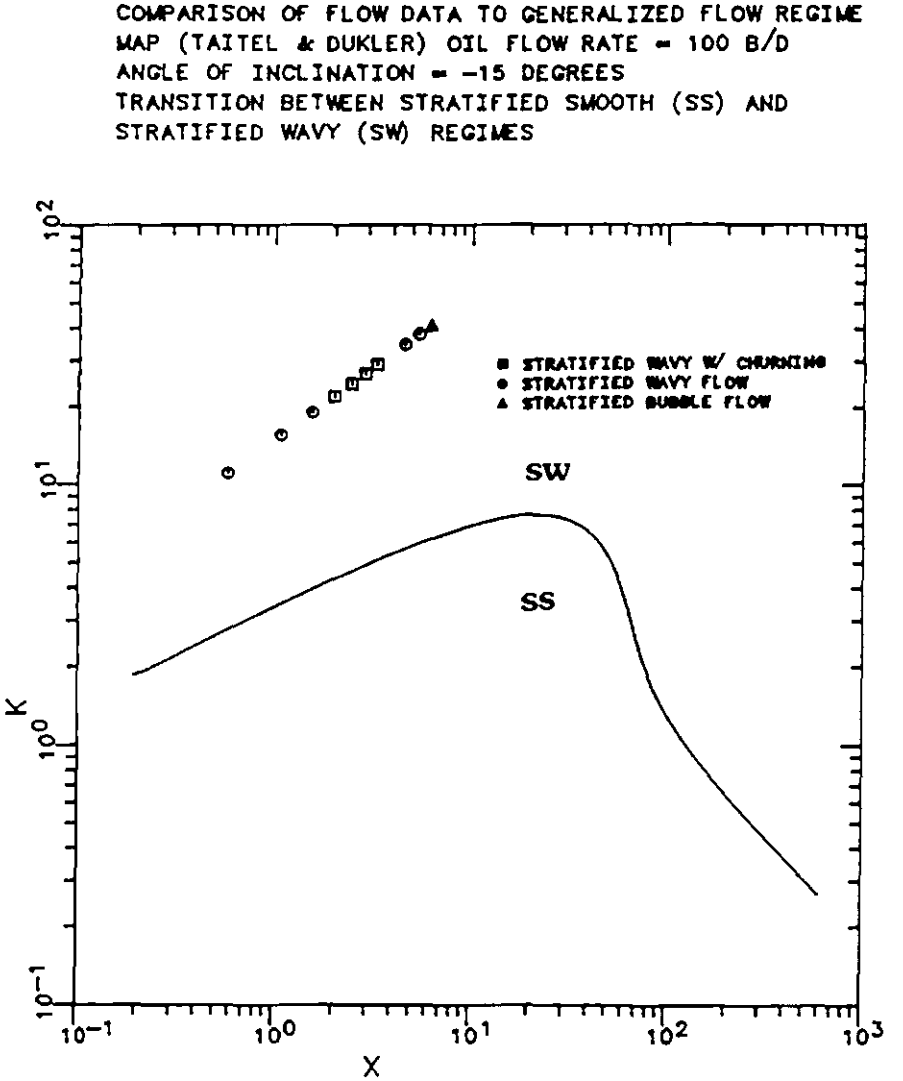

Figure 40

Comparison of Flow Data to Generalized Flow Regime Map (Taitel & Dukler)

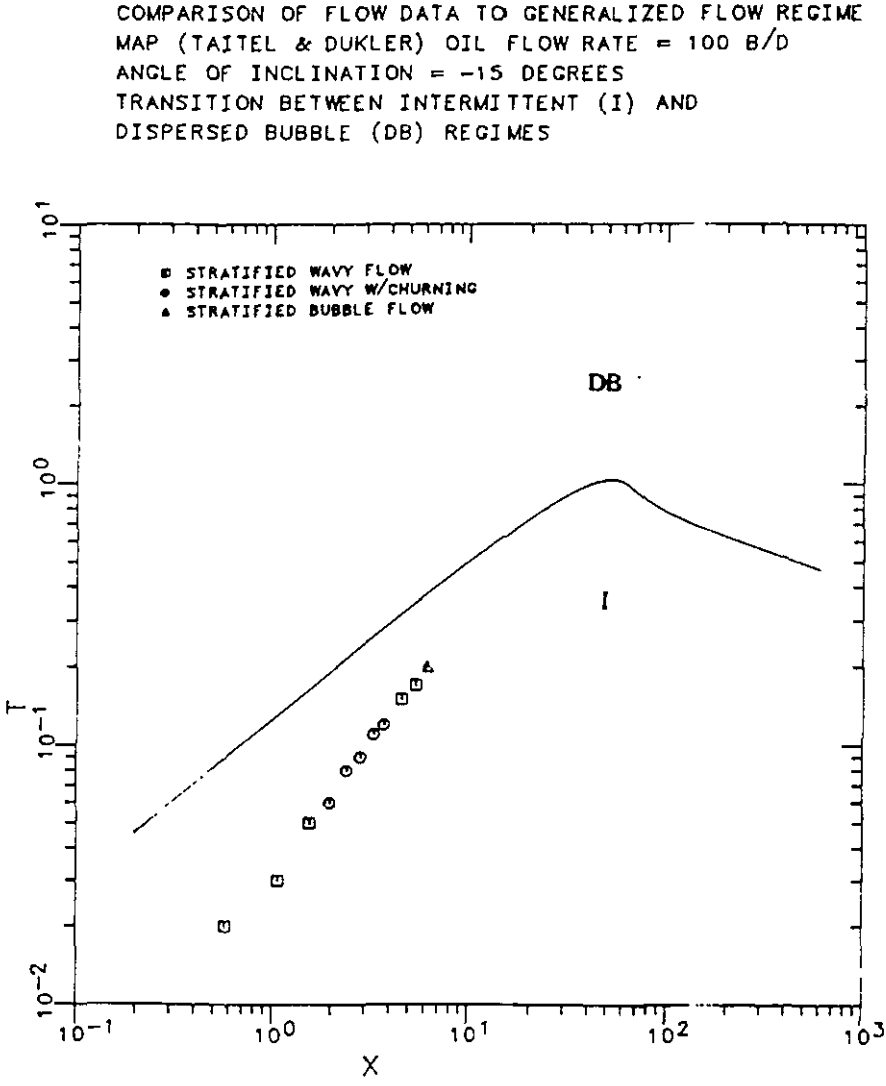

Figure 41

Comparison of Flow Data to Generalized Flow Regime Map (Taitel & Dukler)

data is intermittent flow of any kind (neither slug nor plug) and stratified wavy can be described as being close to dispersed bubble, the conclusion is that this, along with the previous comparisons, has indicated that the transition boundaries generated in this specific case are not valid for the data points in liquid-liquid flow.

Three additional sets of plots were made at -15 degrees. Oil flow rates of 300, 500 and 700 B/D were used. The generalized flow regime plot of 700 B/D of oil, Figure 42, shows some distortion of the flow boundary lines when compared to the horizontal, generalized flow map, Figure 32. This overall distortion, due to the sensitivity of the Martinelli Parameter to the oil flow rate and angle of inclination seems to be somewhat less than the flow map at an oil rate of 100 B/D. The transition lines shift less to the right from the original placement in the generalized map at horizontal flow as the oil rate increases. Therefore at 100 B/D of oil the transition boundaries are shifted as far to the right as possible under the present conditions. The plots of Lines A, B, C and D were similar to the plots at 100 B/D of oil except that in the plots of Line A and Line B, Figures 43 and 44 respectively, the data points were shifted above the stratified wavy/annular-dispersed liquid boundary and into the annular dispersed liquid region. For the Line C plot, Figure 45, the data points were shifted higher into the stratified wavy region while in the Line D plot, Figure 46, the data shifted to the right along with the transition line and therefore the points remained approximately the same distance away from the boundary line as the previous Line D plot, Figure 41. This means that as you increase the flow rate the boundary lines tend to approach the positions

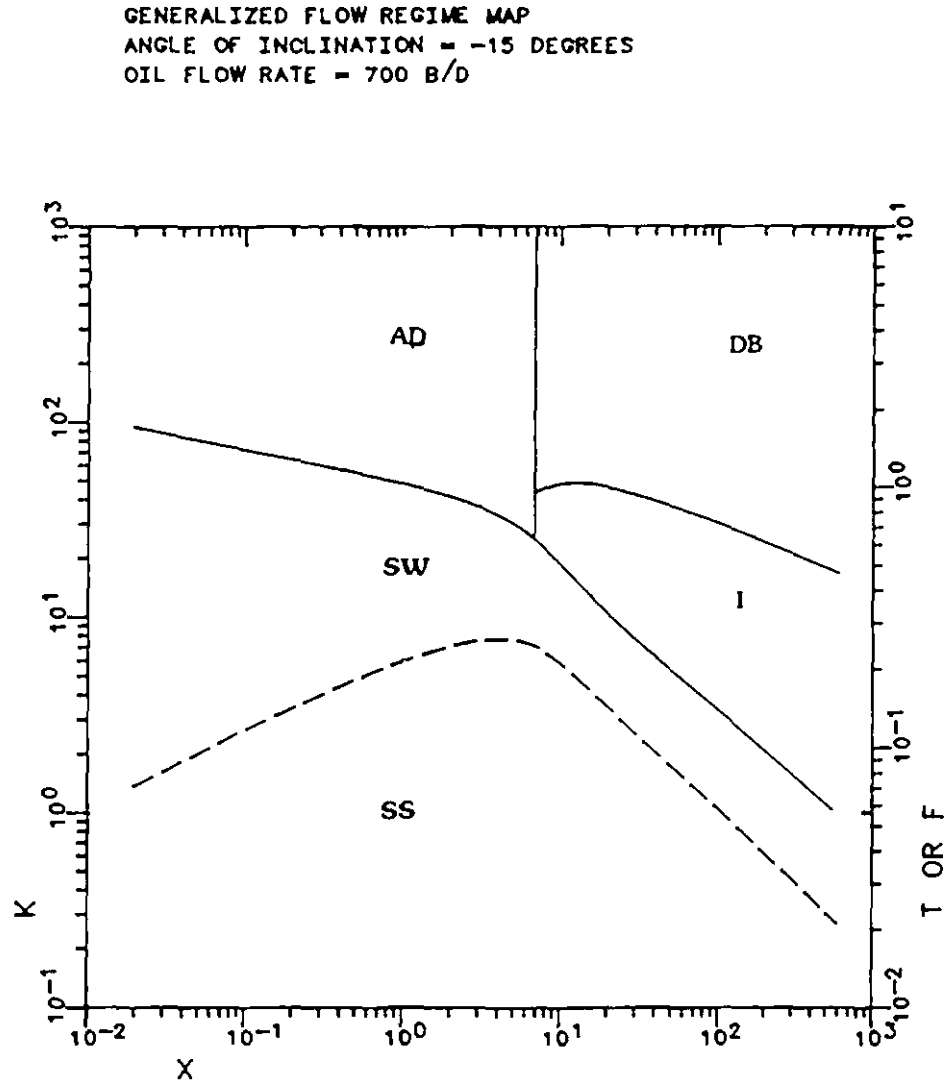

Figure 42

Generalized Flow Regime Map

COMPARISON OF FLOW DATA TO GENERALIZED FLOW REGIME MAP (TAITEL & DUKLER) OIL FLOW RATE = 700 B/D ANGLE OF INCLINATION = -15 DEGREES TRANSITION BETWEEN STRATIFIED (S) AND INTERMITTENT (I) OR ANNULAR-DISPERSED LIQUID (AD) REGIMES

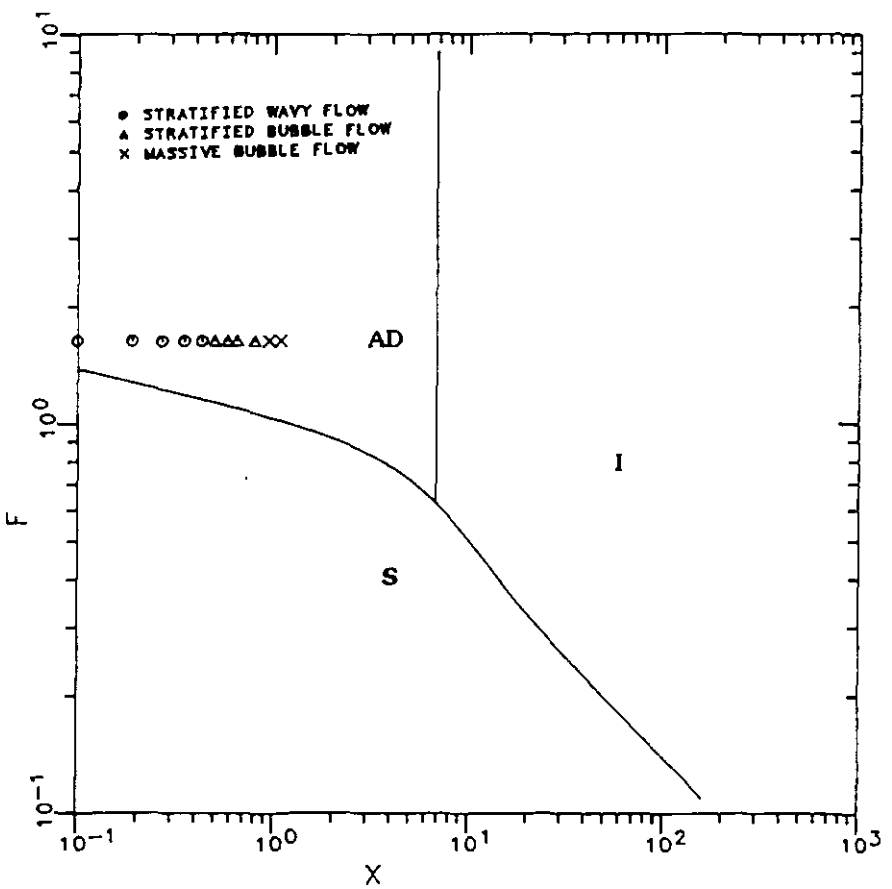

Figure 43

Comparison of Flow Data to Generalized Flow Regime Map (Taitel & Dukler)

COMPARISON OF FLOW DATA TO GENERALIZED FLOW REGIME MAP (TAITEL & DUKLER) OIL FLOW RATE = 700 B/D ANGLE OF INCLINATION = -15 DEGREES TRANSITION BETWEEN INTERMITTENT (I) AND ANNULAR DISPERSED LIQUID (AD) REGIMES

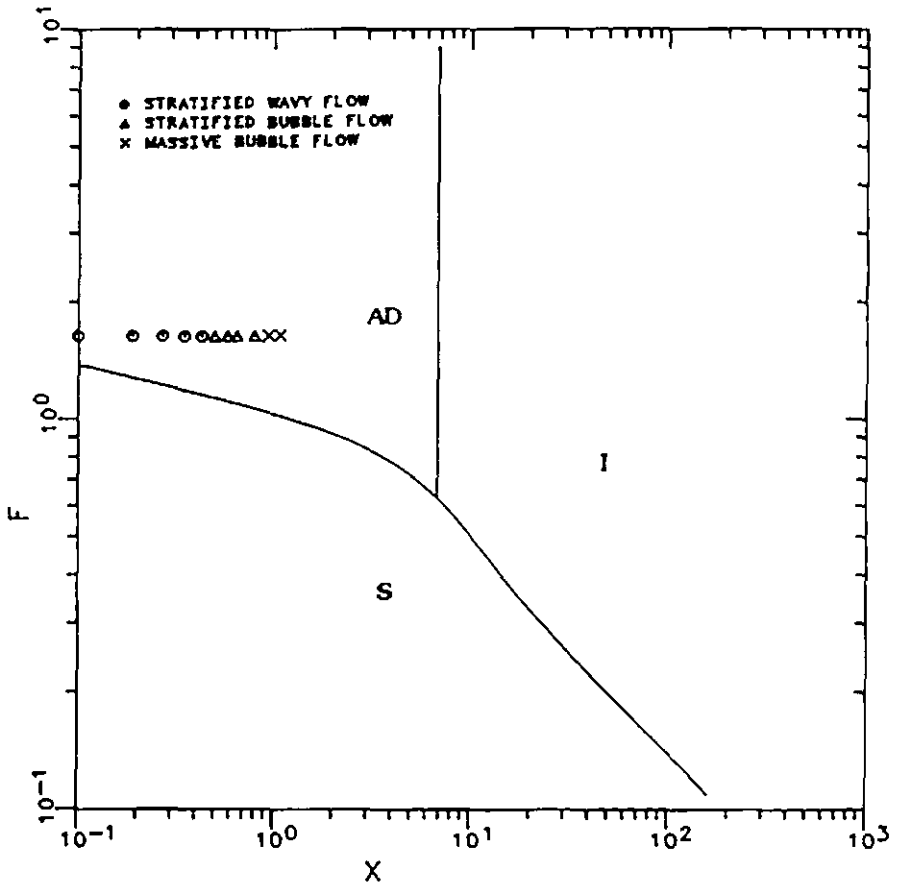

Figure 44

Comparison of Flow Data to Generalized Flow Regime Map (Taitel & Dukler)

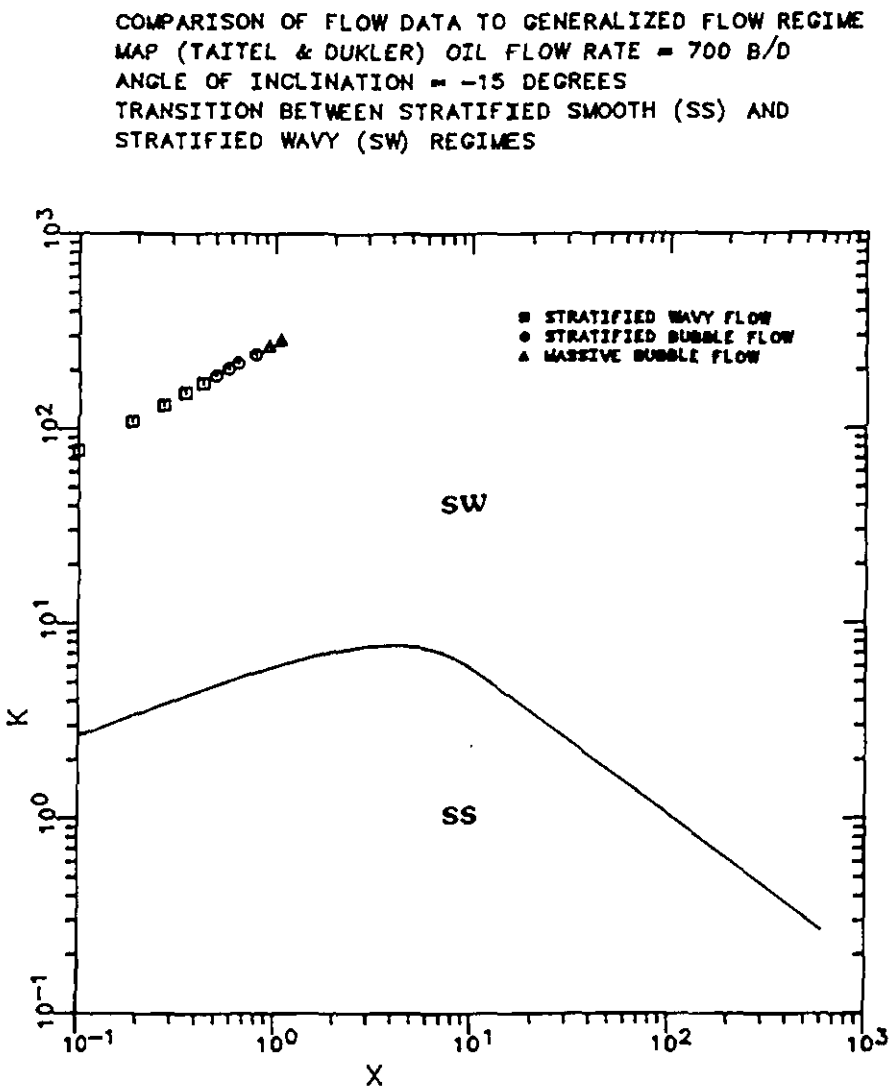

Figure 45

Comparison of Flow Data to Generalized Flow Regime Map (Taitel & Dukler)

COMPARISON OF FLOW DATA TO GENERALIZED FLOW REGIME
MAP (TAITEL & DUKLER) OIL FLOW RATE = 700 B/D
ANGLE OF INCLINATION = -15 DEGREES
TRANSITION BETWEEN INTERMITTENT (I) AND
DISPERSED BUBBLE (DB) REGIMES

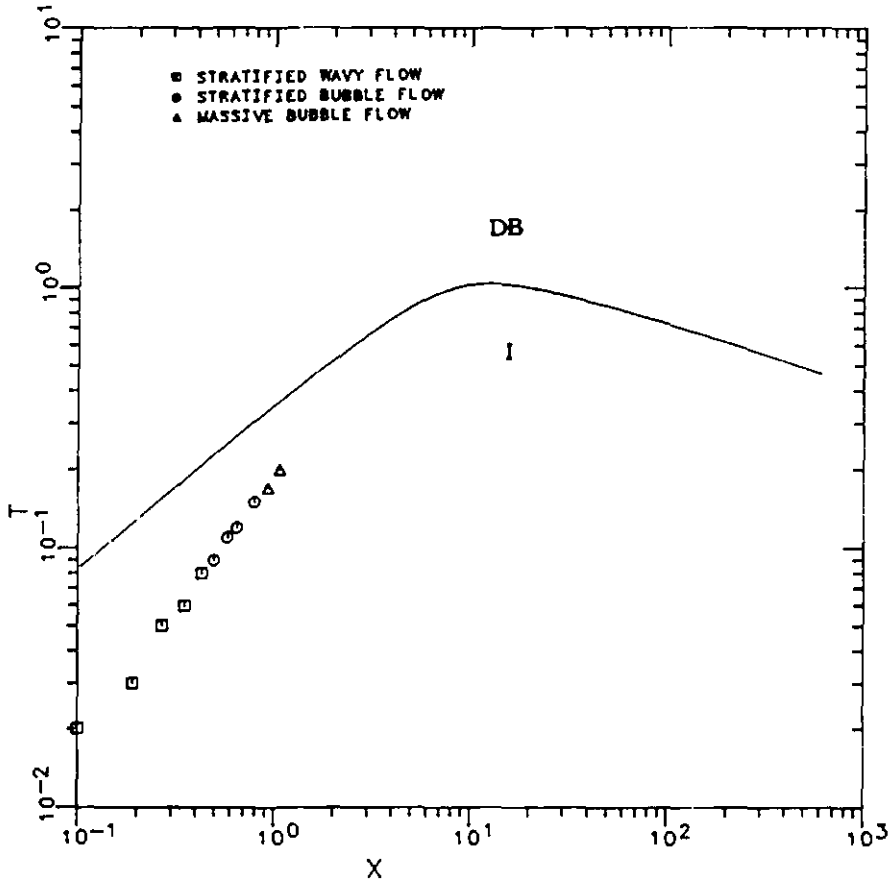

Figure 46

Comparison of Flow Data to Generalized Flow Regime Map (Taitel & Dukler)

they were in at horizontal flow, where the Martinelli parameter X, was not affected by oil flow rate or the angle of inclination because Y is zero at that horizontal flow. The other sets of plots involving oil flow rates of 300 and 500 B/D are included in Appendix III.

The following sets of flow regime boundary plots were developed for -30 degrees (down hill flow) and at oil flow rates of 100, 300, 500 and 700 B/D, respectively. The generalized map at 100 B/D of oil, Figure 47, was compared to the generalized flow maps at -15 degrees and 100 B/D of oil and 0 degrees. The boundary lines at this angle and oil flow rate did not shift as far to the right as the boundary lines for plot at -15 degrees. With the data obtained it shows a possible trend that at some angle between -30 and 0 degrees the maximum shift in the regime boundaries is achieved, and then they will shift back to the left toward the positions occupied by the boundary line at horizontal flow. However, there is not enough data at other angles of inclinations above or below these angles to confirm this idea. When the Line A plot for 100 B/D of oil, Figure 48, was compared with the same plot at -15 degrees, the data points were essentially in the same location for both plots. This also was the case for the Line B plot, Figure 49, in which the position of the data did not change appreciably. According to the Line C plot, Figure 50, the data points are shifted a little farther away from the boundary line than in the Line C plot at -15 degrees. In Figure 51, the Line D plot for -30 degrees at 100 B/D of oil, the data points tend to be just a little closer to the flow boundary than the -15 degree plot.

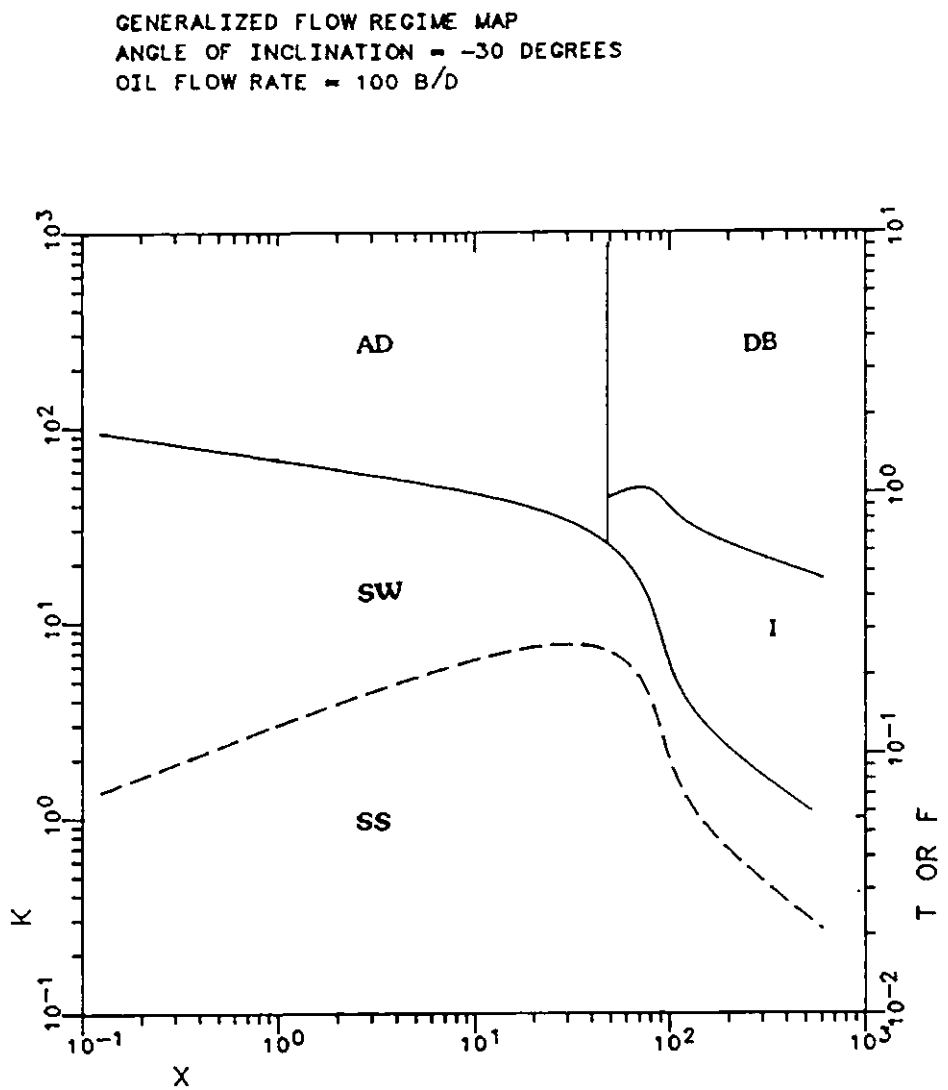

Figure 47

Generalized Flow Regime Map

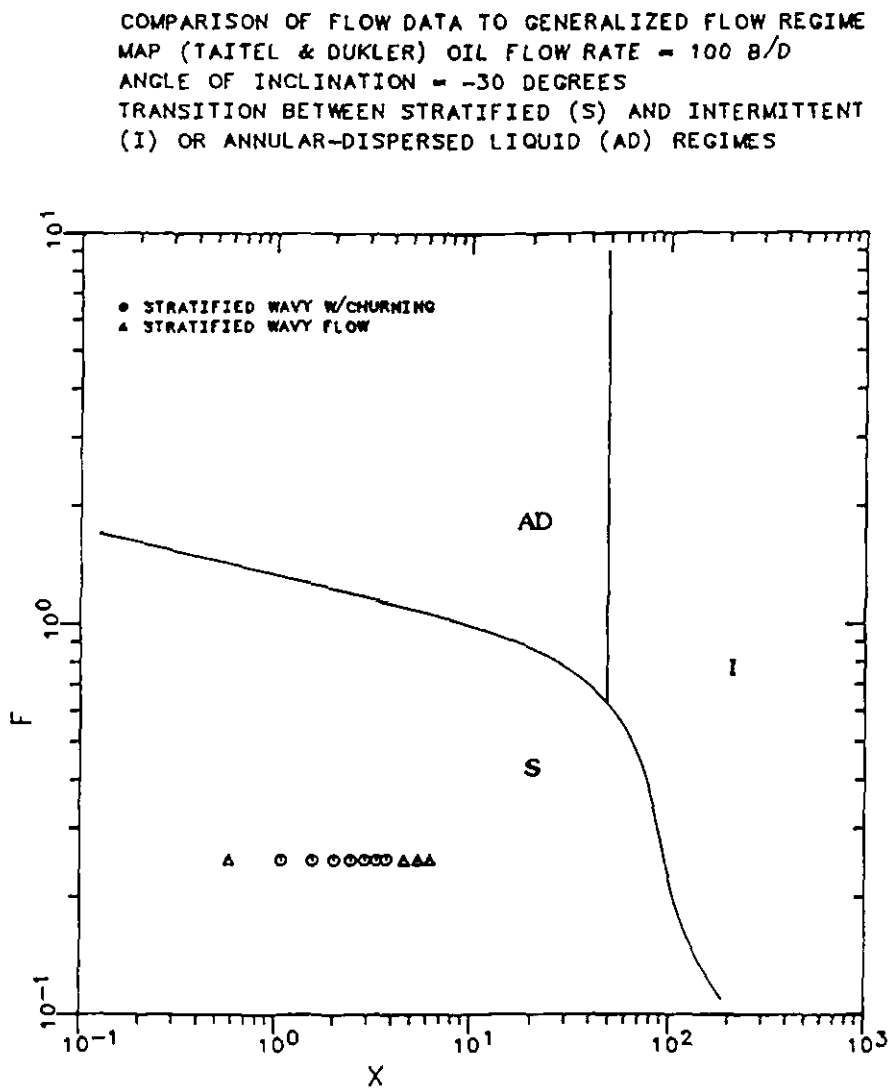

Figure 48

Comparison of Flow Data to Generalized Flow Regime Map (Taitel & Dukler)

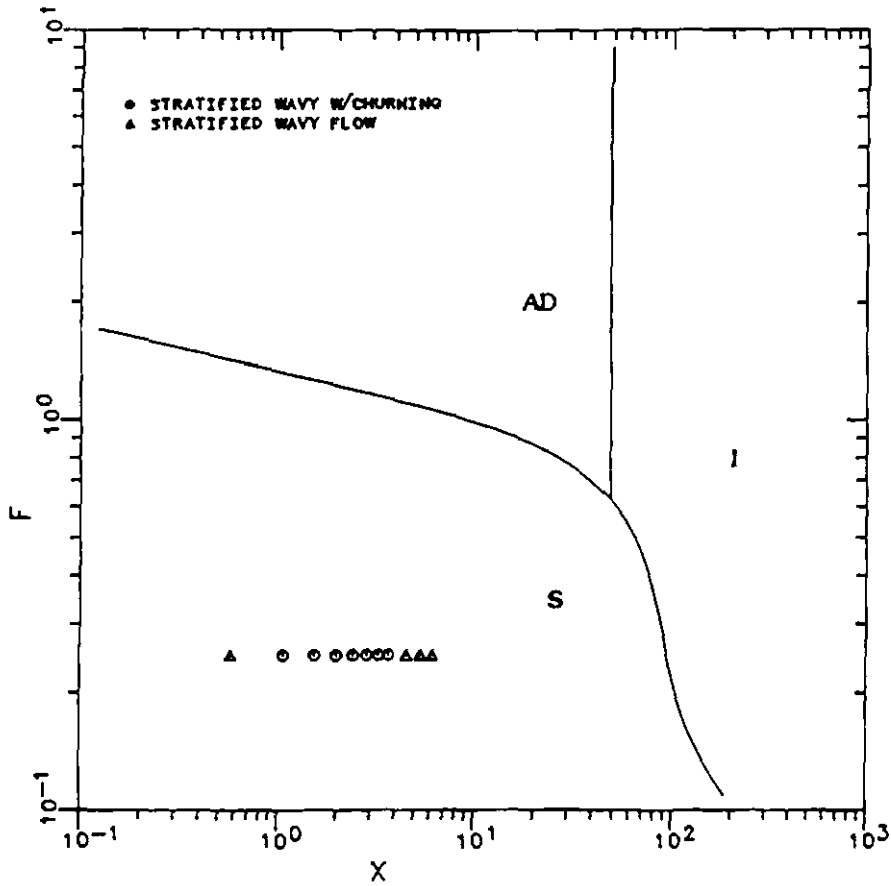

Figure 49

Comparison of Flow Data to Generalized Flow Regime Map (Taitel & Dukler)

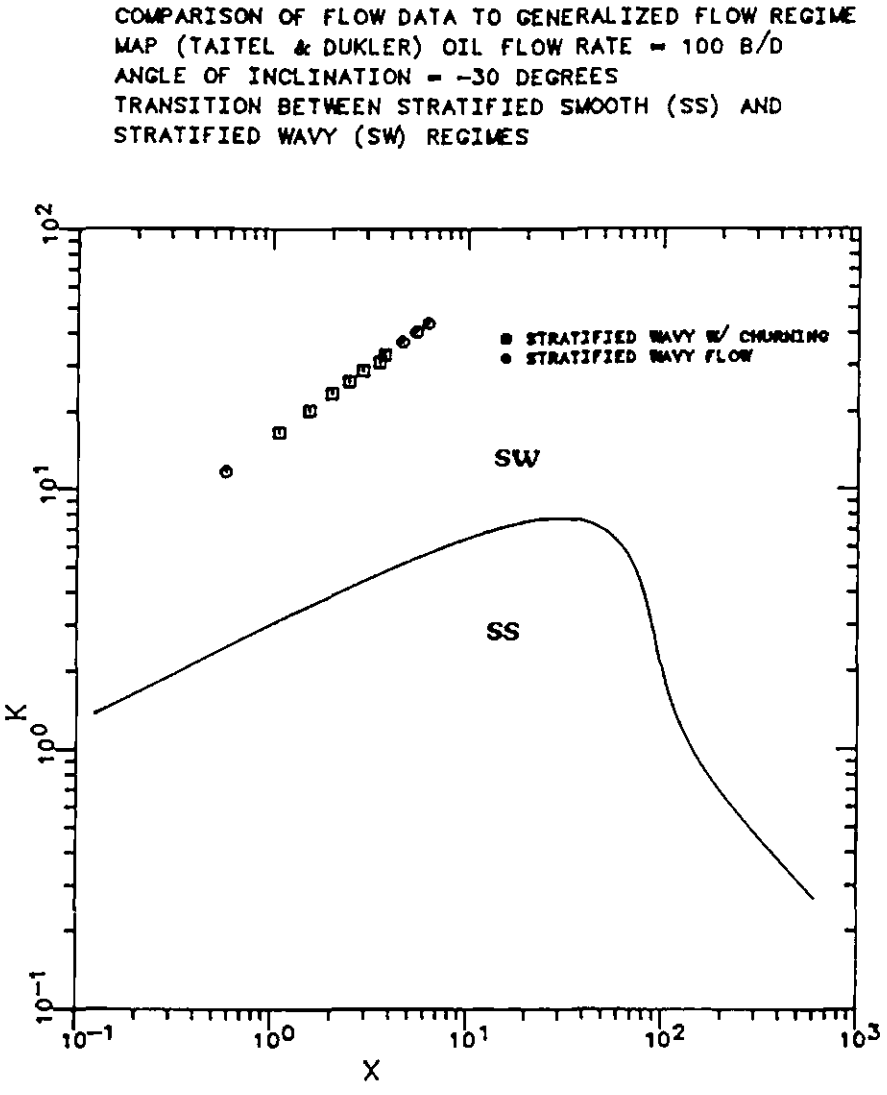

Figure 50

Comparison of Flow Data to Generalized Flow Regime Map (Taitel & Dukler)

COMPARISON OF FLOW DATA TO GENERALIZED FLOW REGIME
MAP (TAITEL & DUKLER) OIL FLOW RATE = 100 B/D
ANGLE OF INCLINATION = -30 DEGREES
TRANSITION BETWEEN INTERMITTENT (I) AND
DISPERSED BUBBLE (DB) REGIMES

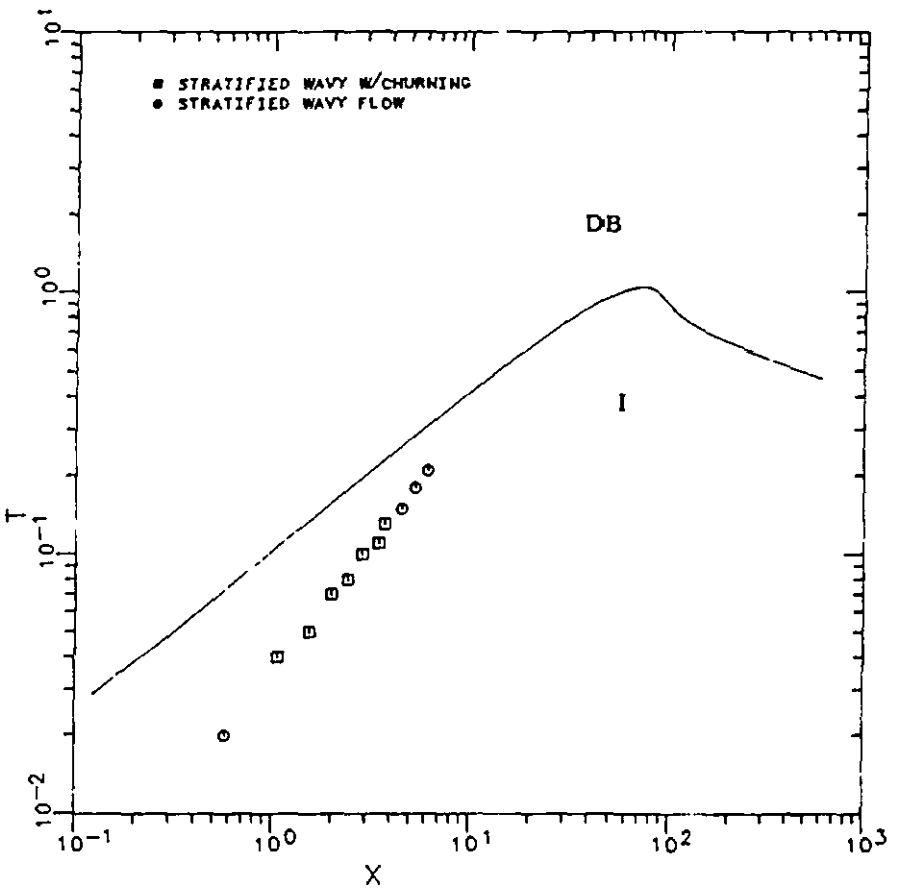

Figure 51

Comparison of Flow Data to Generalized Flow Regime Map (Taitel & Dukler)

The generalized flow regime map, in Figure 52, at -30 degrees with an oil flow rate of 700 B/D seems to resemble the flow map at -15 degrees with the identical flow rate. This trend continued through the next set of transition plots. The plots of Lines A, B, C and D, Figure 53, 54, 55 and 56, respectively, all continued to exhibit the same trends when compared to the plots of the same transition boundary lines at -15 degrees and the same flow rate. The other sets of plots involving flow rates of 300 and 500 B/D are included in Appendix III.

From the information just presented the results are twofold. First, from all the data used, it is important to note that even though the dimensionless flow regime variables developed by Taitel and Dukler were modified from gas-liquid parameters to liquid-liquid parameters, the end results in the plots indicate that something more must be done with the initial assumptions used in these dimensionless variables or that it is not possible to use the Taitel and Dukler variables with liquid-liquid flow in their present forms. Secondly, within the plots that were developed using the modified dimensionless variables, the dependence upon the flow rate of oil has a more significant effect on the location of the transition boundaries and data points than the angle of inclination of the pipe. However, it is not known if the further modification of the dimensionless variables assumptions will change this cause and effect relationship.

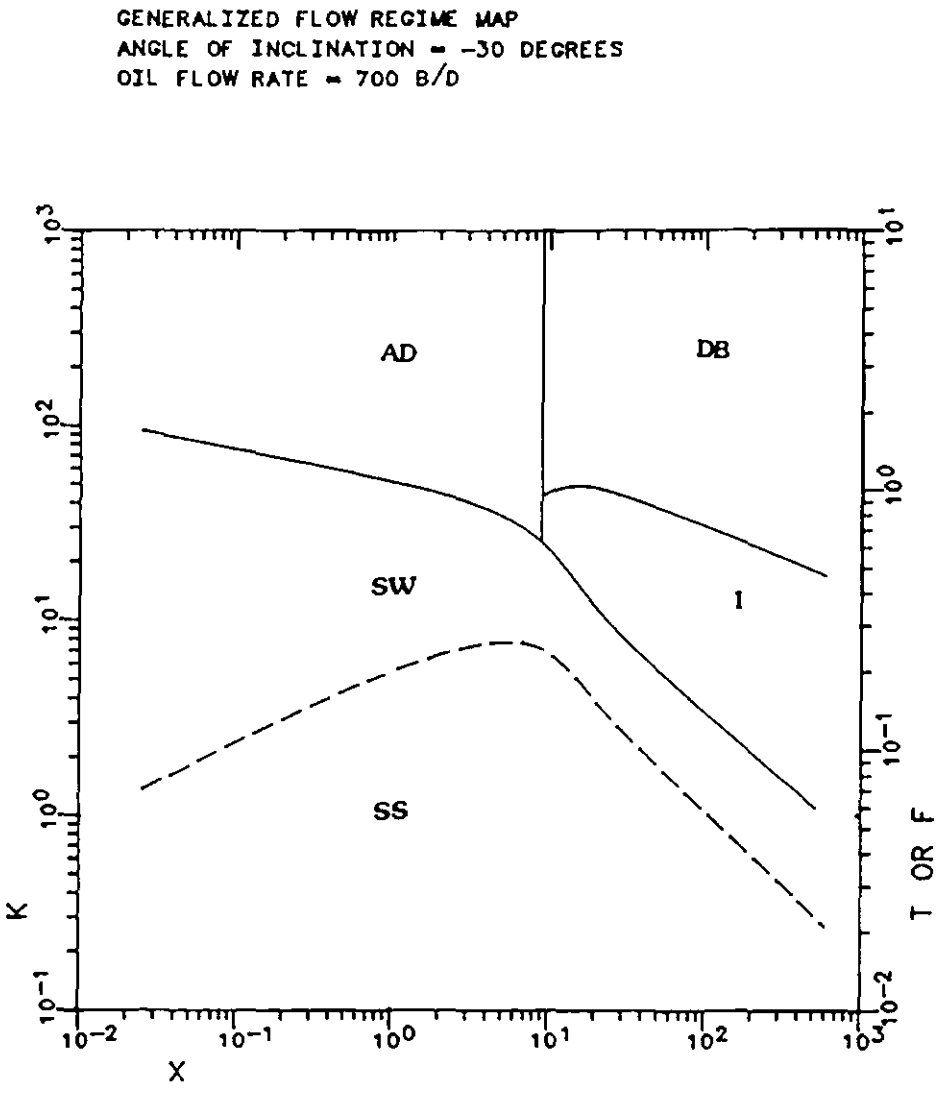

Figure 52

Generalized Flow Regime Map

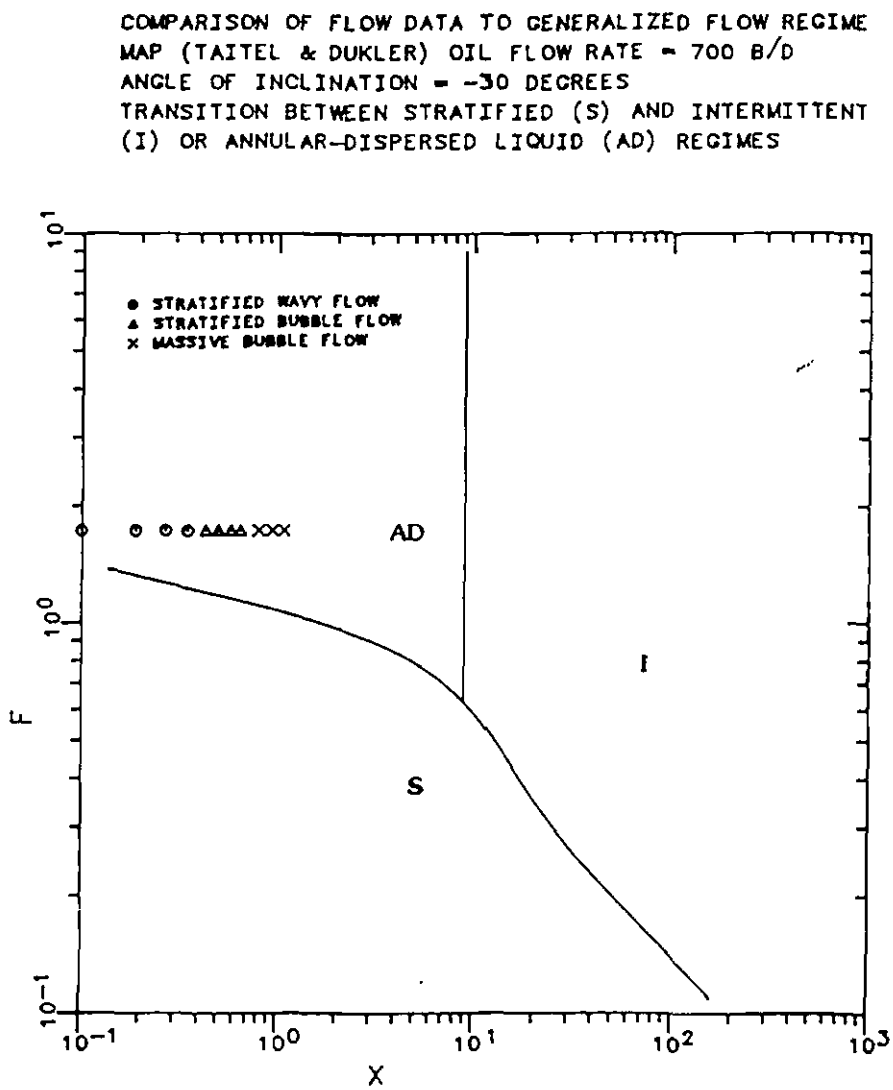

Figure 53

Comparison of Flow Data to Generalized Flow Regime Map (Taitel & Dukler)

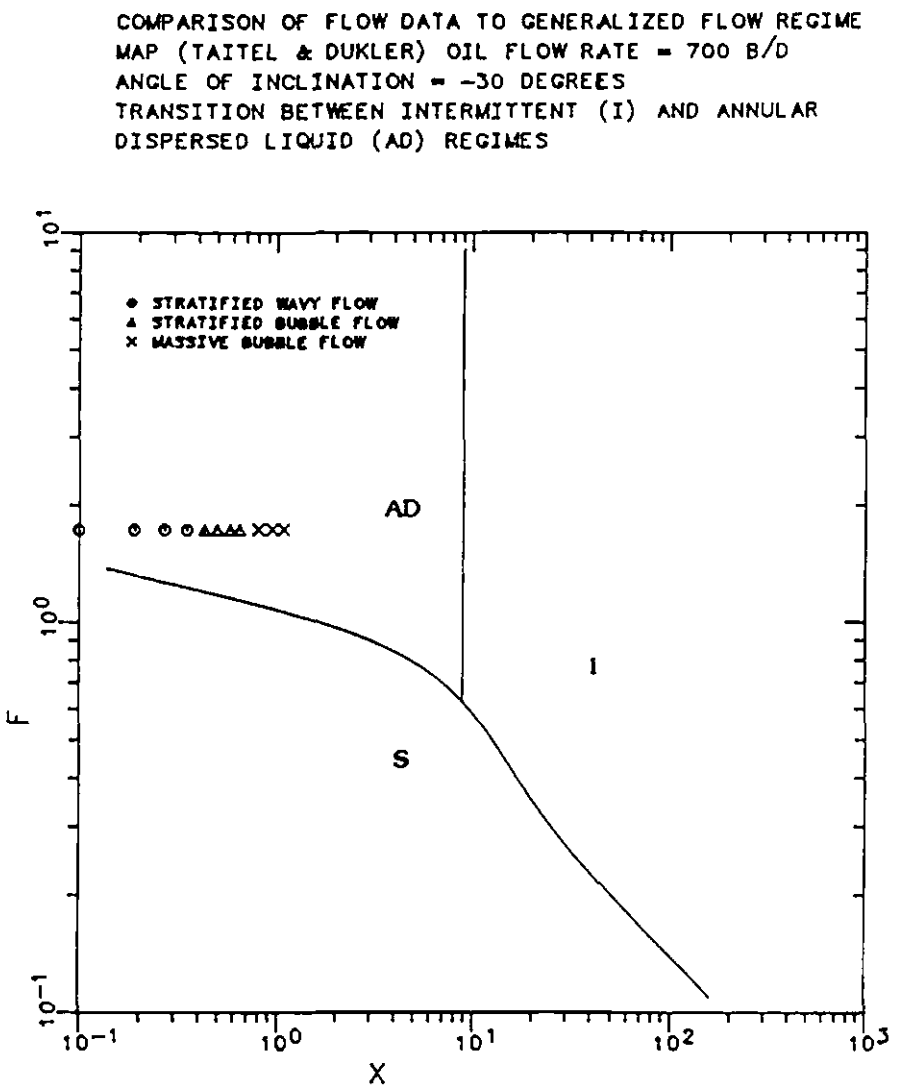

Figure 54

Comparison of Flow Data to Generalized Flow Regime Map (Taitel & Dukler)

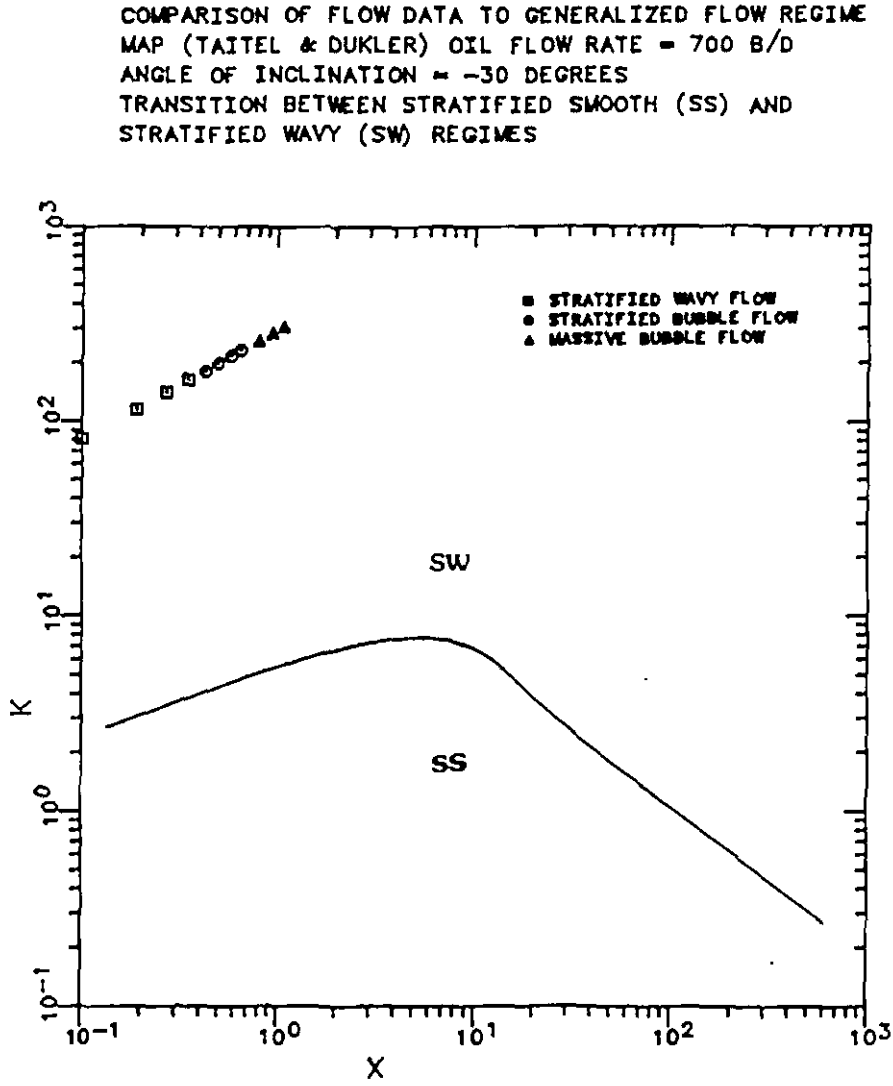

Figure 55

Comparison of Flow Data to Generalized Flow Regime Map (Taitel & Dukler)

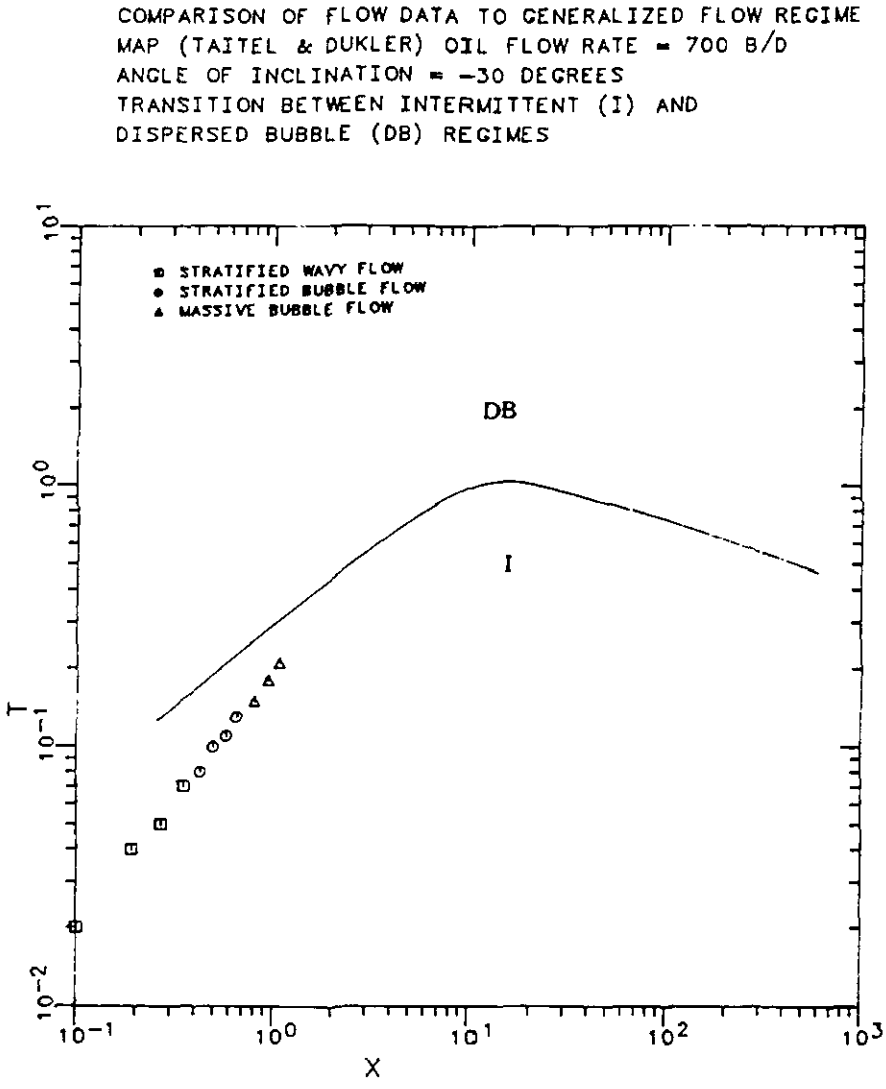

Figure 56

Comparison of Flow Data to Generalized Flow Regime Map (Taitel & Dukler)

HOLDUP

Normally, in two-phase in downhill liquid-liquid flow, the more dense phase will move faster than the less dense phase. Oil is considered the lighter phase and water is considered the heavier phase in the present experimentation. Because of this phenomena called holdup, the in situ volume fraction of the more dense phase will be less than the input volume fraction of the more dense phase. This relationship is defined by the parameter called holdup as follows:

$$\text{Holdup } (H_w) = \frac{\text{Volume of denser phase in a pipe segment}}{\text{Volume of the pipe segment}}$$

REASONS FOR MEASURING HOLDUP

It appears, at first glance, that holdup could be calculated simply by knowing flow rates, pressure, temperature and fluid properties. This simplistic method will work only when there is no slip velocity between the two phases. Slip velocity is defined as the difference in average velocities of the two phases. In this study, slip velocity will indicate the difference between the ratios of the superficial velocity and holdup of the oil and water phase, respectively. This condition of "no slip" does not exist to a great extent under actual flowing conditions but it can be approached in certain cases. The proof that "no slip" between the phases can exist between oil and water in horizontal flow, is shown in Figure 57. Values

for water holdup (assuming no slip velocity between the phases exists) are calculated by

$$H_w \text{ (no slip)} = \frac{Q_w}{Q_w + Q_o}$$

where Q_w and Q_o are the volumetric flow rates of the water and oil, respectively, considered at the same conditions at which the experimental water holdup data is gathered. This holdup (no slip) valve is the same as the input fraction of the water phase (λ_w). The "no slip" holdup valves and the experimental holdup data are compared in Figure 57.

In horizontal flow, almost all the data approximates the "no slip" holdup. This is the case in situations where the oil flow rate is less than the water rate. However, when the water and oil flow rates are fairly close in magnitude or when the constant water flow rate is less than the oil rate, the velocity of the oil tends to be greater, thus, it slips by the water phase and causes an increase in the water holdup. This would seem to hold true for upward inclined flow in both liquid-liquid and gas-liquid flow and be the reverse in downward liquid-liquid and gas-liquid flow.

Since actual values of holdup cannot be calculated directly, the parameter must be measured experimentally. Holdup data is necessary for the calculation of the real average linear velocities of each liquid phase. These velocities allow for the calculation of kinetic energy, Reynolds numbers and often significant parameters which involve mass

transport. Knowing the water holdup also allows for the prediction of the two-phase flowing mixture density. The density of a flowing oil-water mixture is defined by

$$\rho_m = \rho_w H_w + \rho_o (1 - H_w)$$

Yet, a knowledge of water holdup does not indicate what the real fluid distribution is in the pipe. The same value of holdup can come from two totally different flow regime geometries. The real value of knowing holdup quantitatively is being able to observe the effect of holdup on pressure drops in the areas where two-phase flow occurs.

It seems that the logical conclusion to these facts is that a correlation between holdup and liquid-liquid flow rates, angle of inclination, fluid properties and flow patterns would be very beneficial for the calculation of real average velocities of the oil and water phases for design usage.

Data for water holdup was obtained experimentally by the use of "quick-closing" ball values as discussed in the previous chapter.

Holdup data compared with other selected parameters that were discussed previously including pipe inclination will be analyzed to see if any correlation between holdup and those parameters does, in fact, exist.

Mukherjee, Brill and Beggs[14] developed a liquid-liquid holdup correlation involving several parameters including pipe inclination (both uphill and downhill flow) and Reynold's number. After

COMPARISON OF MEASURED FLOWING WATER HOLDUP
WITH CALCULATED NO-SLIP WATER HOLDUP

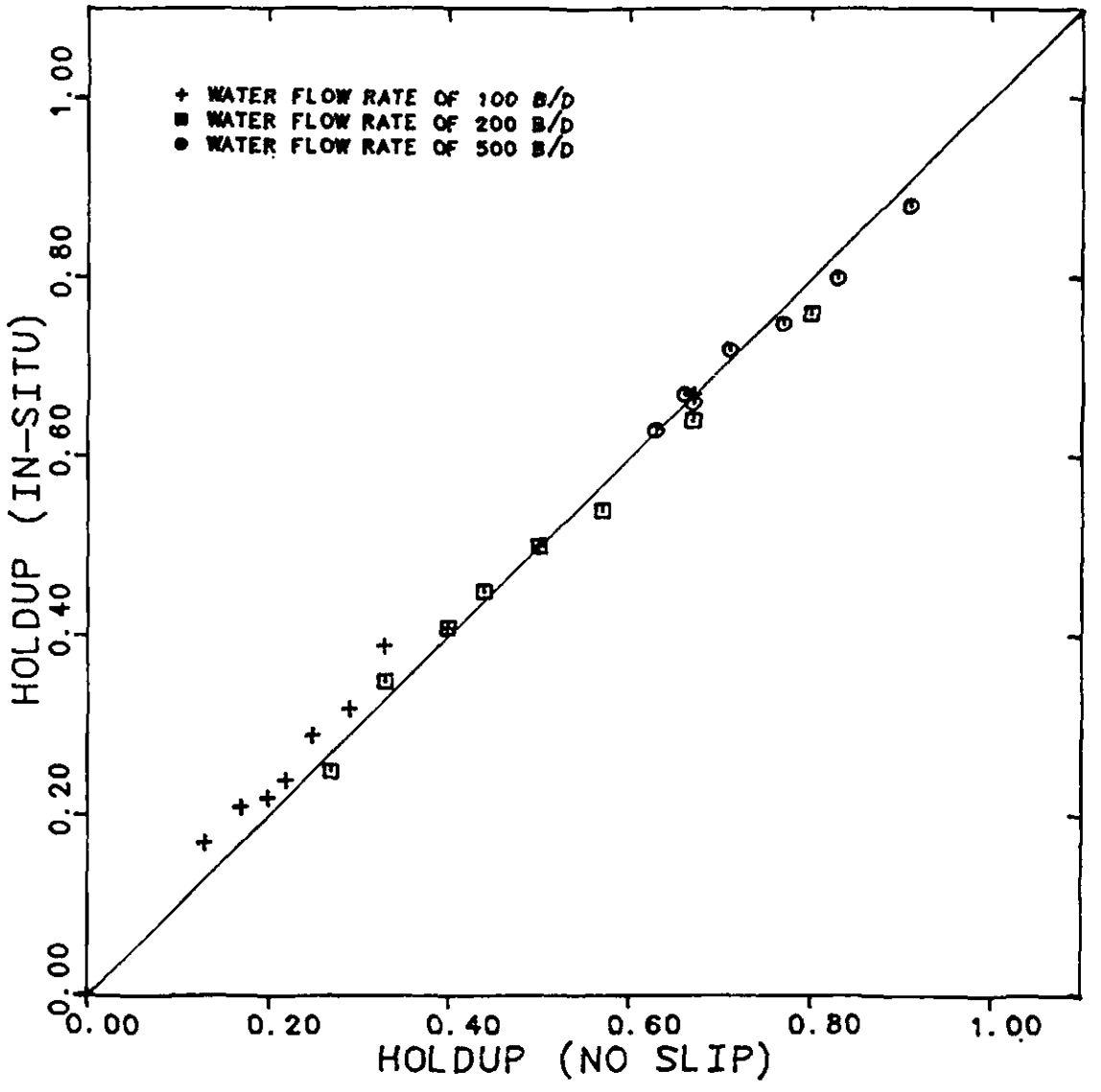

Figure 57

Comparison of Measured Flowing Water Holdup

with Calculated No-Slip Water Holdup

the initial comparison of holdup with the other parameters discussed previously is completed, a comparison of actual holdup data with the developed correlation will be shown to discover if the correlation is valid over the range of parameters and conditions used in the present experimentation.

ANALYSIS OF HOLDUP DATA

The change in water holdup with the angle of inclination is depicted in Figure 58. Several observations can be made from Figure 58.

Since water is the more dense phase and therefore heavier, the force of gravity should come into effect and cause the water to "slip" past the oil in downward flow which would results in $H_w < \lambda_w$. Figure 58 definitely proves the last statement when referring to the change from 0 degrees to -15 degrees. However, one would assume as the angle of inclination gets steeper (i.e. changes from -15 to -30 degrees) the holdup would decrease further. This does not occur in this situation when dealing with the angle change from -15 to -30 degrees. The holdup measured in two cases (λ_w = 0.2 and 0.4) is approximately the same and in the other two cases (λ_w = 0.6 and 0.8), a somewhat larger holdup value is observed. This anomalous behavior could be caused by forces other than the buoyancy and gravity effects on the oil and water phases, respectively.

Another measure of the holdup phenomenon, at the holdup ratio, is used quite frequently in correlation work with two-phase flow. This relationship is presented as

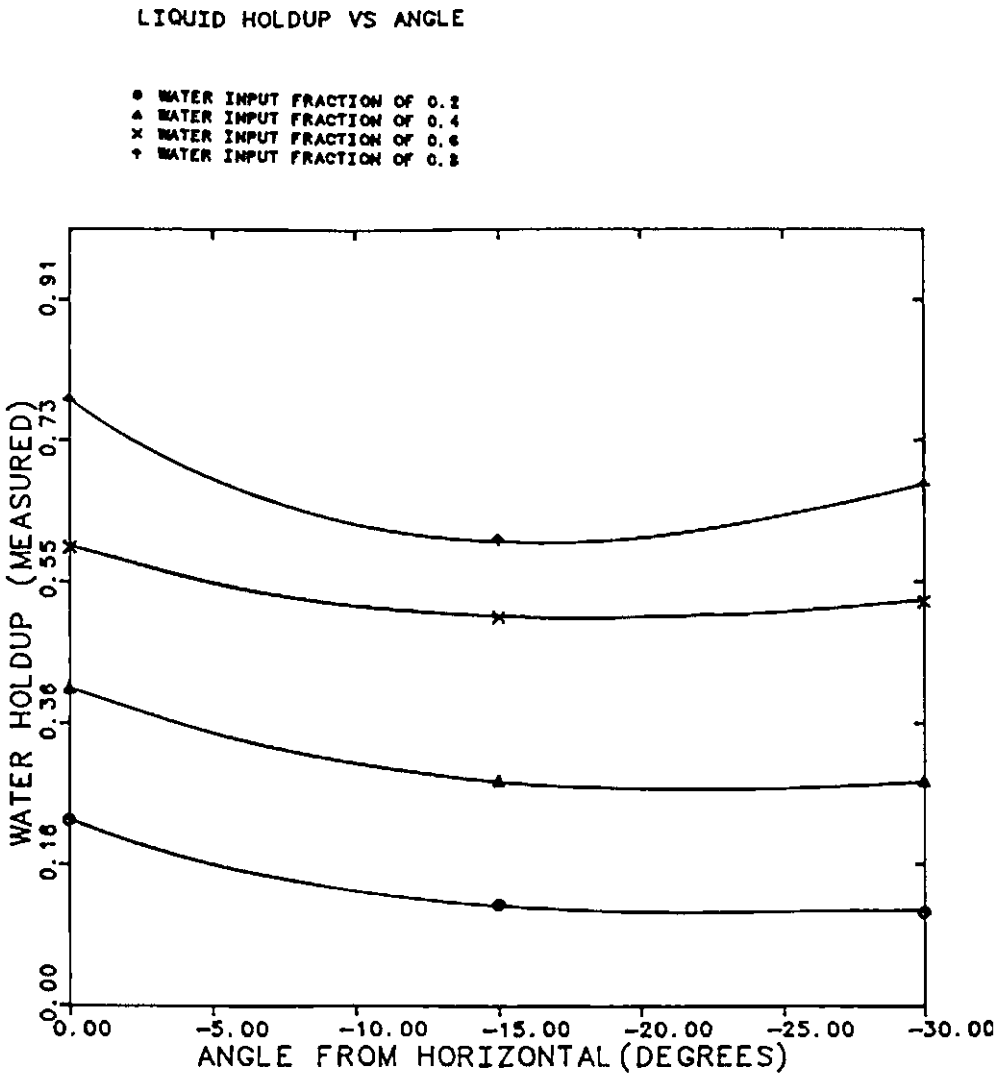

Figure 58

Liquid Holdup Compared to Angle of Inclination

(Holdup Ratio) $$R_H = \frac{H_w/H_o}{\lambda_w/\lambda_o} = \frac{H_w/H_o}{Q_w/Q_o}$$

The holdup ratio will provide a clear means to understand the degree of slip taking place between the two flowing phases, when

$R_H = 1$ no slip is occurring between phases

or, if $R_H > 1$ the less dense phase is moving faster than the denser phase

and finally, if

$R_H < 1$ the denser phase is moving faster than the less dense phase

Figure 59 shows the holdup ratio, R_H compared to superficial oil velocity, V_{so} for various constant superficial water velocities with the corresponding flow regimes regions for the data points at 0 degrees. Considering a constant low water velocity, 0.15 ft/sec, as the oil velocity is increased the holdup ratio tends to increase from 1.0. This indicates that the lighter phase, oil, is moving faster than the more dense phase, water. Notice that when the water velocity is held constant at a higher velocity, such as 2.1 ft/sec, the holdup ratio is less than 1.0, which implies that the heavier phase is traveling faster

HOLDUP RATIO VS FLOW RATE
ANGLE OF INCLINATION = 0 DEGREES
(ALL VELOCITIES ARE SUPERFICIAL)

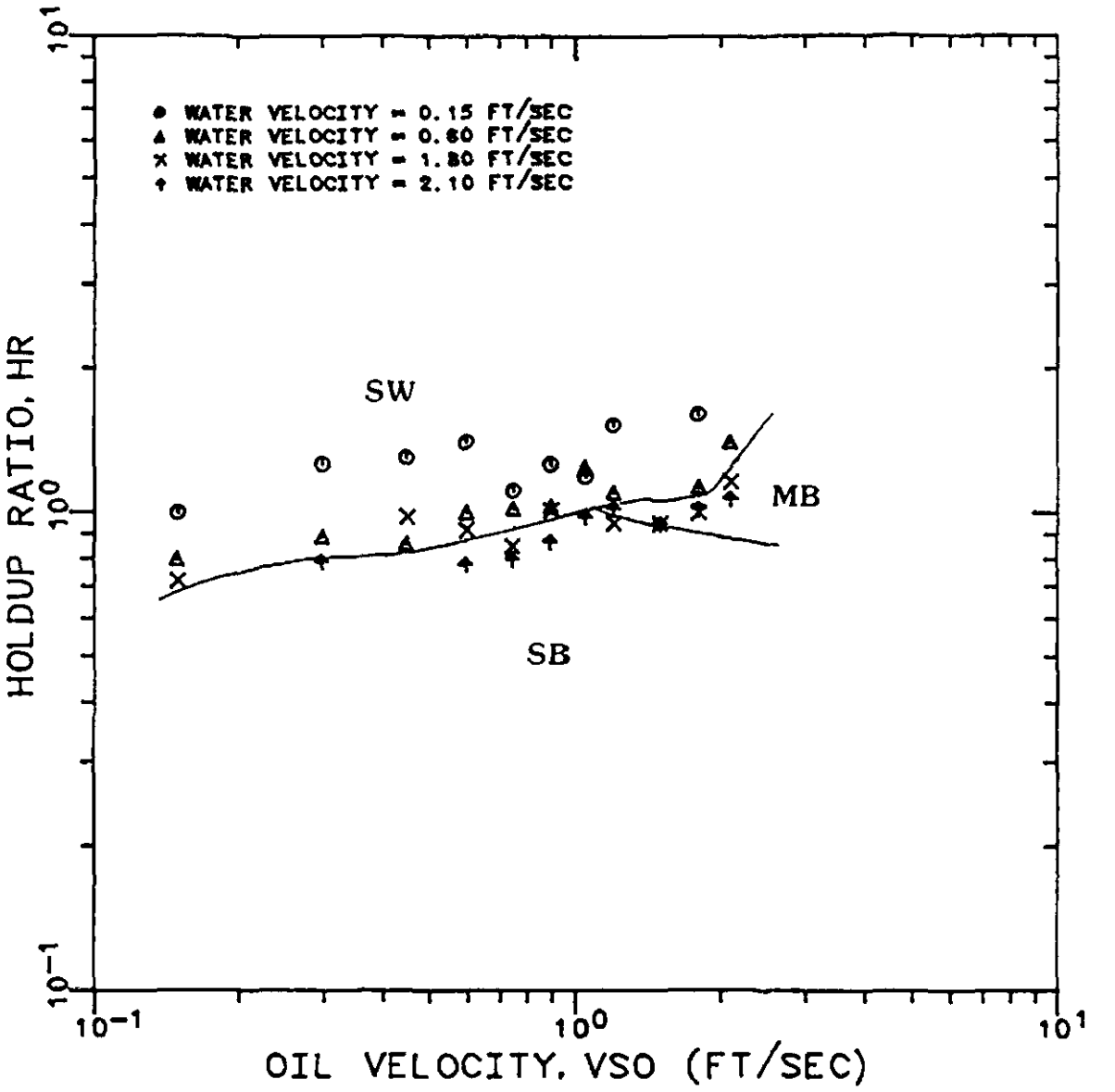

Figure 59

Holdup Ratio Compared to Flow Rate

than the lighter phase. This is true until the oil velocity reaches a point where the flow regime changes from stratified bubble to massive bubble - then the holdup ratio approaches 1.0. This situation could be caused by the fact that massive bubble flow is a continuous phase of water with oil drops and could resemble single phase flow. The higher constant water velocity causes the low holdup ratio because at low oil velocities, the water, even though the oil phase is lighter, will flow faster, thus, causing slippage past the oil.

When the angle of inclination is changed to -15 degrees (downhill flow), Figure 60, and all other conditions remain the same, the holdup ratios will, in almost all cases, be less than 1.0, which indicate that the heavier phase, water is slipping past the oil. The reason for this particular cause and effect is the importance of the gravity effect on the two phases. When considering downhill flow, gravity causes the heavier phase to travel faster. Only when the flow regime approaches massive bubble does the holdup ratio approach 1.0. The possible explanation for this action was explained previously for horizontal flow.

In Figure 61, at an inclination angle equal to -30 degrees, approximately the same results occur as with -15 degrees. In almost all cases, the holdup ratio indicated that the more dense phase was moving faster than the less dense phase. Again, when the flow regime changed to massive bubble the holdup ratio implied that there is no slippage between the phases or that they are flowing at approximately the same velocity.

HOLDUP RATIO VS FLOW RATE
ANGLE OF INCLINATION = -15 DEGREES
(ALL VELOCITIES ARE SUPERFICIAL)

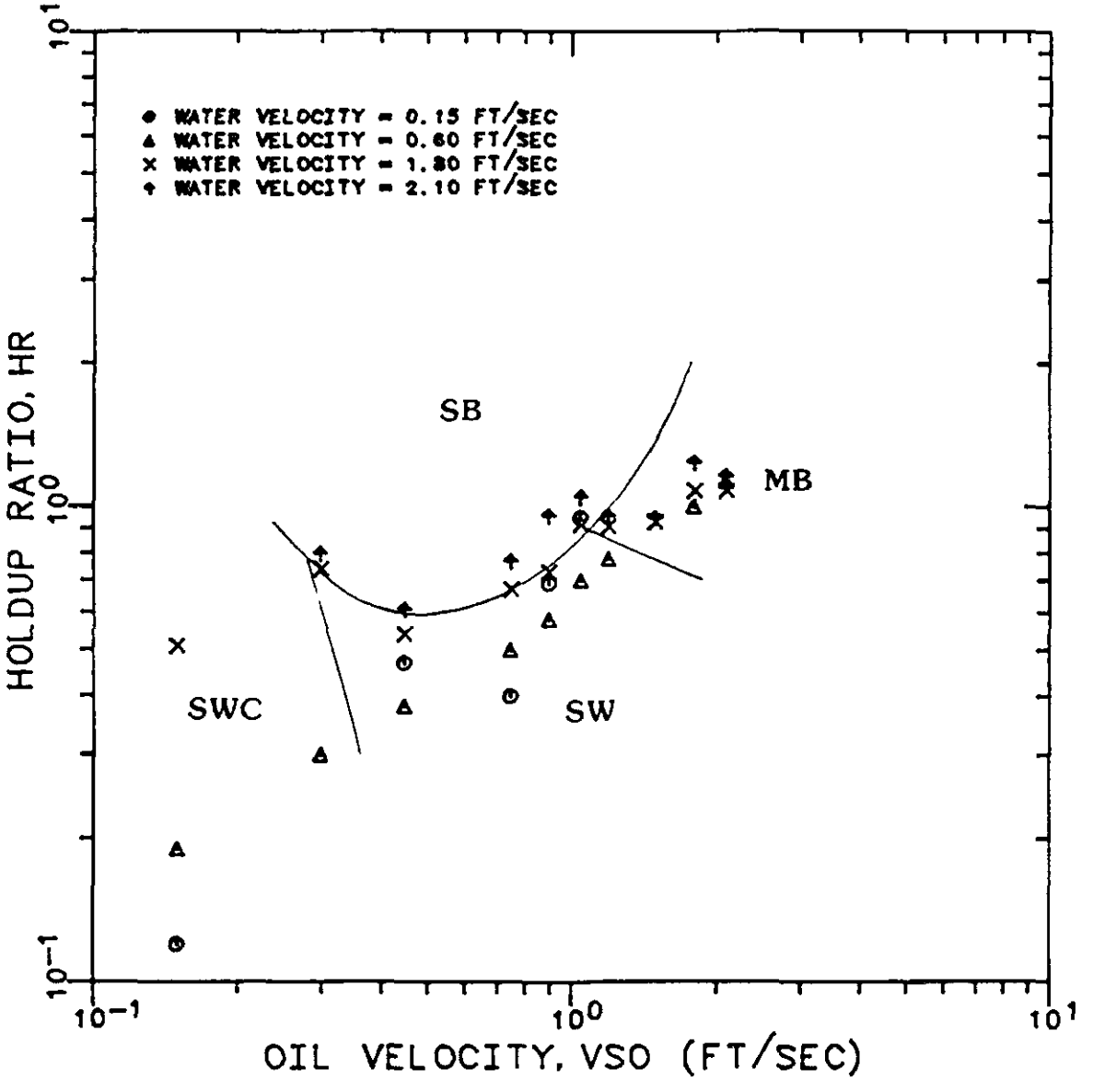

Figure 60

Holdup Ratio Compared to Flow Rate

HOLDUP RATIO VS FLOW RATE
ANGLE OF INCLINATION = -30 DEGREES
(ALL VELOCITIES ARE SUPERFICIAL)

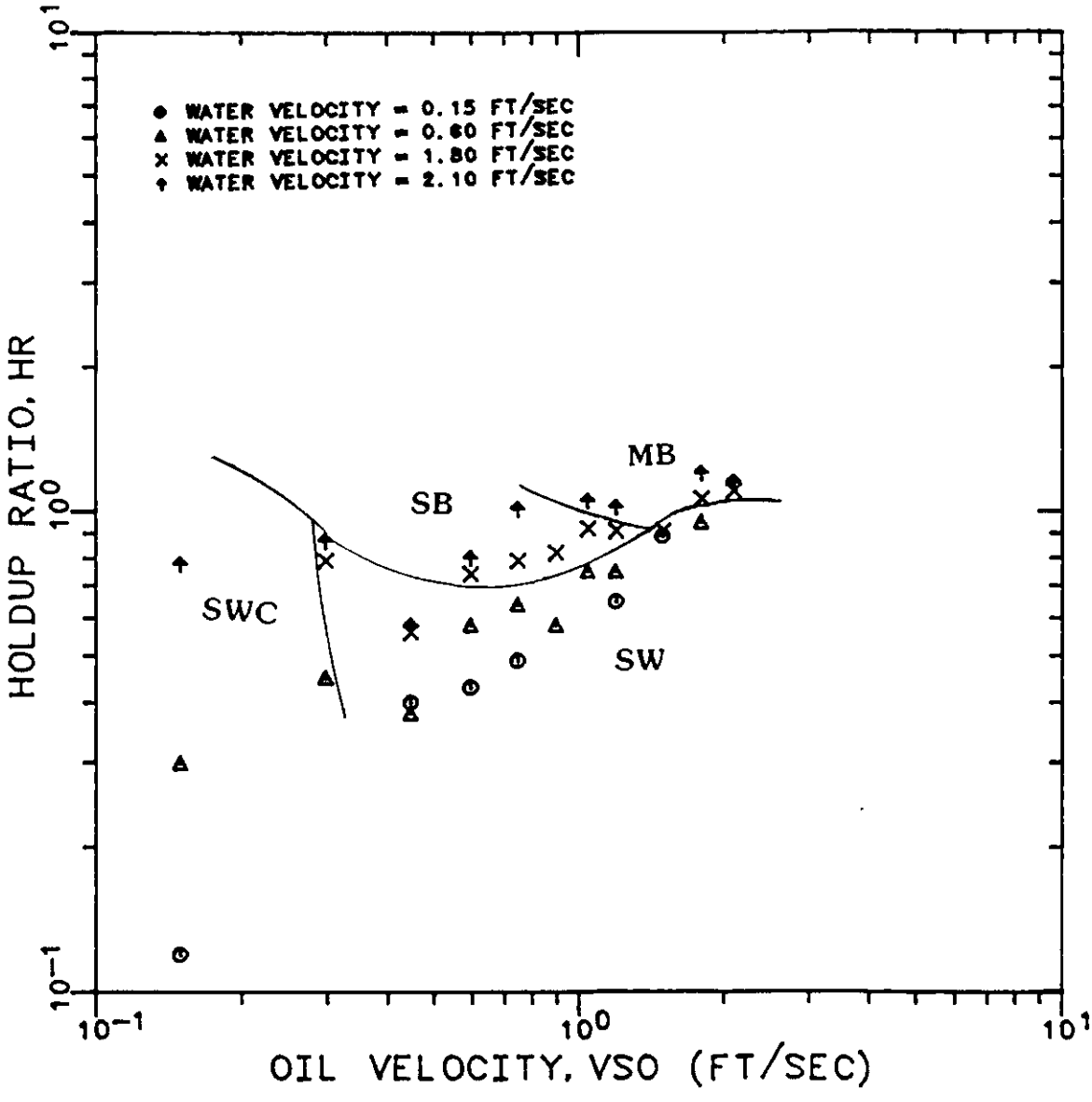

Figure 61

Holdup Ratio Compared to Flow Rate

Therefore, from the previous work, gravity seems to play an important part in the effect of inclination on the phase slippage in two phase flow. This phase slippage depends upon the possible flow regimes generated under the flowing conditions. When the flow regime is stratified, the date indicates that there is a greater slippage past the oil phase by the water phase. As the flow regime data trends toward massive bubble flow, the holdup ratio approaches 1.0 which shows that phase slippage is less severe.

Figure 62 shows a comparison of measured water holdup and water input fraction at horizontal. In the case of a constant water flow rate of 100 B/D, the water holdup is somewhat larger than the water input fraction which indicates that oil is slipping past the water. The slip velocity calculated for a water input fraction of .70 is approximately -0.23 ft/sec, which from the definition stated previously supports the premise that the oil is slipping past the water. When the water flow rate is increased to 400 B/D, the water holdups are approximately the same as the corresponding water input fractions. The slip velocity for this example (λ_w = .70) approximates 0 ft/sec. This indicate that the relative velocities are approximately the same, which implies that there is little or no slippage between the phases. However, when the water flow rates was increased to 700 B/D the input fraction of water was larger, in most cases, than the related measured holdup. The slip velocity calculated for this case (λ_w = .70) equals 0.47 ft/sec. This seems to indicate that the water was slipping past the oil phase.

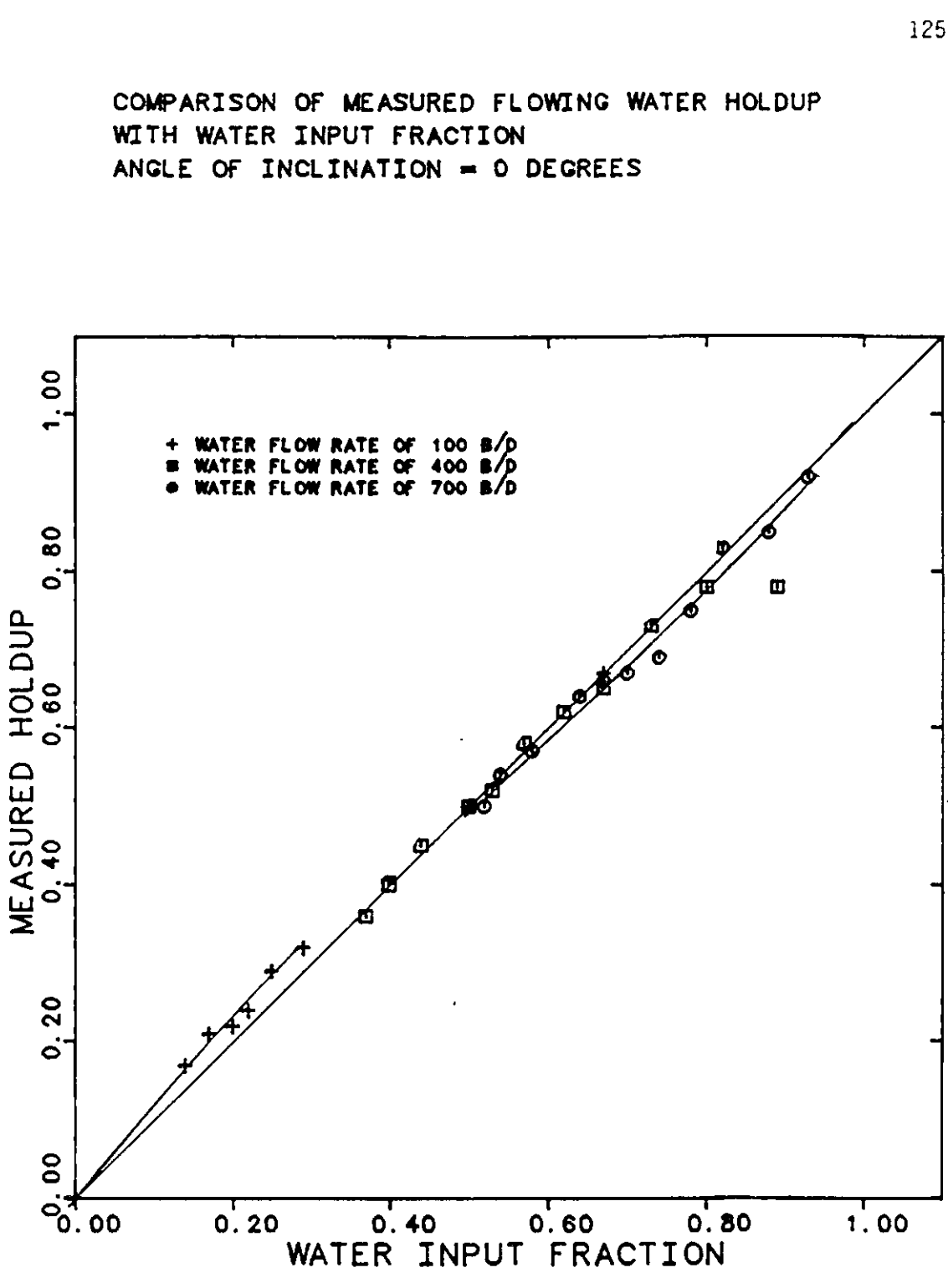

Figure 62

Comparison of Measured Flowing Water Holdup with Water Input Fraction

Next, the angle of inclination was changed to -15 degrees, the resulting plot of measured holdup vs. water input fraction is depicted in Figure 63. When the water flow rate was set at a constant value of 100 B/D, the resulting holdups were much less than the corresponding water input fractions. For this example, at a water input fraction of .67, the slip velocity calculated is 1.17 ft/sec. This shows that the water velocities are much greater than the oil velocities, therefore, slippage between the phases occurs. When the water flow rate was raised to a level of 400 B/D, the resulting trend line from the data indicates that the water phase is moving faster than the oil phase, but, the average velocity difference, slip velocity, which approximates 1.1 ft/sec in this case, is not as great as the slip velocity for the previous constant water flow rate. Finally, the flow rate of water was increased to 700 B/D, and the resulting data points shows that the slip velocity approximates .19 ft/sec at an input water fraction of .67 is the smallest for any of the cases. This means that the water phase is moving just a little faster than the oil phase which causes the measured holdup to be slightly less than the water input fraction.

For the comparison of measured water holdup with water input fraction, the angle of inclination was set at -30 degrees, with the results shown in Figure 64. Again, as detailed in the previous discussion with -15 degrees, the trend lines of the data points indicate slippage between the oil and water phases. When the flow rate of water was set at a constant rate of 50 B/D, the results exhibit a large slip velocity with the water moving much faster than the oil. This is borne out by the fact that the water holdups measured are much smaller than

COMPARISON OF MEASURED FLOWING WATER HOLDUP
WITH WATER INPUT FRACTION
ANGLE OF INCLINATION = -15 DEGREES

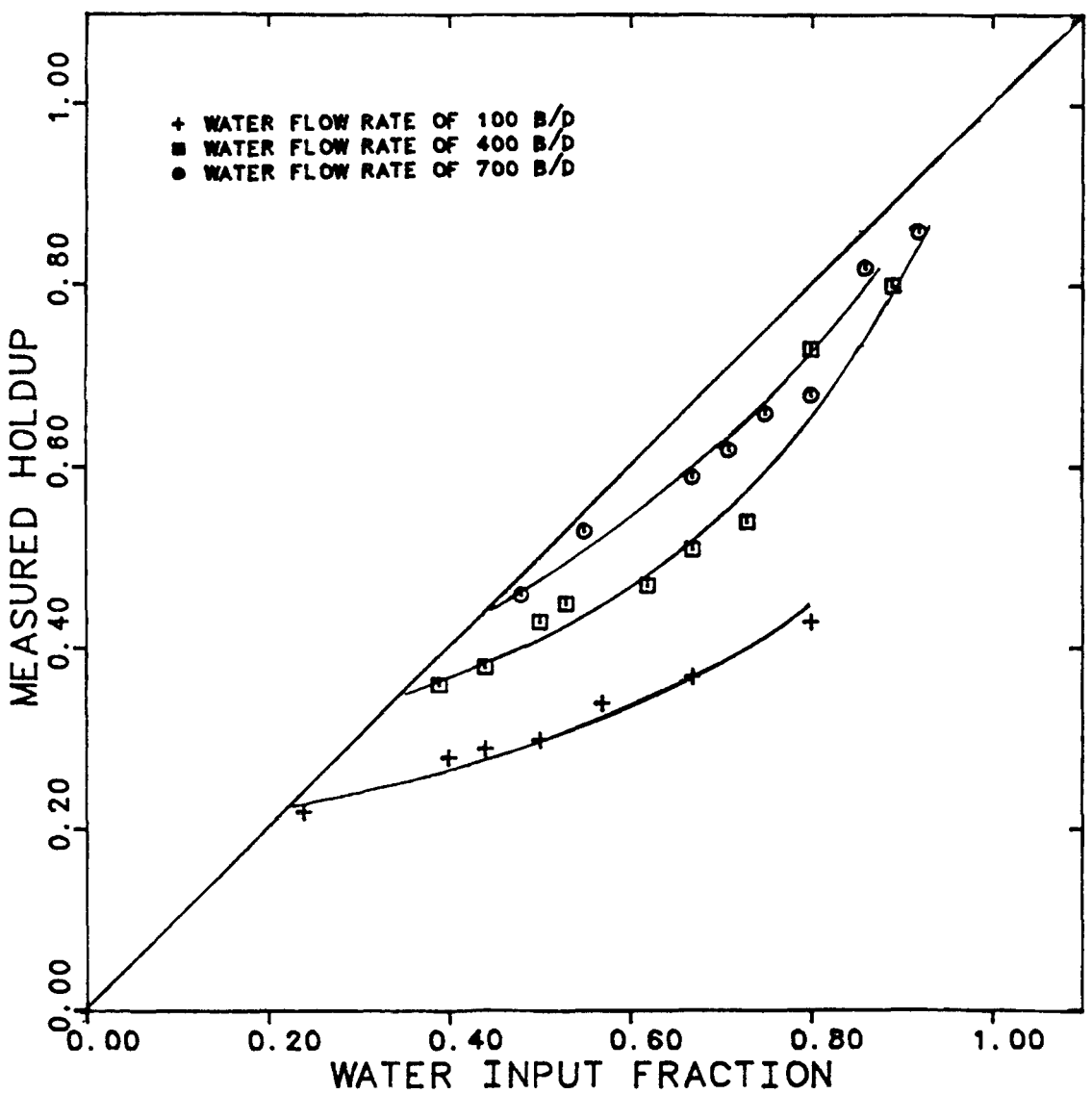

Figure 63

Comparison of Measured Flowing Water Holdup with Water Input Fraction

COMPARISON OF MEASURED FLOWING WATER HOLDUP
WITH WATER INPUT FRACTION
ANGLE OF INCLINATION = -30 DEGREES

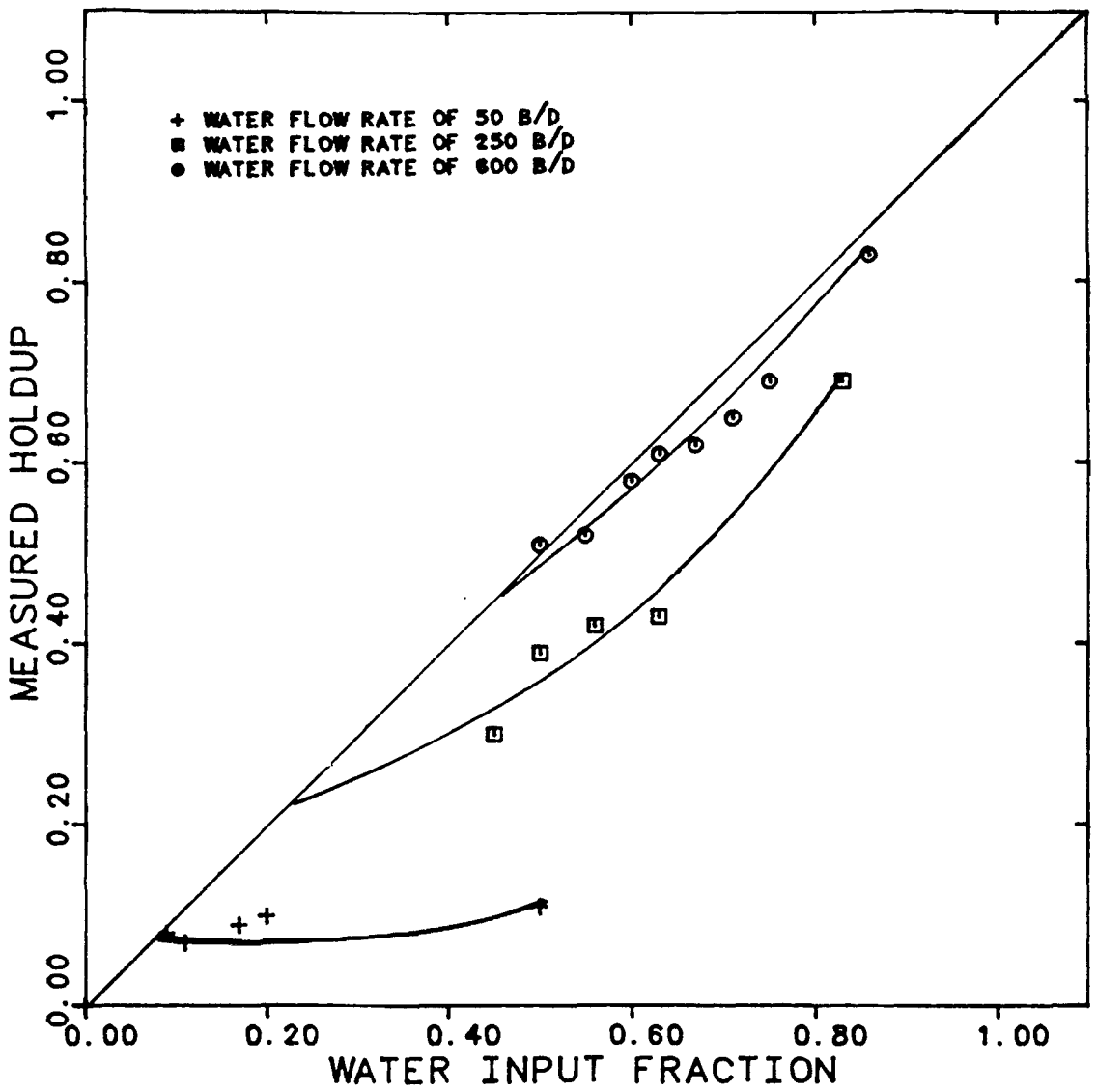

Figure 64

Comparison of Measured Flowing Water Holdup with Water Input Fraction

velocity. Finally, at a water rate of 600 B/D, the resulting holdups approach the associated input water fractions, which denotes that a very small slip velocity of .14 ft/sec is present.

the input water fractions and that the slip velocity for this case at an input water fraction of .50 approximates 1.2 ft/sec. At a constant water rate of 250 B/D, the results imply that there is still a slip velocity between the phases, which approximates .7 ft/sec at the same input water fraction, but is somewhat smaller than the previous slip

The observations just presented lead to the following conclusions: first, in horizontal flow, at smaller flow rates the oil phase "slips" past the water phase due to the fact that oil has a viscosity which is somewhat less than the viscosity for water; therefore, the oil has less of a drag, which will cause it to travel faster. Also, as the flow rate of water is increased, the measured holdups approach the input water fractions. When the angle of inclination is changed to downhill flow (-15 and -30 degrees), the trend reverses and the water phase "slips" past the oil phase. This is due, in part, to the gravity effect. It would, at first, seem logical that the data will indicate that as you increase the constant water flow rate, the flowing water holdup would decrease, since the higher rate would tend to increase the water velocity, thus, causing more slippage of water past the oil phase. However, as the previous data has shown, this is not the case, in fact, the exact opposite seems to be true. As the water flow rate is increased the holdup approaches the corresponding water input fraction. One possible explanation for this phenomena is based on the correlation of flow regimes with holdup. At the low flow

rates of 50 B/D and 100 B/D, the flow regime consists of stratified wavy flow, which was defined previously as distinct phase separation with a rippled or wavy interface. This type of pattern would allow the water phase to move freely past the oil phase at one point, the interface. Moreover, if the rates of water flow were increased to 400, 600 or 700 B/D, the flow patterns could change from stratified wavy to stratified bubble and then to massive bubble flow. This would create a situation where the water would flow as a continuous phase and therefore, more water would be in contact with the wall, thus causing a viscous drag which leads to a decrease in velocity and an increase in holdup. In fact, when massive bubble flow occurs at the higher flow rates, it could almost seem to display characteristics similar to single phase flow.

Mukherjee et al.[14] developed an empirical water holdup correlation for downhill flow using experimental data. A stepwise regression analysis procedure was applied to their generated data with the resulting holdup correlation:

$$H_w \text{ (downhill flow)} = 8.3763 \frac{\lambda_w^{1.2428} (\sin \theta)^{0.4947}}{N_{Re}^{0.2093}} \qquad (39)$$

A computer program, MBBCORR, is displayed in Appendix V along with the generated output. This program incorporates the holdup correlation with the experimental input parameters. The calculated holdup by this method was compared with the experimental holdup data at -15 and -30 degrees, respectively. The resulting plots are shown in Figure 65 and Figure 66. The total velocity of the oil and water varied from 1.95 to 2.45 ft/sec

in accordance with the guideline set by the authors, also horizontal flow data was not used since the sine function in the correlation would cause all holdup values to equal zero. Since the angles of interest used by Mukherjee et al. were -30 to -90 degrees, the correlation does not take into account inclination angles smaller than -30 degrees, where the authors stated that important slippage occurs, and that the correlation probably would lead to erroneous calculated water holdups. The purpose of this comparison of the Mukherjee et al. correlation to experimental holdups is to see if the correlation is close enough to give close, reasonable answers for the specific input parameters. The two plots comparing the calculated holdup with the experimental holdup indicated that there was not much agreement between the calculated and experimental holdup. In both cases, the calculated holdup was greater than the measured holdup. What seemed surprising was there seemed to be less agreement in the plot at -30 degrees than with the plot at -15 degrees, even though the correlation had included data obtained at -30 degrees. It would seem that a separate correlation should be developed at angles of inclinations smaller than -30 degrees since it has been observed that the most important slippage occurs at those important angles of inclination.

It was noted, however, that at low experimental holdup values, there was some agreement with the calculated holdup values. One possible reason for this is the fact that flow regimes in the experiments performed by Mukherjee, Brill and Beggs were dispersed and resembled single phase flow. The low holdups in the present experimentation were the result of high oil flow rates which create low

water holdups and this would tend to duplicate the situation under which the correlation equation was developed.

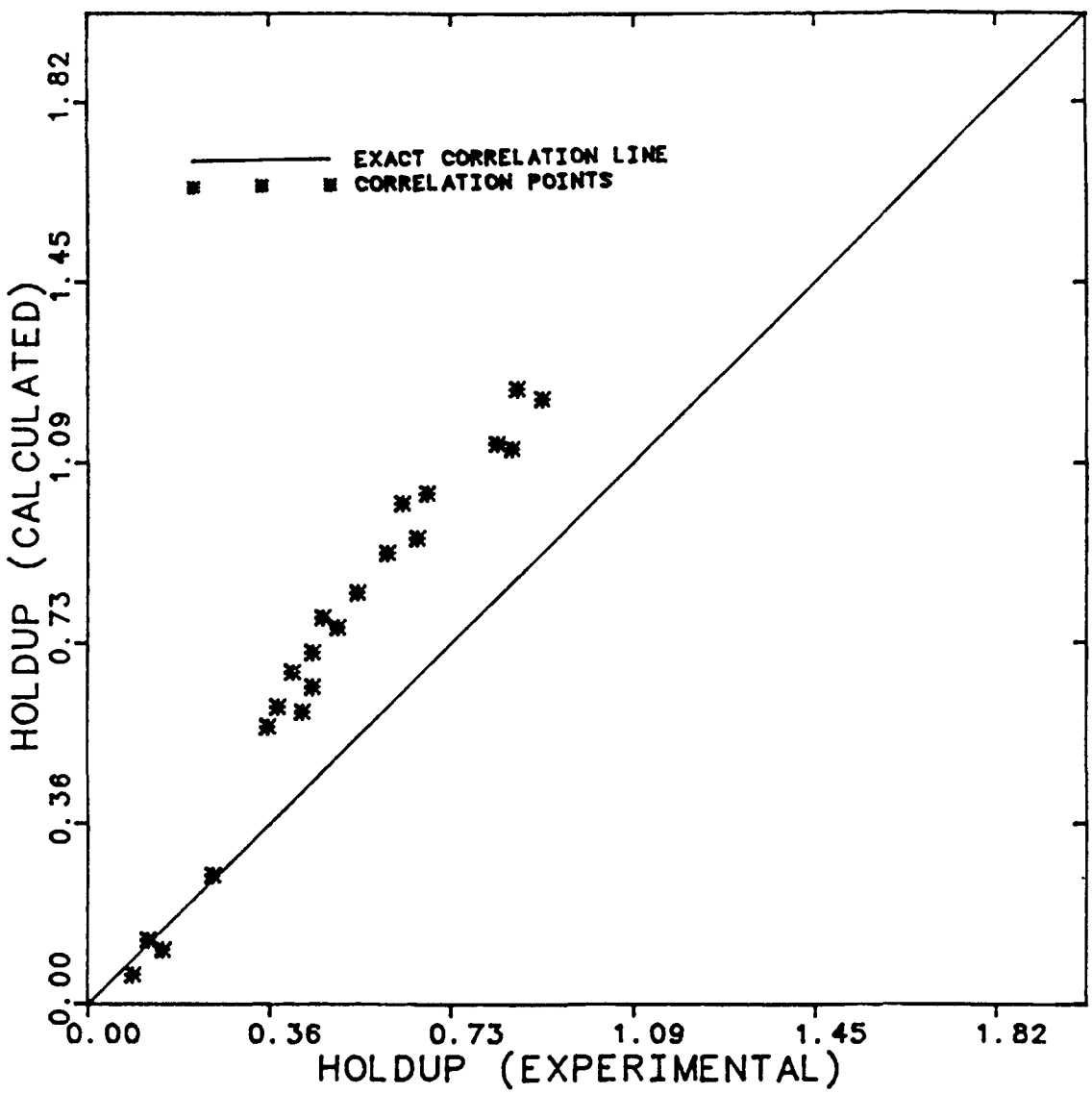

Figure 65

Comparison of Mukherjee, Brill and Beggs Holdup Correlation for Downhill Flow with Experimental Holdup Data

COMPARISON OF MUKHERJEE. BRILL AND BEGGS
HOLDUP CORRELATION FOR DOWNHILL FLOW
WITH EXPERIMENTAL HOLDUP DATA
ANGLE OF INCLINATION = -30 DEGREES

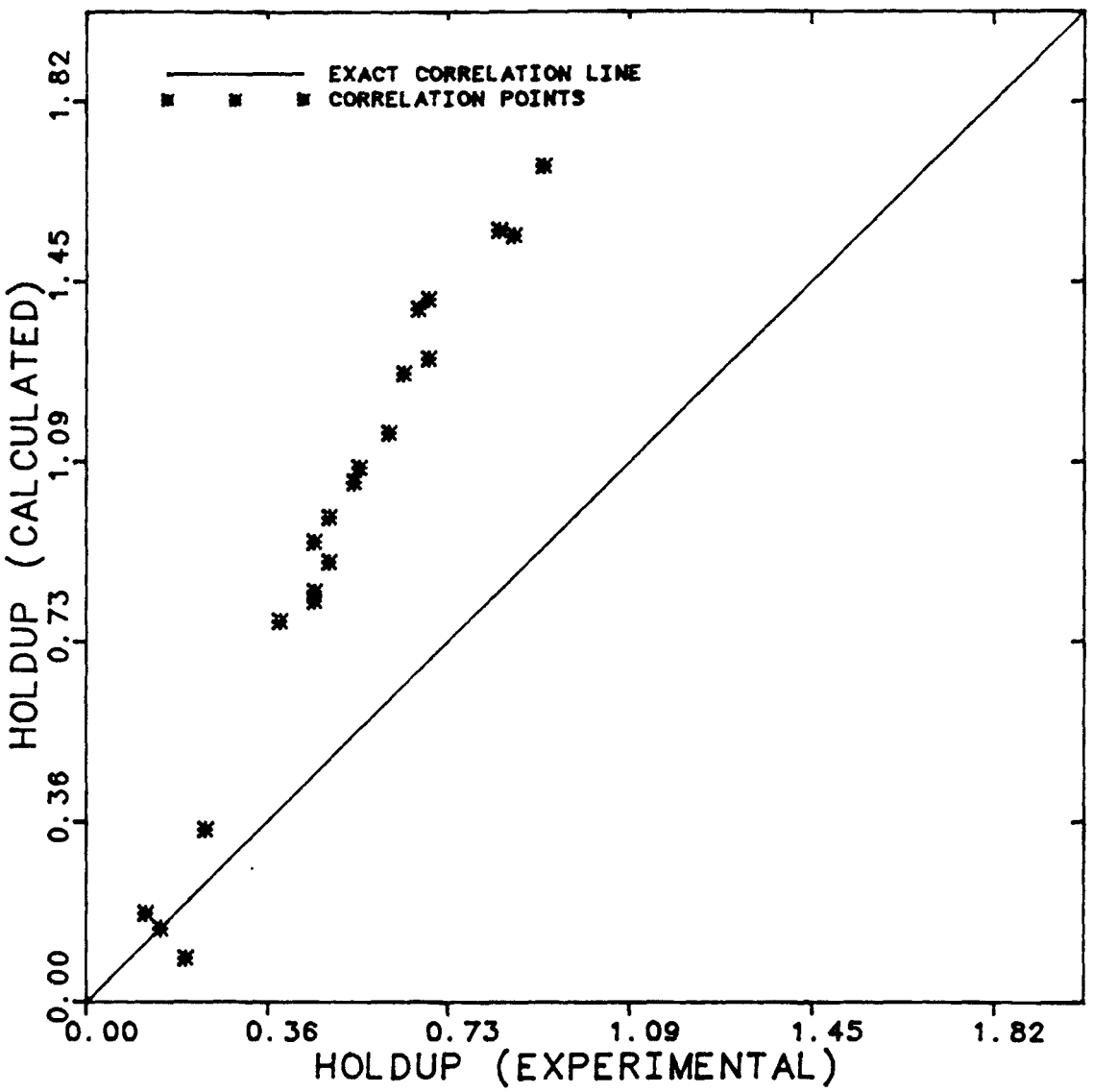

Figure 66

Comparison of Mukherjee, Brill and Beggs Holdup Correlation for Downhill Flow with Experimental Holdup Data

CHAPTER IV

CONCLUSIONS AND RECOMMENDATIONS

Conclusions

The present study of horizontal and downhill, two-phase, oil-water flow has led to several conclusions that the author considers important. The conclusions are limited to the range of data obtained and the type of liquids used. Use of the results to check with significantly different parameters; pipe sizes, oil densities and viscosities, inclination angle and flow rates is not advisable. The conclusions are:

(1) Flow regime formation is dependent on the angle of inclination of the flow system. The change from horizontal (0 degrees) to either -15 or -30 degrees will have the greatest effect on flow regime formation.

(2) The comparison of the experimental data to the Taitel and Dukler generalized gas-liquid flow map modified for liquid-liquid flow indicated that no feasible correlation exists with the present form of modification of the generalized, dimensionless variables.

(3) Water-oil slippage is a function of the inclination angle of the pipe and was highest at -15 degrees, which was between the two other inclination angles studied.

(4) Water holdup seems to be dependent on the flow regimes. Holdup approaches unity, at all inclination angles studied, when the flow regime becomes massive bubble, which consists of oil drops in a continuous water phase.

(5) Oil slippage past water in horizontal flow occurs at low water flow rates. At higher water rates the slippage becomes less severe, and at the highest water flow rates, there is almost no slippage.

(6) Gravity is a significant factor in causing increasing slip velocity and decreasing water holdup in downhill oil-water flow.

(7) Water will slip past the oil phase in downhill flow at low flow rates with a large slip velocity. As the flow rates of water increase, however, the slip velocity decreases, which indicates that there is less slippage between the oil and water and at maximum flow rates of water, there is almost no slip velocity.

(8) In both situations of downhill flow, -15 and -30 degrees, respectively, the experimental holdup did not correlate well with the calculated values from the Mukherjee et al. empirical, downhill water holdup correlation.

Recommendations

Future study of horizontal and downhill two-phase oil-water flow should be extended to cover the following:

(1) Future studies should vary more experimental parameters such as oil viscosity, oil density and pipe diameter to ensure a full understanding of the effect that changing conditions have on the formation and transition of flow regimes.

(2) Consideration should be given to the further study of the initial assumptions used in the mechanistic model for analytical prediction of transition between regimes developed by Taitel and Dukler to discover if any further assumptions or modifications are possible to completely transform the gas-liquid generalized dimensionless variables into usable liquid-liquid dimensionless variables.

(3) Future work involving oil-water flow should include the effects of flow regime formation and holdup on pressure drop.

(4) Future work should involve more angles of inclination between 0 and -30 degrees, respectively, since important slippage occurs at those angles.

(5) Future experimentation with oil-water systems should consider using diesel fuel instead of Soltrol 130 or any other type of light mineral oil because of the possibility of algae and bacteria growth which will

lead to replacement of the oil supply and the need for separate storage of the oil and water which will be impractical.

APPENDIX I

Modification of Generalized Flow Regime Dimensionless Groups Developed by Taitel et al. for the Present Flow System

The generalized flow regime map dimensionless groups developed by Taitel and Dukler will be modified for testing on the flow system now being used.

The following is a check to see if these dimensionless groups are applicable to the system.

Taitel et al. used this friction factor equation

$$f = \frac{0.046}{(N_{Re})^{0.2}} \qquad \text{for } 2.1\times10^3 < N_{Re} < 10^5 \tag{A1-1}$$

where $$f = \tfrac{1}{4}\left(\frac{D}{L}\right)\frac{\Delta P}{\frac{1}{2}\rho \bar{v}^2} \qquad N_{Re} = \frac{\bar{D}v\rho}{\mu} = \frac{\bar{D}v}{\nu} \tag{A1-2}$$

The dimensionless variables used are:

$$X = \left[\frac{(dP/dx)_L^S}{(dP/dx)_G^S}\right]^{\frac{1}{2}} \tag{A1-3}$$

$$T = \left[\frac{|(dP/dx)_L^S|}{(\rho_L - \rho_G)g\cos\alpha}\right]^{\frac{1}{2}} \tag{A1-4}$$

$$Y = \frac{(\rho_L - \rho_G)g\sin\alpha}{|(dP/dx)_G^S|} \tag{A1-5}$$

$$F = \frac{\rho_G}{\sqrt{\rho_L - \rho_G}} \quad \frac{U_G^S}{\sqrt{D\ g\ \cos\alpha}} \tag{A1-6}$$

$$K = F \left(\frac{D\ U_L^S}{\nu_L} \right)^{\frac{1}{2}} = F\ [(R_e)_L^S]^{\frac{1}{2}} \tag{A1-7}$$

Now, check to see if the Blassius equation is applicable in the flow rates of interest; 0 → 2000 B/D. The pipe diameter (D) is 2-inch ID.

$$N_{Re} = \frac{\bar{v}D}{\nu} \quad \text{where } \bar{v} = \frac{Q}{A} \quad \text{and } A = (\pi/4)\ D^2 = 0.02182\ ft^2$$

From the data sheet of the oil used, Soltrol 130, in Table III:

ν_o (32 degrees F) = 2.775 cs = 2.581 ft²/D

ν_o (100 degrees F) = 1.358 cs = 1.263 ft²/D

Assuming the kinematic viscosity of the oil behaves as a linear function:

At the experimental temperature of 77 degrees F,

$$\nu_o = 1.709\ ft^2/D$$

For N_{Re} = 2100 = $\frac{Q_o D}{\nu_o}$

therefore, Q = 126 B/D

It follows that for ν_o = 2.775 cs, when N_{Re} = 10^5, then Q_o = 6018 B/D and when N_{Re} = 2100, then Q_o = 61.8 B/D.

Similarly, when ν_o = 1.358 cs,

and N_{Re} = 10^5, Q = 2944 B/D

when N_{Re} = 2100, Q = 61.9 B/D.

Now, for the oil,

$$f_o = \frac{0.046}{(N_{Re})^{0.20}} = \frac{0.046}{((D\bar{v})/\nu)} \qquad \text{with } \bar{v} = Q_o/A$$

Q_o needs to be in B/D

Therefore $$f_o = \frac{0.046}{[(D/A)(Q_o/\nu_o]^{0.20}}$$

Simplifying down to a convenient form,

$$f_o = \frac{0.024}{(Q_o)^{0.2}} \qquad \text{(A1-8)}$$

Now, for water, the Blassius equation will be the same. However, the kinematic viscosity at 77 degrees F is

$$\nu_w = 0.9935 \text{ cs} = 0.924 \text{ ft}^2/\text{D}$$

Similarly, with all other parameters being the same, the equation will simplify down to

$$f_w = \frac{0.0214}{(Q_w)^{0.2}} \qquad \text{(A1-9)}$$

From the previous work,

$$x = \left[\frac{(dP/dx)_w^S}{(dP/dx)_o^S} \right]^{\frac{1}{2}}$$

with w = water and o = oil

$$f = \tfrac{1}{4} \left(\frac{D}{L} \right) \frac{\Delta P}{\frac{1}{2} \rho \bar{v}^2}$$

then $\Delta P/L \cong dP/dx = (2f\rho\bar{v}^2)/D$

so $(dP/dx)_w^S = (2 f_w \rho_w \bar{v}_w^2)/D$

with ρ_w (77 degrees F) = 62.24 lbm/ft^3

Q_w must be in B/D, therefore,

$$(dP/dx)_w^S = 1.418 \times 10^{-4} (Q_w^2/Q_w^{0.2}) (\text{lbm/ft}^2\text{sec}^2))$$

Since the answer in units of lbf/ft^3 is preferred, $(dP/dx)_w^S$ must be divided by g_c,

therefore,

$$(dP/dx)_w^S = 4.407 \times 10^{-6} Q_w^{1.8} \text{ lbf/ft}^3$$

Since every variable in the equation for $(dP/dx)_o^S$ is the same as $(dP/dx)_w^S$ except for viscosity and density, (ν_o = 1.709 ft^2/D and ρ_o = 47.0 lbm/ft^3)

therefore, $(dP/dx)_o^S = (2 f_o \rho_o \bar{v}^2)/D$

Similarly, $(dP/dx)_o^S = 3.732 \times 10^{-6} Q_o^{1.8}$ lbf/ft^3

Now to simplify the generalized form for X,

$$X = \left[\frac{(dP/dx)_w^S}{(dP/dx)_o^S} \right]^{\frac{1}{2}} = \left[\frac{4.407 \times 10^{-6} Q_w^{1.8} \text{lbf/ft}^3}{3.732 \times 10^{-6} Q_o^{1.8} \text{lbf/ft}^3} \right]^{\frac{1}{2}}$$

Now in a reduced form,

$$X = 1.09 \, (Q_w/Q_o)^{0.9} \tag{A1-10}$$

Accordingly,

$$T = \left[\frac{|(dP/dx)_w^S|}{(\rho_w - \rho_o) g \cos \alpha} \right]^{\frac{1}{2}}$$

in a simplified form,

$$T = \frac{5.367 \times 10^{-4} Q_w^{0.9}}{\sqrt{\cos \alpha}} \tag{A1-11}$$

Next, Y is reduced into a similar form as in previous examples.

$$Y = \frac{(\rho_w - \rho_o) g \sin \alpha}{|(dP/dx)_o^S|}$$

is then reduced to

$$Y = 4.06 \times 10^6 \quad \frac{\sin \alpha}{Q_o^{1.8}} \tag{A1-12}$$

Similarly, F is reduced down to a simple form from:

$$F = \frac{\rho_o}{\sqrt{\rho_w - \rho_o}} \quad \frac{U_G^S}{\sqrt{D \, g \cos \alpha}}$$

$$\text{to } F = 0.0023 \quad \frac{Q_o}{\sqrt{\cos \alpha}} \tag{A1-13}$$

Finally,

$$K = F \left(\frac{D\, U_w^S}{\nu_w} \right)^{\frac{1}{2}} \quad \text{with} \quad U_w^S = \frac{Q_w}{A}$$

therefore substituting for the appropriate parameters,

$$K = 0.01533 \quad \frac{Q_o\, Q_w 0.5}{\sqrt{\cos \alpha}} \tag{A1-14}$$

In summary:

$$X = 1.09\, (Q_w/Q_o)^{0.9}$$

$$T = \frac{5.367 \times 10^{-4} Q_w^{0.9}}{\sqrt{\cos \alpha}}$$

$$Y = 4.06 \times 10^{6} \quad \frac{\sin \alpha}{Q_o^{1.8}}$$

$$F = 0.0023 \quad \frac{Q_o}{\sqrt{\cos \alpha}}$$

$$K = 0.01533 \quad \frac{Q_o\, Q_w 0.5}{\sqrt{\cos \alpha}}$$

These dimensionless groups will incorporate the data gathered from the flow system to generate a dimensionless flow regime map for liquid-liquid flow. This map should be similar to the map generated by Taitel and Dukler for gas-liquid flow.

The following computer program, FMAP, calculates the dimensionless parameters X, T, Y, F and K used by Taitel and Dukler in creating their generalized flow regime map, using the data from the present experimentation.

```
      PROGRAM FMAP(INPUT,OUTPUT,TAPE5=INPUT,TAPE6=OUTPUT)
C*****************************************************************
C                                                                *
C PURPOSE:                                                       *
C                                                                *
C  PROGRAM FMAP CALCULATES THE DIMENSIONLESS PARAMETERS X,T,Y,F AND *
C  K USED BY TAITEL AND DUKLER (ALCHE J. 1976) IN CREATING THEIR  *
C  GENERALIZED FLOW REGIME MAP.  THESE PARAMETERS WERE DEVELOPED  *
C  FOR USE WITH THE FLOW SYSTEM USED IN THE PRESENT EXPERIMENTATION *
C                                                                *
C INPUT PARAMETERS:                                              *
C                                                                *
C  QOIL     -  FLOW RATE OF OIL, B/D                            *
C  QWATER   -  FLOW RATE OF WATER, B/D                          *
C  ANGLE    -  ANGLE OF INCLINATION, DEGREES                    *
C  FR       -  FLOW REGIME OBSERVED AT GIVEN FLOW RATES         *
C                                                                *
C  OUTPUT PARAMETERS:                                            *
C                                                                *
C  QOIL     -  FLOW RATE OF OIL, B/D                            *
C  QWATER   -  FLOW RATE OF WATER, B/D                          *
C  ANGLE    -  ANGLE OF INCLINATION, DEGREES                    *
C  X        -  DIMENSIONLESS MARTINELLI PARAMETER               *
C  T        -  DIMENSIONLESS DISPERSED BUBBLE FLOW PARAMETER    *
C  Y        -  DIMENSIONLESS INCLINATION PARAMETER              *
C  K        -  DIMENSIONLESS WAVY FLOW PARAMETER                *
C  FR       -  FLOW REGIME OBSERVED AT GIVEN FLOW RATES         *
C                                                                *
C*****************************************************************
      REAL QWATER(1000),QOIL(1000),ANGLE(1000)
      REAL X(1000),T(1000),Y(1000),F(1000),K(1000)
      INTEGER FR(1000)
C-----------------------------------------------------------------
C     NUMBER OF OIL AND WATER FLOW RATES
C-----------------------------------------------------------------
      N=363
C-----------------------------------------------------------------
C     CALCULATION OF OUTPUT PARAMETERS
C-----------------------------------------------------------------
      DO 7 I=1,N
        READ(5,10)QOIL(I),QWATER(I),ANGLE(I),FR(I)
        ANGLE(I)=-(ANGLE(I)*3.14/180.0)
        X(I)=1.08*(QWATER(I)/QOIL(I))**(0.9)
        T(I)=(0.0005367*(QWATER(I)**0.9))/(COS(ANGLE(I))**0.5)
        Y(I)=(4110000.0*SIN(ANGLE(I)))/(QOIL(I)**1.80)
        F(I)=(0.00225*QOIL(I))/(COS(ANGLE(I))**0.5)
        K(I)=(0.01533*QOIL(I)*(QWATER(I)**0.5))/(COS(ANGLE(I))**0.5)
        ANGLE(I)=-(ANGLE(I)*180/3.14)
      CONTINUE
```

```
      II=1
      NCOUNT=1
      DO 8 J=1,7
        WRITE(6,20)
         DO 6 II=II,NCOUNT*48
C-------------------------------------------------------------------------
C     PRINT OUT CALCULATED VALUES
C-------------------------------------------------------------------------
            WRITE(6,30) QOIL(II),QWATER(II),ANGLE(II),X(II),T(II),Y(II),
     $      F(II),K(II),FR(II)
         CONTINUE
      II=NCOUNT*(48)
      NCOUNT=NCOUNT+1
      CONTINUE
C-------------------------------------------------------------------------
C     FORMAT STATEMENTS
C-------------------------------------------------------------------------
      FORMAT(F6.1,F6.1,F6.1,A5,F6.1)
      FORMAT(1H1,T5,*QOIL*,T15,*QWATER*,T26,*ANGLE*,T39,*X*,
     $T49,*T*,T59,*Y*,T68,*F*,T77,*K*,T85,*OBSERVED FLOW REGIME*,/,
     $T5,4(*-*),T15,6(*-*),T26,5(*-*),T38,4(*-*),T48,3(*-*),T58,3(*-*),
     $T58,3(*-*),T67,3(*-*),T75,5(*-*),T85,20(*-*),)
      FORMAT(1X,T3,F6.1,T14,F6.1,T26,F5.1,T36,F6.2,T45,F6.2,
     $T54,F8.2,T64,F6.2,T75,F6.2,T93,A5)
      END
```

SOIL	WATER	ANGLE	X	T	V	F	K	OBSERVED FLOW REGIME
50.0	50.0	0	1.08	.02	0	11	5.42	##
50.0	100.0	0	2.02	.03	0	11	7.67	##
50.0	150.0	0	2.90	.05	0	11	9.39	##
50.0	200.0	0	3.76	.06	0	11	10.84	##
50.0	250.0	0	4.60	.08	0	11	12.12	##
50.0	300.0	0	5.42	.09	0	11	13.28	##
50.0	350.0	0	6.22	.10	0	11	14.34	##
50.0	400.0	0	7.02	.12	0	11	15.33	##
50.0	500.0	0	8.58	.14	0	11	17.14	##
50.0	600.0	0	10.11	.17	0	11	18.78	##
50.0	700.0	0	11.61	.20	0	11	20.28	##
100.0	50.0	0	.58	.02	0	23	10.84	##
100.0	100.0	0	1.08	.03	0	23	15.33	##
100.0	150.0	0	1.56	.05	0	23	18.78	##
100.0	200.0	0	2.02	.06	0	23	21.68	##
100.0	250.0	0	2.46	.08	0	23	24.24	##
100.0	300.0	0	2.90	.09	0	23	26.55	##
100.0	350.0	0	3.33	.10	0	23	28.68	##
100.0	400.0	0	3.76	.12	0	23	30.66	##
100.0	500.0	0	4.60	.14	0	23	34.28	##
100.0	600.0	0	5.42	.17	0	23	37.55	##
100.0	700.0	0	6.22	.20	0	23	40.56	##
150.0	50.0	0	.40	.02	0	34	16.26	##
150.0	100.0	0	.75	.03	0	34	23.00	##
150.0	150.0	0	1.08	.05	0	34	28.16	##
150.0	200.0	0	1.40	.06	0	34	32.52	##
150.0	250.0	0	1.71	.08	0	34	36.36	##
150.0	300.0	0	2.02	.09	0	34	39.83	##
150.0	350.0	0	2.32	.10	0	34	43.02	##
150.0	400.0	0	2.61	.12	0	34	45.99	##
150.0	500.0	0	3.19	.14	0	34	51.42	##
150.0	600.0	0	3.76	.17	0	34	56.33	##
150.0	700.0	0	4.32	.20	0	34	60.84	##
200.0	50.0	0	.31	.02	0	45	21.68	##
200.0	100.0	0	.58	.03	0	45	30.66	##
200.0	150.0	0	.83	.05	0	45	37.55	##
200.0	200.0	0	1.08	.06	0	45	43.36	##
200.0	250.0	0	1.32	.08	0	45	48.48	##
200.0	300.0	0	1.56	.09	0	45	53.10	##
200.0	350.0	0	1.79	.10	0	45	57.36	##
200.0	400.0	0	2.02	.12	0	45	61.32	##
200.0	500.0	0	2.46	.14	0	45	68.56	##
200.0	600.0	0	2.90	.17	0	45	75.10	##
200.0	700.0	0	3.33	.20	0	45	81.12	##
250.0	50.0	0	.25	.02	0	56	27.10	##
250.0	100.0	0	.47	.03	0	56	38.32	##
250.0	150.0	0	.68	.05	0	56	46.94	##
250.0	200.0	0	.88	.06	0	56	54.20	##
250.0	250.0	0	1.08	.08	0	56	60.60	##
250.0	300.0	0	1.27	.09	0	56	66.38	##
250.0	350.0	0	1.46	.10	0	56	71.70	##
250.0	400.0	0	1.65	.12	0	56	76.65	##
250.0	500.0	0	2.02	.14	0	56	85.70	##
250.0	600.0	0	2.37	.17	0	56	93.88	##
250.0	700.0	0	2.73	.20	0	56	101.40	##
300.0	50.0	0	.22	.02	0	68	32.52	##
300.0	100.0	0	.40	.03	0	68	45.99	##
300.0	150.0	0	.58	.05	0	68	56.33	##
300.0	200.0	0	.75	.06	0	68	65.04	##
300.0	250.0	0	.92	.08	0	68	72.72	##

OOIL	OWATER	ANOLE	X	T	Y	F	K	OBSERVED FLOW REGIME
300.0	250.0	0	.92	.08	0	66	72 72	SW
300.0	300.0	0	1.08	.09	0	66	79.66	SW
300 0	350.0	0	1.24	.10	0	66	86.04	SW
300.0	400.0	0	1.40	12	0	66	91 98	SW
300.0	500.0	0	1.71	14	0	66	102 84	SW
300.0	600.0	0	2.02	17	0	66	112 65	SB
300.0	700.0	0	2.32	20	0	66	121.68	SB
350.0	50.0	0	19	02	0	79	37 94	SW
350.0	100.0	0	35	.03	0	79	53 65	SW
350.0	150 0	0	50	05	0	79	65 71	SW
350.0	200.0	0	.65	.06	0	79	75 88	SW
350.0	250.0	0	.80	.08	0	79	84.84	SW
350.0	300.0	0	.94	09	0	79	72 93	SW
350 0	350.0	0	1.08	.10	0	79	100 38	SW
350.0	400.0	0	1.22	12	0	79	107.31	SW
350.0	500.0	0	1.49	.14	0	79	119.98	SB
350.0	600.0	0	1.75	.17	0	79	131.43	SB
350.0	700.0	0	2.02	20	0	79	141.96	SB
400.0	50.0	0	17	02	0	90	43 36	SW
400.0	100.0	0	.31	03	0	90	61 32	SW
400.0	150.0	0	.45	.05	0	90	75.10	SW
400.0	200.0	0	58	.06	0	90	86.72	SW
400.0	250.0	0	71	.08	0	90	96 96	SW
400.0	300.0	0	.83	09	0	90	106 21	SW
400.0	350.0	0	.96	.10	0	90	114 72	SW
400.0	400.0	0	1.08	.12	0	90	122 64	SW
400.0	500.0	0	1.32	.14	0	90	137.12	SB
400.0	600.0	0	1.56	.17	0	90	150.20	SB
400.0	700.0	0	1.79	.20	0	90	162.24	SB
500.0	50.0	0	.14	.02	0	1.13	54.20	SW
500.0	100.0	0	.25	.03	0	1.13	76.65	SW
500.0	150.0	0	.37	.05	0	1.13	93.88	SW
500.0	200.0	0	.47	.06	0	1.13	108.40	SW
500.0	250.0	0	.58	.08	0	1.13	121.19	SW
500.0	300.0	0	.68	.09	0	1.13	132.76	SW
500.0	350.0	0	.78	.10	0	1.13	143.40	SW
500.0	400.0	0	.88	.12	0	1.13	153.30	SB
500.0	500.0	0	1.08	.14	0	1.13	171.39	SB
500.0	600.0	0	1.27	.17	0	1.13	187.75	SB
500.0	700.0	0	1.46	.20	0	1.13	202.80	SB
400.0	50.0	0	.12	.02	0	1.35	65.04	SW
400.0	100.0	0	.22	.03	0	1.35	91.98	SW
400.0	150.0	0	.31	.05	0	1.35	112.65	SW
400.0	200.0	0	.40	.06	0	1.35	130.08	SW
400.0	250.0	0	.49	.08	0	1.35	145.43	SW
400.0	300.0	0	.58	.09	0	1.35	159.31	SW
400.0	350.0	0	.66	.10	0	1.35	172.08	SB
400.0	400.0	0	.75	.12	0	1.35	183.96	SB
400.0	500.0	0	.92	.14	0	1.35	205.67	SB
400.0	600.0	0	1.08	.17	0	1.35	225.30	SB
400.0	700.0	0	1.24	.20	0	1.35	243.36	SB
700.0	50.0	0	.10	.02	0	1.58	75.88	SW
700.0	100.0	0	.19	.03	0	1.58	107.31	SW
700.0	150.0	0	.27	.05	0	1.58	131.43	SW
700.0	200.0	0	.35	.06	0	1.58	151.76	SW
700.0	250.0	0	.43	.08	0	1.58	169.67	SW
700.0	300.0	0	.50	.09	0	1.58	185.87	SW
700.0	350.0	0	.58	.10	0	1.58	200.76	SB
700.0	400.0	0	.65	.12	0	1.58	214.62	SB
700.0	500.0	0	.80	14	0	1 58	239 95	SB

OIL	WATER	ANGLE	X	T	V	F	K	OBSERVED FLOW REGIME
700.0	600.0	0	.94	.17	0	1.00	262.85	MB
700.0	700.0	0	1.08	.20	0	1.00	283.92	MB
50.0	50.0	-15.0	1.08	.02	929.99	11	5.51	SW
50.0	100.0	-15.0	2.02	.03	929.99	11	7.80	SW
50.0	150.0	-15.0	2.90	.05	929.99	11	9.55	SWC
50.0	200.0	-15.0	3.76	.06	929.99	11	11.03	SWC
50.0	250.0	-15.0	4.60	.08	929.99	11	12.33	SWC
50.0	300.0	-15.0	5.42	.09	929.99	11	13.51	SWC
50.0	350.0	-15.0	6.22	.11	929.99	11	14.59	SWC
50.0	400.0	-15.0	7.02	.12	929.99	11	15.60	SWC
50.0	500.0	-15.0	8.58	.15	929.99	11	17.44	SWC
50.0	600.0	-15.0	10.11	.17	929.99	11	19.10	SWC
50.0	700.0	-15.0	11.61	.20	929.99	11	20.63	SW
100.0	50.0	-15.0	.58	.02	267.07	23	11.03	SW
100.0	100.0	-15.0	1.08	.03	267.07	23	15.60	SW
100.0	150.0	-15.0	1.56	.05	267.07	23	19.10	SW
100.0	200.0	-15.0	2.02	.06	267.07	23	22.06	SWC
100.0	250.0	-15.0	2.46	.08	267.07	23	24.66	SWC
100.0	300.0	-15.0	2.90	.09	267.07	23	27.02	SWC
100.0	350.0	-15.0	3.33	.11	267.07	23	29.18	SWC
100.0	400.0	-15.0	3.76	.12	267.07	23	31.20	SWC
100.0	500.0	-15.0	4.60	.15	267.07	23	34.88	SW
100.0	600.0	-15.0	5.42	.17	267.07	23	38.21	SW
100.0	700.0	-15.0	6.22	.20	267.07	23	41.27	SB
150.0	50.0	-15.0	.40	.02	128.72	.34	16.54	SW
150.0	100.0	-15.0	.75	.03	128.72	.34	23.40	SW
150.0	150.0	-15.0	1.08	.05	128.72	.34	28.65	SW
150.0	200.0	-15.0	1.40	.06	128.72	.34	33.09	SW
150.0	250.0	-15.0	1.71	.08	128.72	.34	36.99	SW
150.0	300.0	-15.0	2.02	.09	128.72	.34	40.52	SW
150.0	350.0	-15.0	2.32	.11	128.72	.34	43.77	SW
150.0	400.0	-15.0	2.61	.12	128.72	.34	46.79	SW
150.0	500.0	-15.0	3.19	.15	128.72	.34	52.32	SW
150.0	600.0	-15.0	3.76	.17	128.72	.34	57.31	SW
150.0	700.0	-15.0	4.32	.20	128.72	.34	61.90	SB
200.0	50.0	-15.0	.31	.02	76.70	.46	22.06	SW
200.0	100.0	-15.0	.58	.03	76.70	.46	31.20	SW
200.0	150.0	-15.0	.83	.05	76.70	.46	38.21	SW
200.0	200.0	-15.0	1.08	.06	76.70	.46	44.12	SW
200.0	250.0	-15.0	1.32	.08	76.70	.46	49.32	SW
200.0	300.0	-15.0	1.56	.09	76.70	.46	54.03	SW
200.0	350.0	-15.0	1.79	.11	76.70	.46	58.36	SW
200.0	400.0	-15.0	2.02	.12	76.70	.46	62.39	SW
200.0	500.0	-15.0	2.46	.15	76.70	.46	69.76	SW
200.0	600.0	-15.0	2.90	.17	76.70	.46	76.41	SW
200.0	700.0	-15.0	3.33	.20	76.70	.46	82.54	SB
250.0	50.0	-15.0	.25	.02	51.33	.57	27.57	SW
250.0	100.0	-15.0	.47	.03	51.33	.57	38.99	SW
250.0	150.0	-15.0	.68	.05	51.33	.57	47.76	SW
250.0	200.0	-15.0	.88	.06	51.33	.57	55.15	SW
250.0	250.0	-15.0	1.08	.08	51.33	.57	61.66	SW
250.0	300.0	-15.0	1.27	.09	51.33	.57	67.54	SW
250.0	350.0	-15.0	1.46	.11	51.33	.57	72.95	SW
250.0	400.0	-15.0	1.65	.12	51.33	.57	77.99	SW
250.0	500.0	-15.0	2.02	.15	51.33	.57	87.19	SW
250.0	600.0	-15.0	2.37	.17	51.33	.57	95.52	SB
250.0	700.0	-15.0	2.73	.20	51.33	.57	103.17	SB
300.0	50.0	-15.0	.22	.02	36.97	.69	33.09	SW
300.0	100.0	-15.0	.40	.03	36.97	.69	46.79	SW
300.0	150.0	-15.0	.58	.05	36.97	.69	57.31	SW

QOIL	QWATER	ANGLE	X	T	Y	F	K	OBSERVED FLOW REGIME
300.0	200.0	-15.0	.75	.06	36.97	.69	66.18	SW
300.0	250.0	-15.0	.92	.08	36.97	.69	73.99	SW
300.0	300.0	-15.0	1.08	.09	36.97	.69	81.05	SW
300.0	350.0	-15.0	1.24	11	36.97	.69	87.54	SW
300.0	400.0	-15.0	1.40	12	36.97	.69	93.59	SW
300.0	500.0	-15.0	1.71	15	36.97	.69	104.63	SW
300.0	600.0	-15.0	2.02	17	36.97	.69	114.62	SB
300.0	700.0	-15.0	2.32	20	36.97	.69	123.80	SB
350.0	50.0	-15.0	.19	02	28.01	.80	38.60	SW
350.0	100.0	-15.0	.35	03	28.01	.80	54.59	SW
350.0	150.0	-15.0	.50	05	28.01	.80	66.86	SW
350.0	200.0	-15.0	.65	06	28.01	.80	77.21	SW
350.0	250.0	-15.0	.80	08	28.01	.80	86.32	SW
350.0	300.0	-15.0	.94	.09	28.01	.80	94.56	SW
350.0	350.0	-15.0	1.08	11	28.01	.80	102.13	SW
350.0	400.0	-15.0	1.22	12	28.01	.80	109.18	SW
350.0	500.0	-15.0	1.49	15	28.01	.80	122.07	SW
350.0	600.0	-15.0	1.75	.17	28.01	.80	133.72	SB
350.0	700.0	-15.0	2.02	20	28.01	.80	144.44	SB
400.0	50.0	-15.0	.17	02	22.02	.92	44.12	SW
400.0	100.0	-15.0	.31	.03	22.02	.92	62.39	SW
400.0	150.0	-15.0	.45	.05	22.02	.92	76.41	SW
400.0	200.0	-15.0	.58	.06	22.02	92	88.23	SW
400.0	250.0	-15.0	71	.08	22.02	92	98.45	SW
400.0	300.0	-15.0	83	09	22.02	92	108.06	SW
400.0	350.0	-15.0	96	11	22.02	92	116.72	SW
400.0	400.0	-15.0	1.08	.12	22.02	.92	124.78	SW
400.0	500.0	-15.0	1.32	.15	22.02	.92	139.51	SB
400.0	600.0	-15.0	1.56	17	22.02	.92	152.83	MB
400.0	700.0	-15.0	1.79	.20	22.02	.92	165.07	MB
500.0	50.0	-15.0	.14	.02	14.74	1.14	55.15	SW
500.0	100.0	-15.0	.25	.03	14.74	1.14	77.99	SW
500.0	150.0	-15.0	.37	05	14.74	1.14	95.52	SW
500.0	200.0	-15.0	.47	06	14.74	1.14	110.29	SW
500.0	250.0	-15.0	.58	.08	14.74	1.14	123.31	SW
500.0	300.0	-15.0	.68	.09	14.74	1.14	135.08	SW
500.0	350.0	-15.0	.78	.11	14.74	1.14	145.90	SW
500.0	400.0	-15.0	.88	.12	14.74	1.14	155.98	SB
500.0	500.0	-15.0	1.08	.15	14.74	1.14	174.39	SB
500.0	600.0	-15.0	1.27	.17	14.74	1.14	191.03	MB
500.0	700.0	-15.0	1.46	.20	14.74	1.14	206.34	MB
600.0	50.0	-15.0	.12	.02	10.42	1.37	66.18	SW
600.0	100.0	-15.0	.22	.03	10.42	1.37	93.59	SW
600.0	150.0	-15.0	.31	.05	10.42	1.37	114.62	SW
600.0	200.0	-15.0	.40	.06	10.42	1.37	132.35	SW
600.0	250.0	-15.0	.49	.08	10.42	1.37	147.97	SW
600.0	300.0	-15.0	.58	.09	10.42	1.37	162.10	SB
600.0	350.0	-15.0	.66	.11	10.42	1.37	175.08	SB
600.0	400.0	-15.0	.75	.12	10.42	1.37	187.17	SB
600.0	500.0	-15.0	.92	.15	10.42	1.37	209.27	SB
600.0	600.0	-15.0	1.08	.17	10.42	1.37	229.24	MB
600.0	700.0	-15.0	1.24	.20	10.42	1.37	247.41	MB
700.0	50.0	-15.0	.10	.02	8.04	1.60	77.21	SW
700.0	100.0	-15.0	.19	.03	8.04	1.60	109.18	SW
700.0	150.0	-15.0	.27	05	8.04	1.60	133.72	SW
700.0	200.0	-15.0	.35	06	8.04	1.60	154.41	SW
700.0	250.0	-15.0	.43	.08	8.04	1.60	172.44	SB
700.0	300.0	-15.0	.50	.09	8.04	1.60	189.11	SB
700.0	350.0	-15.0	58	11	8.04	1.60	204.27	SB
700.0	400.0	-15.0	65	12	8.04	1.60	218.37	SB

OIL	WATER	ANGLE	X	T	V	F	K	OBSERVED FLOW REGIME
700.0	500.0	-15.0	.80	.15	8.04	1.60	244.14	SB
700.0	600.0	-15.0	.94	.17	8.04	1.60	267.45	MB
700.0	700.0	-15.0	1.08	.20	8.04	1.60	288.87	MB
50.0	50.0	-30.0	1.08	.02	1796.66	.12	5.82	SWC
50.0	100.0	-30.0	2.02	.04	1796.66	.12	8.24	SWC
50.0	150.0	-30.0	2.90	.05	1796.66	.12	10.09	SWC
50.0	200.0	-30.0	3.76	.07	1796.66	.12	11.65	SWC
50.0	250.0	-30.0	4.60	.08	1796.66	.12	13.02	SWC
50.0	300.0	-30.0	5.42	.10	1796.66	.12	14.27	SWC
50.0	350.0	-30.0	6.22	.11	1796.66	.12	15.41	SWC
50.0	400.0	-30.0	7.02	.13	1796.66	.12	16.47	SWC
50.0	500.0	-30.0	8.58	.15	1796.66	.12	18.42	SWC
50.0	600.0	-30.0	10.11	.18	1796.66	.12	20.17	SW
50.0	700.0	-30.0	11.61	.21	1796.66	.12	21.79	SW
100.0	50.0	-30.0	.58	.02	515.96	.24	11.65	SW
100.0	100.0	-30.0	1.08	.04	515.96	.24	16.47	SWC
100.0	150.0	-30.0	1.56	.05	515.96	.24	20.17	SWC
100.0	200.0	-30.0	2.02	.07	515.96	.24	23.29	SWC
100.0	250.0	-30.0	2.46	.08	515.96	.24	26.04	SWC
100.0	300.0	-30.0	2.90	.10	515.96	.24	28.53	SWC
100.0	350.0	-30.0	3.33	.11	515.96	.24	30.82	SWC
100.0	400.0	-30.0	3.76	.13	515.96	.24	32.94	SWC
100.0	500.0	-30.0	4.60	.15	515.96	.24	36.83	SW
100.0	600.0	-30.0	5.42	.18	515.96	.24	40.35	SW
100.0	700.0	-30.0	6.22	.21	515.96	.24	43.58	SW
150.0	50.0	-30.0	.40	.02	248.68	.36	17.47	SW
150.0	100.0	-30.0	.75	.04	248.68	.36	24.71	SW
150.0	150.0	-30.0	1.08	.05	248.68	.36	30.26	SW
150.0	200.0	-30.0	1.40	.07	248.68	.36	34.94	SW
150.0	250.0	-30.0	1.71	.08	248.68	.36	39.07	SW
150.0	300.0	-30.0	2.02	.10	248.68	.36	42.80	SW
150.0	350.0	-30.0	2.32	.11	248.68	.36	46.22	SW
150.0	400.0	-30.0	2.61	.13	248.68	.36	49.42	SW
150.0	500.0	-30.0	3.19	.15	248.68	.36	55.25	SW
150.0	600.0	-30.0	3.76	.18	248.68	.36	60.52	SB
150.0	700.0	-30.0	4.32	.21	248.68	.36	65.37	SB
200.0	50.0	-30.0	.31	.02	148.17	.48	23.29	SW
200.0	100.0	-30.0	.58	.04	148.17	.48	32.94	SW
200.0	150.0	-30.0	.83	.05	148.17	.48	40.35	SW
200.0	200.0	-30.0	1.08	.07	148.17	.48	46.59	SW
200.0	250.0	-30.0	1.32	.08	148.17	.48	52.09	SW
200.0	300.0	-30.0	1.56	.10	148.17	.48	57.06	SW
200.0	350.0	-30.0	1.79	.11	148.17	.48	61.63	SW
200.0	400.0	-30.0	2.02	.13	148.17	.48	65.89	SW
200.0	500.0	-30.0	2.46	.15	148.17	.48	73.66	SB
200.0	600.0	-30.0	2.90	.18	148.17	.48	80.70	SB
200.0	700.0	-30.0	3.33	.21	148.17	.48	87.16	SB
250.0	50.0	-30.0	.23	.02	99.16	.60	29.12	SW
250.0	100.0	-30.0	.47	.04	99.16	.60	41.18	SW
250.0	150.0	-30.0	.68	.05	99.16	.60	50.43	SW
250.0	200.0	-30.0	.88	.07	99.16	.60	58.24	SW
250.0	250.0	-30.0	1.08	.08	99.16	.60	65.11	SW
250.0	300.0	-30.0	1.27	.10	99.16	.60	71.33	SW
250.0	350.0	-30.0	1.46	.11	99.16	.60	77.04	SW
250.0	400.0	-30.0	1.65	.13	99.16	.60	82.36	SW
250.0	500.0	-30.0	2.02	.15	99.16	.60	92.08	SB
250.0	600.0	-30.0	2.37	.18	99.16	.60	100.87	SB
250.0	700.0	-30.0	2.73	.21	99.16	.60	108.95	SB
300.0	50.0	-30.0	.22	.02	71.42	.73	34.94	SW
300.0	100.0	-30.0	.40	.04	71.42	.73	49.42	SW

SOIL	WATER	ANGLE	X	T	Y	F	K	OBSERVED FLOW REGIME
300.0	150.0	-30.0	.58	05	71.42	73	60.52	SW
300.0	200.0	-30.0	.75	07	71.42	73	69.88	SW
300.0	250.0	-30.0	.92	08	71.42	73	78.13	SW
300.0	300.0	-30.0	1.08	10	71.42	73	85.59	SW
300.0	350.0	-30.0	1.24	11	71.42	73	92.45	SW
300.0	400.0	-30.0	1.40	13	71.42	73	98.83	SW
300.0	500.0	-30.0	1.71	15	71.42	73	110.50	SB
300.0	600.0	-30.0	2.02	18	71.42	73	121.04	SB
300.0	700.0	-30.0	2.33	21	71.42	73	130.74	MB
350.0	50.0	-30.0	.19	02	54.11	85	40.77	SW
350.0	100.0	-30.0	.35	04	54.11	85	57.65	SW
350.0	150.0	-30.0	.50	05	54.11	85	70.61	SW
350.0	200.0	-30.0	.65	07	54.11	85	81.53	SW
350.0	250.0	-30.0	.80	08	54.11	85	91.16	SW
350.0	300.0	-30.0	.94	10	54.11	85	99.86	SW
350.0	350.0	-30.0	1.08	11	54.11	85	107.86	SW
350.0	400.0	-30.0	1.22	13	54.11	85	115.30	SW
350.0	500.0	-30.0	1.49	15	54.11	85	129.91	SW
350.0	600.0	-30.0	1.75	18	54.11	85	141.22	SB
350.0	700.0	-30.0	2.02	21	54.11	85	152.53	SB
400.0	50.0	-30.0	.17	02	42.55	97	46.59	SW
400.0	100.0	-30.0	.31	04	42.55	97	65.89	SW
400.0	150.0	-30.0	.45	05	42.55	97	80.70	SW
400.0	200.0	-30.0	.58	07	42.55	97	93.18	SW
400.0	250.0	-30.0	.71	08	42.55	97	104.18	SW
400.0	300.0	-30.0	.83	10	42.55	97	114.12	SW
400.0	350.0	-30.0	.96	11	42.55	97	123.26	SW
400.0	400.0	-30.0	1.08	13	42.55	97	131.78	SB
400.0	500.0	-30.0	1.32	15	42.55	97	147.33	SB
400.0	600.0	-30.0	1.56	18	42.55	97	161.39	MB
400.0	700.0	-30.0	1.79	21	42.55	97	174.32	MB
500.0	50.0	-30.0	.14	02	28.48	1.21	58.24	SW
500.0	100.0	-30.0	.25	04	28.48	1.21	82.36	SW
500.0	150.0	-30.0	.37	05	28.48	1.21	100.87	SW
500.0	200.0	-30.0	.47	07	28.48	1.21	116.47	SW
500.0	250.0	-30.0	.58	08	28.48	1.21	130.22	SB
500.0	300.0	-30.0	.68	10	28.48	1.21	142.65	SB
500.0	350.0	-30.0	.78	11	28.48	1.21	154.08	SB
500.0	400.0	-30.0	.88	13	28.48	1.21	164.72	SB
500.0	500.0	-30.0	1.08	15	28.48	1.21	184.14	SB
500.0	600.0	-30.0	1.27	18	28.48	1.21	201.74	MB
500.0	700.0	-30.0	1.44	21	28.48	1.21	217.90	MB
600.0	50.0	-30.0	.12	02	20.51	1.45	69.88	SW
600.0	100.0	-30.0	.22	04	20.51	1.45	98.83	SW
600.0	150.0	-30.0	.31	05	20.51	1.45	121.04	SW
600.0	200.0	-30.0	.40	07	20.51	1.45	139.77	SW
600.0	250.0	-30.0	.49	08	20.51	1.45	156.27	SB
600.0	300.0	-30.0	.58	10	20.51	1.45	171.18	SB
600.0	350.0	-30.0	.66	11	20.51	1.45	184.90	SB
600.0	400.0	-30.0	.75	13	20.51	1.45	197.66	SB
600.0	500.0	-30.0	.92	15	20.51	1.45	220.99	SB
600.0	600.0	-30.0	1.08	18	20.51	1.45	242.09	MB
600.0	700.0	-30.0	1.24	21	20.51	1.45	261.48	MB
700.0	50.0	-30.0	.10	02	15.54	1.69	81.53	SW
700.0	100.0	-30.0	.19	04	15.54	1.69	115.30	SW
700.0	150.0	-30.0	.27	05	15.54	1.69	141.22	SW
700.0	200.0	-30.0	.35	07	15.54	1.69	163.06	SW
700.0	250.0	-30.0	.43	08	15.54	1.69	182.31	SB
700.0	300.0	-30.0	.50	10	15.54	1.69	199.71	SB
700.0	350.0	-30.0	.58	11	15.54	1.69	215.71	SB
700.0	400.0	-30.0	.65	13	15.54	1.69	230.61	SB
700.0	500.0	-30.0	.80	15	15.54	1.69	257.83	MB
700.0	600.0	-30.0	.94	18	15.54	1.69	282.43	MB
700.0	700.0	-30.0	1.08	21	15.54	1.69	305.06	MB

APPENDIX II

Calculation of the Martinelli Parameter in Horizontal and Inclined Flow

It was necessary to transform Equation (3) into a dimensionless form, Equation (7), which has all variables dependent upon only $\tilde{h}_L = h_L/D$ (liquid level/pipe diameter) designated by a tilde (~) so that Figure 12 can be used to calculate an X value for a given $\tilde{h}_L$ value.

$$\tau_{WG}\ \frac{S_G}{A_G} - \tau_{WL}\ \frac{S_L}{A_L} + \tau_i S_i \left(\frac{1}{A_L} + \frac{1}{A_G} \right)(\rho_L - \rho_G)\ g \sin \alpha = 0 \qquad (3)$$

The corresponding dimensionless equation from previous work is:

$$X^2 \left[(\tilde{U}_L \tilde{D}_L)^{-n}\ \tilde{U}_L^2\ \frac{\tilde{S}_L}{\tilde{A}_L} \right] - \left[(\tilde{U}_G \tilde{D}_G)^{-m}\ \tilde{U}_G^2\ \left(\frac{\tilde{S}_G}{\tilde{A}_G} + \frac{\tilde{S}_i}{\tilde{A}_L} + \frac{\tilde{S}_i}{\tilde{A}_G} \right) \right] - 4Y = 0 \qquad (7)$$

All of the dimensionless variables with the superscript ~ that depend only on $\tilde{h}_L$ can be seen from equations (10) through (16) in Chapter 3. Since at horizontal, where $\alpha = 0$, Y, in Equation (9) also equals zero. Therefore, Equation (7) can be rearranged to yield a value for X for a particular $\tilde{h}_L$ value.

Starting with equations (10) through (16), the following letters will designate certain parts of these equations.

$$A = (2\tilde{h}_L - 1) \tag{A2-1}$$

$$B = \cos^{-1}(2\tilde{h}_L - 1) = \cos^{-1}A \tag{A2-2}$$

$$C = \pi - \cos^{-1}(2\tilde{h}_L - 1) = \pi - B \tag{A2-3}$$

$$D = \sqrt{1 - (2\tilde{h}_L - 1)^2} = \sqrt{1 - A^2} \tag{A2-4}$$

Next, Equation (7) is separated into four sections for easy simplification.

$$FS = \left(X^2 \quad (\tilde{U}_L \tilde{D}_L)^{-n} \quad \tilde{U}_L^2 \quad \frac{\tilde{S}_L}{\tilde{A}_L} \right) \tag{A2-5}$$

$$SS = (\tilde{U}_G \tilde{D}_G)^{-m} \quad \tilde{U}_G^2 \tag{A2-6}$$

$$TS = \frac{\tilde{S}_G}{\tilde{A}_G} + \frac{\tilde{S}_i}{\tilde{A}_G} \tag{A2-7}$$

$$FHS = \frac{\tilde{S}_i}{\tilde{A}_L} \tag{A2-8}$$

For the first section (FS)

Substitute Equation (6) and (15) and simplifying,

$$FS = X^2 \left[\left(\frac{\tilde{A}}{\tilde{A}_L} \frac{4\tilde{A}_L}{\tilde{S}_L} \right)^{-n} \left(\frac{\tilde{A}}{\tilde{A}_L} \right) \frac{\tilde{S}_L}{\tilde{A}_L} \right] \qquad \text{(A2-9)}$$

where $n = 0.2$ and $\tilde{A} = \pi/4$ from previous work

$$FS = X^2 \left[\left(\frac{4\tilde{A}}{\tilde{S}_L} \right)^{-0.2} \left(\frac{\tilde{A}}{\tilde{A}_L} \right)^2 \frac{\tilde{S}_L}{\tilde{A}_L} \right]$$

$$= X^2 \left[\left(\frac{\tilde{S}_L}{4\tilde{A}} \right)^{0.2} \frac{\tilde{A}^2}{\tilde{A}_L^2} \frac{\tilde{S}_L}{\tilde{A}_L} \right]$$

$$= 0.758\, X^2 \left[\frac{\tilde{S}_L^{0.2}}{\tilde{A}^{0.2}} \frac{\tilde{A}^2}{\tilde{A}_L^2} \frac{\tilde{S}_L}{\tilde{A}_L} \right]$$

$$= 0.758\, X^2 \left[\frac{\tilde{S}_L^{1.2}\, \tilde{A}^{1.8}}{\tilde{A}_L^3} \right]$$

$$= 0.758 \left(\frac{\pi}{4} \right)^{1.8} X^2 \left[\frac{\tilde{S}_L^{1.2}}{\tilde{A}_L^3} \right]$$

Now substituting Equations (10) through (14) into this equation gives

$$FS = 0.491\, X^2 \left[\frac{(\pi - \cos^{-1}(2\tilde{h}_L - 1))^{1.2}}{0.25(\pi - \cos^{-1}(2\tilde{h}_L - 1) + (2\tilde{h}_L - 1)\sqrt{1 - (2\tilde{h}_L - 1)^2})^3} \right]$$

or more simply, using the previous letter designation for the equations,

$$FS = 0.491\ X^2 \left(\frac{C^{1.2}}{0.25\ (C + A \times D)^3} \right) \qquad \text{(A2-10)}$$

For the second section, (SS), substitute Equation (6) and (16) and simplify:

$$SS = \left(\frac{\tilde{A}}{\tilde{A}_G} \frac{4\tilde{A}_G}{\tilde{S}_G + \tilde{S}_i} \right)^{-m} \left(\frac{\tilde{A}}{\tilde{A}_G} \right) \qquad \text{(A2-11)}$$

where m = 0.2 from previous work

$$SS = \left(\frac{4\tilde{A}}{\tilde{S}_G + \tilde{S}_i} \right)^{-0.2} \left(\frac{\tilde{A}^2}{\tilde{A}_G^2} \right)$$

$$= \left(\frac{\tilde{S}_G + \tilde{S}_i}{4\tilde{A}} \right)^{0.2} \left(\frac{\tilde{A}^2}{\tilde{A}_G^2} \right)$$

$$= 0.758 \left(\frac{(\tilde{S}_G + \tilde{S}_i)^{0.2}}{\tilde{A}^{0.2}} \frac{\tilde{A}^2}{\tilde{A}_G^2} \right)$$

$$= 0.758 \left(\frac{(\tilde{S}_G + \tilde{S}_i)^{0.2}\ \tilde{A}^{1.8}}{\tilde{A}_G^2} \right)$$

this simplifies to:

$$SS = 0.491 \left(\frac{(B + D)^{0.2}}{(0.25(B - A \times D))^2} \right) \qquad \text{(A2-12)}$$

Similarly, the third section (TS) becomes

$$TS = \frac{\tilde{S}_G}{\tilde{A}_G} + \frac{\tilde{S}_i}{\tilde{A}_G} \qquad \text{(A2-13)}$$

$$TS = \frac{\tilde{S}_G + \tilde{S}_i}{\tilde{A}_G}$$

$$\text{therefore, } TS = \frac{B + D}{0.25\ (B - A \times D)} \qquad \text{(A2-14)}$$

Finally, the fourth section (FHS) is

$$FHS = \frac{\tilde{S}_i}{\tilde{A}_L} \qquad \text{(A2-15)}$$

$$FHS = \frac{D}{0.25(C + A \times D)} \qquad \text{(A2-16)}$$

Now combining all four sections gives the following arrangement:

$$X^2\ FS - SS \times (TS + FHS) + 4(Y) = 0 \qquad \text{(A2-17)}$$

Solving for X at horizontal flow (Y = 0):

$$X = \sqrt{\frac{SS \times (TS + FHS)}{FS}} \qquad \text{(A2-18)}$$

This equation will be used to calculate an X value for a given $\tilde{h}_L$ value, at horizontal flow.

Now for an angle of inclination of the system away from horizontal, the Y value, will not equal zero and must be taken into account when calculating X values from $\tilde{h}_L$ values. Using Equation (9) and Figure 12, X values can be located at certain Y values which are dependent upon the flow rate of the lighter phase and the angle of inclination (in this case, downhill flow is used). In this work, Y is calculated for a specific flow rate of oil and set angle of inclination. Substitute Y into Equation (7) and the result after simplification is:

$$X = \sqrt{\frac{SS \times (TS + FHS) + 4Y}{FS}} \qquad \text{(A2-19)}$$

This equation calculates an X value for a given $\tilde{h}_L$ and a constant Y value.

The following computer programs HLD and HLDXDK calculate the appropriate values of the Martinelli parameter X for horizontal and inclined flow, respectively.

```
      PROGRAM HLD(INPUT,OUTPUT,TAPE5=INPUT,TAPE6=OUTPUT)
C*****************************************************************
C                                                                *
C  PURPOSE:                                                      *
C                                                                *
C   PROGRAM HLD CALCULATES THE APPROPIATE VALUE OF THE MARTINELLI *
C   PARAMETER X FOR HORIZONTAL FLOW FROM EQUATIONS ASSOCIATED WITH *
C   THE EQUILIBRIUM LEVEL FOR STRATIFIED FLOW CURVES ON FIGURE 12 *
C   IN THE TEXT.                                                 *
C                                                                *
C  OUTPUT PARAMETERS:                                            *
C                                                                *
C   X     -  DIMENSIONLESS MARTINELLI PARAMETER                  *
C   HL    -  EQUILIBRIUM LEVEL FOR STRATIFIED FLOW FROM FIGURE   *
C            12 FOR HORIZONTAL FLOW                              *
C                                                                *
C*****************************************************************
      REAL X(1000),HL(1000)
      REAL A(1000),B(1000),C(1000),D(1000),FS(1000)
      REAL SS(1000),TS(1000),FHS(1000)
      NHLD=95
      ADDHLD=0.01
C-----------------------------------------------------------------
C     CALCULATION OF X PARAMETER
C-----------------------------------------------------------------
      DO 1 I=1,NHLD
        HL(I)=ADDHLD+0.01*I
        A(I)=(2*HL(I)-1.0)
        B(I)=ACOS(A(I))
        C(I)=3.1415-B(I)
        D(I)=SQRT(1.0-(A(I)**2.0))
        FS(I)=(C(I)**1.2/(0.25*(C(I)+A(I)*D(I))**3.0))
        SS(I)=((B(I)+D(I))**0.2)/(0.25*(B(I)-A(I)*D(I))**2.0)
        TS(I)=D(I)/(0.25*(C(I)+A(I)*D(I)))
        FHS(I)=(B(I)+D(I))/(0.25*(B(I)-A(I)*D(I)))
        X(I)=SQRT((SS(I)*(TS(I)+FHS(I)))/FS(I))
   1  CONTINUE
      WRITE(6,10)
C-----------------------------------------------------------------
C     PRINT OUT CALCULATED VALUES
C-----------------------------------------------------------------
      DO 5 I=1,NHLD
        WRITE(6,20)X(I),HL(I)
   5  CONTINUE
C-----------------------------------------------------------------
C     FORMAT STATEMENTS
C-----------------------------------------------------------------
  10  FORMAT(1H1,T25,*X*,T45,*HL/D*/,T24,3(*-*),T45,4(*-*)//)
  20  FORMAT(3X,T23,F7.3,T43,F6.2)
      END
```

MARTINELLI PARAMETER (X)	HL/D
.012	.02
.023	.03
.035	.04
.048	.05
.064	.06
.081	.07
.099	.08
.119	.09
.140	.10
.163	.11
.188	.12
.214	.13
.241	.14
.271	.15
.301	.16
.334	.17
.368	.18
.404	.19
.442	.20
.482	.21
.524	.22
.568	.23
.615	.24
.663	.25
.715	.26
.768	.27
.824	.28
.884	.29
.946	.30
1.011	.31
1.079	.32
1.151	.33
1.226	.34
1:306	.35
1.389	.36
1.477	.37
1.569	.38
1.666	.39
1.769	.40
1.877	.41
1.990	.42
2.110	.43
2.237	.44

MARTINELLI PARAMETER (X)	HL/D
2.371	.45
2.512	.46
2.662	.47
2.821	.48
2.989	.49
3.168	.50
3.357	.51
3.559	.52
3.773	.53
4.002	.54
4.246	.55
4.506	.56
4.785	.57
5.084	.58
5.404	.59
5.749	.60
6.119	.61
6.519	.62
6.951	.63
7.418	.64
7.925	.65
8.476	.66
9.077	.67
9.733	.68
10.452	.69
11.242	.70
12.112	.71
13.074	.72
14.142	.73
15.331	.74
16.660	.75
18.153	.76
19.838	.77
21.749	.78
23.930	.79
26.434	.80
29.329	.81
32.701	.82

MARTINELLI PARAMETER (X)	HL/D
36.663	.83
41.362	.84
46.996	.85
53.833	.86
62.246	.87
72.768	.88
86.175	.89
103.644	.90
127.026	.91
159.368	.92
205.988	.93
276.877	.94
392.694	.95
602.202	.96

```
      PROGRAM HLDXDK(INPUT,OUTPUT,TAPE5=INPUT,TAPE6=OUTPUT)
C*****************************************************************
C                                                                *
C  PURPOSE:                                                      *
C                                                                *
C   PROGRAM HLDXDK CALCULATES A DIMENSIONLESS MATRINELLI PARAMETER *
C   (X) FROM EQUATIONS ASSOCIATED WITH THE EQUILIBRIUM LEVEL FOR  *
C   STRATIFIED FLOW CURVES ON FIGURE 12 IN THE TEXT.  EACH VALUE  *
C   OF X CALCULATED IS DEPENDENT ON THE Y INPUT VALUE.  FOR IN-   *
C   CLINED FLOW, THE Y VALUE WILL VARY ACCORDING TO THE ANGLE OF  *
C   INCLINATION AND OIL FLOW RATE.  Y VALUES ARE CALCULATED FROM  *
C   PROGRAM FMAP.                                                *
C                                                                *
C  INPUT PARAMETERS:                                             *
C                                                                *
C   QOIL      -  OIL FLOW RATE,  B/D                             *
C   ANG       -  ANGLE OF INCLINATION,  DEGREES                  *
C   Y         -  DIMENSIONLESS INCLINATION PARAMETER             *
C                                                                *
C  OUTPUT PARAMETERS:                                            *
C                                                                *
C   X         -  DIMENSIONLESS MARTINELLI PARAMETER              *
C   HLD       -  EQUILIBRIUM LEVEL FOR STRATIFIED FLOW FROM      *
C                FIGURE 12                                       *
C                                                                *
C*****************************************************************
      REAL X(1000),HLD(1000)
      REAL A(1000),B(1000),C(1000),D(1000),FS(1000)
      REAL SS(1000),TS(1000),FHS(1000)
      NHLD=95
      ADDHLD=0.01
C-----------------------------------------------------------------
C     READ INPUT PARAMETERS
C-----------------------------------------------------------------
      READ(5,*)QOIL,ANG,Y
      FOURY=4*Y
C-----------------------------------------------------------------
C     CALCULATION OF X PARAMETER
C-----------------------------------------------------------------
      DO 1 I=1,NHLD
        HLD(I)=ADDHLD+0.01*I
        A(I)=(2*HLD(I)-1.0)
        B(I)=ACOS(A(I))
        C(I)=3.1415-B(I)
        D(I)=SQRT(1.0-(A(I)**2.0))
        FS(I)=(C(I)**1.2/(0.25*(C(I)+A(I)*D(I))**3.0))*0.491
        SS(I)=(((B(I)+D(I))**0.2)/(0.25*(B(I)-A(I)*D(I))**2.0))
     $  *0.491
        TS(I)=D(I)/(0.25*(C(I)+A(I)*D(I)))
        FHS(I)=(B(I)+D(I))/(0.25*(B(I)-A(I)*D(I)))
        X(I)=SQRT(((SS(I)*(TS(I)+FHS(I)))+FOURY)/FS(I))
   1  CONTINUE
```

```
C-----------------------------------------------------------------------
C     WRITE HEADING
C-----------------------------------------------------------------------
      WRITE(6,7)
      WRITE(6,8)QOIL,ANG,Y
      WRITE(6,10)
      DO 5 I=1,NHLD
C-----------------------------------------------------------------------
C     PRINT OUT CALCULATED VALUES
C-----------------------------------------------------------------------
        WRITE(6,20)X(I),HLD(I)
   5  CONTINUE
C-----------------------------------------------------------------------
C     FORMAT STATEMENTS
C-----------------------------------------------------------------------
   7  FORMAT(1H1,T20,*QOIL (B/D)*,T40,*ANGLE*,T60,*Y*/,T19,11(*-*),
     $T39,7(*-*),T58,6(*-*))
   8  FORMAT(2X,T20,F5.1,T40,F5.1,T58,F6.2//)
  10  FORMAT(8X,T25,*X*,T45,*HL/D*/,T24,3(*-*),T45,4(*-*)//)
  20  FORMAT(3X,T23,F7.3,T43,F6.2)
      END
```

QOIL (B/D)	ANGLE	Y
100.0	-15.0	267.0

MARTINELLI PARAMETER (X)	HL/D
.091	.02
.200	.03
.349	.04
.536	.05
.761	.06
1.021	.07
1.317	.08
1.648	.09
2.012	.10
2.408	.11
2.837	.12
3.296	.13
3.785	.14
4.304	.15
4.851	.16
5.426	.17
6.029	.18
6.657	.19
7.311	.20
7.989	.21
8.692	.22
9.418	.23
10.166	.24
10.936	.25
11.728	.26
12.539	.27
13.370	.28
14.220	.29
15.088	.30
15.974	.31
16.876	.32
17.794	.33
18.728	.34
19.676	.35
20.638	.36
21.613	.37
22.600	.38
23.599	.39

MARTINELLI PARAMETER (X)	HL/D
24.609	.40
25.629	.41
26.659	.42
27.697	.43
28.744	.44
29.798	.45
30.858	.46
31.925	.47
32.997	.48
34.073	.49
35.154	.50
36.237	.51
37.323	.52
38.412	.53
39.501	.54
40.591	.55
41.682	.56
42.772	.57
43.861	.58
44.949	.59
46.035	.60
47.119	.61
48.200	.62
49.280	.63
50.357	.64
51.432	.65
52.505	.66
53.578	.67
54.651	.68
55.725	.69
56.804	.70
57.889	.71
58.984	.72
60.096	.73
61.229	.74
62.394	.75
63.601	.76
64.866	.77
66.210	.78
67.659	.79
69.251	.80
71.036	.81

MARTINELLI PARAMETER (X)	HL/D
73.082	.82
75.484	.83
78.374	.84
81.938	.85
86.440	.86
92.258	.87
99.945	.88
110.320	.89
124.617	.90
144.768	.91
173.914	.92
217.473	.93
285.532	.94
398.831	.95
606.201	.96

OIL (B/D)	ANGLE	Y
300.0	-15.0	37.0

MARTINELLI PARAMETER (X)	HL/D
.036	.02
.077	.03
.134	.04
.205	.05
.289	.06
.388	.07
.499	.08
.623	.09
.760	.10
.909	.11
1.070	.12
1.243	.13
1.427	.14
1.622	.15
1.828	.16
2.044	.17
2.270	.18
2.506	.19
2.752	.20
3.008	.21
3.272	.22
3.545	.23
3.827	.24
4.117	.25
4.416	.26
4.722	.27
5.036	.28
5.357	.29
5.685	.30
6.020	.31
6.362	.32
6.710	.33
7.064	.34
7.424	.35
7.790	.36
8.161	.37
8.538	.38
8.920	.39

MARTINELLI PARAMETER (X)	HL/D
9.307	.40
9.698	.41
10.094	.42
10.495	.43
10.900	.44
11.309	.45
11.722	.46
12.138	.47
12.559	.48
12.984	.49
13.412	.50
13.845	.51
14.281	.52
14.722	.53
15.166	.54
15.616	.55
16.070	.56
16.530	.57
16.996	.58
17.468	.59
17.948	.60
18.437	.61
18.936	.62
19.446	.63
19.970	.64
20.510	.65
21.070	.66
21.651	.67
22.260	.68
22.901	.69
23.580	.70
24.306	.71
25.088	.72
25.937	.73
26.870	.74
27.903	.75
29.059	.76
30.366	.77
31.858	.78
33.581	.79

MARTINELLI PARAMETER (X)	HL/D
35.588	.80
37.950	.81
40.759	.82
44.130	.83
48.218	.84
53.225	.85
59.429	.86
67.210	.87
77.108	.88
89.909	.89
106.797	.90
129.630	.91
161.462	.92
207.617	.93
278.092	.94
393.550	.95
602.757	.96

QOIL (B/D)	ANGLE	Y
500.0	-15.0	15.0

MARTINELLI PARAMETER (X)	HL/D
.025	.02
.052	.03
.089	.04
.135	.05
.191	.06
.254	.07
.327	.08
.407	.09
.496	.10
.593	.11
.697	.12
.808	.13
.927	.14
1.053	.15
1.187	.16
1.326	.17
1.473	.18
1.626	.19
1.785	.20
1.951	.21
2.122	.22
2.300	.23
2.483	.24
2.671	.25
2.865	.26
3.064	.27
3.269	.28
3.478	.29
3.692	.30
3.911	.31
4.135	.32
4.363	.33
4.596	.34
4.833	.35
5.074	.36
5.320	.37
5.569	.38
5.823	.39
6.081	.40
6.342	.41

MARTINELLI PARAMETER (X)	HL/D
6.608	.42
6.878	.43
7.151	.44
7.429	.45
7.711	.46
7.997	.47
8.287	.48
8.582	.49
8.882	.50
9.187	.51
9.498	.52
9.815	.53
10.138	.54
10.468	.55
10.806	.56
11.153	.57
11.510	.58
11.877	.59
12.257	.60
12.652	.61
13.063	.62
13.492	.63
13.943	.64
14.418	.65
14.923	.66
15.461	.67
16.038	.68
16.660	.69
17.337	.70
18.076	.71
18.889	.72
19.790	.73
20.795	.74
21.924	.75
23.200	.76
24.654	.77
26.320	.78
28.243	.79
30.478	.80
33.096	.81

MARTINELLI PARAMETER (X)	HL/D
36.185	.82
39.859	.83
44.270	.84
49.616	.85
56.169	.86
64.305	.87
74.558	.88
87.708	.89
104.934	.90
128.088	.91
160.220	.92
206.650	.93
277.370	.94
393.041	.95
602.427	.96

QOIL (B/D)	ANGLE	Y
700.0	-15.0	8.0

MARTINELLI PARAMETER (X)	HL/D
.020	.02
.041	.03
.069	.04
.104	.05
.146	.06
.194	.07
.248	.08
.308	.09
.375	.10
.447	.11
.525	.12
.608	.13
.697	.14
.791	.15
.891	.16
.995	.17
1.105	.18
1.219	.19
1.338	.20
1.462	.21
1.591	.22
1.724	.23
1.861	.24
2.003	.25
2.149	.26
2.299	.27
2.453	.28
2.611	.29
2.773	.30
2.939	.31
3.109	.32
3.282	.33
3.459	.34
3.641	.35
3.825	.36
4.014	.37
4.206	.38
4.402	.39
4.602	.40
4.806	.41
5.014	.42

MARTINELLI PARAMETER (X)	HL/D
5.225	.43
5.441	.44
5.662	.45
5.887	.46
6.117	.47
6.352	.48
6.592	.49
6.838	.50
7.091	.51
7.350	.52
7.617	.53
7.892	.54
8.176	.55
8.471	.56
8.776	.57
9.095	.58
9.427	.59
9.775	.60
10.141	.61
10.528	.62
10.937	.63
11.374	.64
11.840	.65
12.341	.66
12.882	.67
13.468	.68
14.107	.69
14.808	.70
15.579	.71
16.434	.72
17.384	.73
18.448	.74
19.644	.75
20.996	.76
22.535	.77
24.294	.78
26.318	.79
28.662	.80
31.394	.81
34.602	.82
38.401	.83
42.937	.84
48.411	.85

MARTINELLI PARAMETER (X)	HL/D
55.091	.86
63.353	.87
73.728	.88
86.996	.89
104.334	.90
127.594	.91
159.823	.92
206.341	.93
277.140	.94
392.879	.95
602.322	.96

OIL (B/D)	ANGLE	Y
100.0	-30.0	516.0

MARTINELLI PARAMETER (X)	HL/D
.126	.02
.277	.03
.484	.04
.744	.05
1.056	.06
1.418	.07
1.829	.08
2.288	.09
2.794	.10
3.344	.11
3.939	.12
4.577	.13
5.257	.14
5.978	.15
6.738	.16
7.537	.17
8.373	.18
9.246	.19
10.154	.20
11.097	.21
12.073	.22
13.081	.23
14.120	.24
15.190	.25
16.289	.26
17.416	.27
18.570	.28
19.750	.29
20.956	.30
22.185	.31
23.438	.32
24.712	.33
26.008	.34
27.324	.35
28.659	.36
30.012	.37
31.381	.38
32.767	.39
34.168	.40

MARTINELLI PARAMETER (X)	HL/D
35.583	.41
37.010	.42
38.450	.43
39.900	.44
41.361	.45
42.830	.46
44.307	.47
45.790	.48
47.280	.49
48.774	.50
50.272	.51
51.772	.52
53.274	.53
54.777	.54
56.280	.55
57.781	.56
59.280	.57
60.776	.58
62.268	.59
63.755	.60
65.236	.61
66.711	.62
68.178	.63
69.637	.64
71.089	.65
72.531	.66
73.965	.67
75.390	.68
76.807	.69
78.217	.70
79.621	.71
81.021	.72
82.420	.73
83.822	.74
85.233	.75
86.661	.76
88.117	.77
89.614	.78
91.175	.79

MARTINELLI PARAMETER (X)	HL/D
92.825	.80
94.603	.81
96.564	.82
98.783	.83
101.368	.84
104.477	.85
108.339	.86
113.295	.87
119.860	.88
128.821	.89
141.400	.90
159.546	.91
186.460	.92
227.662	.93
293.373	.94
404.471	.95
609.907	.96

QOIL(B/D)	ANGLE	Y
300.0	-30.0	71.0

MARTINELLI PARAMETER (X)	HL/D
.048	.02
.105	.03
.182	.04
.280	.05
.396	.06
.531	.07
.685	.08
.856	.09
1.044	.10
1.250	.11
1.472	.12
1.709	.13
1.963	.14
2.232	.15
2.515	.16
2.813	.17
3.125	.18
3.450	.19
3.789	.20
4.141	.21
4.505	.22
4.881	.23
5.269	.24
5.668	.25
6.078	.26
6.499	.27
6.931	.28
7.372	.29
7.823	.30
8.283	.31
8.752	.32
9.229	.33
9.714	.34
10.208	.35
10.709	.36
11.217	.37
11.732	.38
12.253	.39

MARTINELLI PARAMETER (X)	HL/D
12.780	.40
13.314	.41
13.853	.42
14.397	.43
14.946	.44
15.500	.45
16.058	.46
16.620	.47
17.186	.48
17.756	.49
18.330	.50
18.907	.51
19.487	.52
20.070	.53
20.656	.54
21.246	.55
21.838	.56
22.434	.57
23.033	.58
23.637	.59
24.244	.60
24.857	.61
25.475	.62
26.101	.63
26.734	.64
27.377	.65
28.033	.66
28.702	.67
29.390	.68
30.099	.69
30.835	.70
31.604	.71
32.414	.72
33.274	.73
34.197	.74
35.199	.75
36.298	.76
37.520	.77
38.897	.78
40.468	.79

MARTINELLI PARAMETER (X)	HL/D
42.287	.80
44.422	.81
46.960	.82
50.019	.83
53.752	.84
58.366	.85
64.142	.86
71.468	.87
80.891	.88
93.208	.89
109.614	.90
131.977	.91
163.362	.92
209.103	.93
279.205	.94
394.335	.95
603.268	.96

QOIL (B/D)	ANGLE	Y
500.0	-30.0	28.0

MARTINELLI PARAMETER (X)	HL/D
.032	.02
.068	.03
.118	.04
.180	.05
.254	.06
.339	.07
.437	.08
.545	.09
.665	.10
.795	.11
.936	.12
1.086	.13
1.247	.14
1.417	.15
1.597	.16
1.785	.17
1.983	.18
2.189	.19
2.404	.20
2.627	.21
2.858	.22
3.097	.23
3.343	.24
3.597	.25
3.857	.26
4.125	.27
4.399	.28
4.680	.29
4.967	.30
5.261	.31
5.560	.32
5.864	.33
6.175	.34
6.490	.35
6.811	.36

MARTINELLI PARAMETER (X)	HL/D
7.137	.37
7.468	.38
7.803	.39
8.143	.40
8.487	.41
8.836	.42
9.189	.43
9.546	.44
9.907	.45
10.272	.46
10.641	.47
11.014	.48
11.391	.49
11.772	.50
12.157	.51
12.547	.52
12.941	.53
13.340	.54
13.745	.55
14.155	.56
14.572	.57
14.996	.58
15.428	.59
15.869	.60
16.320	.61
16.783	.62
17.260	.63
17.753	.64
18.265	.65
18.799	.66
19.359	.67
19.950	.68
20.578	.69
21.249	.70
21.972	.71
22.757	.72
23.617	.73
24.567	.74
25.626	.75
26.817	.76
28.169	.77

MARTINELLI PARAMETER (X)	HL/D
29.717	.78
31.506	.79
33.592	.80
36.044	.81
38.953	.82
42.435	.83
46.643	.84
51.779	.85
58.117	.86
66.037	.87
76.075	.88
89.015	.89
106.039	.90
129.001	.91
160.955	.92
207.222	.93
277.797	.94
393.342	.95
602.622	.96

QOIL (B/D)	ANGLE	Y
700.0	-30.0	16.0

MARTINELLI PARAMETER (X)	HL/D
.025	.02
.054	.03
.092	.04
.139	.05
.196	.06
.262	.07
.337	.08
.420	.09
.511	.10
.610	.11
.718	.12
.833	.13
.956	.14
1.086	.15
1.223	.16
1.367	.17
1.518	.18
1.676	.19
1.840	.20
2.011	.21
2.188	.22
2.370	.23
2.559	.24
2.753	.25
2.953	.26
3.159	.27
3.369	.28
3.585	.29
3.806	.30
4.031	.31
4.262	.32
4.497	.33
4.736	.34
4.980	.35
5.229	.36
5.481	.37
5.738	.38

MARTINELLI PARAMETER (X)	HL/D
5.999	.39
6.264	.40
6.532	.41
6.805	.42
7.082	.43
7.363	.44
7.648	.45
7.937	.46
8.230	.47
8.528	.48
8.830	.49
9.137	.50
9.449	.51
9.766	.52
10.090	.53
10.419	.54
10.756	.55
11.100	.56
11.452	.57
11.814	.58
12.187	.59
12.572	.60
12.971	.61
13.386	.62
13.818	.63
14.272	.64
14.750	.65
15.256	.66
15.795	.67
16.372	.68
16.994	.69
17.668	.70
18.405	.71
19.214	.72
20.110	.73
21.109	.74
22.231	.75
23.498	.76

MARTINELLI PARAMETER (X)	HL/D
24.942	.77
26.596	.78
28.507	.79
30.729	.80
33.332	.81
36.405	.82
40.063	.83
44.457	.84
49.786	.85
56.321	.86
64.440	.87
74.675	.88
87.809	.89
105.019	.90
128.159	.91
160.276	.92
206.694	.93
277.403	.94
393.064	.95
602.442	.96

APPENDIX III

COMPUTER PROGRAM DUKMAP AND GENERATED FLOW REGIME MAPS

```
      PROGRAM DUKMAP(INPUT,OUTPUT,TAPE5,INPUT,TAPE6=OUTPUT)
C*****************************************************************
C                                                                *
C  PURPOSE:                                                      *
C                                                                *
C   PROGRAM DUKMAP CALCULATES THE APPROXIMATE TRANSITION BOUNDARY *
C   LINES IN THE GENERALIZED GAS-LIQUID FLOW REGIME MAP DEVELOPED *
C   BY TAITEL AND DUKLER (AICHE J. 1976) USING PARAMETERS MODIFIED*
C   FOR THE CONDITIONS OF THE EXPERIMENTS PERFORMED.  THE GENER-  *
C   ATED BOUNDARY LINES WILL BE ASSOCIATED WITH LIQUID-LIQUID     *
C   FLOW.                                                        *
C                                                                *
C  INPUT PARAMETERS:                                             *
C                                                                *
C   NX       -  MARTINELLI PARAMETER CALCULATED FROM PROGRAM HLD  *
C               FOR HORIZONTAL FLOW OR PROGRAM HLDXDK FOR INCLINED*
C               FLOW                                             *
C   HL       -  EQUILIBRIUM LEVEL FOR STATIFIED FLOW CALCULATED   *
C               FROM APPROPIATE PROGRAM                          *
C                                                                *
C                                                                *
C  OUTPUT PARAMETERS:                                            *
C                                                                *
C   NX       -  MARTINELLI PARAMETER                              *
C   ALINE    -  PARAMETER THAT SATISFIES THE CRITERIA FOR THE     *
C               TRANSITION BETWEEN STRATIFIED (S) AND INTERMIT-  *
C               TENT (I) OR ANNULAR-DISPERSED LIQUID (AD) REGIMES*
C   BLINE    -  PARAMETER THAT SATISFIES THE CRITERIA FOR THE     *
C               TRANSITION BETWEEN INTERMITTENT (I) AND ANNULAR  *
C               DISPERSED LIQUID (AD) REGIMES                    *
C   CLINE    -  PARAMETER THAT SATISFIES THE CRITERIA FOR THE     *
C               TRANSITION BETWEEN STRATIFIED SMOOTH (SS) AND    *
C               STRATIFIED WAVY (SW) REGIMES                     *
C   DLINE    -  PARAMETER THAT SATISFIES THE CRITERIA FOR THE     *
C               TRANSITION BETWEEN INTERMITTENT (I) AND DISPERSED*
C               BUBBLE (DB) REGIMES                              *
C                                                                *
C*****************************************************************
      REAL UWL(500),UOL(500),AWL(500),AOL(500),HL(500)
      REAL SIL(500),SWL(500),ALINE(500),C2(500),NX(500),SWL(500)
      REAL SOL(500),DOL(500),DWL(500),CLINE(500),DLINE(500)
```

```
C-----------------------------------------------------------------------
C     READ NUMBER OF INPUT PAIRS
C-----------------------------------------------------------------------
      READ(5,*)NVALUE
      DO 1 I=1,NVALUE
C-----------------------------------------------------------------------
C     READ INPUT PAIRS
C-----------------------------------------------------------------------
        READ(5,*)NX(I),HL(I)
   1  CONTINUE
      CALL DUKNUM(HL,AWL,AOL,SIL,UWL,UOL,C2,DWL,NVALUE)
      CALL LINEA(NVALUE,C2,UOL,HL,AOL,ALINE)
      CALL LINEC(NVALUE,UOL,UWL,CLINE)
      CALL LINED(NVALUE,AOL,UWL,SIL,DWL,DLINE)
      WRITE (6,10)
      DO 2 I=1,NVALUE
C-----------------------------------------------------------------------
C     PRINT OUT CALCULATED VALUES
C-----------------------------------------------------------------------
        WRITE(6,20)NX(I),ALINE(I),CLINE(I),DLINE(I)
   2  CONTINUE
C-----------------------------------------------------------------------
C     FORMAT STATEMENTS
C-----------------------------------------------------------------------
   10 FORMAT(1H1,T15,*X*,T35,*LINE A*,T55,*LINE C*,T75,*LINE D*/,T14,
     $3(*-*),T35,6(*-*),T55,6(*-*),T75,6(*-*)//)
   20 FORMAT(3X,T13,F8.3,T35,F6.3,T55,F6.3,T75,F6.3)
      STOP
      END

      SUBROUTINE DUKNUM (HL,AWL,AOL,SIL,UWL,UOL,C2,DWL,NVALUE)
C**********************************************************************
C                                                                     *
C  PURPOSE:                                                           *
C                                                                     *
C   SUBROUTINE DUKNUM CALCULATES VARIABLES THAT ARE DEPENDENT ON      *
C   THE DIMENSIONLESS VALUE OF HL.  THESE VARIABLES WILL BE USED      *
C   IN THE FOLLOWING SUBROUTINES TO CALCULATE THE APPROPRIATE FLOW    *
C   FLOW REGIME TRANSITION BOUNDARIES FOR THE GIVEN INPUT DATA.       *
C                                                                     *
C**********************************************************************
      REAL UWL(500),UOL(500),AWL(500),AOL(500),HL(500)
      REAL C2(500),SOL(500),DWL(500),DOL(500),SIL(500)
      DO 1 I=1,NVALUE
        AL=0.7854
        AWL(I)=0.25*(3.1415-ACOS(2*HL(I)-1)+(2*HL
```

```
     $  (I)-1)*SQRT(1-((2*HL(I)-1)**2.0)))
        AOL(I)=0.25*(ACOS(2*HL(I)-1)-(2*HL(I)-1)*
     $  SQRT(1-((2*HL(I)-1)**2.0)))
        SOL(I)=ACOS(2*HL(I)-1)
        SWL(I)=3.1415-ACOS(2*HL(I)-1)
        SIL(I)=SQRT(1-(2*HL(I)-1)**2)
        UWL(I)=(AL/(AWL(I)))
        UOL(I)=(AL/(AOL(I)))
        C2(I)=1.0-HL(I)
        DWL(I)=(4*AWL(I))/SWL(I)
        DOL(I)=(4*AOL(I))/(SIL(I)+SOL(I))
    1  CONTINUE
       RETURN
       END


C*********************************************************************
C                                                                    *
C  PURPOSE:                                                          *
C                                                                    *
C   SUBROUTINE LINEA CALCULATES THE DIMENSIONLESS PARAMETER F        *
C   WHICH STATISFIES THE CRITIERIA FOR THE TRANSITION BETWEEN        *
C   STATIFIED AND INTERMITTENT OR ANNULAR DISPERSED LIQUID           *
C   REGIMES FOR THE GIVEN VALUES OF THE MARTINELLI PARAMETER X       *
C   FROM PROGRAM DUKMAP                                              *
C                                                                    *
C*********************************************************************
       REAL UOL(500),AWL(500),AOL(500),HL(500)
       REAL ALINE(500),C2(500),SOL(500),DOL(500)
       REAL DWL(500)
       DO 1 I=1,NVALUE
         ALINE(I)=SQRT(1.0/((C2(I)**2)*((UOL(I)**2)*
      $  SQRT(1-(2*HL(I)-1)**2)/AOL(I))))
    1  CONTINUE
       RETURN
       END

C*********************************************************************
C                                                                    *
C   LINEB IS THE TRANSITION BETWEEN INTERMITTENT AND ANNULAR DIS-    *
C   PERSED LIQUID REGIMES.  SINCE THIS TRANSITION TAKES PLACE AT     *
C   A CONSTANT VALUE OF HL=0.5, A SINGLE VALUE OF X CHARACTERIZES    *
C   THE CHANGE IN THE REGIME FOR ANY DIMENSIONLESS Y PARAMETER       *
C   VALUE.  FOR HORIZONTAL FLOW, Y=0, AND X=3.17 FROM THE DATA       *
C   GENERATED FROM PROGRAM HLD.  FOR INCLINED FLOW, THE Y PARA-      *
C   METER WILL VARY ACCORDING TO THE FLOW RATE OF OIL AND ANGLE      *
C   OF INCLINATION.  THE X PARAMETER IN THIS CASE IS CALCULATED      *
C   BY PROGRAM HLDXDK.                                               *
C                                                                    *
C*********************************************************************
```

```
      SUBROUTINE LINEC(NVALUE,UOL,UWL,CLINE)
C*****************************************************************
C                                                                *
C  PURPOSE:                                                      *
C                                                                *
C   SUBROUTINE LINEC CALCULATES THE DIMENSIONLESS PARAMETER K    *
C   WHICH SATISFIES THE CRITERIA FOR THE TRANSITION BETWEEN      *
C   STRATIFIED SMOOTH AND STRATIFIED WAVY REGIMES UNDER THE GIVEN *
C   VALUES OF THE MARTINELLI X PARAMETER                         *
C                                                                *
C*****************************************************************
      REAL UWL(500),UOL(500),AWL(500),CLINE(500)
      REAL SOL(500),DOL(500),DWL(500)
      DO 1 I=1,NVALUE
        CLINE(I)=2.0/((SQRT(UWL(I)))*UOL(I)*(SQRT(0.01)))
   1  CONTINUE
      RETURN
      END


      SUBROUTINE LINED(NVALUE,AOL,UWL,SIL,DWL,DLINE)
C*****************************************************************
C                                                                *
C  PURPOSE:                                                      *
C                                                                *
C   SUBROUTINE LINED CALCULATES THE DIMENSIONLESS PARAMETER T    *
C   WHICH SATISFIES THE CRITERIA FOR THE TRANSITION BETWEEN IN-   *
C   TERMITTENT AND DISPERSED BUBBLE FLOW REGIMES UNDER THE GIVEN  *
C   VALUES OF THE MARTINELLI PARAMETER X CALCULATED BY PROGRAM    *
C   DUKMAP.                                                      *
C                                                                *
C*****************************************************************

      REAL UWL(500),AOL(500),SIL(500),DWL(500),DLINE(500)
      DO 1 I=1,NVALUE
        DLINE(I)=SQRT((8.0*AOL(I))/(SIL(I)*(UWL(I)**2.0)/((UWL(I)
     $  *DWL(I))**0.2)))
   1  CONTINUE
      RETURN
      END
```

GENERALIZED FLOW REGIME MAP
ANGLE OF INCLINATION = -15 DEGREES
OIL FLOW RATE = 300 B/D

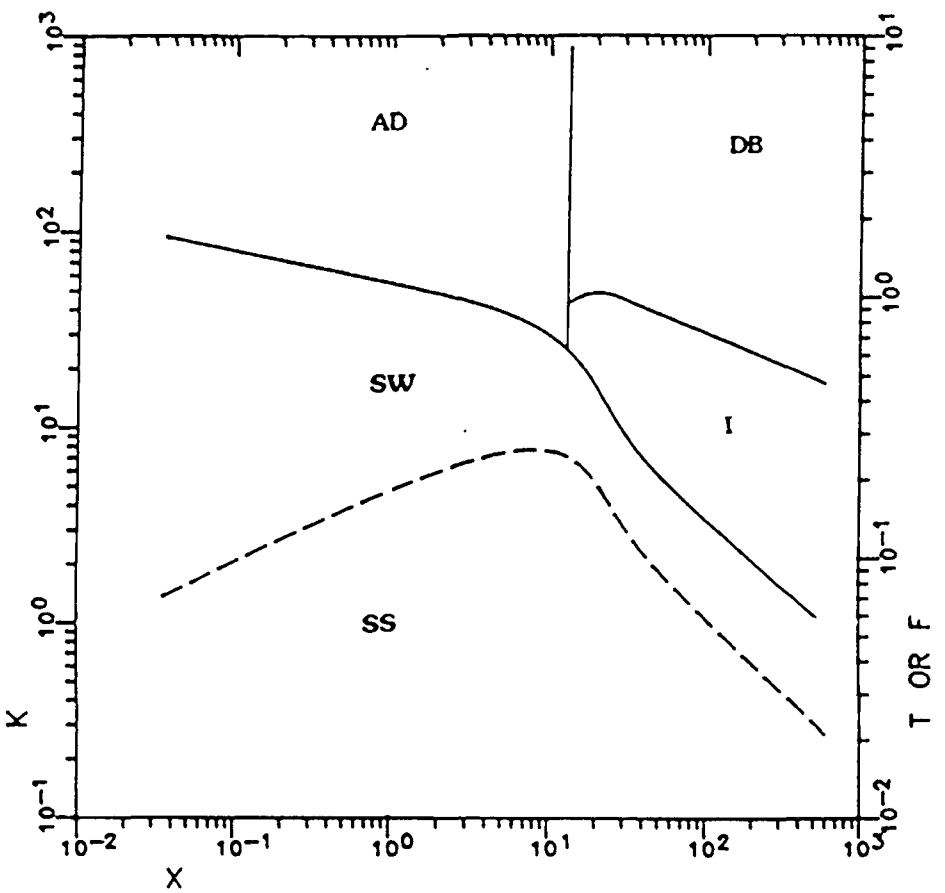

COMPARISON OF FLOW DATA TO GENERALIZED FLOW REGIME MAP (TAITEL & DUKLER) OIL FLOW RATE = 300 B/D
ANGLE OF INCLINATION = -15 DEGREES
TRANSITION BETWEEN STRATIFIED (S) AND INTERMITTENT (I) OR ANNULAR-DISPERSED LIQUID (AD) REGIMES

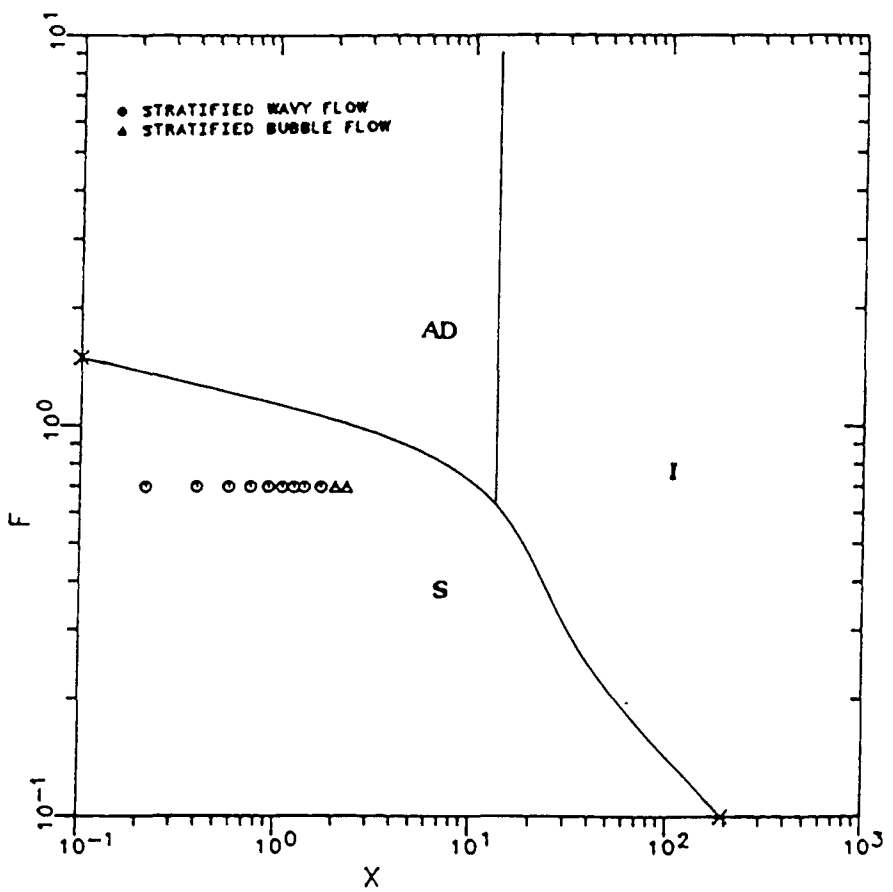

COMPARISON OF FLOW DATA TO GENERALIZED FLOW REGIME MAP (TAITEL & DUKLER) OIL FLOW RATE = 300 B/D
ANGLE OF INCLINATION = -15 DEGREES
TRANSITION BETWEEN INTERMITTENT (I) AND ANNULAR-DISPERSED LIQUID (AD) REGIMES

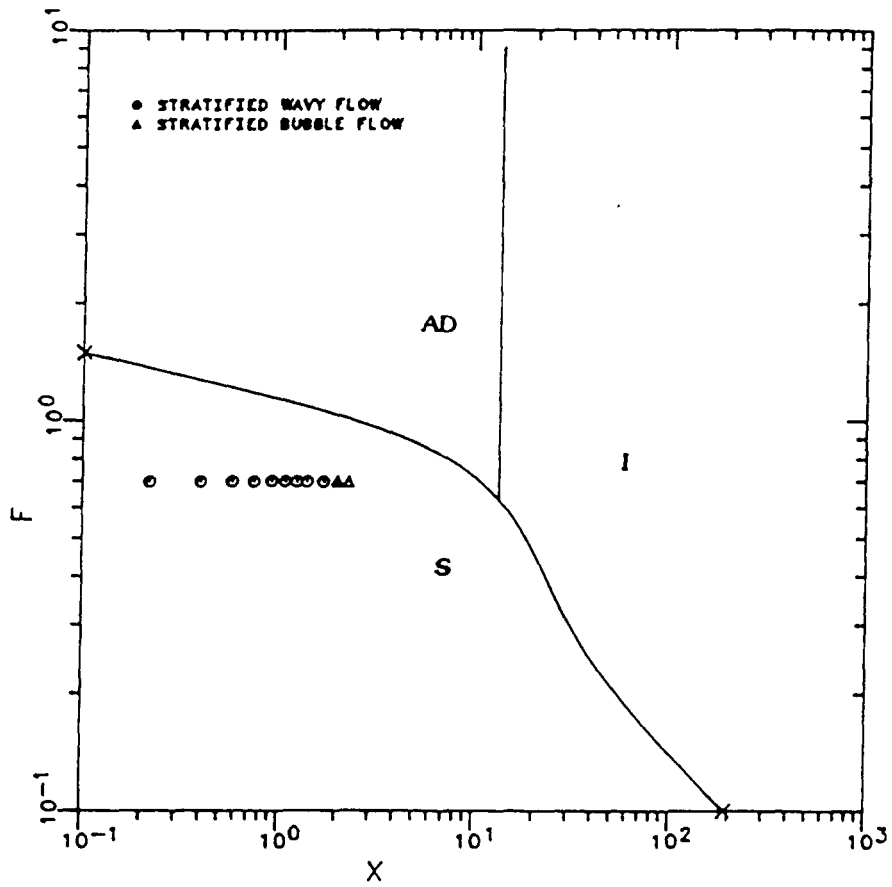

COMPARISON OF FLOW DATA TO GENERALIZED FLOW REGIME MAP (TAITEL & DUKLER) OIL FLOW RATE = 300 B/D
ANGLE OF INCLINATION = -15 DEGREES
TRANSITION BETWEEN STRATIFIED SMOOTH (SS) AND STRATIFIED WAVY (SW) REGIMES

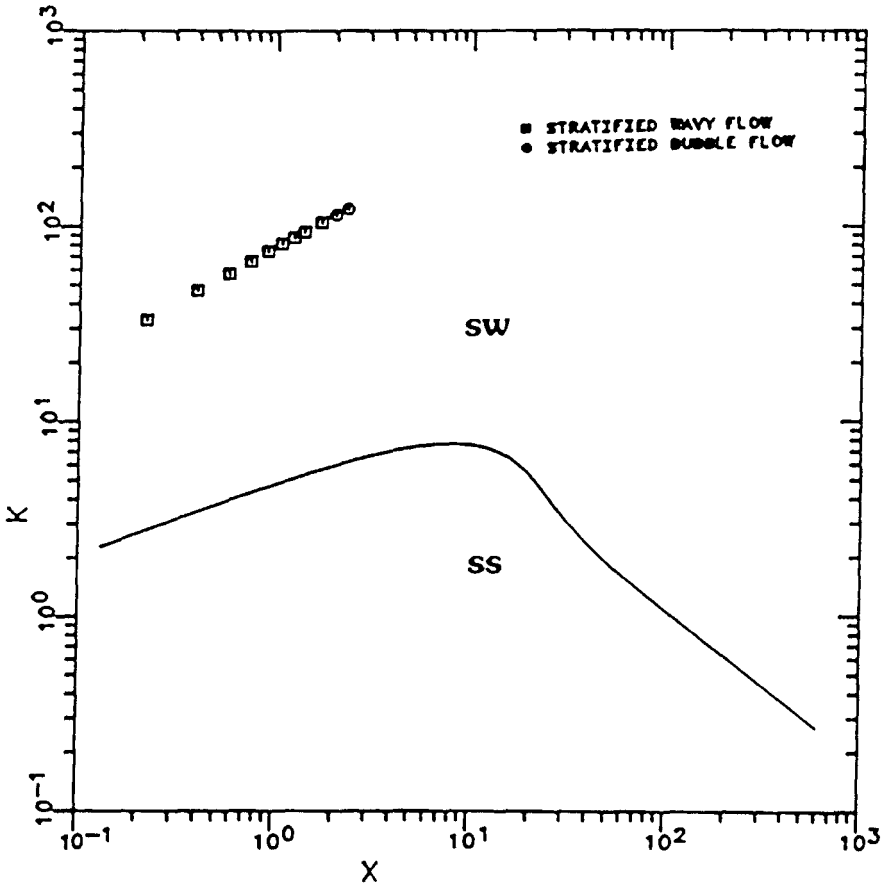

COMPARISON OF FLOW DATA TO GENERALIZED FLOW REGIME
MAP (TAITEL & DUKLER) OIL FLOW RATE = 300 B/D
ANGLE OF INCLINATION = -15 DEGREES
TRANSITION BETWEEN INTERMITTENT (I) AND
DISPERSED BUBBLE (DB) REGIMES

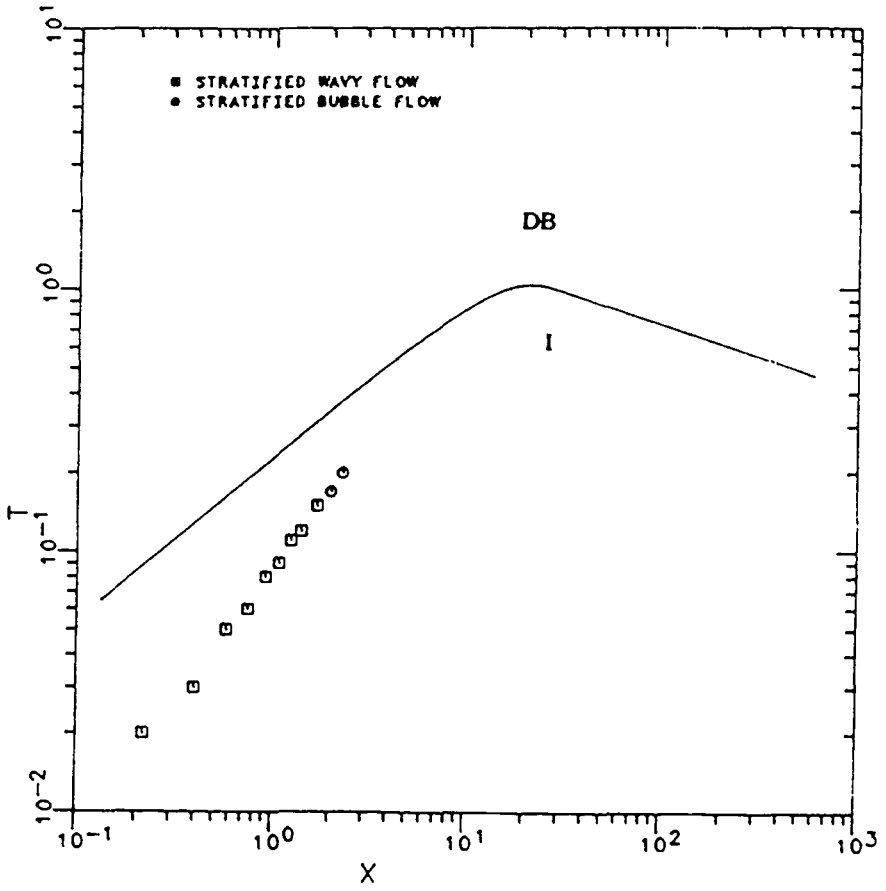

GENERALIZED FLOW REGIME MAP
ANGLE OF INCLINATION = -15 DEGREES
OIL FLOW RATE = 500 B/D

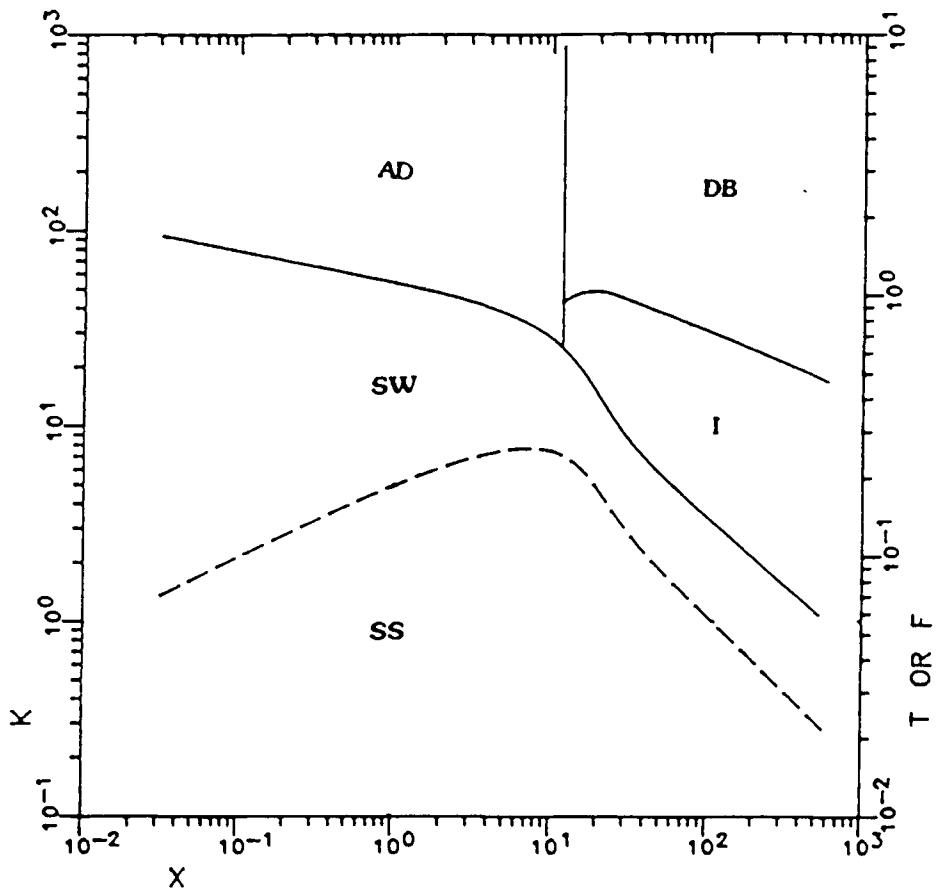

COMPARISON OF FLOW DATA TO GENERALIZED FLOW REGIME MAP (TAITEL & DUKLER) OIL FLOW RATE = 500 B/D
ANGLE OF INCLINATION = -15 DEGREES
TRANSITION BETWEEN STRATIFIED (S) AND INTERMITTENT (I) OR ANNULAR-DISPERSED LIQUID (AD) REGIMES

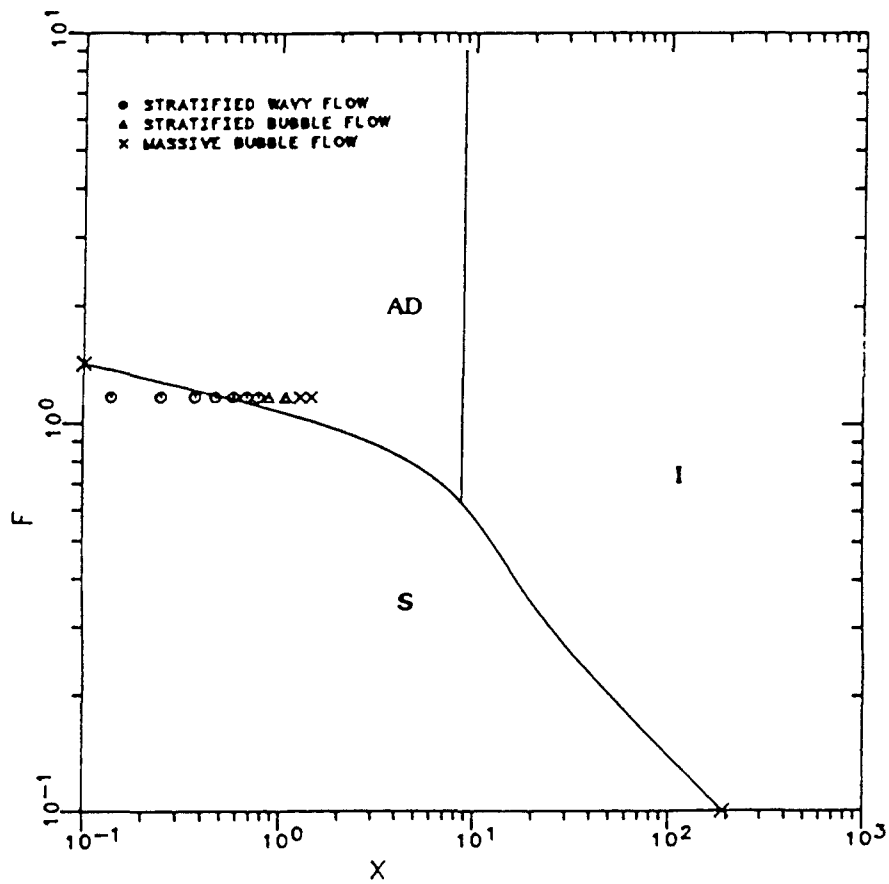

COMPARISON OF FLOW DATA TO GENERALIZED FLOW REGIME
MAP (TAITEL & DUKLER) OIL FLOW RATE = 500 B/D
ANGLE OF INCLINATION = -15 DEGREES
TRANSITION BETWEEN INTERMITTENT (I) AND
ANNULAR-DISPERSED LIQUID (AD) REGIMES

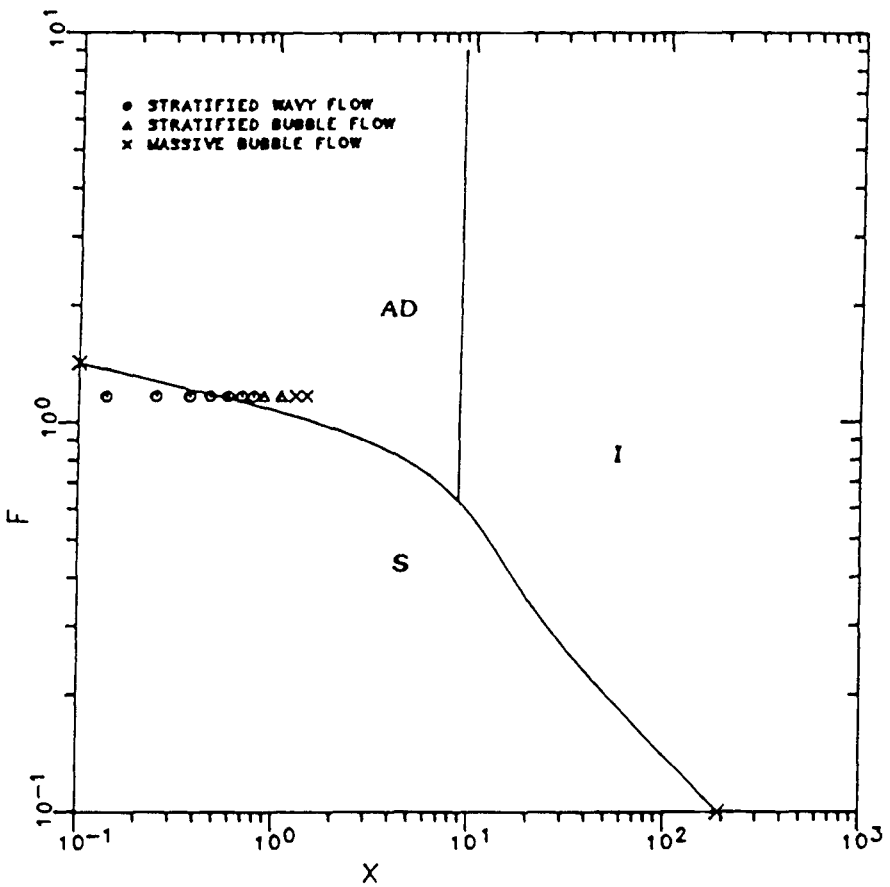

COMPARISON OF FLOW DATA TO GENERALIZED FLOW REGIME MAP (TAITEL & DUKLER) OIL FLOW RATE = 500 B/D
ANGLE OF INCLINATION = -15 DEGREES
TRANSITION BETWEEN STRATIFIED SMOOTH (SS) AND STRATIFIED WAVY (SW) REGIMES

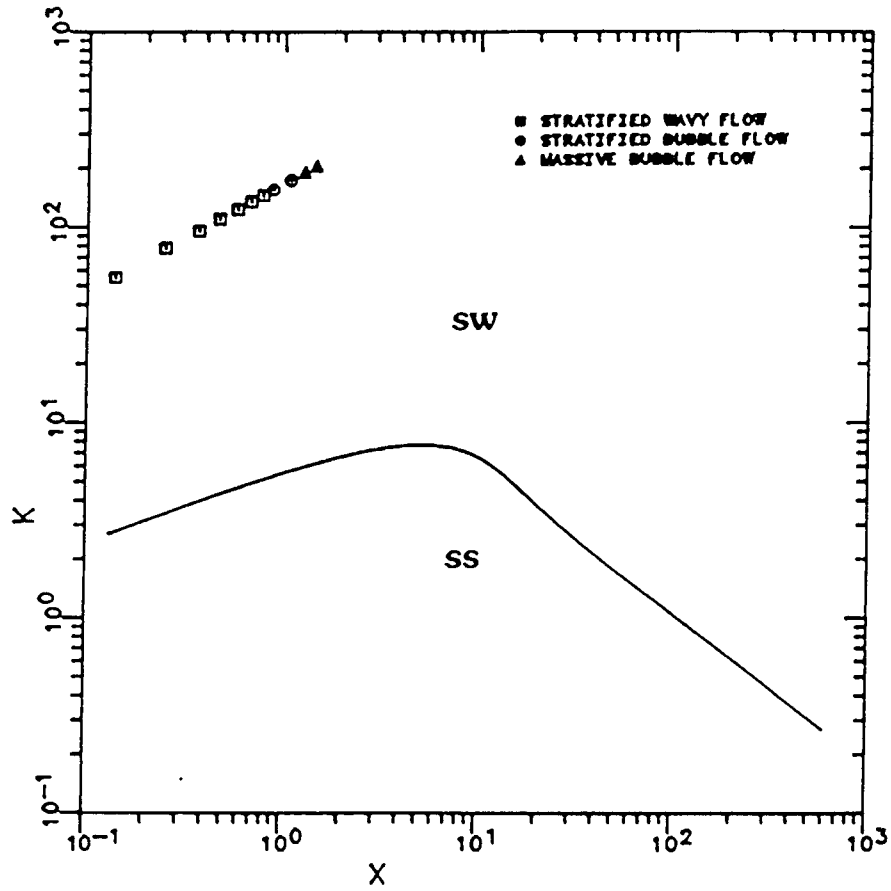

COMPARISON OF FLOW DATA TO GENERALIZED FLOW REGIME MAP (TAITEL & DUKLER) OIL FLOW RATE = 500 B/D ANGLE OF INCLINATION = -15 DEGREES TRANSITION BETWEEN INTERMITTENT (I) AND DISPERSED BUBBLE (DB) REGIMES

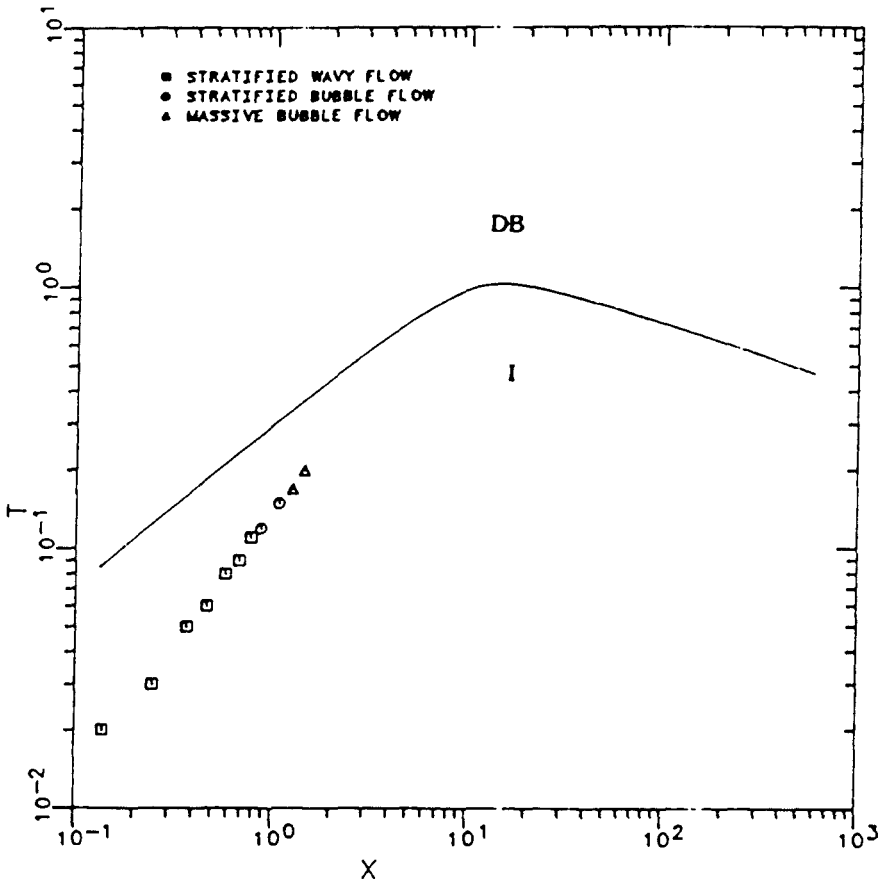

GENERALIZED FLOW REGIME MAP
ANGLE OF INCLINATION = -30 DEGREES
OIL FLOW RATE = 300 B/D

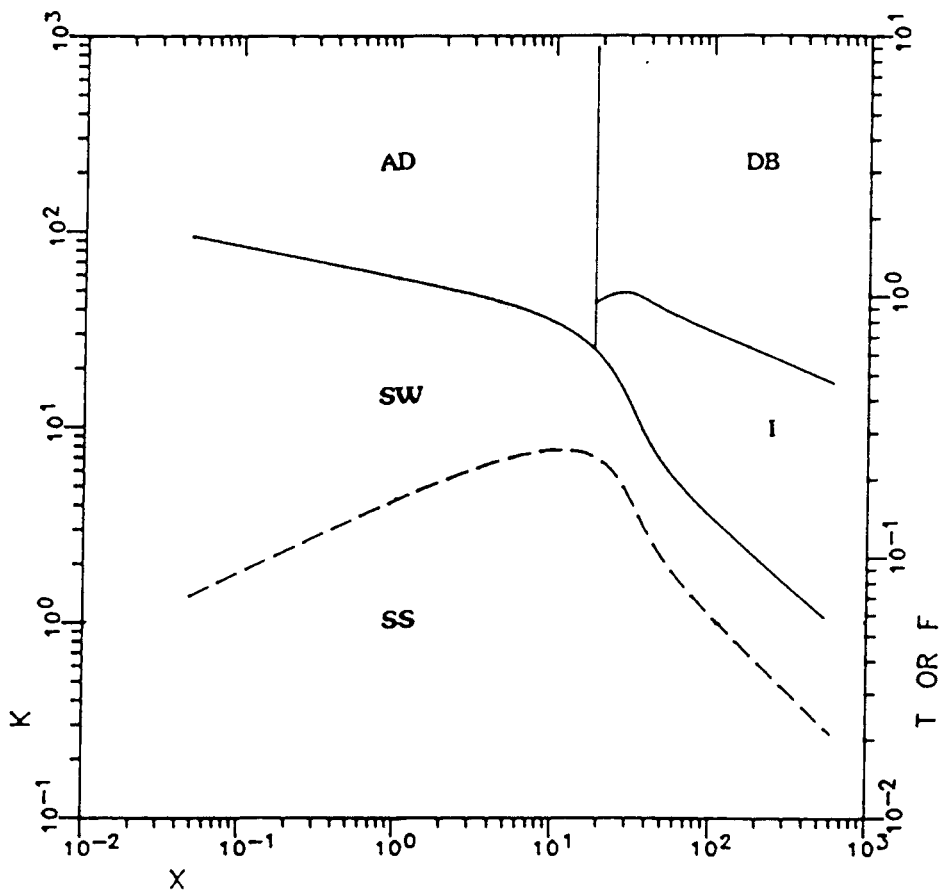

COMPARISON OF FLOW DATA TO GENERALIZED FLOW REGIME MAP (TAITEL & DUKLER) OIL FLOW RATE = 300 B/D
ANGLE OF INCLINATION = -30 DEGREES
TRANSITION BETWEEN STRATIFIED (S) AND INTERMITTENT (I) OR ANNULAR-DISPERSED LIQUID (AD) REGIMES

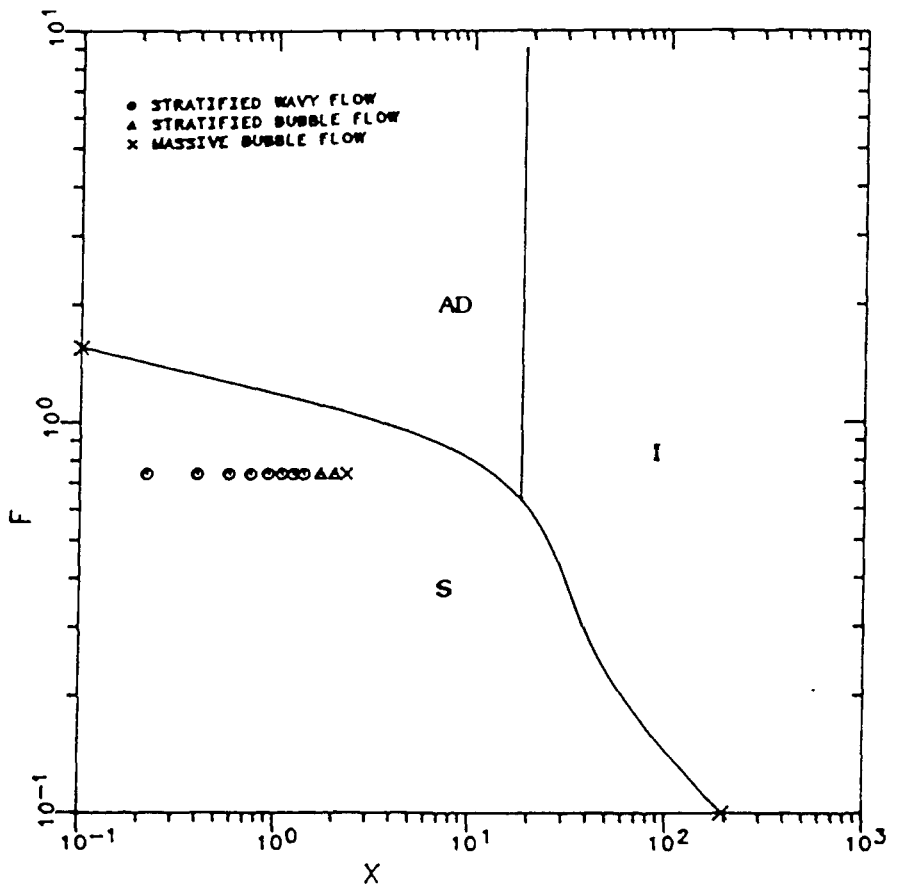

COMPARISON OF FLOW DATA TO GENERALIZED FLOW REGIME MAP (TAITEL & DUKLER) OIL FLOW RATE = 300 B/D ANGLE OF INCLINATION = -30 DEGREES TRANSITION BETWEEN INTERMITTENT (I) AND ANNULAR-DISPERSED LIQUID (AD) REGIMES

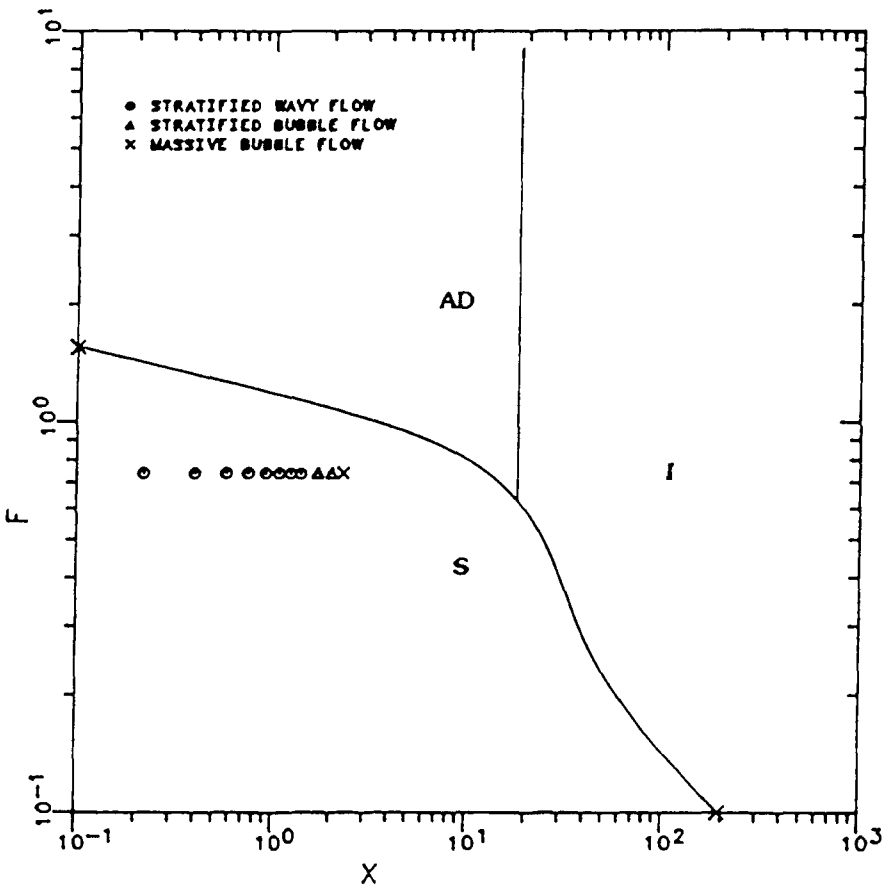

COMPARISON OF FLOW DATA TO GENERALIZED FLOW REGIME MAP (TAITEL & DUKLER) OIL FLOW RATE = 300 B/D
ANGLE OF INCLINATION = -30 DEGREES
TRANSITION BETWEEN STRATIFIED SMOOTH (SS) AND STRATIFIED WAVY (SW) REGIMES

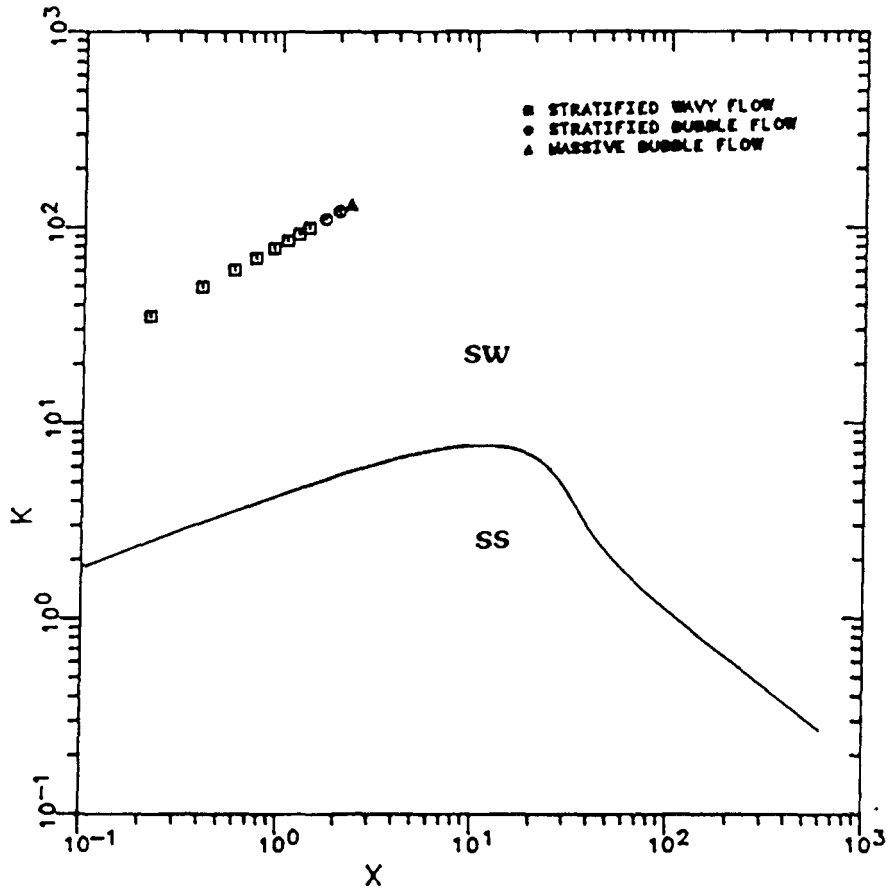

COMPARISON OF FLOW DATA TO GENERALIZED FLOW REGIME MAP (TAITEL & DUKLER) OIL FLOW RATE = 300 B/D
ANGLE OF INCLINATION = -30 DEGREES
TRANSITION BETWEEN INTERMITTENT (I) AND DISPERSED BUBBLE (DB) REGIMES

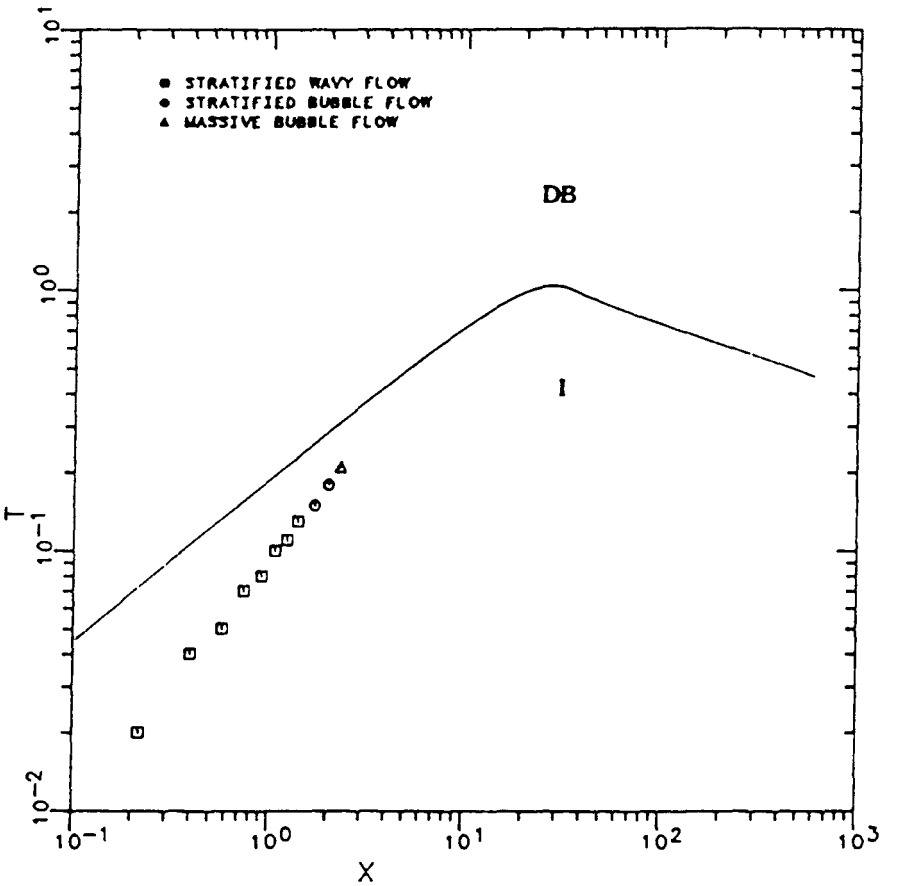

GENERALIZED FLOW REGIME MAP
ANGLE OF INCLINATION = -30 DEGREES
OIL FLOW RATE = 500 B/D

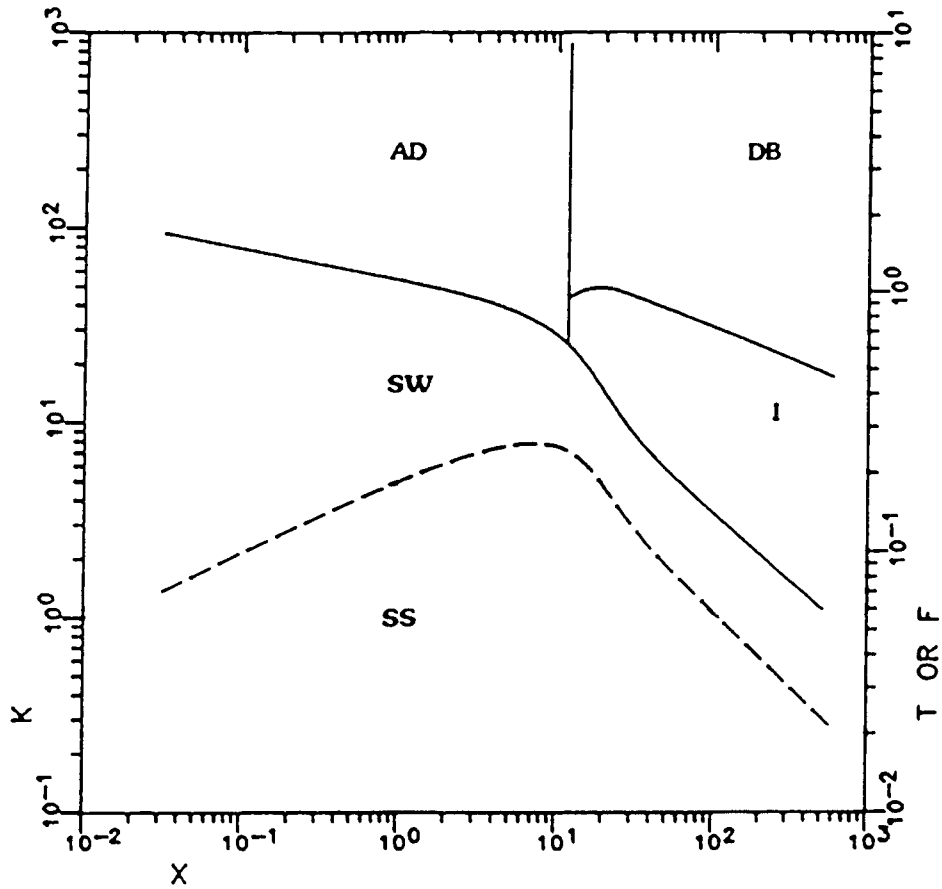

COMPARISON OF FLOW DATA TO GENERALIZED FLOW REGIME MAP (TAITEL & DUKLER) OIL FLOW RATE = 500 B/D
ANGLE OF INCLINATION = -30 DEGREES
TRANSITION BETWEEN STRATIFIED (S) AND INTERMITTENT (I) OR ANNULAR-DISPERSED LIQUID (AD) REGIMES

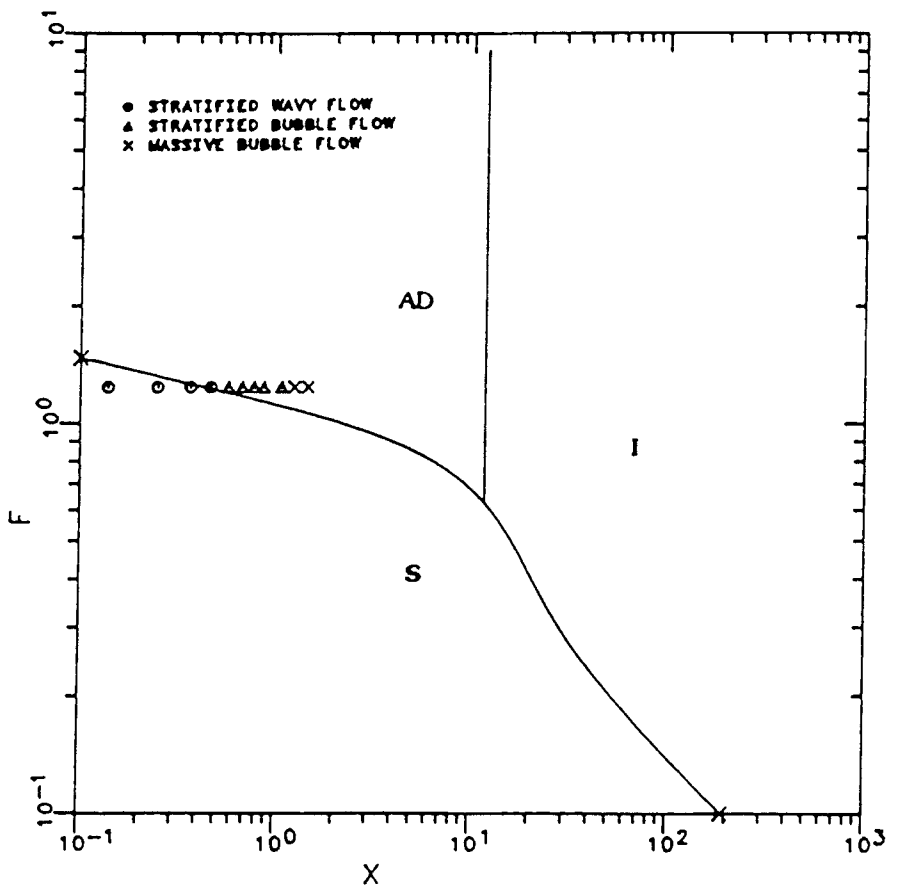

COMPARISON OF FLOW DATA TO GENERALIZED FLOW REGIME MAP (TAITEL & DUKLER) OIL FLOW RATE = 500 B/D ANGLE OF INCLINATION = -30 DEGREES TRANSITION BETWEEN INTERMITTENT (I) AND ANNULAR-DISPERSED LIQUID (AD) REGIMES

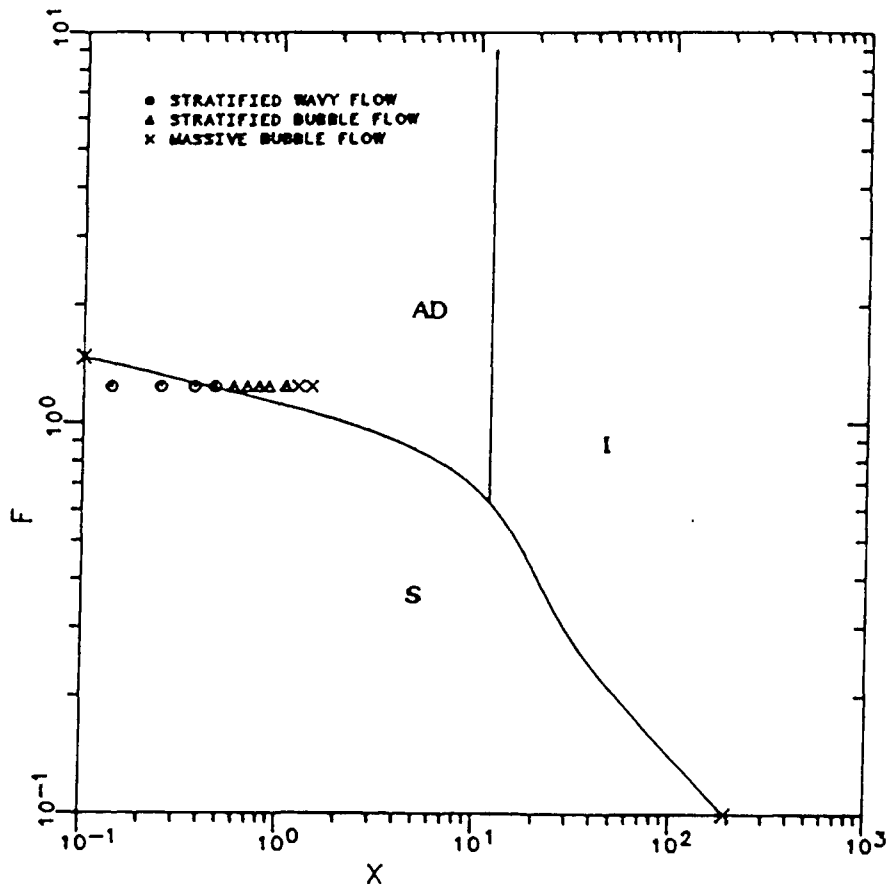

COMPARISON OF FLOW DATA TO GENERALIZED FLOW REGIME MAP (TAITEL & DUKLER) OIL FLOW RATE = 500 B/D ANGLE OF INCLINATION = -30 DEGREES TRANSITION BETWEEN STRATIFIED SMOOTH (SS) AND STRATIFIED WAVY (SW) REGIMES

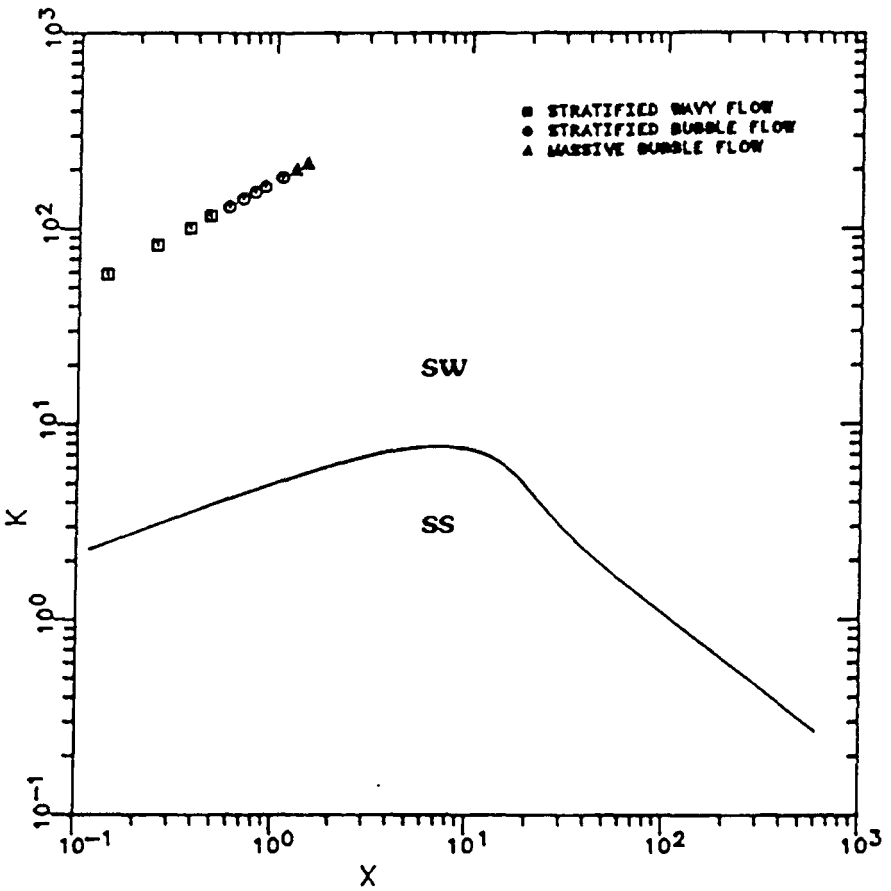

COMPARISON OF FLOW DATA TO GENERALIZED FLOW REGIME MAP (TAITEL & DUKLER) OIL FLOW RATE = 500 B/D
ANGLE OF INCLINATION = -30 DEGREES
TRANSITION BETWEEN INTERMITTENT (I) AND DISPERSED BUBBLE (DB) REGIMES

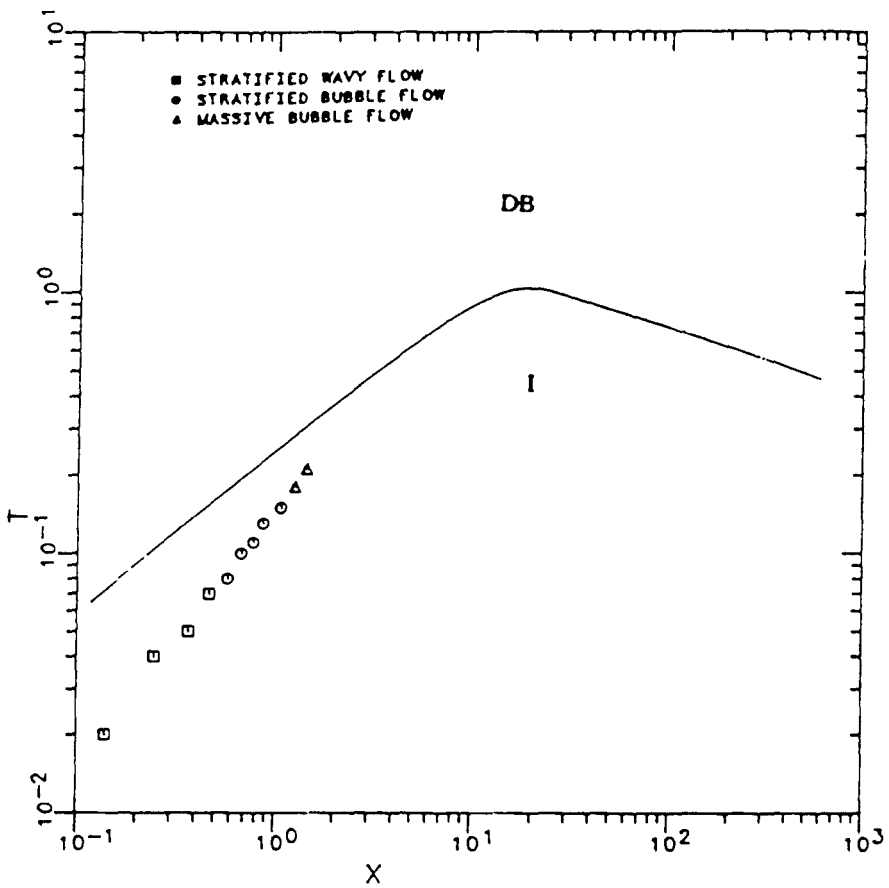

APPENDIX IV

COMPUTER PROGRAM HOLDUP AND GENERATED OUTPUT

```
      PROGRAM HOLDUP(INPUT,OUTPUT,TAPE5=INPUT,TAPE6=OUTPUT)
C*****************************************************************
C                                                                *
C  PURPOSE:                                                      *
C                                                                *
C   PROGRAM HOLDUP CALCULATES THE VOLUME FRACTION OF THE PIPE    *
C   OCCUPIED BY THE MORE DENSE PHASE.  THIS VOLUME FRACTION      *
C   IS REFERRED TO AS HOLDUP.                                    *
C                                                                *
C  INPUT PARAMETERS:                                             *
C                                                                *
C   N          -  NUMBER OF INPUT DATA LINES                     *
C   QOIL       -  OIL FLOW RATE, B/D                             *
C   QWATER     -  WATER FLOW RATE, B/D                           *
C   ANGLE      -  ANGLE OF INCLINATION, DEGREES                  *
C   FR         -  FLOW REGIME OBSERVED AT GIVEN FLOW             *
C                 RATES OF OIL AND WATER                         *
C   DTI        -  DISTANCE TO INTERFACE, CM                      *
C                                                                *
C  OUTPUT PARAMETERS:                                            *
C                                                                *
C   QOIL       -  OIL FLOW RATE, B/D                             *
C   QWATER     -  WATER FLOW RATE, B/D                           *
C   ANGLE      -  ANGLE OF INCLINATION, DEGREES                  *
C   FR         -  FLOW REGIME OBSERVED AT GIVEN FLOW             *
C                 RATES OF OIL AND WATER                         *
C   HU         -  HOLDUP OF THE MORE DENSE PHASE                 *
C   VF         -  VOID FRACTION                                  *
C   OIF        -  OIL INPUT FRACTION                             *
C   WIF        -  WATER INPUT FRACTION                           *
C   HUR        -  HOLDUP RATIO                                   *
C                                                                *
C*****************************************************************
      REAL QOIL(1000),QWATER(1000),ANGLE(1000),DTI(1000),VF(1000)
      REAL VOLW(1000),HU(1000),WIF(1000),OIF(1000),HUR(1000)
      INTEGER FR(1000)
      READ(5,*)N
      VOLT=2861.5
C-----------------------------------------------------------------
C     READ INPUT PARAMETERS
C-----------------------------------------------------------------
      DO 1 I=1,N
        READ(5,7)QOIL(I),QWATER(I),ANGLE(I),FR(I),DTI(I)
```

```
C-----------------------------------------------------------------
C     CALCULATION OF OUTPUT PARAMETERS
C-----------------------------------------------------------------
        VOLW(I)=356.13+20.268*DTI(I)
        HU(I)=VOLW(I)/VOLT
        VF(I)=1.0-HU(I)
        WIF(I)=QWATER(I)/(QWATER(I)+QOIL(I))
        OIF(I)=1.0-WIF(I)
        HUR(I)=((HU(I)/VF(I))/(WIF(I)/OIF(I)))
  1   CONTINUE
      WRITE(6,10)
C-----------------------------------------------------------------
C     PRINT OUT CALCULATED PARAMETERS
C-----------------------------------------------------------------
      DO 2 I=1,N
        WRITE(6,20)QOIL(I),QWATER(I),ANGLE(I),FR(I),HU(I),VF(I),
     $  WIF(I),OIF(I),HUR(I)
  2   CONTINUE
C-----------------------------------------------------------------
C     FORMAT STATEMENTS
C-----------------------------------------------------------------
  7   FORMAT(F6.1,F6.1,F6.1,A5,F6.1)
  10  FORMAT(1H1,T2,*QOIL*,T11,*QWATER*,T22,*ANGLE*,T32,
     $*FLOW REGIME*,T48,*HOLDUP*,T59,*VOID FRACTION*,T76,
     $*WATER INPUT*,T92,*OIL INPUT*,T106,*HOLDUP*/,T3,*B/D*,T13,
     $*B/D*,T34,*OBSERVED*,T77,*FRACTION*,T93,*FRACTION*,T107,
     $*RATIO*/,T2,4(*-*),T11,6(*-*),T22,5(*-*),T32,11(*-*),
     $T48,6(*-*),T59,13(*-*),T76,11(*-*),T92,9(*-*),T106,
     $6(*-*)/)
 20   FORMAT(2X,T2,F5.1,T11,F5.1,T22,F5.1,T36,A4,T49,F4.2,T63,F4.2,
     $T80,F4.2,T95,F4.2,T107,F4.2)
      END
```

QOIL B/D	QWATER B/D	ANGLE	FLOW REGIME OBSERVED	HOLDUP	VOID FRACTION	WATER INPUT FRACTION	OIL INPUT FRACTION	HOLDUP RATIO
50 0	50 0	0	SS	50	50	50	50	1 00
50 0	100 0	0	SW	67	33	67	33	1 01
50 0	150 0	0	SW	71	29	75	25	80
50 0	200 0	0	SW	76	24	80	20	80
50 0	250 0	0	SW	78	22	83	17	71
50 0	300 0	0	SW	84	16	84	14	91
50 0	350 0	0	SW	85	15	88	13	79
50 0	400 0	0	SW	86	14	89	11	76
50 0	500 0	0	SW	88	12	91	09	70
50 0	600 0	0	SW	90	10	92	08	72
50 0	700 0	0	SW	92	08	93	07	85
100 0	50 0	0	SW	39	61	33	67	1 26
100 0	100 0	0	SW	50	50	50	50	1 00
100 0	150 0	0	SW	57	43	60	40	89
100 0	200 0	0	SW	64	36	67	33	89
100 0	250. 0	0	SW	68	32	71	29	87
100 0	300 0	0	SW	71	29	75	25	82
100. 0	350 0	0	SW	73	27	78	22	76
100. 0	400 0	0	SW	78	22	80	20	87
100 0	500 0	0	SW	80	20	83	17	.79
100 0	600 0	0	SW	82	18	86	14	75
100 0	700 0	0	SB	85	15	88	13	79
150 0	50 0	0	SW	30	70	25	75	1 30
150 0	100. 0	0	SW	41	59	40	60	1 06
150 0	150 0	0	SW	50	50	50	50	1 00
150 0	200. 0	0	SW	54	46	57	43	86
150 0	250. 0	0	SW	61	39	63	38	95
150 0	300 0	0	SW	66	34	67	33	.97
150 0	350 0	0	SW	70	30	70	30	.98
150 0	400. 0	0	SW	73	27	73	27	1.00
150 0	500 0	0	SW	75	25	77	23	92
150 0	600. 0	0	SW	80	20	80	20	98
150 0	700 0	0	SB	83	17	82	18	1.08
200 0	50 0	0	SW	26	74	20	80	1.40
200 0	100 0	0	SW	39	61	33	67	1 26
200 0	150 0	0	SW	41	59	43	57	95
200 0	200 0	0	SW	50	50	50	50	1.00
200 0	250 0	0	SW	56	44	56	44	1.03
200 0	300 0	0	SW	61	39	60	40	1.03
200 0	350. 0	0	SW	.63	.37	64	36	.99
200. 0	400. 0	0	SW	.65	.35	67	33	.94
200. 0	500. 0	0	SW	72	.28	71	29	1.03
200 0	600 0	0	SW	73	.27	75	25	92
200 0	700 0	0	SB	75	25	78	22	85
250 0	50 0	0	SW	18	82	17	83	1 11
250 0	100. 0	0	SW	32	68	29	71	1 15
250. 0	150. 0	0	SW	40	.60	38	.63	1 11
250 0	200 0	0	SW	45	55	44	56	1.02
250 0	250 0	0	SW	51	.49	50	50	1.03
250 0	300 0	0	SW	56	.44	55	45	1 08
250 0	350 0	0	SW	58	.42	58	42	1 01
250. 0	400 0	0	SW	62	.38	62	38	1.01
250. 0	500 0	0	SW	66	34	67	33	95
250 0	600 0	0	SW	67	33	71	29	85
250 0	700. 0	0	SB	69	.31	74	26	80
300 0	50 0	0	SW	17	83	14	86	1 26
300 0	100. 0	0	SW	29	71	25	75	1 24
300 0	150 0	0	SW	36	64	33	67	1 12

QOIL B/D	QWATER B/D	ANGLE	FLOW REGIME OBSERVED	HOLDUP	VOID FRACTION	WATER INPUT FRACTION	OIL INPUT FRACTION	HOLDUP RATIO
300 0	200 0	0	SW	41	59	40	60	1 03
300 0	250 0	0	SW	48	52	45	55	1 10
300 0	300 0	0	SW	51	49	50	50	1 03
300 0	350 0	0	SW	54	46	54	46	1 05
300 0	400 0	0	SW	58	42	57	43	1 06
300 0	500 0	0	SW	63	37	63	38	1 01
300 0	600 0	0	SB	65	35	67	33	92
300 0	700 0	0	SB	67	33	70	30	87
350 0	50 0	0	SW	15	85	13	88	1 19
350 0	100 0	0	SW	24	76	22	78	1 09
350 0	200 0	0	SW	41	59	36	64	1 24
350 0	250 0	0	SW	44	56	42	58	1 08
350 0	300. 0	0	SW	48	52	46	54	1 07
350 0	350 0	0	SW	51	49	50	50	1 03
350 0	400 0	0	SW	52	48	53	47	96
350 0	500 0	0	SB	59	41	59	41	1 02
350 0	600 0	0	SB	65	35	63	37	1 08
350 0	700 0	0	SB	66	34	67	33	98
400 0	50 0	0	SW	16	84	11	89	1.52
400 0	100. 0	0	SW	22	78	20	80	1 15
400 0	200. 0	0	SW	35	65	33	67	1 10
400 0	400 0	0	SW	50	50	50	50	1 00
400 0	600 0	0	SB	59	41	60	40	95
400 0	700 0	0	MB	64	36	64	36	1 02
500 0	50 0	0	SW	08	92	09	91	89
500 0	100 0	0	SW	21	79	17	83	1.32
500 0	400 0	0	SB	45	55	44	56	1 02
500 0	600. 0	0	SB	53	.47	55	45	95
500 0	700. 0	0	MB	57	.43	58	42	.93
600. 0	50 0	0	SW	12	.08	.08	92	1.60
600 0	100. 0	0	SW	17	83	14	86	1.26
600 0	200. 0	0	SW	27	73	25	75	1.13
600 0	400. 0	0	SB	40	60	40	60	1.02
600. 0	600. 0	0	MB	50	.50	50	50	1.00
600 0	700 0	0	MB	54	46	54	46	1.02
700 0	100. 0	0	SW	17	83	13	88	1 42
700 0	200 0	0	SW	29	71	22	78	1 40
700 0	400 0	0	SB	37	63	36	64	1 03
700. 0	600. 0	0	MB	50	50	46	54	1 16
700. 0	700 0	0	MB	52	48	50	50	1.07
50 0	50. 0	-15. 0	SWC	11	.89	50	50	12
50 0	100. 0	-15. 0	SWC	22	78	67	33	14
50 0	150. 0	-15. 0	SWC	30	70	.75	25	15
50 0	200. 0	-15 0	SWC	43	.57	80	20	19
50 0	250. 0	-15. 0	SWC	58	.42	.83	17	28
50 0	300. 0	-15. 0	SWC	68	32	86	14	35
50 0	350. 0	-15. 0	SWC	72	28	88	13	37
50 0	400 0	-15. 0	SWC	.80	20	89	11	49
50 0	500. 0	-15. 0	SWC	84	16	91	09	52
50 0	600. 0	-15. 0	SWC	86	.14	92	08	51
50. 0	700. 0	-15 0	SW	91	09	93	07	73
100 0	100 0	-15. 0	SWC	26	74	50	50	35
100 0	200. 0	-15. 0	SWC	37	63	67	33	30
100 0	400 0	-15 0	SWC	73	27	80	20	69
100 0	600. 0	-15 0	SW	82	18	.86	14	74
100 0	700 0	-15 0	SW	85	15	88	13	80
150 0	50 0	-15. 0	SW	14	86	25	75	47
150 0	100 0	-15 0	SW	20	80	40	60	36

QOIL B/D	QWATER B/D	ANGLE	FLOW REGIM OBSERVED	HOLDUP	VOID FRACTION	WATER INPUT FRACTION	OIL INPUT FRACTION	HOLDUP RATIO
150.0	150.0	-15.0	SW	.27	.73	.50	.50	.37
150.0	200.0	-15.0	SW	.34	.66	.57	.43	.38
150.0	250.0	-15.0	SW	.39	.61	.63	.38	.38
150.0	300.0	-15.0	SW	.44	.56	.67	.33	.39
150.0	350.0	-15.0	SW	.48	.52	.70	.30	.39
150.0	400.0	-15.0	SW	.54	.46	.73	.27	.44
150.0	500.0	-15.0	SW	.63	.37	.77	.23	.51
150.0	600.0	-15.0	SW	.68	.32	.80	.20	.54
150.0	700.0	-15.0	SB	.74	.26	.82	.18	.61
200.0	50.0	-15.0	SW	.10	.90	.20	.80	.43
200.0	100.0	-15.0	SW	.17	.83	.33	.67	.42
200.0	150.0	-15.0	SW	.27	.73	.43	.57	.49
200.0	200.0	-15.0	SW	.30	.70	.50	.50	.43
200.0	250.0	-15.0	SW	.37	.63	.56	.44	.47
200.0	300.0	-15.0	SW	.41	.59	.60	.40	.46
200.0	350.0	-15.0	SW	.45	.55	.64	.36	.47
200.0	400.0	-15.0	SW	.51	.49	.67	.33	.53
200.0	500.0	-15.0	SW	.60	.40	.71	.29	.61
200.0	600.0	-15.0	SW	.66	.34	.75	.25	.66
200.0	700.0	-15.0	SB	.69	.31	.78	.22	.64
250.0	50.0	-15.0	SW	.07	.93	.17	.83	.40
250.0	100.0	-15.0	SW	.17	.83	.29	.71	.53
250.0	150.0	-15.0	SW	.23	.77	.38	.63	.49
250.0	200.0	-15.0	SW	.29	.71	.44	.56	.50
250.0	250.0	-15.0	SW	.36	.64	.50	.50	.56
250.0	300.0	-15.0	SW	.41	.59	.55	.45	.57
250.0	350.0	-15.0	SW	.44	.56	.58	.42	.57
250.0	400.0	-15.0	SW	.47	.53	.62	.38	.56
250.0	500.0	-15.0	SW	.54	.46	.67	.33	.59
250.0	600.0	-15.0	SB	.62	.38	.71	.29	.67
250.0	700.0	-15.0	SB	.68	.32	.74	.26	.77
300.0	50.0	-15.0	SW	.10	.90	.14	.86	.69
300.0	100.0	-15.0	SW	.15	.85	.25	.75	.54
300.0	150.0	-15.0	SW	.25	.75	.33	.67	.66
300.0	200.0	-15.0	SW	.28	.72	.40	.60	.58
300.0	250.0	-15.0	SW	.33	.67	.45	.55	.59
300.0	300.0	-15.0	SW	.37	.63	.50	.50	.59
300.0	350.0	-15.0	SW	.41	.59	.54	.46	.59
300.0	400.0	-15.0	SW	.45	.55	.57	.43	.61
300.0	500.0	-15.0	SW	.50	.50	.63	.38	.61
300.0	600.0	-15.0	SB	.59	.41	.67	.33	.73
300.0	700.0	-15.0	SB	.69	.31	.70	.30	.96
350.0	50.0	-15.0	SW	.12	.88	.13	.88	.95
350.0	100.0	-15.0	SW	.24	.76	.22	.78	1.09
350.0	200.0	-15.0	SW	.29	.71	.36	.64	.70
350.0	250.0	-15.0	SW	.33	.67	.42	.58	.70
350.0	300.0	-15.0	SW	.36	.64	.46	.54	.65
350.0	350.0	-15.0	SW	.38	.62	.50	.50	.61
350.0	400.0	-15.0	SW	.45	.55	.53	.47	.70
350.0	500.0	-15.0	SW	.49	.51	.59	.41	.66
350.0	600.0	-15.0	SB	.61	.39	.63	.37	.92
350.0	700.0	-15.0	SB	.68	.32	.67	.33	1.05
400.0	50.0	-15.0	SW	.10	.90	.11	.89	.92
400.0	100.0	-15.0	SW	.15	.85	.20	.80	.73
400.0	200.0	-15.0	SW	.28	.72	.33	.67	.78
400.0	400.0	-15.0	SW	.43	.57	.50	.50	.75
400.0	600.0	-15.0	MB	.58	.42	.60	.40	.91
400.0	700.0	-15.0	MB	.63	.37	.64	.36	.96

QOIL B/D	QWATER B/D	ANGLE	FLOW REGIME OBSERVED	HOLDUP	VOID FRACTION	WATER INPUT FRACTION	OIL INPUT FRACTION	HOLDUP RATIO
500 0	50 0	-15 0	SW	08	92	09	91	89
500 0	100. 0	-15 0	SW	12	88	17	83	71
500 0	400 0	-15 0	SB	38	62	44	56	76
500 0	600 0	-15 0	MB	53	47	55	45	93
500 0	700 0	-15 0	MB	57	43	58	42	95
600 0	50 0	-15 0	SW	09	91	08	92	1 17
600 0	100 0	-15 0	SW	12	88	14	86	85
600 0	200 0	-15 0	SW	25	75	25	75	1 00
600 0	400. 0	-15 0	SB	39	61	40	60	97
600 0	600 0	-15 0	MB	52	48	50	50	1 08
600 0	700 0	-15 0	MB	59	41	54	46	1 24
700 0	100 0	-15 0	SW	15	85	13	88	1 26
700 0	200. 0	-15 0	SW	24	76	22	78	1 13
700 0	400 0	-15 0	SB	39	61	36	64	1 14
700 0	600 0	-15 0	MB	48	52	46	54	1. 08
700 0	700 0	-15 0	MB	54	46	50	50	1. 16
50 0	50. 0	-30. 0	SWC	11	89	50	50	.12
50 0	100 0	-30 0	SWC	25	75	67	33	16
50 0	150. 0	-30 0	SWC	47	53	75	25	29
50 0	200. 0	-30 0	SWC	54	46	80	20	30
50 0	250 0	-30 0	SWC	69	31	83	17	44
50. 0	300. 0	-30 0	SWC	78	22	86	14	58
50 0	350. 0	-30 0	SWC	79	21	88	13	53
50. 0	400. 0	-30 0	SWC	85	15	89	11	69
50 0	700. 0	-30 0	SW	92	08	93	07	78
100 0	100. 0	-30. 0	SWC	24	76	50	50	.32
100 0	200. 0	-30. 0	SWC	47	53	67	33	45
100. 0	400. 0	-30. 0	SWC	79	.21	80	20	.95
100 0	600. 0	-30 0	SW	83	17	.86	14	79
100 0	700. 0	-30. 0	SW	86	.14	88	13	.87
150 0	50. 0	-30. 0	SW	12	88	25	75	.40
150. 0	100. 0	-30. 0	SW	20	80	40	60	.38
150 0	150. 0	-30. 0	SW	30	70	50	50	.43
150 0	200. 0	-30 0	SW	34	66	57	43	.38
150 0	250 0	-30. 0	SW	43	57	63	38	45
150 0	300 0	-30 0	SW	47	53	67	33	45
150 0	350. 0	-30. 0	SW	51	49	70	30	.45
150 0	400. 0	-30. 0	SW	61	39	73	.27	.56
150. 0	500. 0	-30. 0	SW	67	33	77	23	.61
150 0	600. 0	-30. 0	SB	69	.31	.80	.20	.56
150 0	700 0	-30. 0	SB	73	.27	.82	.18	.58
200. 0	50. 0	-30. 0	SW	10	90	20	80	43
200 0	100. 0	-30. 0	SW	22	78	33	67	.35
200 0	150. 0	-30. 0	SW	26	74	43	57	.47
200 0	200. 0	-30. 0	SW	37	63	50	50	58
200. 0	250. 0	-30. 0	SW	42	.58	56	.44	59
200. 0	300. 0	-30. 0	SW	46	.54	.60	.40	.57
200. 0	350. 0	-30. 0	SW	.51	.49	64	36	.59
200 0	400. 0	-30 0	SW	57	.43	67	.33	.65
200. 0	500. 0	-30. 0	SB	64	.36	71	29	.72
200. 0	600. 0	-30. 0	SB	69	31	75	25	.74
200 0	700 0	-30. 0	SB	74	26	.78	22	.80
250 0	50. 0	-30. 0	SW	09	91	17	83	49
250 0	100 0	-30. 0	SW	18	82	29	71	.35
250 0	150. 0	-30. 0	SW	27	.73	38	63	.63
250 0	200 0	-30 0	SW	34	66	44	56	64
250 0	250. 0	-30. 0	SW	39	61	50	50	64
250 0	300. 0	-30. 0	SW	47	53	55	45	73

OIL B/D	WATER B/D	ANGLE	FLOW REGIM OBSERVED	HOLDUP	VOID FRACTION	WATER INPUT FRACTION	OIL INPUT FRACTION	HOLDUP RATIO
					49	58	42	75
250 0	350 0	-30 0	SW	51	45	62	38	76
250 0	400 0	-30 0	SW	55	39	67	33	78
250 0	500 0	-30 0	SB	61	35	71	29	79
250 0	600 0	-30 0	SB	65	26	74	26	1 01
250 0	700 0	-30 0	SB	74	88	14	86	80
300 0	50 0	-30 0	SW	12	85	25	.75	53
300 0	100 0	-30 0	SW	15	75	33	67	67
300 0	150. 0	30 0	SW	25	72	40	60	58
300 0	200 0	30 0	SW	28	70	45	55	52
300 0	250 0	30 0	SW	30	62	50	50	62
300 0	300 0	-30 0	SW	38	54	54	46	74
300 0	350 0	-30 0	SW	46	51	57	43	71
300 0	400 0	-30 0	SW	49	46	63	38	69
300 0	500 0	-30 0	SB	54	38	67	33	82
300 0	600 0	-30 0	SW	62	31	70	30	94
300 0	700 0	-30 0	MB	69	13	13	88	1 06
350 0	50 0	-30 0	SW	13	78	22	78	1 01
350 0	100. 0	-30 0	SW	22	70	36	64	75
350 0	200. 0	-30 0	SW	30	66	42	58	72
350 0	250. 0	-30 0	SW	34	61	46	54	74
350. 0	300. 0	-30. 0	SW	39	54	50	50	84
350 0	350. 0	-30 0	SW	46	51	53	47	85
350 0	400. 0	-30 0	SW	49	42	59	41	95
350 0	500. 0	-30 0	SW	58	39	63	37	92
350 0	600. 0	-30 0	SB	61	32	67	.33	1. 05
350. 0	700. 0	-30. 0	SB	68	93	11	89	.65
400. 0	50. 0	-30 0	SW	07	85	20	80	68
400 0	100. 0	-30. 0	SW	15	73	33	67	75
400 0	200. 0	-30. 0	SW	27	54	50	.50	87
400 0	400. 0	-30 0	SB	46	42	60	40	.91
400 0	600. 0	-30 0	MB	58	36	64	36	1 02
400 0	700. 0	-30 0	MB	64	92	09	91	89
500. 0	50. 0	-30. 0	SW	08	84	17	83	95
500 0	100. 0	-30 0	SW	16	60	44	.56	82
500 0	400. 0	-30. 0	SB	40	48	55	.45	91
500 0	600. 0	-30. 0	SB	52	43	58	.42	96
500. 0	700. 0	-30. 0	MB	57	.80	08	.92	2. 91
600. 0	50. 0	-30. 0	SW	20	88	14	.86	.80
600. 0	100. 0	-30. 0	SW	12	.76	25	75	.96
600. 0	200. 0	-30. 0	SW	24	.59	.40	.60	1. 03
600. 0	400. 0	-30. 0	SB	41	49	50	.50	1. 06
600 0	600. 0	-30. 0	MB	51	42	54	46	1. 20
600 0	700. 0	-30 0	MB	58	85	13	88	1 26
700 0	100 0	-30 0	SW	15	71	22	.78	1. 41
700. 0	200. 0	-30 0	SW	29	.61	36	.64	1. 14
700 0	400. 0	-30 0	SB	39	51	46	.54	1 10
700 0	600. 0	-30. 0	MB	49	46	50	50	1 15
700 0	700. 0	-30 0	MB	54				

APPENDIX V

COMPUTER PROGRAM MBBCORR AND GENERATED OUTPUT

```
      PROGRAM MBBCORR(INPUT,OUTPUT,TAPE5=INPUT,TAPE6=OUTPUT)
C*****************************************************************
C                                                                *
C   PURPOSE:                                                     *
C                                                                *
C    PROGRAM MBBCORR CALCULATES WATER HOLDUP FOR CERTAIN INPUT    *
C    PARAMETERS.  THIS EMPIRICAL WATER HOLDUP CORRELATION WAS     *
C    DEVELOPED BY MUKHERJEE,BRILL AND BEGGS (TRANS. OF ASME,      *
C    1981) FOR DOWNHILL FLOW OF OIL AND WATER.                    *
C                                                                *
C   INPUT PARAMETERS:                                            *
C                                                                *
C    N       - NUMBER OF INPUT DATA LINES                        *
C    QOIL    - OIL FLOW RATE, B/D                                *
C    QWATER  - WATER FLOW RATE, B/D                              *
C    ANG     - ANGLE OF INCLINATION FROM HORIZONTAL, DEGREES     *
C    OVIS    - OIL VISCOSITY, CP                                 *
C    WVIS    - WATER VISCOSITY, CP                               *
C    ODEN    - OIL DENSITY, LB/GAL                               *
C    WDEN    - WATER DENSITY, LB/GAL                             *
C    PD      - PIPE DIAMETER (ID), INCHES                        *
C                                                                *
C   OUTPUT PARAMETERS:                                           *
C                                                                *
C    QOIL    - OIL FLOW RATE, B/D                                *
C    QWATER  - WATER FLOW RATE, B/D                              *
C    ANG     - ANGLE OF INCLINATION FROM HORIZONTAL, DEGREES     *
C    HUW     - HOLDUP OF WATER (CALCULATED)                      *
C                                                                *
C*****************************************************************
      REAL QOIL(500),QWATER(500),ANG(500),VSO(500),VSW(500)
      REAL OIF(500),WIF(500),MVIS(500),MDEN(500),MVEL(500),MNRE(500)
      REAL HUW(500)
      READ(5,*)N
C-----------------------------------------------------------------
C     READ INPUT PARAMETERS
C-----------------------------------------------------------------
      READ(5,*)OVIS,WVIS,ODEN,WDEN,PD
      DO 1 I=1,N
        READ(5,*)QOIL(I),QWATER(I),ANG(I)
```

```
C-----------------------------------------------------------------------
C     CALCULATION OF OUTPUT PARAMETERS
C-----------------------------------------------------------------------
        ANG(I)=-(ANG(I)*3.14/180.0)
        VSO(I)=0.003*QOIL(I)
        VSW(I)=0.003*QWATER(I)
        WIF(I)=QWATER(I)/(QWATER(I)+QOIL(I))
        OIF(I)=1.0-WIF(I)
        MVIS(I)=OIF(I)*OVIS+WIF(I)*WVIS
        MDEN(I)=OIF(I)*ODEN+WIF(I)*WDEN
        MVEL(I)=VSO(I)+VSW(I)
        MNRE(I)=(MDEN(I)*MVEL(I)*PD)/MVIS(I)
        HUW(I)=8.3763*(WIF(I)**1.2428)*(SIN(ANG(I))**0.4947)
     $  /MNRE(I)**0.2093
        ANG(I)=-(ANG(I)*180/3.14)
   1  CONTINUE
      WRITE(6,10)
C-----------------------------------------------------------------------
C     PRINT OUT CALCULATED PARAMETERS
C-----------------------------------------------------------------------
      DO 2 I=1,N
        WRITE(6,20)QOIL(I),QWATER(I),ANG(I),HUW(I)
   2  CONTINUE
C-----------------------------------------------------------------------
C     FORMAT STATEMENTS
C-----------------------------------------------------------------------
   10 FORMAT(1H1,T3,*QOIL*,T11,*QWATER*,T22,*ANGLE*,T32,*WATER*/,
     $T4,*B/D*,T13,*B/D*,T21,*DEGREES*,T32,*HOLDUP*/,T3,4(*-*),T11,
     $6(*-*),T21,7(*-*),T32,6(*-*)/)
  20  FORMAT(2X,T3,F5.1,T11,F5.1,T22,F5.1,T34,F4.2)
      END
```

QOIL B/D	QWATER B/D	ANGLE DEGREES	WATER HOLDUP
50.0	50.0	-15.0	.91
50.0	100.0	-15.0	1.17
50.0	150.0	-15.0	1.26
50.0	200.0	-15.0	1.29
50.0	250.0	-15.0	1.30
50.0	300.0	-15.0	1.30
50.0	350.0	-15.0	1.30
50.0	400.0	-15.0	1.29
50.0	500.0	-15.0	1.27
50.0	600.0	-15.0	1.24
50.0	700.0	-15.0	1.22
100.0	100.0	-15.0	.78
100.0	200.0	-15.0	1.01
100.0	400.0	-15.0	1.12
100.0	600.0	-15.0	1.13
100.0	700.0	-15.0	1.12
150.0	50.0	-15.0	.34
150.0	100.0	-15.0	.57
150.0	150.0	-15.0	.72
150.0	200.0	-15.0	.82
150.0	250.0	-15.0	.88
150.0	300.0	-15.0	.93
150.0	350.0	-15.0	.96
150.0	400.0	-15.0	.98
150.0	500.0	-15.0	1.01
150.0	600.0	-15.0	1.03
150.0	700.0	-15.0	1.03
200.0	50.0	-15.0	.25
200.0	100.0	-15.0	.44
200.0	150.0	-15.0	.58
200.0	200.0	-15.0	.68
200.0	250.0	-15.0	.75
200.0	300.0	-15.0	.80
200.0	350.0	-15.0	.84
200.0	400.0	-15.0	.87
200.0	500.0	-15.0	.91
200.0	600.0	-15.0	.94
200.0	700.0	-15.0	.96
250.0	50.0	-15.0	.19
250.0	100.0	-15.0	.36
250.0	150.0	-15.0	.48

QOIL B/D	QWATER B/D	ANGLE DEGREES	WATER HOLDUP
250.0	200.0	-15.0	.58
250.0	250.0	-15.0	.65
250.0	300.0	-15.0	.70
250.0	350.0	-15.0	.75
250.0	400.0	-15.0	.78
250.0	500.0	-15.0	.83
250.0	600.0	-15.0	.87
250.0	700.0	-15.0	.89
300.0	50.0	-15.0	.15
300.0	100.0	-15.0	.30
300.0	150.0	-15.0	.41
300.0	200.0	-15.0	.50
300.0	250.0	-15.0	.57
300.0	300.0	-15.0	.62
300.0	350.0	-15.0	.67
300.0	400.0	-15.0	.71
300.0	500.0	-15.0	.76
300.0	600.0	-15.0	.80
300.0	700.0	-15.0	.83
350.0	50.0	-15.0	.13
350.0	100.0	-15.0	.25
350.0	200.0	-15.0	.43
350.0	250.0	-15.0	.50
350.0	300.0	-15.0	.56
350.0	350.0	-15.0	.60
350.0	400.0	-15.0	.64
350.0	500.0	-15.0	.70
350.0	600.0	-15.0	.74
350.0	700.0	-15.0	.78
400.0	50.0	-15.0	.11
400.0	100.0	-15.0	.22
400.0	200.0	-15.0	.38
400.0	400.0	-15.0	.59
400.0	600.0	-15.0	.69
400.0	700.0	-15.0	.73
500.0	50.0	-15.0	.08
500.0	100.0	-15.0	.17
500.0	400.0	-15.0	.50
500.0	600.0	-15.0	.61
500.0	700.0	-15.0	.65
600.0	50.0	-15.0	.06
600.0	100.0	-15.0	.13

QOIL B/D	QWATER B/D	ANGLE DEGREES	WATER HOLDUP
600.0	200.0	-15.0	.26
600.0	400.0	-15.0	.43
600.0	600.0	-15.0	.54
600.0	700.0	-15.0	.58
700.0	100.0	-15.0	.11
700.0	200.0	-15.0	.22
700.0	400.0	-15.0	.38
700.0	600.0	-15.0	.48
700.0	700.0	-15.0	.52
50.0	50.0	-30.0	1.25
50.0	100.0	-30.0	1.61
50.0	150.0	-30.0	1.74
50.0	200.0	-30.0	1.79
50.0	250.0	-30.0	1.80
50.0	300.0	-30.0	1.80
50.0	350.0	-30.0	1.79
50.0	400.0	-30.0	1.78
50.0	700.0	-30.0	1.69
100.0	100.0	-30.0	1.09
100.0	200.0	-30.0	1.40
100.0	400.0	-30.0	1.55
100.0	600.0	-30.0	1.56
100.0	700.0	-30.0	1.55
150.0	50.0	-30.0	.47
150.0	100.0	-30.0	.79
150.0	150.0	-30.0	1.00
150.0	200.0	-30.0	1.13
150.0	250.0	-30.0	1.22
150.0	300.0	-30.0	1.28
150.0	350.0	-30.0	1.33
150.0	400.0	-30.0	1.36
150.0	500.0	-30.0	1.40
150.0	600.0	-30.0	1.42
150.0	700.0	-30.0	1.43
200.0	50.0	-30.0	.34
200.0	100.0	-30.0	.62
200.0	150.0	-30.0	.80
200.0	200.0	-30.0	.94
200.0	250.0	-30.0	1.04
200.0	300.0	-30.0	1.11

QOIL B/D	QWATER B/D	ANGLE DEGREES	WATER HOLDUP
200.0	350.0	-30.0	1.17
200.0	400.0	-30.0	1.21
200.0	500.0	-30.0	1.27
200.0	600.0	-30.0	1.30
200.0	700.0	-30.0	1.32
250.0	50.0	-30.0	.27
250.0	100.0	-30.0	.49
250.0	150.0	-30.0	.67
250.0	200.0	-30.0	.80
250.0	250.0	-30.0	.90
250.0	300.0	-30.0	.97
250.0	350.0	-30.0	1.03
250.0	400.0	-30.0	1.08
250.0	500.0	-30.0	1.15
250.0	600.0	-30.0	1.20
250.0	700.0	-30.0	1.23
300.0	50.0	-30.0	.21
300.0	100.0	-30.0	.41
300.0	150.0	-30.0	.56
300.0	200.0	-30.0	.69
300.0	250.0	-30.0	.78
300.0	300.0	-30.0	.86
300.0	350.0	-30.0	.93
300.0	400.0	-30.0	.98
300.0	500.0	-30.0	1.05
300.0	600.0	-30.0	1.11
300.0	700.0	-30.0	1.15
350.0	50.0	-30.0	.18
350.0	100.0	-30.0	.35
350.0	200.0	-30.0	.60
350.0	250.0	-30.0	.69
350.0	300.0	-30.0	.77
350.0	350.0	-30.0	.83
350.0	400.0	-30.0	.89
350.0	500.0	-30.0	.97
350.0	600.0	-30.0	1.03
350.0	700.0	-30.0	1.07
400.0	50.0	-30.0	.15
400.0	100.0	-30.0	.30
400.0	200.0	-30.0	.53
400.0	400.0	-30.0	.81
400.0	600.0	-30.0	.96
400.0	700.0	-30.0	1.01
500.0	50.0	-30.0	.11
500.0	100.0	-30.0	.23

QOIL B/D	QWATER B/D	ANGLE DEGREES	WATER HOLDUP
500.0	400.0	-30.0	.69
500.0	600.0	-30.0	.84
500.0	700.0	-30.0	.89
600.0	50.0	-30.0	.09
600.0	100.0	-30.0	.18
600.0	200.0	-30.0	.35
600.0	400.0	-30.0	.59
600.0	600.0	-30.0	.75
600.0	700.0	-30.0	.80
700.0	100.0	-30.0	.15
700.0	200.0	-30.0	.30
700.0	400.0	-30.0	.52
700.0	600.0	-30.0	.67
700.0	700.0	-30.0	.72

APPENDIX VI

DATA TABLE

QOIL (B/D)	QWATER (B/D)	ANGLE DEGREES	FLOW REGIME	DISTANCE TO INTERFACE (CM)
50.0	50.0	0.0	SS	53.0
50.0	100.0	0.0	SW	77.0
50.0	150.0	0.0	SW	82.0
50.0	200.0	0.0	SW	90.0
50.0	250.0	0.0	SW	92.7
50.0	300.0	0.0	SW	101.7
50.0	350.0	0.0	SW	102.0
50.0	400.0	0.0	SW	103.7
50.0	500.0	0.0	SW	106.0
50.0	600.0	0.0	SW	109.0
50.0	700.0	0.0	SW	112.7
100.0	50.0	0.0	SW	37.0
100.0	100.0	0.0	SW	53.0
100.0	150.0	0.0	SW	63.3
100.0	200.0	0.0	SW	72.7
100.0	250.0	0.0	SW	79.0
100.0	300.0	0.0	SW	82.7
100.0	350.0	0.0	SW	85.2
100.0	400.0	0.0	SW	92.0
100.0	500.0	0.0	SW	95.0
100.0	600.0	0.0	SW	98.0
100.0	700.0	0.0	SB	102.0
150.0	50.0	0.0	SW	25.0
150.0	100.0	0.0	SW	41.0
150.0	150.0	0.0	SW	53.0
150.0	200.0	0.0	SW	58.0
150.0	250.0	0.0	SW	69.0
150.0	300.0	0.0	SW	75.7
150.0	350.0	0.0	SW	80.7
150.0	400.0	0.0	SW	85.0
150.0	500.0	0.0	SW	89.0
150.0	600.0	0.0	SW	95.0
100.0	700.0	0.0	SB	100.3
200.0	50.0	0.0	SW	19.0
200.0	100.0	0.0	SW	37.0
200.0	150.0	0.0	SW	41.0
200.0	200.0	0.0	SW	53.0
200.0	250.0	0.0	SW	62.0
200.0	300.0	0.0	SW	68.0

QOIL (B/D)	QWATER (B/D)	ANGLE DEGREES	FLOW REGIME	DISTANCE TO INTERFACE (CM)
200.0	350.0	0.0	SW	72.0
200.0	400.0	0.0	SW	74.5
200.0	500.0	0.0	SW	84.0
200.0	600.0	0.0	SW	86.0
200.0	700.0	0.0	SB	88.0
250.0	50.0	0.0	SW	8.0
250.0	100.0	0.0	SW	27.0
250.0	150.0	0.0	SW	39.0
250.0	200.0	0.0	SW	46.0
250.0	250.0	0.0	SW	54.0
250.0	300.0	0.0	SW	62.0
250.0	350.0	0.0	SW	65.0
250.0	400.0	0.0	SW	69.7
250.0	500.0	0.0	SW	75.0
250.0	600.0	0.0	SW	77.0
200.0	700.0	0.0	SB	80.0
300.0	50.0	0.0	SW	7.0
300.0	100.0	0.0	SW	23.7
300.0	150.0	0.0	SW	33.0
300.0	200.0	0.0	SW	39.8
300.0	250.0	0.0	SW	50.0
300.0	300.0	0.0	SW	54.0
300.0	350.0	0.0	SW	59.3
300.0	400.0	0.0	SW	65.0
300.0	500.0	0.0	SW	71.0
300.0	600.0	0.0	SB	74.0
300.0	700.0	0.0	SB	77.0
350.0	50.0	0.0	SW	3.0
350.0	100.0	0.0	SW	16.0
350.0	200.0	0.0	SW	41.0
350.0	250.0	0.0	SW	44.0
350.0	300.0	0.0	SW	50.0
350.0	350.0	0.0	SW	54.0
350.0	400.0	0.0	SW	56.3
350.0	500.0	0.0	SB	66.0
350.0	600.0	0.0	SB	74.0
300.0	700.0	0.0	SB	76.0
400.0	50.0	0.0	SW	5.0
400.0	100.0	0.0	SW	14.0
400.0	200.0	0.0	SW	32.5
400.0	400.0	0.0	SW	53.0
400.0	600.0	0.0	SB	65.3

QOIL (B/D)	QWATER (B/D)	ANGLE DEGREES	FLOW REGIME	DISTANCE TO INTERFACE (CM)
400.0	700.0	0.0	MB	73.0
500.0	50.0	0.0	SW	-6.0
500.0	100.0	0.0	SW	12.0
500.0	400.0	0.0	SB	46.0
500.0	600.0	0.0	SB	57.5
500.0	700.0	0.0	MB	63.0
600.0	50.0	0.0	SW	-1.0
600.0	100.0	0.0	SW	7.0
600.0	200.0	0.0	SW	21.0
600.0	400.0	0.0	SB	39.6
600.0	600.0	0.0	MB	53.0
600.0	700.0	0.0	MB	59.3
700.0	100.0	0.0	SW	6.3
700.0	200.0	0.0	SW	22.7
700.0	400.0	0.0	SB	34.7
700.0	600.0	0.0	MB	52.7
700.0	700.0	0.0	MB	55.3
50.0	50.0	-15.0	SWC	-2.0
50.0	100.0	-15.0	SWC	13.0
50.0	150.0	-15.0	SWC	25.3
50.0	200.0	-15.0	SWC	42.5
50.0	250.0	-15.0	SWC	64.3
50.0	300.0	-15.0	SWC	78.0
50.0	350.0	-15.0	SWC	84.0
50.0	400.0	-15.0	SWC	95.0
50.0	500.0	-15.0	SWC	101.0
50.0	600.0	-15.0	SWC	103.7
50.0	700.0	-15.0	SW	111.0
100.0	100.0	-15.0	SWC	19.2
100.0	200.0	-15.0	SWC	35.0
100.0	400.0	-15.0	SWC	86.0
100.0	600.0	-15.0	SW	97.7
100.0	700.0	-15.0	SB	102.3
150.0	50.0	-15.0	SW	1.5
150.0	100.0	-15.0	SW	11.3
150.0	150.0	-15.0	SW	20.3
150.0	200.0	-15.0	SW	30.3
150.0	250.0	-15.0	SW	37.0

QOIL (B/D)	QWATER (B/D)	ANGLE DEGREES	FLOW REGIME	DISTANCE TO INTERFACE (CM)
150.0	300.0	-15.0	SW	44.0
150.0	350.0	-15.0	SW	49.7
150.0	400.0	-15.0	SW	59.0
150.0	500.0	-15.0	SW	71.0
150.0	600.0	-15.0	SW	79.0
100.0	700.0	-15.0	SB	87.0
200.0	50.0	-15.0	SW	-4.0
200.0	100.0	-15.0	SW	7.0
200.0	150.0	-15.0	SW	20.3
200.0	200.0	-15.0	SW	25.0
200.0	250.0	-15.0	SW	35.3
200.0	300.0	-15.0	SW	40.3
200.0	350.0	-15.0	SW	46.0
200.0	400.0	-15.0	SW	55.0
200.0	500.0	-15.0	SW	67.7
200.0	600.0	-15.0	SW	76.0
200.0	700.0	-15.0	SB	80.0
250.0	50.0	-15.0	SW	-7.0
250.0	100.0	-15.0	SW	7.0
250.0	150.0	-15.0	SW	14.3
250.0	200.0	-15.0	SW	23.0
250.0	250.0	-15.0	SW	33.0
250.0	300.0	-15.0	SW	39.7
250.0	350.0	-15.0	SW	45.0
250.0	400.0	-15.0	SW	49.0
250.0	500.0	-15.0	SW	58.7
250.0	600.0	-15.0	SB	69.7
250.0	700.0	-15.0	SB	78.7
300.0	50.0	-15.0	SW	-3.0
300.0	100.0	-15.0	SW	4.0
300.0	150.0	-15.0	SW	17.3
300.0	200.0	-15.0	SW	21.7
300.0	250.0	-15.0	SW	28.7
300.0	300.0	-15.0	SW	35.0
300.0	350.0	-15.0	SW	40.0
300.0	400.0	-15.0	SW	46.0
300.0	500.0	-15.0	SW	53.7
300.0	600.0	-15.0	SB	66.0
300.0	700.0	-15.0	SB	80.0

QOIL (B/D)	QWATER (B/D)	ANGLE DEGREES	FLOW REIGME	DISTANCE TO INTERFACE (CM)
350.0	50.0	-15.0	SW	-0.7
350.0	100.0	-15.0	SW	16.0
350.0	200.0	-15.0	SW	22.7
350.0	250.0	-15.0	SW	29.7
350.0	300.0	-15.0	SW	33.0
350.0	350.0	-15.0	SW	36.0
350.0	400.0	-15.0	SW	45.3
350.0	500.0	-15.0	SW	51.0
350.0	600.0	-15.0	SB	69.0
350.0	700.0	-15.0	SB	78.0
400.0	50.0	-15.0	SW	-3.0
400.0	100.0	-15.0	SW	4.3
400.0	200.0	-15.0	SW	22.0
400.0	400.0	-15.0	SW	43.0
400.0	600.0	-15.0	MB	64.0
400.0	700.0	-15.0	MB	71.0
500.0	50.0	-15.0	SW	-6.0
500.0	100.0	-15.0	SW	0.0
500.0	400.0	-15.0	SB	36.0
500.0	600.0	-15.0	MB	57.0
500.0	700.0	-15.0	MB	63.0
600.0	50.0	-15.0	SW	-5.0
600.0	100.0	-15.0	SW	0.0
600.0	200.0	-15.0	SW	17.7
600.0	400.0	-15.0	SB	38.0
600.0	600.0	-15.0	MB	55.7
600.0	700.0	-15.0	MB	66.0
700.0	100.0	-15.0	SW	4.0
700.0	200.0	-15.0	SW	17.0
700.0	400.0	-15.0	SB	38.0
700.0	600.0	-15.0	MB	50.3
700.0	700.0	-15.0	MB	58.3
50.0	50.0	-30.0	SWC	-2.0
50.0	100.0	-30.0	SWC	17.3
50.0	150.0	-30.0	SWC	48.7
50.0	200.0	-30.0	SWC	59.0
50.0	250.0	-30.0	SWC	79.7
50.0	300.0	-30.0	SWC	92.3
50.0	350.0	-30.0	SWC	93.7

QOIL (B/D)	QWATER (B/D)	ANGLE DEGREES	FLOW REGIME	DISTANCE TO INTERFACE (CM)
50.0	400.0	-30.0	SWC	102.0
50.0	700.0	-30.0	SW	111.7
100.0	100.0	-30.0	SWC	17.0
100.0	200.0	-30.0	SWC	49.3
100.0	400.0	-30.0	SWC	94.2
100.0	600.0	-30.0	SW	99.0
100.0	700.0	-30.0	SW	103.7
150.0	50.0	-30.0	SW	-1.0
150.0	100.0	-30.0	SW	11.0
150.0	150.0	-30.0	SW	25.0
150.0	200.0	-30.0	SW	30.0
150.0	250.0	-30.0	SW	43.0
150.0	300.0	-30.0	SW	49.0
150.0	350.0	-30.0	SW	54.7
150.0	400.0	-30.0	SW	68.0
150.0	500.0	-30.0	SW	77.0
150.0	600.0	-30.0	SB	80.0
150.0	700.0	-30.0	SB	85.3
200.0	50.0	-30.0	SW	-4.0
200.0	100.0	-30.0	SW	13.0
200.0	150.0	-30.0	SW	19.3
200.0	200.0	-30.0	SW	34.0
200.0	250.0	-30.0	SW	42.3
200.0	300.0	-30.0	SW	47.3
200.0	350.0	-30.0	SW	54.0
200.0	400.0	-30.0	SW	62.3
200.0	500.0	-30.0	SB	73.3
200.0	600.0	-30.0	SB	79.7
200.0	700.0	-30.0	SB	86.3
250.0	50.0	-30.0	SW	-5.0
250.0	100.0	-30.0	SW	8.0
250.0	150.0	-30.0	SW	21.0
250.0	200.0	-30.0	SW	30.0
250.0	250.0	-30.0	SW	37.7
250.0	300.0	-30.0	SW	48.3
250.0	350.0	-30.0	SW	54.7
250.0	400.0	-30.0	SW	60.0
250.0	500.0	-30.0	SB	68.3
250.0	600.0	-30.0	SB	74.7
250.0	700.0	-30.0	SB	86.7
300.0	50.0	-30.0	SW	-1.0
300.0	100.0	-30.0	SW	3.7
300.0	150.0	-30.0	SW	17.7

QOIL (B/D)	QWATER (B/D)	ANGLE DEGREES	FLOW REGIME	DISTANCE TO INTERFACE (CM)
300.0	200.0	-30.0	SW	22.0
300.0	250.0	-30.0	SW	25.0
300.0	300.0	-30.0	SW	36.3
300.0	350.0	-30.0	SW	47.7
300.0	400.0	-30.0	SW	51.0
300.0	500.0	-30.0	SB	58.0
300.0	600.0	-30.0	SB	70.0
300.0	700.0	-30.0	MB	79.3
350.0	50.0	-30.0	SW	1.0
350.0	100.0	-30.0	SW	14.0
350.0	200.0	-30.0	SW	24.7
350.0	250.0	-30.0	SW	30.3
350.0	300.0	-30.0	SW	37.0
350.0	350.0	-30.0	SW	47.0
350.0	400.0	-30.0	SW	52.0
350.0	500.0	-30.0	SW	63.7
350.0	600.0	-30.0	SB	68.7
350.0	700.0	-30.0	SB	78.0
400.0	50.0	-30.0	SW	-7.0
400.0	100.0	-30.0	SW	3.0
400.0	200.0	-30.0	SW	21.0
400.0	400.0	-30.0	SB	48.0
400.0	600.0	-30.0	MB	64.0
400.0	700.0	-30.0	MB	73.0
500.0	50.0	-30.0	SW	-6.0
500.0	100.0	-30.0	SW	5.0
500.0	400.0	-30.0	SB	38.5
500.0	600.0	-30.0	SB	56.0
500.0	700.0	-30.0	MB	63.5
600.0	50.0	-30.0	SW	-10.0
600.0	100.0	-30.0	SW	-1.0
600.0	200.0	-30.0	SW	16.7
600.0	400.0	-30.0	SB	40.0
600.0	600.0	-30.0	MB	55.0
600.0	700.0	-30.0	MB	64.7
700.0	100.0	-30.0	SW	4.0
700.0	200.0	-30.0	SW	23.0
700.0	400.0	-30.0	SB	38.0
700.0	600.0	-30.0	MB	51.0
700.0	700.0	-30.0	MB	58.0

NOMENCLATURE

A = flow cross-sectional area

AD = annular-annular dispersed liquid flow

c = wave velocity

C = coefficient dependent on the size of disturbance; also constant in the friction factor correlation

D = pipe diameter and hydraulic diameter

DB = dispersed bubble flow

f = friction factor

F = modified Froude number, Equation (28)

g = acceleration of gravity

h = liquid level or gas cap

I = intermittent (slug and plug) flow

K = wavy flow, dimensionless parameter, Equation (32)

m = exponent, Equation (5)

n = exponent, Equation (5)

P = pressure

Re = Reynolds number

s = Jefferys' sheltering coefficient

S = perimeter over which the stress acts; also stratified flow

SS = stratified smooth flow

SW = stratified wavy flow

T = dispersed bubble flow dimensionless parameter Equation (38)

U = velocity in the X direction

V = velocity normal to the X direction

x = coordinate in the downstream direction

X = Martinelli parameter, Equation (8)

Y = dimensionless inclination parameter, Equation (9)

Greek symbols

α = angle between the pipe axis and the horizontal, positive for downhill flow

ρ = density

τ = shear stress

ν = kinematic viscosity

Subscripts and Superscripts

G = gas

i = liquid gas interface

L = liquid

s = superficial, for single fluid flow

W = pipe surface

~ = dimensionless variable

' = disturbed variable

• = friction velocity

- = average

BIBLIOGRAPHY

1. Dukler, A. E., Wicks, Moye, and Cleveland, R. G.: "Frictional Pressure Drop in Two-Phase Flow: A Comparison of Existing Correlations for Pressure Loss and Holdup," AIChE Journal, 10, 38-43 (January, 1964).

2. Duns, H. Jr. and Ros, N. C. J.: "Vertical Flow of Gas and Liquid Mixtures in Wells," Sixth World Petroleum Congress, Section 2, Paper 27, Frankfurt, 1963.

3. Ros, N. C. J.: "Simultaneous Flow of Gas and Liquid as Encountered in Well Tubing," Journal of Petroleum Technology, 13, 1037, (October, 1961).

4. Hagedorn, A. R.: "Experimental Study of Pressure Gradients Occurring during Continuous Two-Phase Flow in Small Diameter Vertical Conduits," Ph.D. Dissertation, University of Texas (May, 1964).

5. DeGance, Anthony E., and Atherton, Robert W.: "Vertical and Inclined Flow Correlations," Chemical Engineering, Vol. 77, No. 21, October 5, 1970, p. 87-94.

6. Gregory, G. A.: "Comparison of Methods for the Prediction of Liquid Holdup for Upward Gas-Liquid Flow in Inclined Pipes," Canadian Journal of Chemical Engineering, Vol. 53, August 1975, p. 384-388.

7. Lockhart, R. W., and Martinelli, R. C.: Chemical Engineering Progress, Vol. 45, 1949, p. 39.

8. Guzhov, A. I., Mamayev, V. A., and Odishariya, G. E.: 10th International Gas Conference, Hamburg, Germany, 1967.

9. Beggs, H. Dale, and Brill, James P.: "An Experimental Study of Two-Phase Flow in Inclined Pipes," SPE 4007 presented at the 47th Annual Fall Meeting, San Antonio, Texas, October 1972.

10. Russell, T. W. F., Hodgson, G. W., and Govier, G. W.: Horizontal Pipeline Flow of Mixtures of Oil and Water," Canadian Journal of Chemical Engineering, Vol. 37, p. 9.

11. Charles, M. E., Govier, G. W., and Hodgson, G. W.: "Complexities Inherent in the Study of Two Phase,: Canadian Journal of Chemical Engineering, 1961, p. 67-75.

12. Guzhov, A. I., Grishin, A. D., Medvedev, V. F., and Medvedeva, L. P.: "Formation of Emulsions During Flow of Two Liquids in a Pipe-Line," NEFT KNOZ (in Russian), No. 8, August, 1973, p. 58-61.

13. Soot, P. M., and Knudsen, J. G.: "Two-Phase Liquid-Liquid Flow in Pipes, "AIChE Symposium Series, Vol. 68, No. 118, 1972. p. 38-44.

14. Mukherjee, H., Brill, J. P., and Beggs, H. D.: "Experimental Study of Oil-Water Flow in Inclined Pipes," Transactions of ASME, Vol. 103, p. 56.

15. Eaton, B. A. and Brown, K. A.: "The Prediction of Flow Patterns, Liquid Holdup and Pressure Losses Occurring during Continuous Two-Phase Flow in Horizontal Pipelines", Technical Report, The University of Texas Department of Petroleum Engineering (October, 1965).

16. Baker, O.: "Simultaneous Flow of Oil and Gas," Oil Gas Journal, 53, 185 (July 1954).

17. Taitel, Y., and Dukler, A. E.: "A Model for Predicting Flow Regime Transitions in Horizontal and Near Horizontal Gas-Liquid Flow," AIChE Journal, 22, No. 3, 47-55 (1976).

18. White, P. O., and Huntington, P. L.: "Horizontal Co-Current Two-Phase Flow of Fluids in Pipe Lines," Petroleum Engineer, 27, No. 9, D40 (Aug, 1955).

19. Govier, G. W., and Omer, M. M.: "The Horizontal Pipeline Flow of Air-Water Mixtures," Canadian Journal of Chemical Engineering, 40, 93 (1962).

20. Kosterin, S. I.: Izvestiya Akademii Nauk., SSSR., O. T. N., 12, 1824, USSR (1949).

21. Al-Sheikh, J. N., Saunders, D. E., and Brodkey, R. S.: "Prediction of Flow Patterns in Horizontal Two-Phase Pipe Flow," Canadian Journal of Chemical Engineering, 48, 21 (1970).

22. Mandhane, J. M., Gregory, G. A., and Aziz, K.: "A Flow Pattern Map for Gas-Liquid Flow in Horizontal Pipes," International Journal of Multiphase Flow, I, 537-553 (1974).

23. Hubbard, M. G., and Dukler, A. E.: "The Characterization of Flow Regimes for Horizontal Two-Phase Flow," Proceeding of the 1966 Heat Transfer and Fluid Mechanics Institute, M. A. Saad and J. A. Moller, ed., pp. 100-121, Stanford University Press, California (1966).

24. Agrawal, S. S., Gregory, G. A., and Govier, G. W.: "An analysis of Horizontal Stratified Two-Phase Flow in Pipes," Canadian Journal of Chemical Engineering, 51, 280-286 (1973).

25. Gazley, C.: "Interfacial Shear and Stability in Two-Phase Flow," Ph.D. Thesis, Univ. Del., Newark (1949).

26. Lockhart, R. W., and Martinelli, R. C.: "Proposed Correlation of Data for Isothermal Two-Phase, Two-Component Flow in Pipes," Chemical Engineering Progress, 45, 39-48 (1949).

27. Milne-Thomson, L. M.: Theoretical Hydrodynamics, The MacMillan Co., New York (1960).

28. Jeffreys, H.: "On the Formation of Water Waves by Wind," Proceedings of the Royal Society, A 107, 189 (1925).

29. Benjamin, T. B.: "Gravity Currents and Related Phenomena," Journal of Fluid Mechanics, 31, 209-248 (1968).

30. Fulford, G. D.: "The Flow of Liquids in Thin Films," Advanced Chemical Engineering, 5, 151-236 (1964).

31. Brock, R. R.: "Periodic Permanent Roll Waves," Proceedings of the American Society of Civil Engineers, 96, HYD 12, 2565-2580 (1970).

32. Chu, K. T.: "Statistical Characteristics and Modelling of Wavy Liquid Films in Vertical Two Phase Flow," Ph.D. Dissertation, University of Houston, Houston, Texas (1973).

33. Levich, U. G.: Physicochemical Hydrodynamics, Prentice-Hall, Englewood Cliffs, N. J. (1962).

The vita has been removed from the digitized version of this document.